AD NUMBER: AD0909030
LIMITATION CHANGES
TO: Approved for public release; distribution is unlimited.
FROM: Distribution authorized to US Government Agencies only; Test and Evaluation; 1 Jan 1973. Other requests for this document must be referred to the Air Force Armament Laboratory (DLDG), Eglin AFB, FL 32542
AUTHORITY
AFATL ltr dtd 24 Oct 1975

THIS REPORT HAS BEEN DELIMITED
AND CLEARED FOR PUBLIC RELEASE
UNDER DOD DIRECTIVE 5200.20 AND
NO RESTRICTIONS ARE IMPOSED UPON
ITS USE AND DISCLOSURE.

DISTRIBUTION STATEMENT A

APPROVED FOR PUBLIC RELEASE;
DISTRIBUTION UNLIMITED.

AFATL-TR-73-9

THE SEMI-ARMOR PIERCING HIGH EXPLOSIVE (SAPHE) ENGINEERING DEVEVELOPMENT PROGRAM

HONEYWELL INC.
GOVERNMENT AND AERONAUTICAL PRODUCTS DIVISION

TECHNICAL REPORT AFATL-TR-73-9

JANUARY 1973

Distribution limited to U. S. Government agencies only; this report documents test and evaluation; distribution limitation applied January 1973. Other requests for this document must be referred to the Air Force Armament Laboratory (DLDG), Eglin Air Force Base, Florida 32542.

AIR FORCE ARMAMENT LABORATORY

AIR FORCE SYSTEMS COMMAND • UNITED STATES AIR FORCE

EGLIN AIR FORCE BASE, FLORIDA

The Semi-Armor Piercing High Explosive (SAPHE) Engineering Development Program

Ray A. Hermanson

FOREWORD

This report describes the research and development conducted by Honeywell Inc., Government & Aeronautical Products Division, 200 North Second Street, Hopkins, Minnesota, on the PGU-2/B (SAPHE) projectile under Contract No. F08635-70-C-0009 with the Air Force Armament Laboratory, Eglin Air Force Base, Florida. This report covers the period from 28 August 1968 to 15 August 1972. The program monitor for the Armament Laboratory was Mr. Seymour Slotkin (DLDG).

This report has been reviewed and is approved.

DALE M. DAVIS
Director, Guns and Rockets Division

ABSTRACT

Under this effort a 20mm Semi-Armor Piercing High Explosive (SAPHE) ammunition, designated the PGU-2/B, was designed, developed, fabricated, and evaluated. This design incorporated an all-impact angle base fuze evolved from the feasibility effort under Contract F08635-69-C-0134. The resulting 20mm SAPHE round is designed to meet or exceed the technical requirements of the M50 series ammunition. It is also designed to be directly interchangeable in the present M39 and M61 gun systems without change or modification to the gun or feed (with the exception of coil spring rates). The initial baseline development included contractor design, development tests, and delivery of over 3,000 cartridges for Government evaluations. Additional effort included fuze design modifications to investigate the feasibility of increasing the minimum arming distance to 6 meters, with 15 meters desired, development tests, and delivery of six cutaway display models. Although a safe-separation distance of 6 meters was not achieved within the funds and time available, it is believed that the safe-separation can be increased by using either of the two minor modifications described in the report.

(The reverse of this page is blank)

TABLE OF CONTENTS

TABLE OF CONTENTS (Continued)

TABLE OF CONTENTS (Concluded)

LIST OF FIGURES

LIST OF FIGURES (Continued)

LIST OF FIGURES (Continued)

LIST OF FIGURES (Concluded)

LIST OF TABLES

LIST OF TABLES (Concluded)

SECTION I

INTRODUCTION

Military operations in Southeast Asia have demonstrated the need for 20mm ammunition with longer range and greater terminal effectiveness. A general purpose round combining high explosive (HE) and antiarmor (AP) properties appeared feasible, and its development was authorized in RAD-8-339(1), dated 5 April 1968. The basic requirements are that the complete round shall not exceed the length of the standard 20mm M50 series round and shall be interchangeable in the M39 and M61 gun systems without change or modification. When successfully developed, this round will replace the 20mm API (M53) round and the 20mm HEI (M56) round.

During the period from 30 December 1968 through 31 March 1969, contractor conducted a feasibility study on a new base-mounted, graze-sensitive fuze for a 20mm Semi-Armor Piercing High Explosive (SAPHE) round for the Air Force Armament Laboratory, Eglin Air Force Base, Florida, under Contract F08635-69-C-0134. This program demonstrated the feasibility of the SAPHE fuze through theoretical studies and laboratory and firing tests.

As a result of the feasibility study, AFATL contracted with Honeywell to design, develop and deliver over 3,000 cartridges for Government evaluation. This work, conducted under Contract F08635-70-C-0009 from 28 August 1968 to the completion of hardware delivery on 31 August 1970, is described in Sections III, IV and V of this report.

The contract was subsequently modified on 22 June 1971 to increase the arming delay of the SAPHE fuze without degrading any other function of the round. Section VI of this report describes this effort conducted between 22 June 1971 and 15 August 1972.

SECTION II

SUMMARY AND CONCLUSIONS

Pursuant to the requirements of Contract F08635-70-C-0009, the 20mm Semi-Armor Piercing High Explosive (SAPHE) cartridge, designated PGU-2/B, has been designed and tested. There were two development efforts. The basic contract resulted in a complete projectile assembly and cartridge (Figures 1 and 2).

- Figure 1 (Drawing 28102343) is a cross-sectional layout of the prime concept, which has been tested for strength, safety and arming, function, and sensitivity.
- Figure 2 (Drawing 28102876) represents the cartridge designed to meet the requirements set forth in the contract.

One of the requirements was that the final round shall be dimensionally within the envelope of the presently standard M50 series ammunition. Figure 3 compares the PGU-2/B profile to the M56 profile. Note that minor lengthening of the PGU-2/B is possible.

Another requirement was that the SAPHE round shall use existing ammunition components to the extent feasible (M50 series cartridge case, primers, propellants, explosive mixes, and M505 fuze components) and must be directly interchangeable in the present M39 and M61 gun systems without change to the gun or feed (except for possible stiffening of the recoil springs).

The following ammunition components were used:

- Cartridge case – M103
- Primer – M52A3B1
- Propellant – New ball propellant (Olin Mathieson X2988.1.)

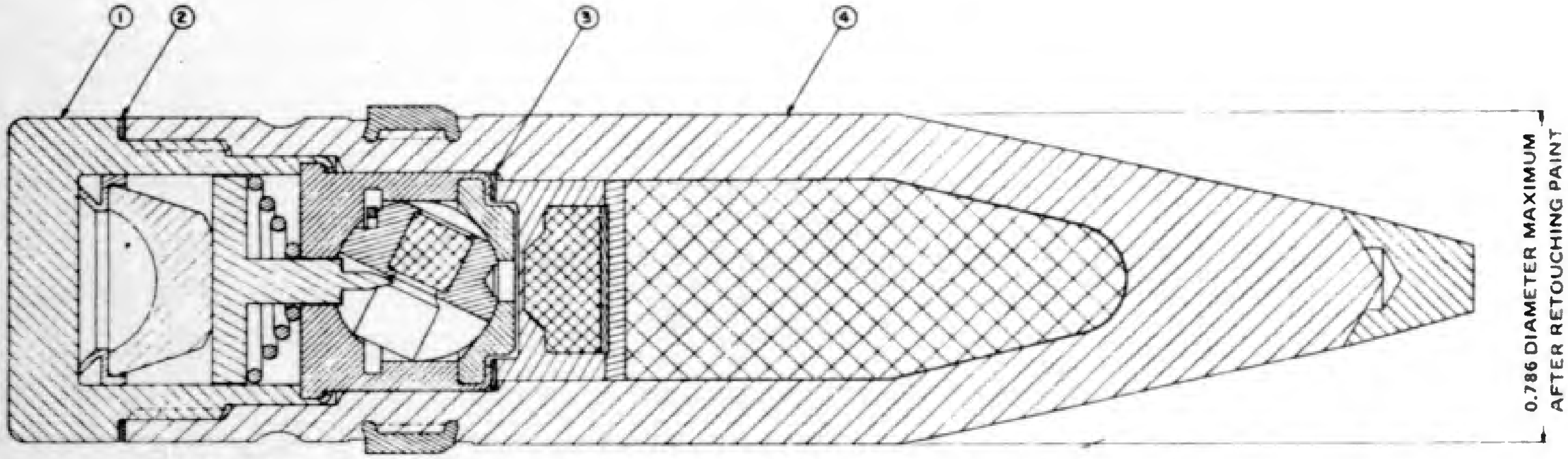

1. FUZE ASSEMBLY
2. SEAL WASHER
3. COMPRESSION WASHER
4. WARHEAD ASSEMBLY

Figure 1. PGU-2/B Projectile

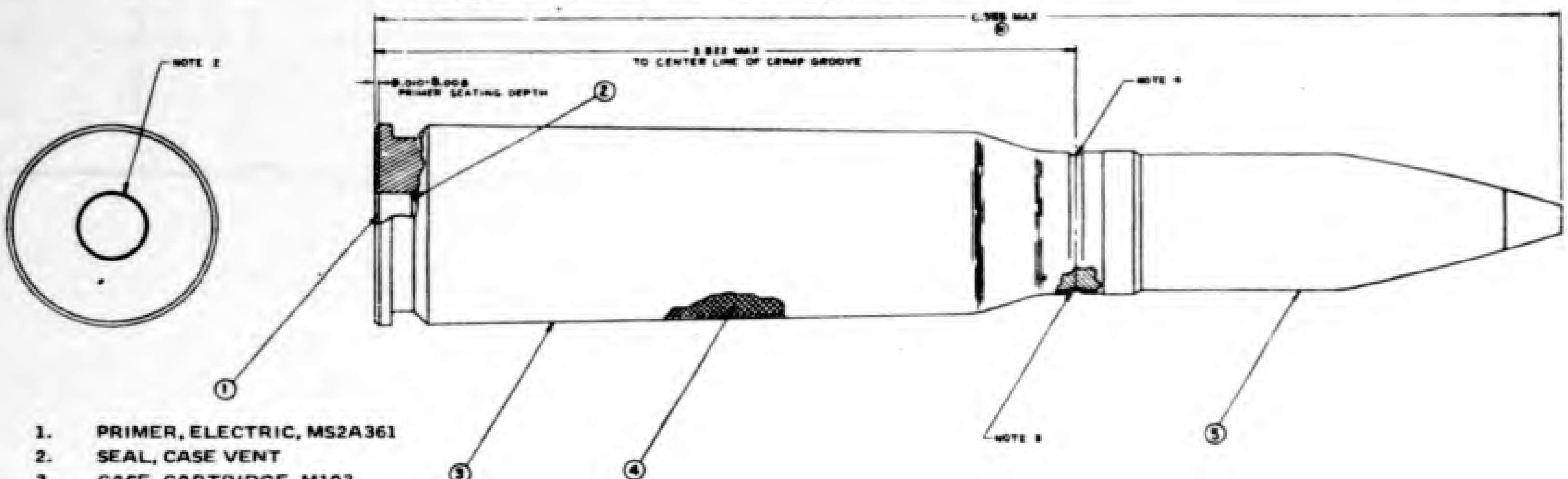

1. PRIMER, ELECTRIC, MS2A361
2. SEAL, CASE VENT
3. CASE, CARTRIDGE, M103
4. PROPELLANT
5. PROJECTILE, 20MM, PGU-2/B

Figure 2. PGU - 2/B Cartridge

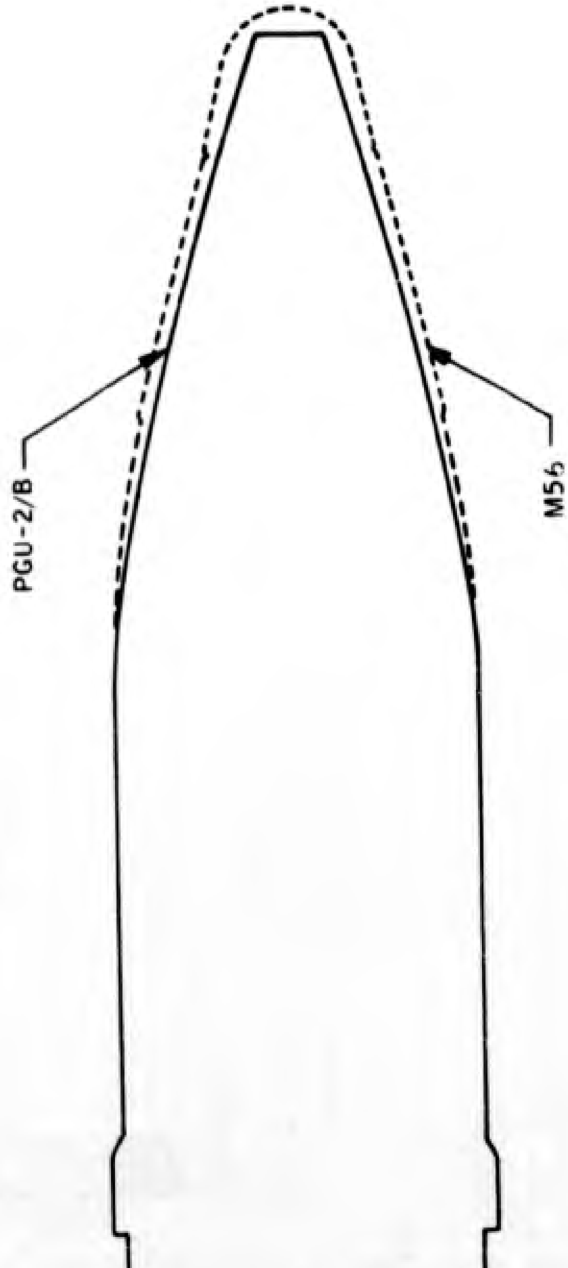

Figure 3. Comparison of PGU-2/B and M56 Profiles

- Explosive – PBXN-5 (Booster)
  LCA Mix No. 1 (Main Charge)

- M505 fuze components – Modified for base fuze application.

The SAPHE round has been test-fired from M39 and M61 gun systems without change to gun or feed.

The warhead, as developed, will survive impact with 1/4-inch Rolled Homogeneous Armor (RHA) at zero degrees and penetrate (without survival) 1/4-inch RHA at 60 degrees impact angle and 3/8-inch RHA at 30 degrees. Effectiveness studies showed that the warhead was more effective than the M56A3 against trucks, armored personnel carriers, parked aircraft, and personnel.

Ballistic studies showed that the round would generally meet its ballistic goals of a downrange velocity of 3,360 fps at 2,000-foot slant range and 1,060 fps at 9,000-foot slant range when fired from an aircraft going 790 KTAS in a 30-degree dive.

Propellant systems were studied and Olin X2988 chosen because it met the requirements with the least variation in pressure and velocity and was a ball propellant with a known resistance to damage from rough handling, vibration, and high temperature storage.

A safing and arming system was developed to partially arm on setback, complete arming during spin, and function on either direct or graze impact. A smaller fuze was investigated to allow an increase in propellant and/or high explosive charge with a probable increase in effectiveness. An explosive train was designed with standard components and shown to be effective by a series of Bruceton tests.

Production by automatic machining was a primary goal of the projectile design. It is believed that quantity production will present no problems.

The estimated safety failure rate of the PGU-2/B was calculated as 0.174×10^{-6}, nearly 5.75 times better than the design goal.

The second development effort began in August 1971 with the objective of providing a minimum arming distance of 6 meters, with 15 meters desired, for the basic SAPHE projectile described above without degrading function. The fuze was modified by changing the rotor, setback spring, firing pin, crush washer, detonator, rear rotor housing and inertia weight.

The configuration at the close of the contract is shown in Figure 4. It is concluded that although this fuze does not completely meet the arming delay requirement, it provides significant improvement over the baseline SAPHE fuze and that further changes will extend the minimum arming distance beyond 6 meters.

To increase the safe separation distance, the ball rotor must be prevented from moving until the projectile is in free flight. This can be done by using setback forces either to lock the ball rotor or to clamp the rotor against its detent spring (C-ring) and prevent the spring from opening until free flight is achieved. Both of these systems have been investigated during the 30mm SAPHE and M505A3 fuze programs described in Appendix I.

The minature detonator was not completely satisfactory in initiating the booster high order, but in the present configuration of the 20mm SAPHE a larger detonator degrades out-of-line safety. It is recommended that the front rotor housing be made in one piece (as successfully demonstrated in the 30mm SAPHE) so that a larger detonator can be used without impairing out-of-line safety.[1]

---

[1] A 30mm SAPHE projectile is being developed by contractor as a candidate for the GAU-8/A gun system.

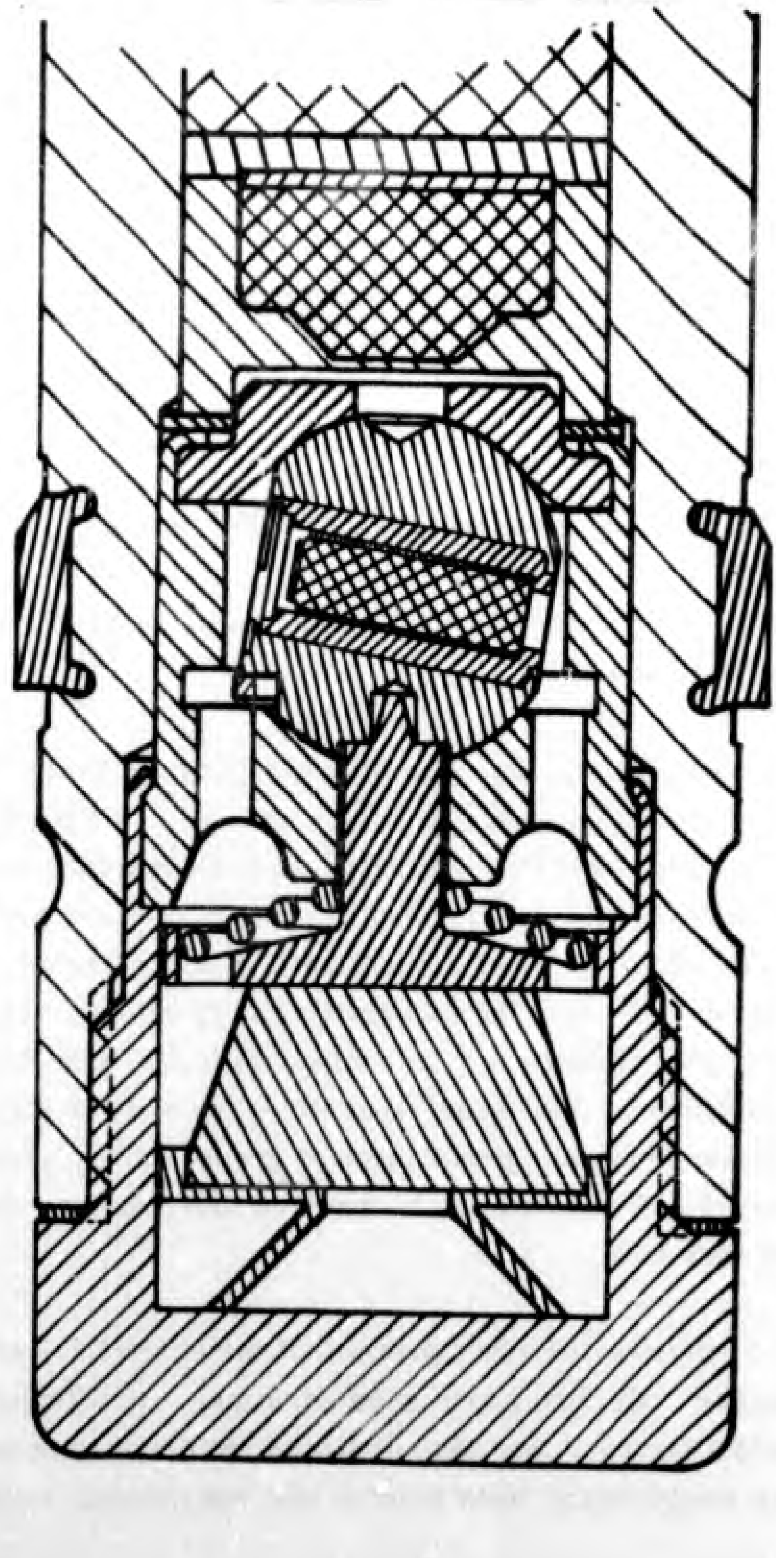

Figure 4. Final SAPHE Fuze Configuration

SECTION III

SUBSYSTEM DEVELOPMENT

A. WARHEAD

The warhead must:

- Protect the fuze and explosive components from the effects of storage and the barrel environment.
- Confine the explosive load.
- Penetrate armor.
- Provide a fragmenting mass for greater effectiveness.

Figure 5 shows the SAPHE warhead which consists of a body, a nose cap, a seal washer and a base plug.

The body forms a two-part cavity. The fuze cavity protects the fuze from the pressure of the propellant gases in the barrel and holds the fuze in position until it has functioned on the target, while the explosive cavity contains the high explosive and booster. For maximum effectiveness, this cavity must remain intact on target impact until it is fragmented by detonation of the explosive. The warhead will survive perpendicular impact with 1/4-inch RHA; the goal of survival after impact with 3/8-inch RHA at 30 degrees was not achieved. The penetrator tip of the body is a standard conical configuration which aids penetration at graze angles. Penetration (without survival) of 1/4-inch RHA at 60 degrees and 3/8-inch RHA at 30 degrees has been achieved.

The cap serves to improve the aerodynamics of the projectile and to reduce the shock load on the body during armor penetration. An alternate body with a thicker wall (Figure 6) was also designed but dropped from consideration after stress analysis and tests proved that the original wall thickness was adequate.

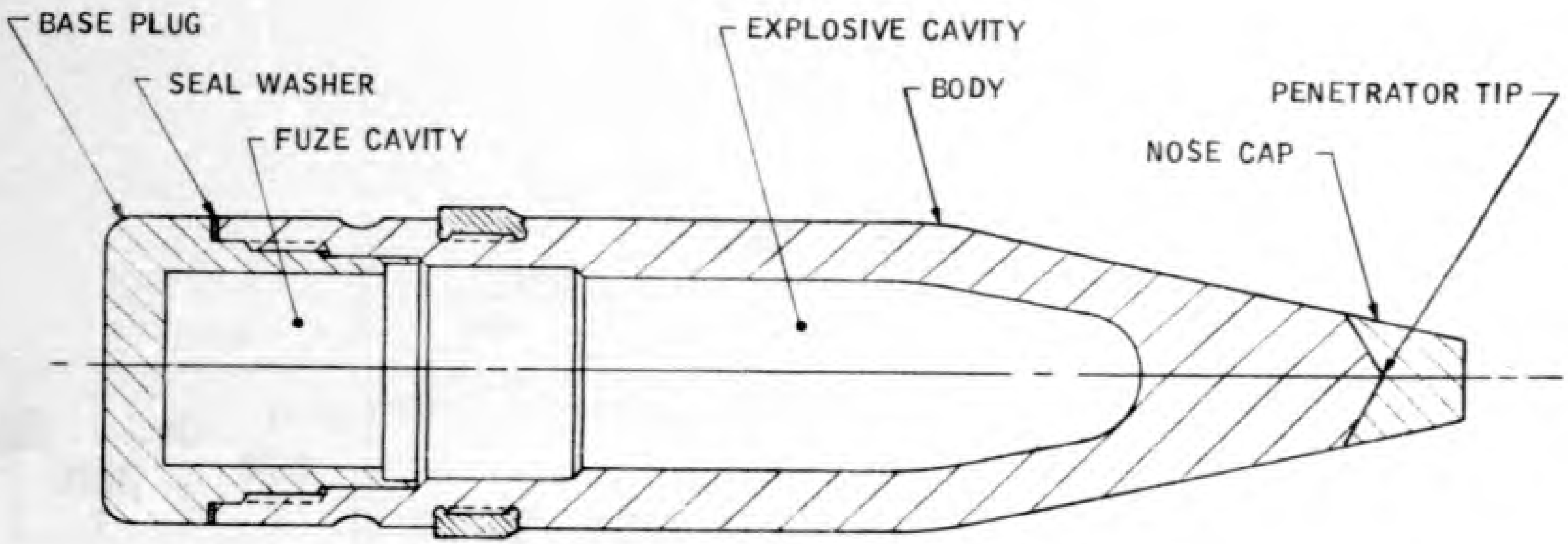

Figure 5. SAPHE Warhead

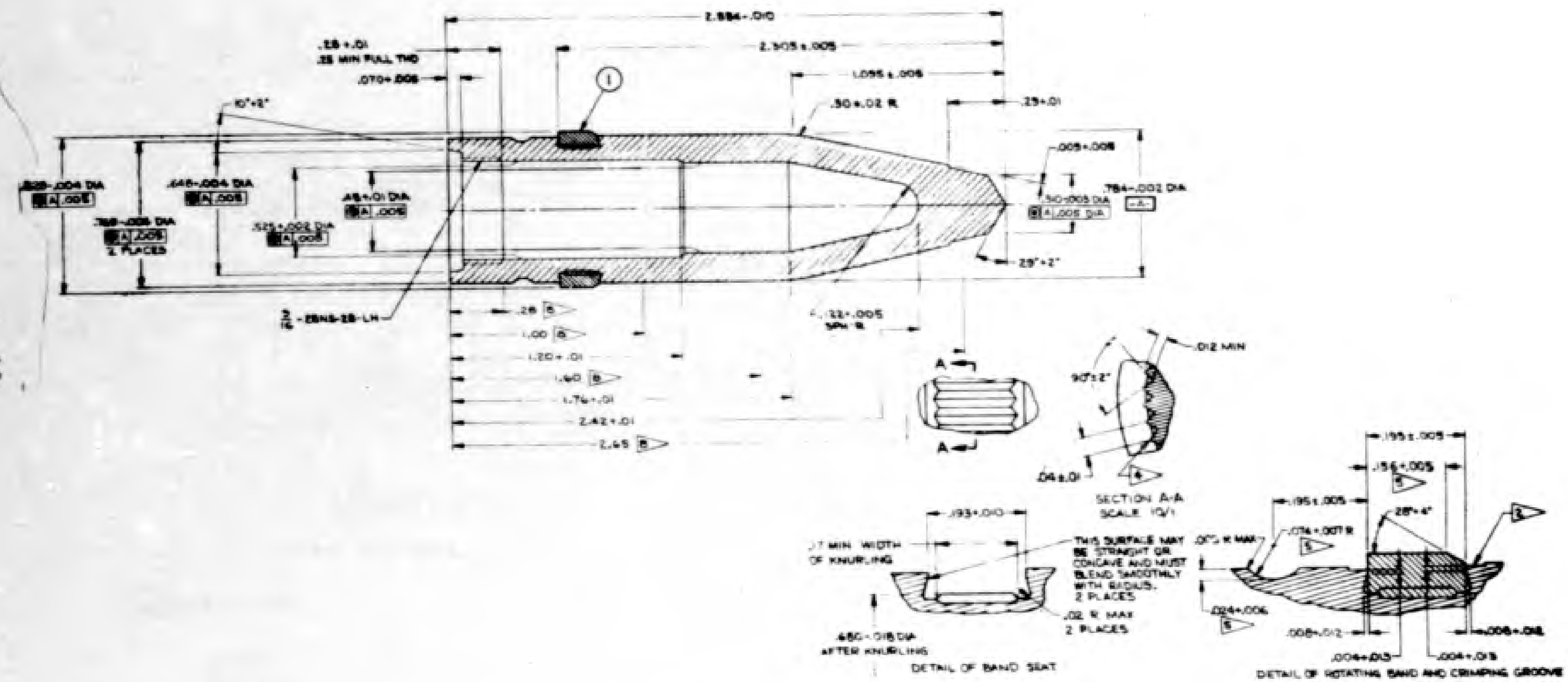

Figure 6. Body and Rotating Band Assembly, Drawing Number 28102098

The seal washer (Figure 7A) is a copper washer 0.020-inch thick compressed beyond its yield point when the base plug and body are screwed together. The seal washer must not leak under propellant pressures of 69,000 psi, and must remain in place in flight. Visual inspection of 16 rounds disassembled after gun firing indicates that there is no gas leakage and that the seal washer remains in place under centrifugal force. The seal washer was also used on all SAPHE propellant proof rounds (300 were fired) with no evidence of gas leakage.

An alternate seal configuration (Figure 7B) was tested for use with the thick wall projectile body and base plug. This configuration permits the base plug to sit directly on the body so that some load can be transferred through the body-to-base-plug interface. In 120 rounds with the alternate seal configuration there were no signs of gas leakage.

However, since the thin wall section in the present body design does not accommodate this seal, and the thick wall section of the present base plug does not require the improved load carrying feature of the alternate seal, this design was not pursued further.

The base plug must withstand barrel pressures and hold the fuze in place until it has functioned on the target. The base plug has never yielded in the barrel but pulls free on armor penetration. The breakage is of no consequence since the fuze will function before the base plug breaks free.

1. Stress Analysis

a. Body

The stresses on the body at points shown in Figure 8 were analyzed by conventional warhead stress analysis procedures. For point 5 the projectile wall was treated as independent cylinders for determining axial stresses and as a one-piece cylinder of equivalent thickness for the hoop and radial stresses (Figure 9).

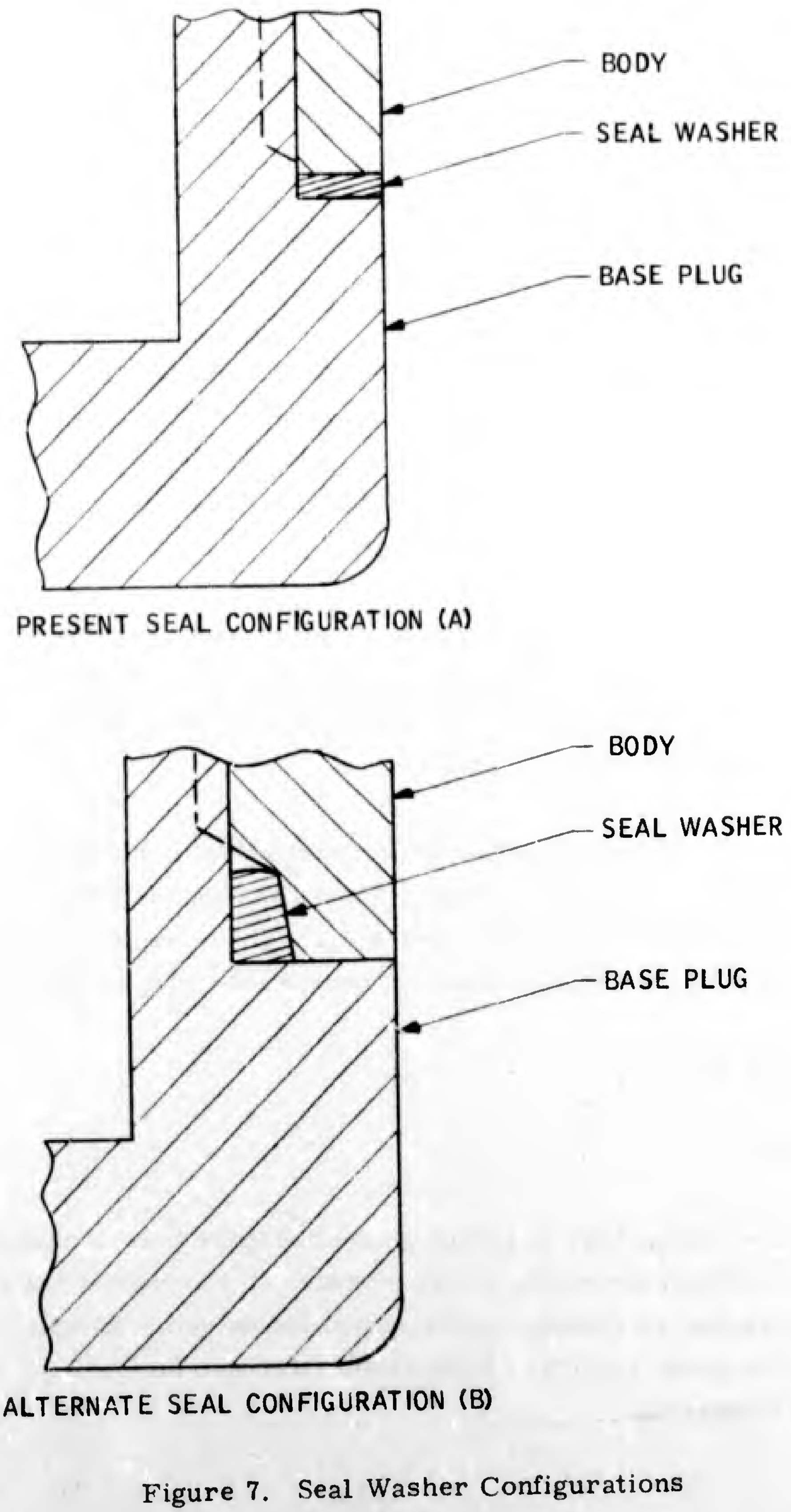

Figure 7. Seal Washer Configurations

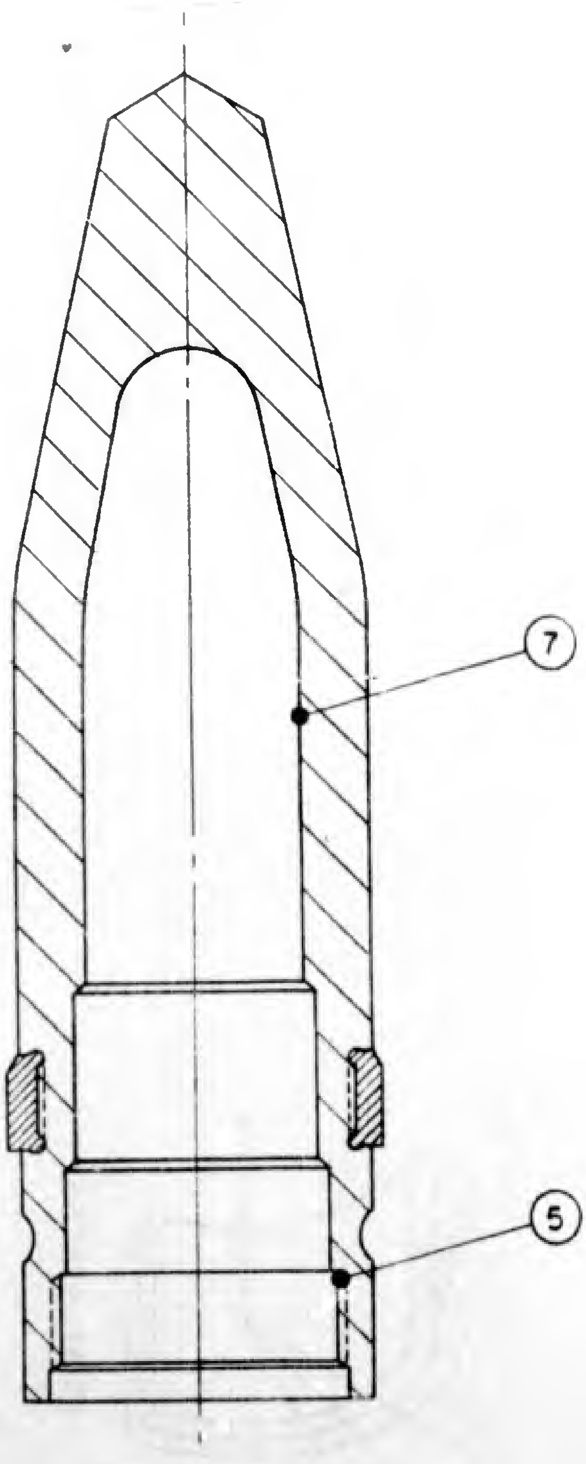

Figure 8. Body Stress Points

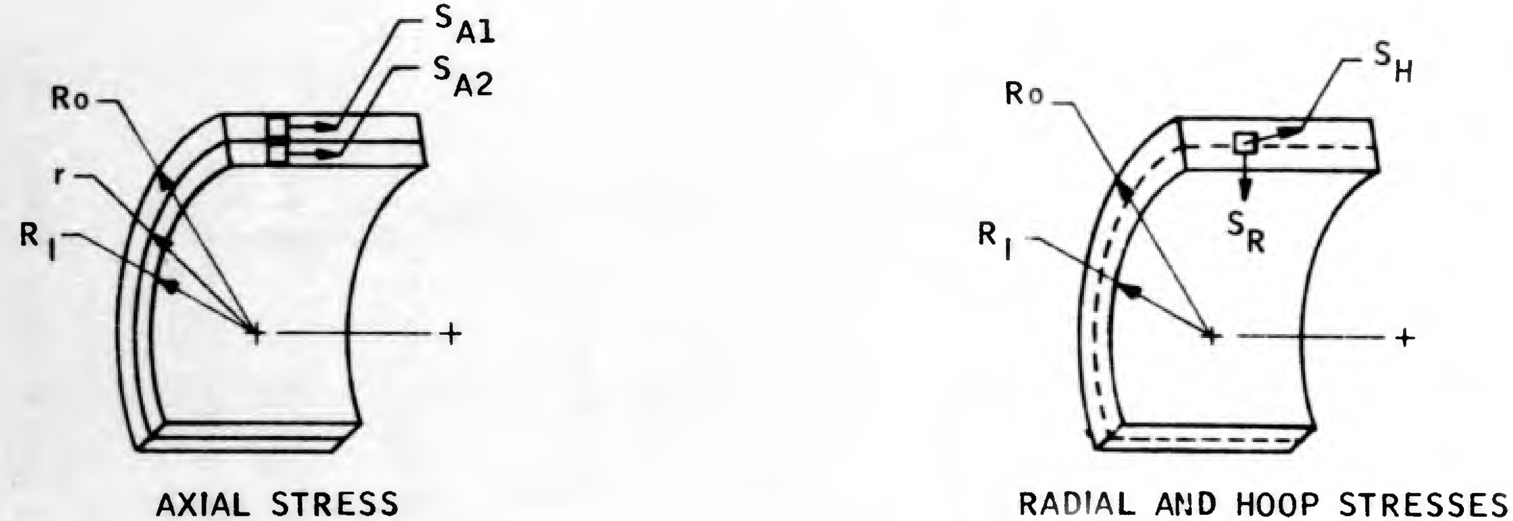

Figure 9. Concentric Cylinder Combination for Point 5 of Stress Analysis

The stresses calculated for velocity of 2,900 fps, pressure of 69,000 psi, and acceleration of 114,000 g, were as follows:

a. Combined stress through threaded section (Pt 5) = 123.2 kpsi

b. Combined stress in wall at rear of explosive cavity (Pt 7) = 65.3 kpsi.

The stresses are less than the yield stress of the 1045 steel body materials (165 kpsi). Failure is not indicated and gun firings of 17 rounds at more than 69,000-psi chamber pressure without a wall failure verify this.

Bodies with thicker wall sections in the base end were designed to reduce the loads on the base plug. When tests proved that the present base plug was adequate, the development of the thick-walled body was discontinued.

b. Base Plug

The stresses on the critical points of the base plug (identified in Figure 10) were also analyzed by conventional stress analysis procedures. The same concentric cylinder simplification used in the body stress analysis was used at points 3 and 6.

Stresses were calculated for the same conditions used for the body with the following results:

- Flexural stress at base center (Pt 1) = 191.7 kpsi
- Shear stress on base edge (Pt 2) = 200.7 kpsi
- Combined stress on fuze wall near cavity bottom (Pt 3) = 239.4 kpsi
- Shear stress on threads (Pt 4) = 97.3 kpsi
- Combined stress on fuze wall near cavity tap (Pt 6) = 209.2 kpsi

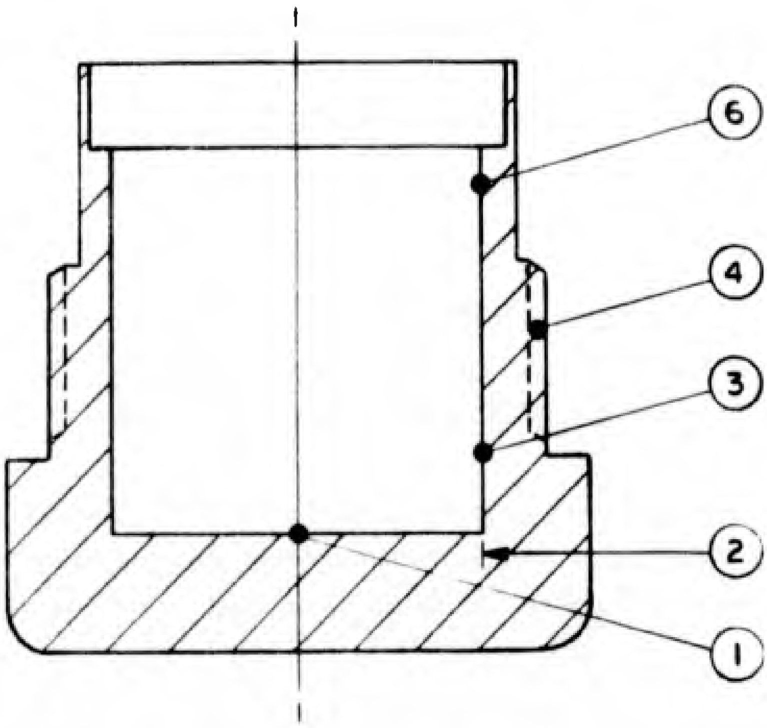

Figure 10. Base Plug Stress Points

The greatest calculated stress of 239.4 kpsi is in excess of the 185.0 kpsi value of the minimum yield strength of 17-4 PH steel; thus, yielding of the base is indicated. However, the calculated values assume that maximum pressure and maximum velocity occur simultaneously which is not true. Therefore, the yield strength of the material is greater than indicated for dynamic conditions and the stress level and material strength approach equality.

The wall strength was tested at 60,000 psi in the gun firings of about 300 projectiles with no failures. Failure was not indicated in gun firings of 17 rounds at more than 69,000 psi chamber pressure.

During armor penetration, the base plug is often broken from the projectile after penetration. Flash X-rays and recovered parts indicate that the failure does not occur until the base plug has entered the armor. The fuze would have functioned before the base plug has separated, so the base plug breakaway is of little consequence.

A parallel effort was conducted to develop a stronger base plug that would mate with a strengthened projectile body. This base plug was designed, and tests proved it satisfactory; but the cavity remaining for the fuze was minimal, and successful tests of the present design proved the stronger-walled version was not necessary.

2. Penetration and Survival

The body must be able to penetrate a target and remain intact (survive) after impact for the explosive and fragmentation to be most effective. To achieve these goals, two tip configurations, three materials, and two heat treatments were investigated.

The final tip design has a 120-degree conical nose configuration which is frequently used on penetrators. Tests indicate that penetration on graze angles is adequate (see Table I).

TABLE I. PENETRATION CAPABILITY OF SAPHE ROUND WITH 120-DEGREE CONICAL TIP

Target	Impact Angle (Degrees)	Minimum Penetration Velocity (Fps)
1/4 in. 425 BHN RHA	0	1, 500
1/4 in. 425 BHN RHA	45	2, 000
1/4 in. 425 BHN RHA	60	2, 200
3/8 in. 425 BHN RHA	0	2, 170
3/8 in. 425 BHN RHA	30	2, 290
1/2 in. 425 BHN RHA	0	2, 860

The body did not survive all of the penetrations. An alternate tip was designed that would eliminate the nose cap and, instead, extend the body tip to replace it (Figure 11). Bodies of this type have survived impact on 1/4-inch 425 BHN armor at 0 degree of obliquity at velocities as high as 2,780 fps (Figure 12) compared with the maximum survival velocity of 2,150 fps for the initial design. The maximum survival velocity for the alternate tip was not determined; it has not been tested at velocities over 2,780 fps at 0 degrees obliquity. Bodies with the alternate tip were also tested against 1/4-inch 425 BHN armor at 60 degrees of obliquity; the minimum velocity tested (2,315 fps) partially penetrated the armor (Figure 13). At this velocity the conical tipped body also penetrates only partially, but a greater portion of the projectile penetrates. Projectiles with the alternate tip left 3/4- to 1-inch-long slip grooves on the armor before penetrating, indicating poor penetration characteristics for this design on graze angles.

For maximum effectiveness the body must remain intact (survive) on target impact. The goal for penetration with survival was 3/8-inch 400-450 BHN armor at 45-degree angle of obliquity; this has not been achieved. Table II contains the survival characteristics of the present conical tip configuration.

TABLE II. SURVIVAL TEST RESULTS FOR UNCAPPED PROJECTILES

Target	Maximum Velocity for No Failure, (Fps)	Maximum Velocity for Tip Only Failure, (Fps)
1/4 x 0° 425 BHN	2,150	2,540
1/4 x 45° 425 BHN	1,990	2,280
1/4 x 60° 425 BHN	No Survival	No Survival
3/8 x 0° 425 BHN	No Survival	No Survival
3/8 x 30° 425 BHN	No Survival	No Survival

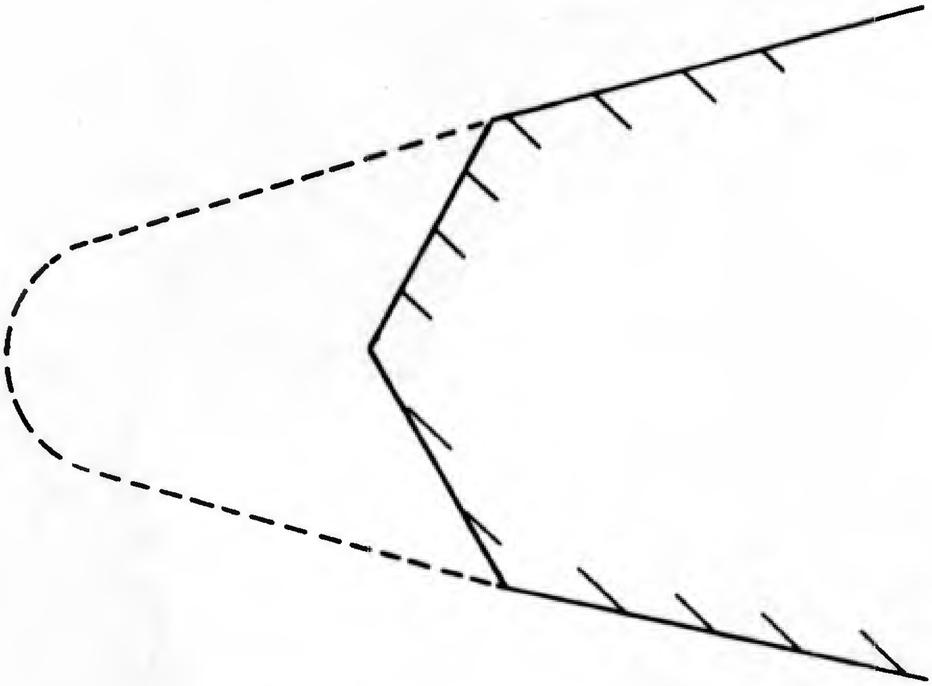

120-DEGREE CONICAL TIP

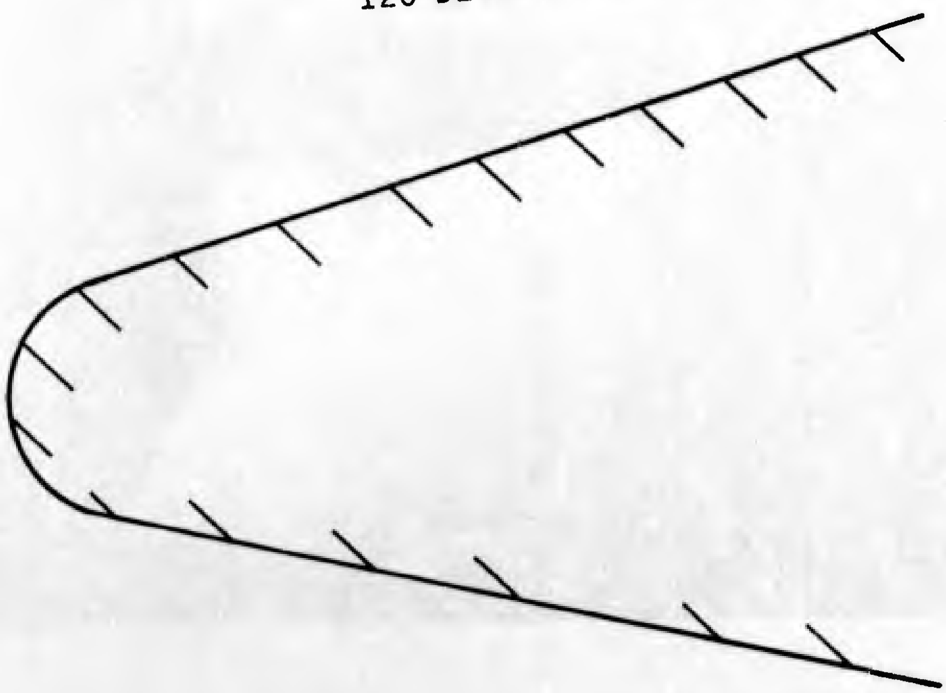

Figure 11. Alternate Nose Tip

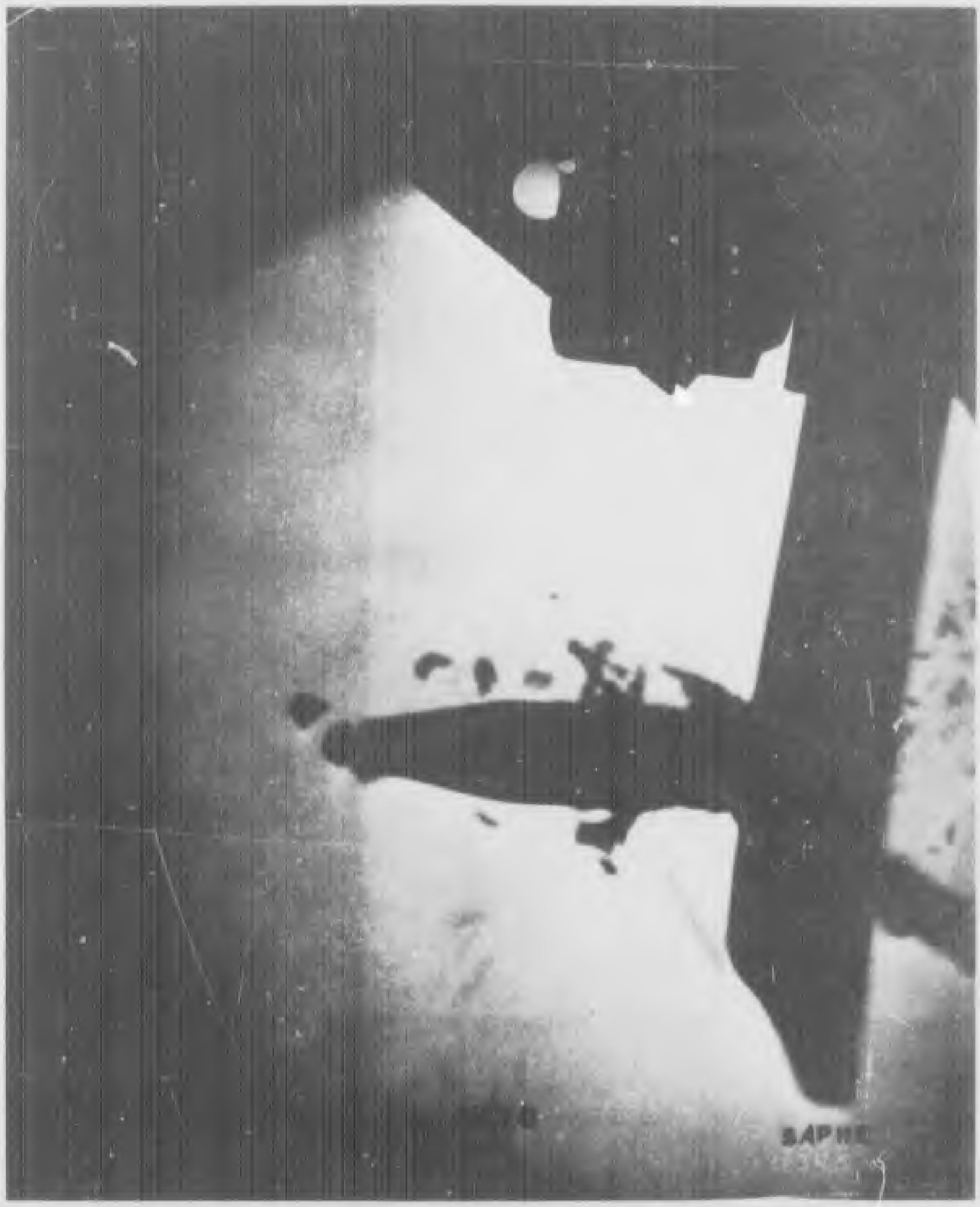

Figure 12. Material 4340, Solid Nose, 0 Degree, 1/4 Inch

Figure 13. Material 1045, 60 Degrees, 1/4 Inch

In this table, a Tip Only failure is one in which the explosive cavity is opened in the forward end due to the loss of the projectile tip; this leaves a 0.250-inch diameter opening at the front of the cavity. A Tip Only failure may reduce the explosive effectiveness of the projectile, but some fragmentation of the body should occur.

Tests were also conducted to determine whether a round that penetrates without survival will retain any effectiveness from brisance and incendiary effects resulting from deflagration of the High Explosive (HE).

The AISI 1045 steel was selected for the final body configuration as a result of penetration testing comparing it with 4340 and 52100 steels. The 4340 steel was selected for its toughness, the 52100 steel for its high strength and fragmentation characteristics. The 1045 steel has the toughness of the 4340, with better forging properties for production purposes. The tests showed that 1045 and 4340 steels behave similarly; the 52100 steel shatters on impact (Figures 14 through 20).

All penetration testing was done on differentially heat-treated rounds with hardnesses of RC 38-45 at the base end and a hardness at the tip end of RC 52 to 58 for the 1045 and 4340 steels and RC 57 to 62 for the 52100 steel. Austempered bodies were also tested, but broke up on impact.

Two configuration changes were made from the initial design to improve the survivability of the body. First the explosive cavity was moved back 0.17 inch (Figure 21) and the rotating band seat was changed to increase the body wall thickness which reduced residual stresses from knurling (Figure 22). From limited testing further explosives cavity changes gave only a modest improvement in survivability (Figure 23).

To determine the feasibility of producing a body that would not bend under the rotating band, test rounds with a 0.480-inch-diameter bore under the rotating band were built for testing. This diameter was chosen as a practical

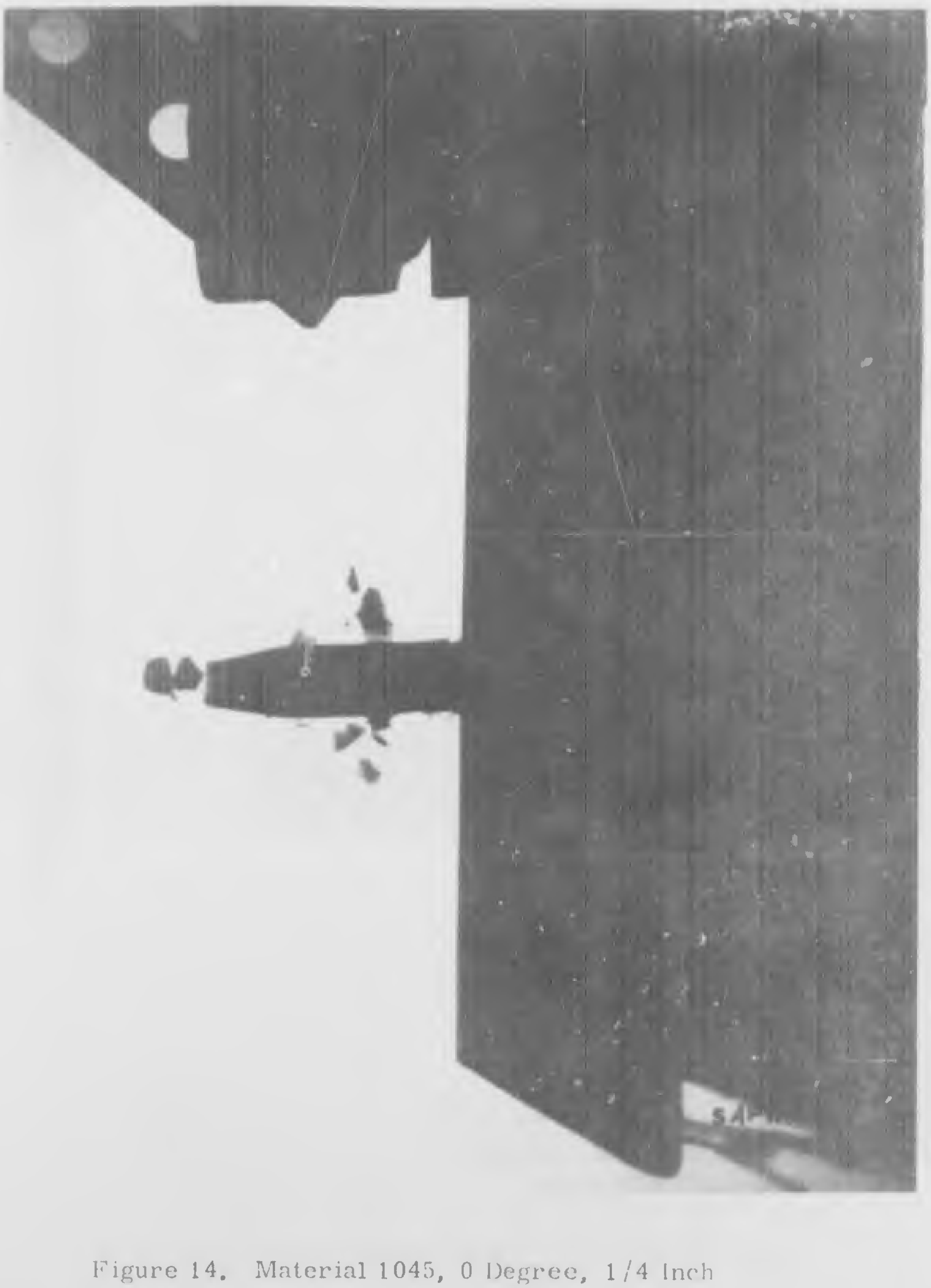

Figure 14. Material 1045, 0 Degree, 1/4 Inch

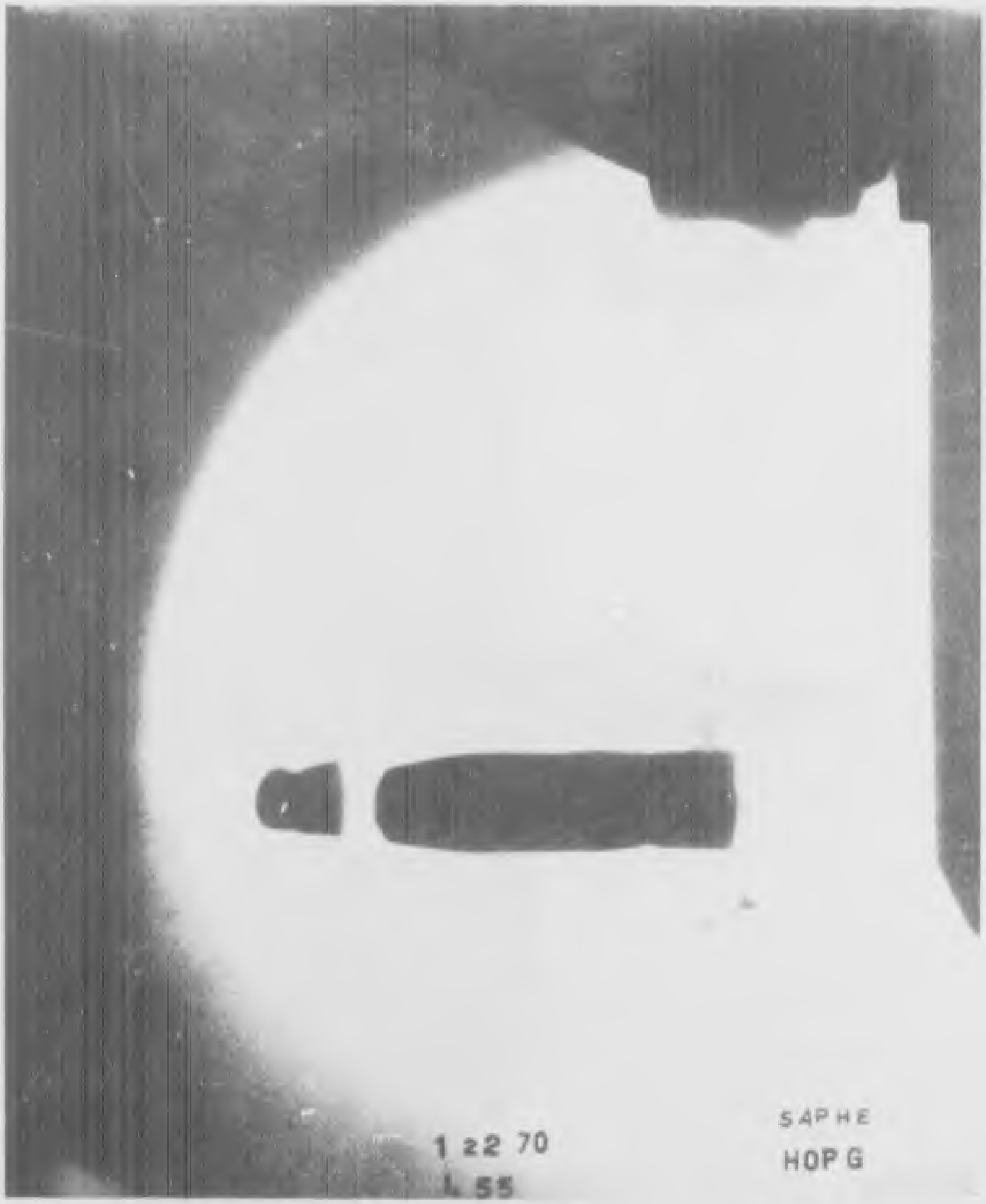

Figure 15. Material 4340, 0 Degree, 1/4 Inch

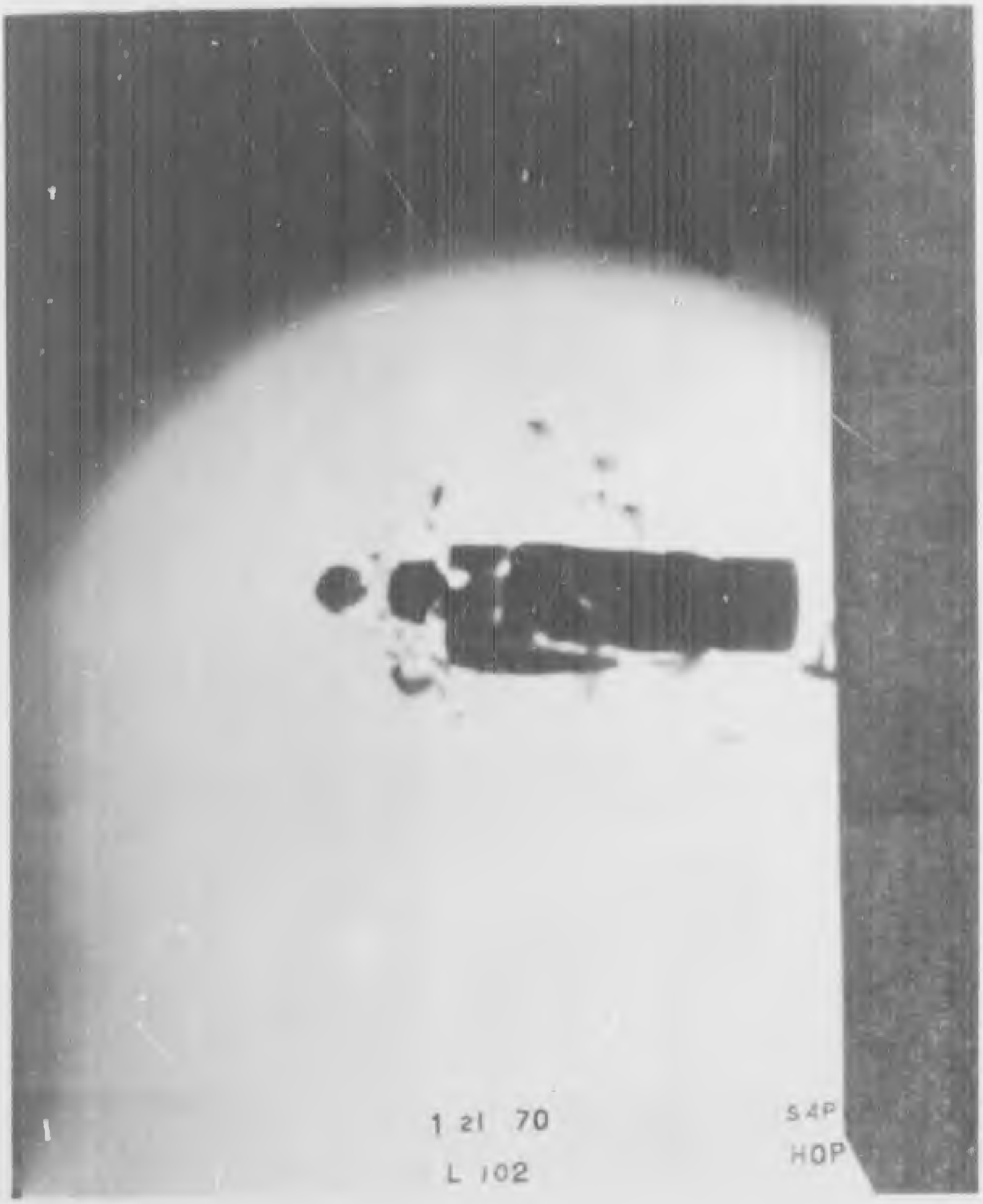

Figure 16. Material 52100, 0 Degree, 1/4 Inch

Figure 17. Material 1045, 30 Degrees, 3/8 Inch

Figure 18. Mate.ial 4340, 30 Degrees, 3/8 Inch

Figure 19. Material 52100, 30 Degrees, 3/8 Inch

Figure 20. Material 4340, Solid Nose, 30 Degrees, 3/8 Inch

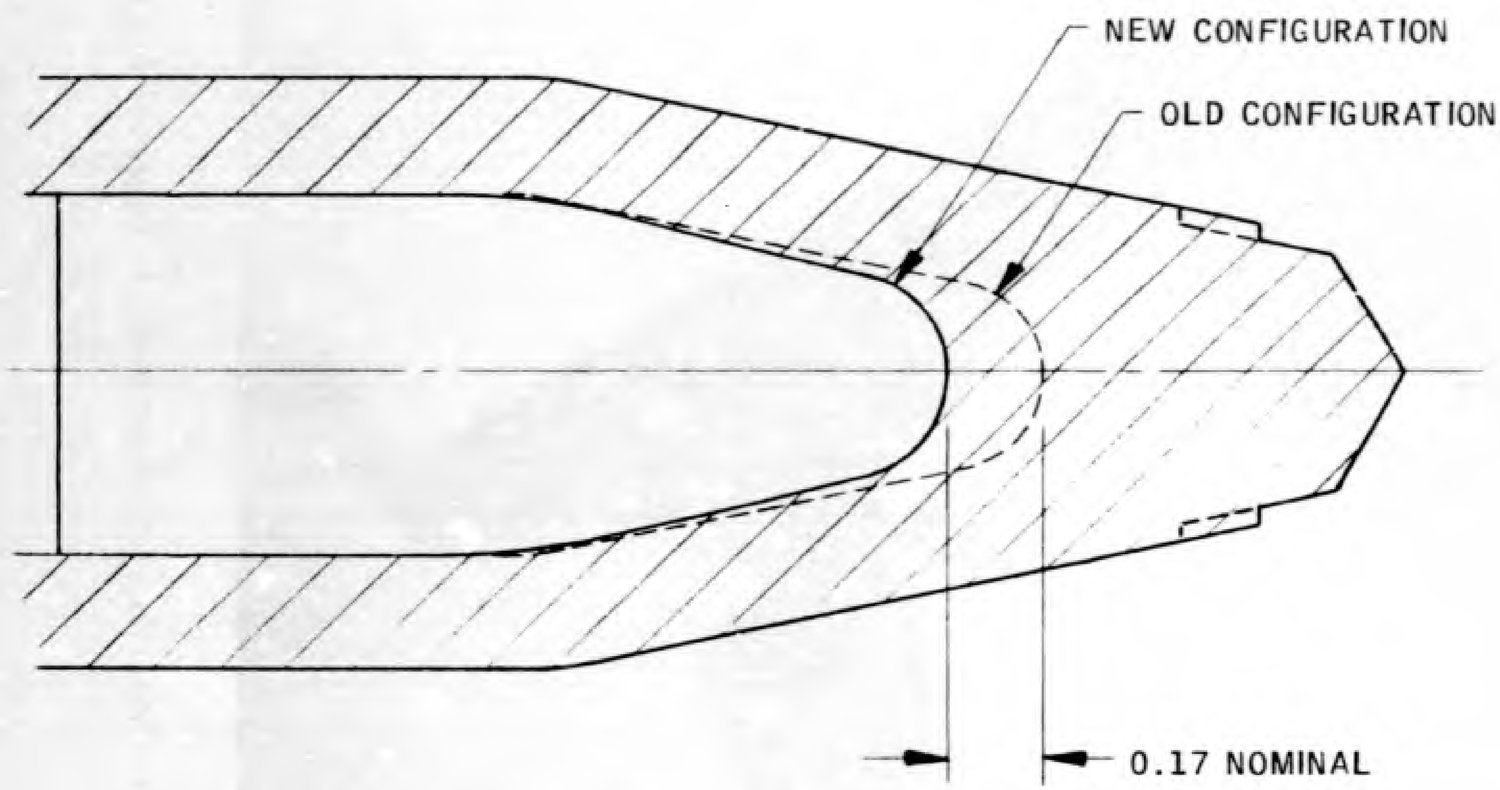

Figure 21. HE Cavity Detail

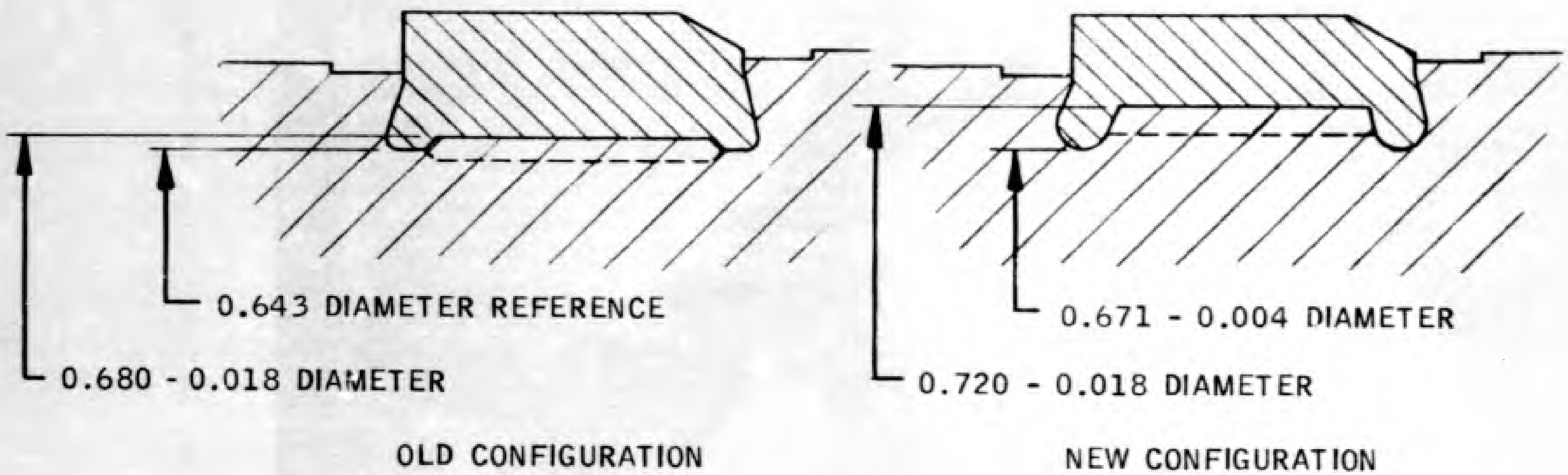

Figure 22. Rotating Band Detail

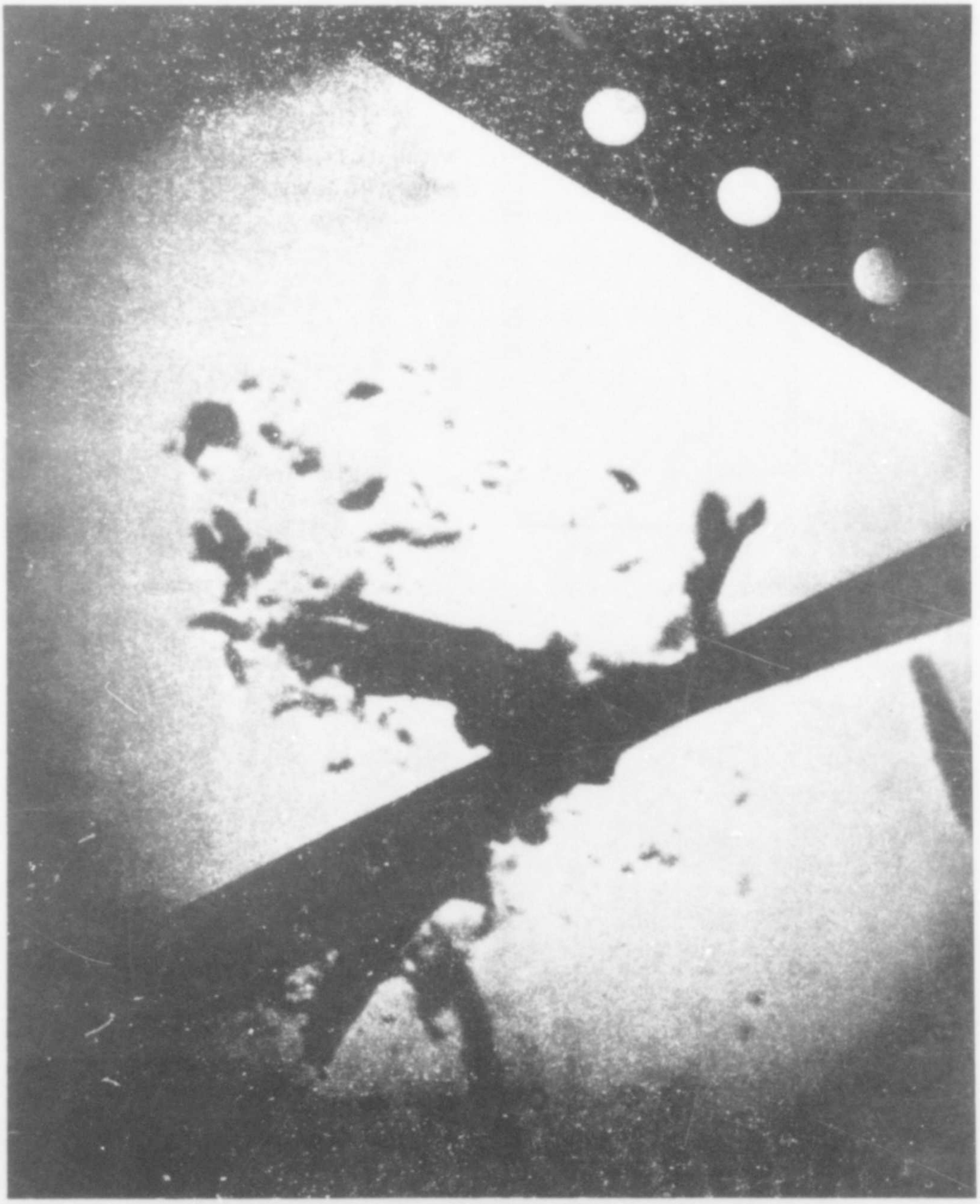

Figure 23. Material 4340, Revised Cavity, 60 Degrees, 1/4 Inch

limit beyond which the explosive cavity could not be loaded and the fuze parts could not fit. Seven such rounds were gun-fired and showed no evidence of bending on impact, but the design required too many compromises in the fuze and was discontinued. Bending is of no significance if it occurs after the detonator has functioned, and slight bending can be tolerated before detonator function. It appears from flash X-rays that bending occurs as the base passes through the armor, except at graze angles greater than 45 degrees, and generally would occur after the detonator had functioned.

Results of the survival tests and HE-loaded-round tests are given in Tables III through VII. Test projectile variables are shown in Figure 24.

It was concluded that the 28102684-001 projectile body (Figure 25) has the best combination of survivability and HE capacity of all the bodies tested. The 28103016-001 body (Figure 26) has better survival characteristics, but the HE capacity of this design is unacceptably low.

The penetration data for the loaded projectiles show that penetration is achieved under conditions which defeat the inert projectiles.

3. Computer Analysis

A study of the impact dynamics of the SAPHE projectile on armor was conducted using a two-dimensional, elastic, Lagrangean, computer, code called the HEMP code. The code was run for 1/2-inch armor of 350 BHN with an impact velocity of 2, 850 fps for three different projectiles:

1. 1045 steel, original explosive cavity (Figure 27).
2. 52100 steel, original explosive cavity (Figure 28).
3. 1045 steel, revised explosive cavity (Figure 29).

TABLE III. SURVIVAL TEST RESULTS, 28102684-001 PROJECTILE BODY

IMPACT CONDITIONS			RESULTS		COMMENTS	OTHER DATA								
TARGET THICKNESS (INCHES)	TARGET ANGLE (DEGREES)	VELOCITY (fps)	PENETRATE TARGET	SURVIVE		SERIAL NUMBER	PROPELLANT	PROPELLANT QUANTITY (GRAMS)	PROJECTILE SHOWN ON X-RAY	PROJECTILE RECOVERED	TARGET PLATE HOLE DIMENSIONS (INCHES)	WITNESS PANEL HOLE DIMENSIONS (INCHES)	FILLER ON TARGET	FILLER ON WITNESS PANEL
0.25	0	---	YES	YES	CONICAL TIP BREAKAGE, YIELDING, NO FILLER LEAKS.	311	WC 870	34.60	NO	YES	0.80 X 0.87	1.55 X 0.80	---	---
0.25	0	3,010				312	WC 870	34.60	YES	YES	0.77 X 0.80	1.10 X 0.80	---	---
0.25	45	---	YES	YES	PROJECTILE GRAZED STAND (NO TEST).	40	WC 870	34.60	YES	NO	1.23 X 0.77	1.90 X 0.75	NO	YES
0.25	45	2,980	YES	YES	YIELDING.	41	WC 870	34.60	YES	NO	1.20 X 0.75	2.30 X 0.80	NO	NO
0.25	45	2,800	YES	---		42	WC 870	32.15	NO	NO	1.20 X 0.80	1.40 X 0.80	NO	NO
0.25	45	---	YES	YES	TIP EROSION, MINOR YIELDING.	43	WC 870	32.15	YES	NO	1.25 X 0.77	2.69 X 0.75	NO	NO
0.25	45	---	YES	YES	TIP CRACKS, YIELDING, SOME FILLER LEAKAGE.	305	WC 870	29.55	YES	YES	1.38 X 0.75	1.90 X 0.80	NO	NO
0.25	45	2,675	YES	YES	TIP EROSION, MINOR YIELDING.	306	WC 870	29.55	YES	NO	1.32 X 0.78	2.10 X 0.80	NO	YES
0.25	45	2,440	YES	YES	TIP CRACKS, YIELDING.	318	WC 870	25.05	YES	NO	1.14 X 0.75	2.85 X 0.85	NO	YES
0.25	45	2,420	YES	YES	YIELDING, SOME FILLER LEAKAGE.	317	WC 870	25.05	NO	YES	1.30 X 0.80	2.10 X 0.77	NO	NO
0.25	60	2,335	YES	NO	BODY SPLIT AXIALLY.	319	WC 870	25.05	YES	NO	1.70 X 0.50	2.70 X 2.60	YES	YES
0.25	60	---	YES	NO	BODY SPLIT AXIALLY.	320	WC 870	25.05	YES	NO	2.20 X 1.00	2.50 X 3.50	YES	YES
0.25	60	2,223	YES	NO	BODY SPLIT AXIALLY.	315	WC 870	23.00	YES	YES	1.45 X 0.70	2.20 X 0.40	YES	YES
0.25	60	2,130	YES	NO	BODY SPLIT AXIALLY.	316	WC 870	23.00	YES	YES	1.30 X 0.70	1.60 X 0.90	YES	YES
0.25	60	1,926	NO	YES	BENDING ONLY, GRAZED TARGET.	314	WC 870	20.00	YES	YES	2.95 X 1.00	0.75 X 0.75	YES	YES
0.25	60	---	NO	YES	GRAZEL TARGET.	313	WC 870	20.00	YES	YES	3.30 X 0.86	3.00 X 0.90	NO	YES

TABLE IV. SURVIVAL TEST RESULTS, 28103016-001 PROJECTILE BODY

IMPACT CONDITIONS			RESULTS		COMMENTS	OTHER DATA								
TARGET THICKNESS (INCHES)	TARGET ANGLE (DEGREES)	VELOCITY (fps)	PENETRATE TARGET	SURVIVE		SERIAL NUMBER	PROPELLANT	PROPELLANT QUANTITY (GRAMS)	PROJECTILE SHOWN ON X-RAY	PROJECTILE RECOVERED	TARGET PLATE HOLE DIMENSIONS (INCHES)	WITNESS PANEL HOLE DIMENSIONS (INCHES)	FILLER ON TARGET	FILLER ON WITNESS PANEL
0.25	45	2,940	YES	YES	TIP EROSION.	362	WC 870	34.60	YES	NO	1.20 X 0.75	1.40 X 0.70	NO	NO
0.25	45	2,915	YES	YES	TIP EROSION, SLIGHT YIELDING.	361	WC 870	34.60	YES	NO	1.35 X 0.85	2.10 X 1.70	NO	NO
0.25	45	2,225	YES	---		363	WC 870	32.15	NO	NO	1.21 X 0.76	2.15 X 0.80	NO	NO
0.25	45	---	YES	YES	YIELDING	364	WC 870	32.15	YES	YES	1.25 X 0.80	2.75 X 0.75	NO	NO
0.25	60	2,375	YES	YES		367	WC 870	29.55	---	YES	1.30 X 0.95	1.80 X 1.70	NO	YES
0.25	60	2,312	YES	YES	TIP EROSION, SLIGHT LEAKAGE.	368	WC 870	29.55	YES	YES	1.25 X 0.75	2.90 X 0.80	NO	NO
0.25	60	2,240	YES	YES	SEVERE TIP EROSION.	369	WC 870	25.05	YES	YES	1.60 X 0.76	2.55 X 0.75	NO	NO
0.25	60	2,230	YES	YES	TIP EROSION.	370	WC 870	25.05	YES	YES	2.20 X 0.72	1.70 X 0.80	NO	NO
0.25	60	1,936	YES	YES	TIP EROSION.	365	WC 870	23.00	YES	NO	1.20 X 0.80	1.95 X 0.70	NO	YES
0.25	60	1,925	NO	YES		366	WC 870	23.00	YES	NO	2.95 X 0.70	1.20 X 0.75	NO	YES

TABLE V. SURVIVAL TEST RESULTS, 28103017-001 PROJECTILE BODY

IMPACT CONDITIONS			RESULTS		COMMENTS	OTHER DATA								
TARGET THICKNESS (INCHES)	TARGET ANGLE (DEGREES)	VELOCITY (fps)	PENETRATE TARGET	SURVIVE		SERIAL NUMBER	PROPELLANT	PROPELLANT QUANTITY (GRAMS)	PROJECTILE SHOWN ON X-RAY	PROJECTILE RECOVERED	TARGET PLATE HOLE DIMENSIONS (INCHES)	WITNESS PANEL HOLE DIMENSIONS (INCHES)	FILLER ON TARGET	FILLER ON WITNESS PANEL
0.25	0	3,000	YES	YES	SEVERE YIELDING, NO LEAKAGE.	331	WC 870	34.60	NO	YES	0.95 X 0.80	2.50 X 0.90	---	---
0.25	0	2,980	YES	YES	SLIGHT YIELDING.	332	WC 870	34.60	NO	YES	---	1.50 X 0.80	---	---
0.25	45	2,980	YES	YES	SEVERE YIELDING, NO LEAKAGE.	321	WC 870	34.60	NO	YES	1.34 X 0.83	2.60 X 0.80	NO	NO
0.25	45	2,980	YES	YES	TIP EROSION.	322	WC 870	34.60	YES	NO	1.32 X 0.75	2.85 X 0.80	NO	NO
0.25	45	2,840	YES	YES	YIELDING, SLIGHT FILLER LEAKAGE.	323	WC 870	32.15	YES	NO	1.32 X 0.80	3.00 X 0.80	NO	NO
0.25	45	2,840	YES	YES	YIELDING, SLIGHT FILLER LEAKAGE.	324	WC 870	32.15	YES	NO	1.34 X 0.76	3.60 X 0.80	NO	YES
0.25	45	2,730	YES	YES	YIELDING, SLIGHT FILLER LEAKAGE.	326	WC 870	29.55	YES	NO	1.34 X 0.80	2.90 X 0.80	---	---
0.25	60	2,360	YES	NO	SPLIT OPEN.	339	WC 870	25.05	YES	NO	2.70 X 0.66	4.00 X 1.80	YES	YES
0.25	60	2,325	YES	NO	SPLIT OPEN.	340	WC 870	25.05	YES	NO	2.50 X 0.80	2.60 X 3.00	YES	YES
0.25	60	2,235	YES	NO	SPLIT OPEN.	335	WC 870	23.00	YES	YES	1.60 X 0.70	5.10 X 3.30	YES	YES
0.25	60	2,158	NO	YES		336	WC 870	23.00	YES	NO	2.80 X 0.60	1.10 X 0.75	NO	YES
0.25	60	1,956	NO	---		333	WC 870	20.00	YES	NO	2.50 X 0.85	1.75 X 1.30	NO	YES
0.25	60	1,910	YES	YES		334	WC 870	20.00	YES	NO	1.50 X 0.80	3.50 X 0.75	YES	NO

TABLE VI. SURVIVAL TEST RESULTS, 28103017-002 PROJECTILE BODY

IMPACT CONDITIONS			RESULTS		COMMENTS	OTHER DATA								
TARGET THICKNESS (INCHES)	TARGET ANGLE (DEGREES)	VELOCITY (fps)	PENETRATE TARGET	SURVIVE		SERIAL NUMBER	PROPELLANT	PROPELLANT QUANTITY (GRAMS)	PROJECTILE SHOWN ON X-RAY	PROJECTILE RECOVERED	TARGET PLATE HOLE DIMENSIONS (INCHES)	WITNESS PANEL HOLE DIMENSIONS (INCHES)	FILLER ON TARGET ✦	FILLER ON WITNESS PANEL
0.25	0	3,000	YES	YES	NOSE YIELDING.	351	WC 870	34.60	NO	NO	0.82 X 0.82	0.95 X 0.75	YES	YES
0.25	0	2,980	YES	YES	MINOR YIELDING.	352	WC 870	34.60	NO	NO	0.80 X 0.80	0.90 X 0.75	YES	YES
0.25	45	3,000	YES	YES	MINOR YIELDING.	342	WC 870	34.60	YES	NO	1.26 X 0.80	2.60 X 0.80	NO	NO
0.25	45	2,970	YES	YES	MINOR YIELDING, CRACK ON TIP.	341	WC 870	34.60	YES	NO	1.20 X 0.75	2.35 X 0.80	NO	YES
0.25	45	2,900	YES	YES	CRACK ON TIP.	343	WC 870	32.15	YES	NO	1.25 X 0.75	2.50 X 0.80	NO	YES
0.25	45	2,860	YES	NO	SPLIT OPEN.	344	WC 870	32.15	YES	YES	1.35 X 0.73	2.75 X 0.72	NO	YES
0.25	45	---	YES	NO	SPLIT OPEN.	345	WC 870	29.55	YES	YES	1.30 X 0.80	2.55 X 0.80	NO	YES
0.25	45	2,440	YES	YES	SEVERE YIELDING, NO FILLER LEAKAGE.	348	WC 870	25.05	YES	YES	1.84 X 0.77	2.95 X 0.74	NO	NO
0.25	60	2,440	YES	NO	SPLIT OPEN.	359	WC 870	25.05	YES	NO	2.00 X 1.15	3.50 X 3.40	YES	YES
0.25	60	2,430	YES	NO	SPLIT OPEN.	360	WC 870	25.05	YES	NO	0.85 X 1.15	3.40 X 2.80	YES	YES
0.25	60	2,010	NO	YES;		350	WC 870	23.0	YES	NO	1.05 X 0.37	3.50 X 1.06	NO	YES
0.25	60	1,971	NO	---		353	WC 870	23.0	NO	NO	2.70 X 0.95	1.25 X 0.75	NO	YES
0.25	60	1,957	NO	YES	BENDING AND TIP EROSION.	349	WC 870	20.0	NO	YES	2.85 X 0.45	3.75 X 1.10	NO	NO
0.25	60	1,913	NO	YES	BENDING AND TIP EROSION.	354	WC 870	20.0	YES	YES	2.60 X 0.80	1.25 X 0.75	NO	YES

TABLE VII. PENETRATION DATA, 28102684-001 PROJECTILE BODY (HE LOADED)

TARGET THICKNESS (INCH)	TARGET ANGLE (DEGREES)	VELOCITY (FPS)	PENETRATE	SERIAL NUMBER
0.50	30	2,920	YES	1071
0.50	30	2,740	YES	1072
0.50	45	2,920	YES	1070
0.50	45	2,730	YES	1069
0.50	45	2,730	YES	1068
0.25	45	1,305	YES	1095
0.25	45	1,300	YES	1094
0.25	45	1,295	YES	1093
0.25	45	1,235	YES	1091
0.25	45	1,225	YES	1092
0.25	45	1,195	YES	1097
0.25	45	1,155	YES	1096
0.25	60	2,970	YES	1014
0.25	60	2,960	YES	1022
0.25	60	2,950	YES	1017
0.25	60	2,940	YES	1020
0.25	60	2,930	YES	1015
0.25	60	2,930	YES	1018
0.25	60	2,910	YES	1021
0.25	60	2,900	YES	1019
0.25	60	1,235	YES	1088
0.25	80	2,930	NO	1280
0.25	80	2,922	NO	1277
0.25	80	2,912	NO	1279
0.25	80	2,907	NO	1278
0.25	80	2,903	NO	1281
0.25	80	2,899	NO	1276
0.25	80	2,892	NO	1282

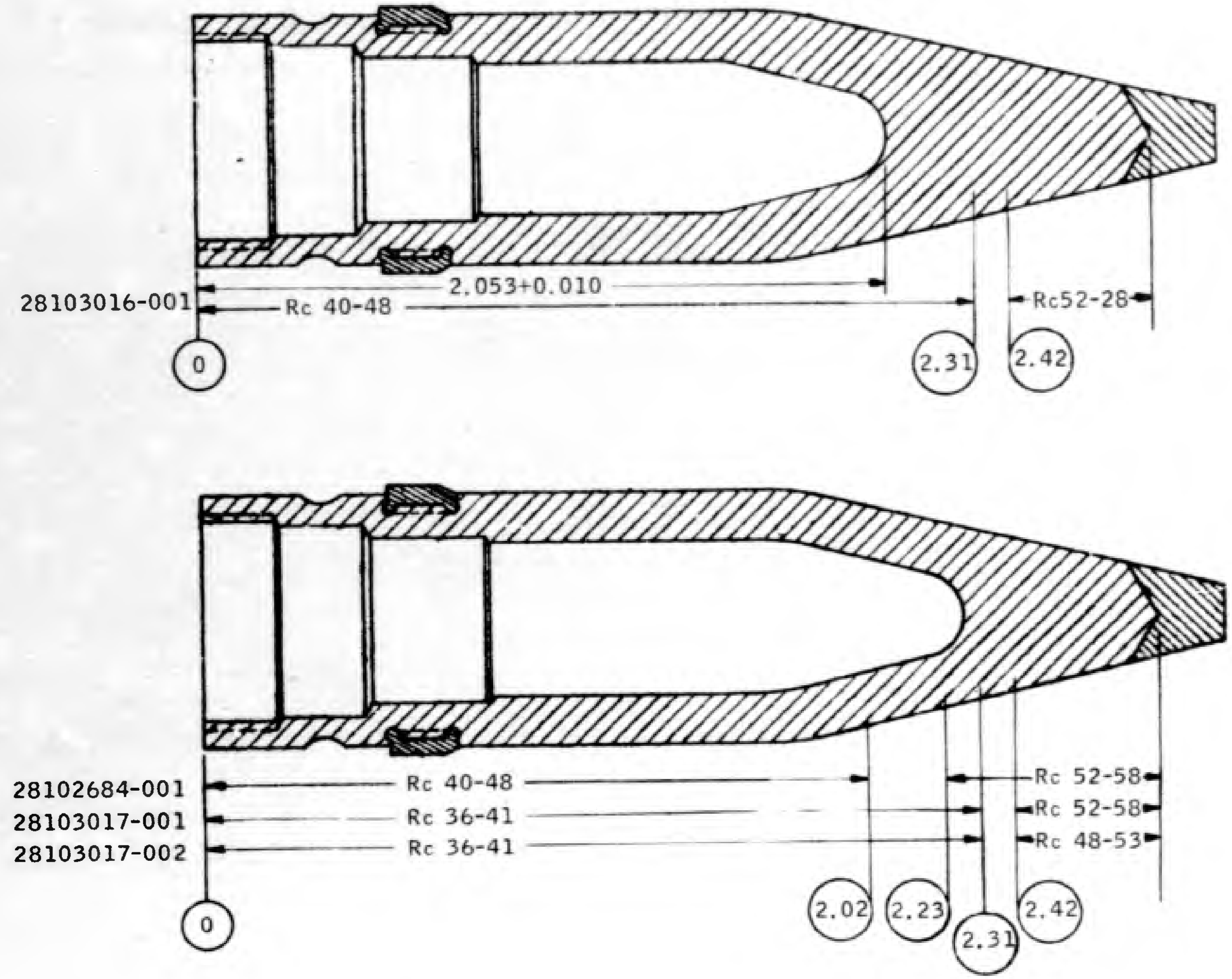

Figure 24. Test Projectile Variables

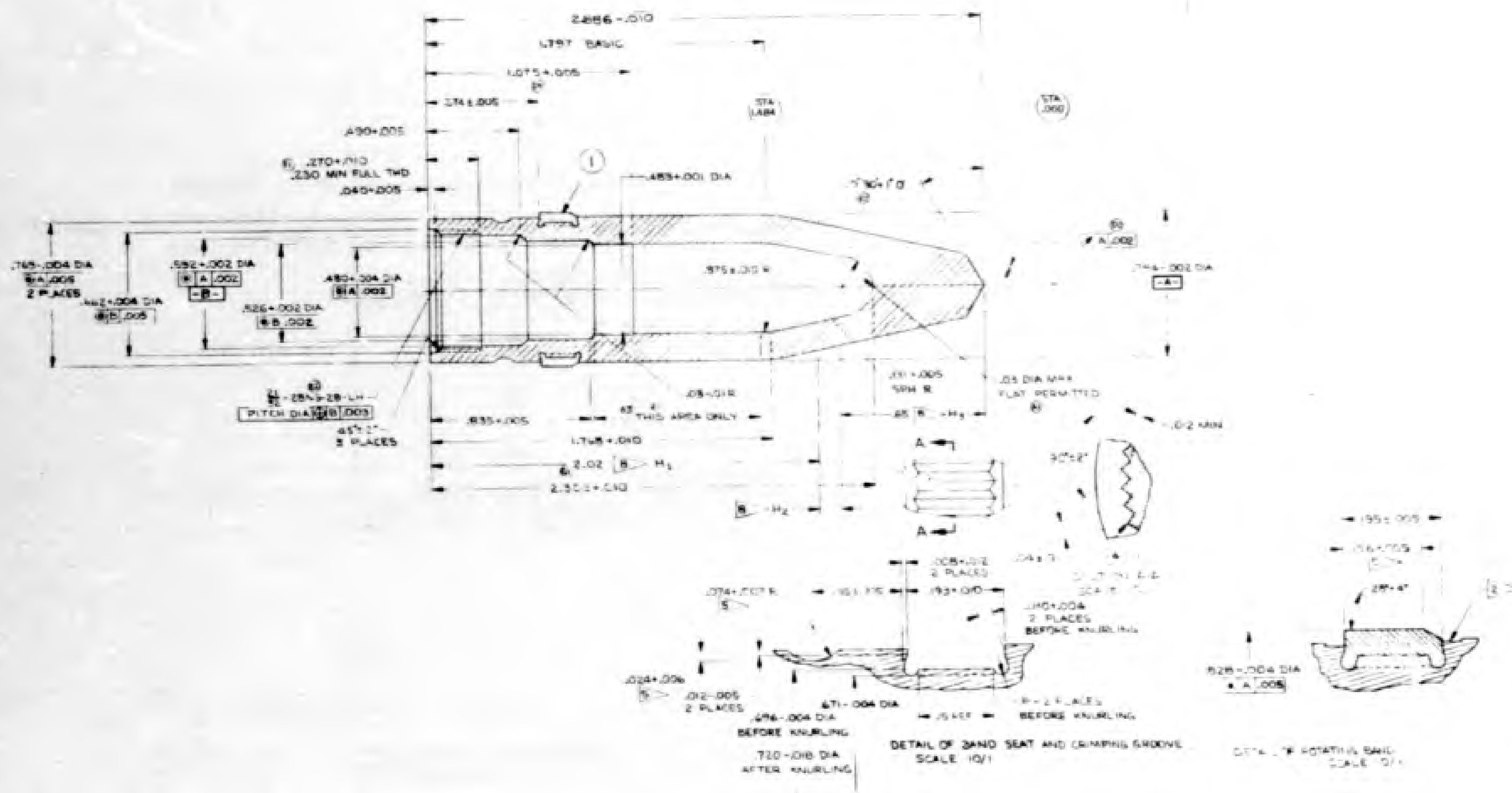

Figure 25. Body and Rotating Band Assembly, Drawing Number 28102684

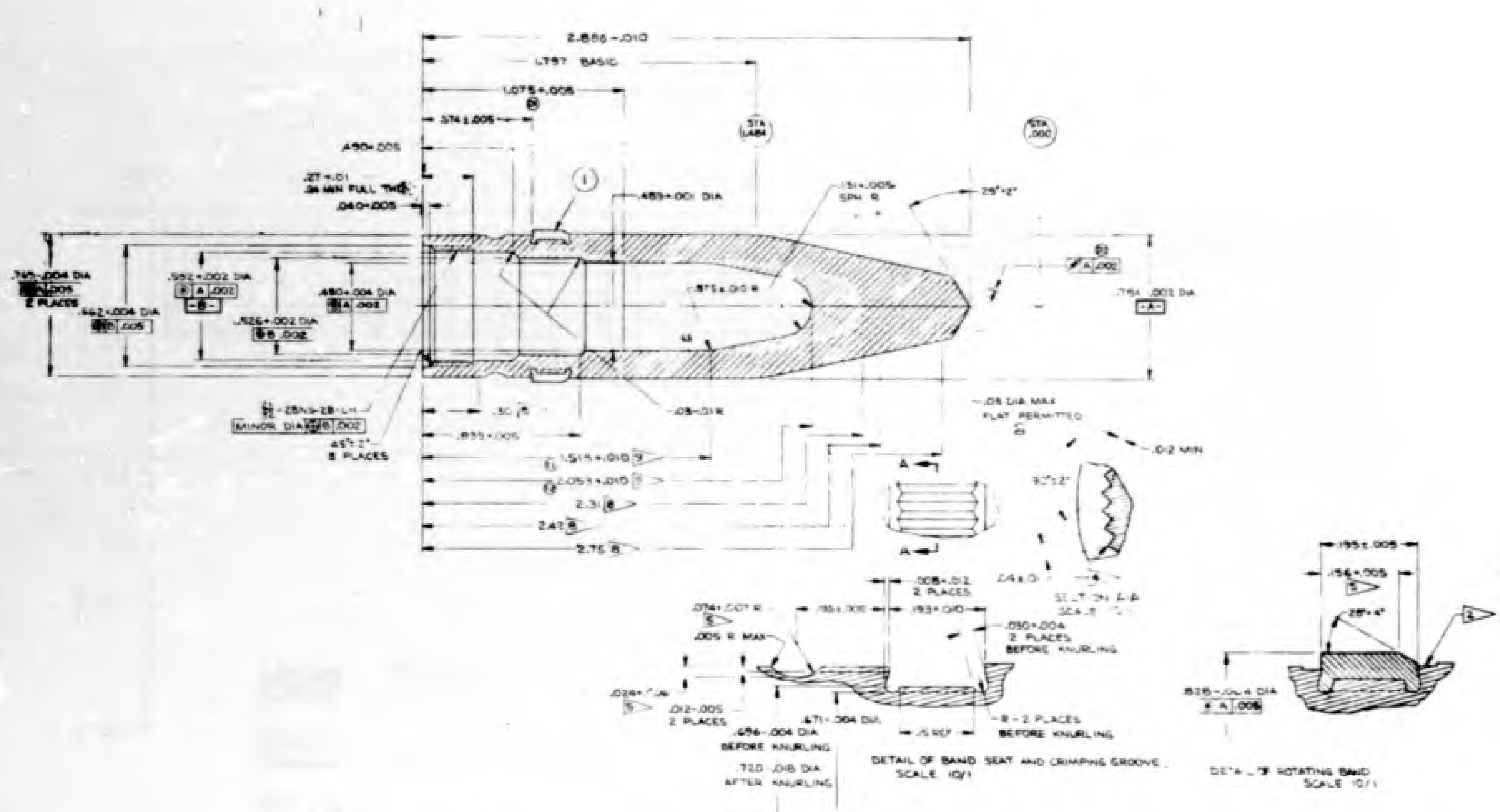

Figure 26. Body and Rotating Band Assembly (Cavity Test), Drawing Number 28103016

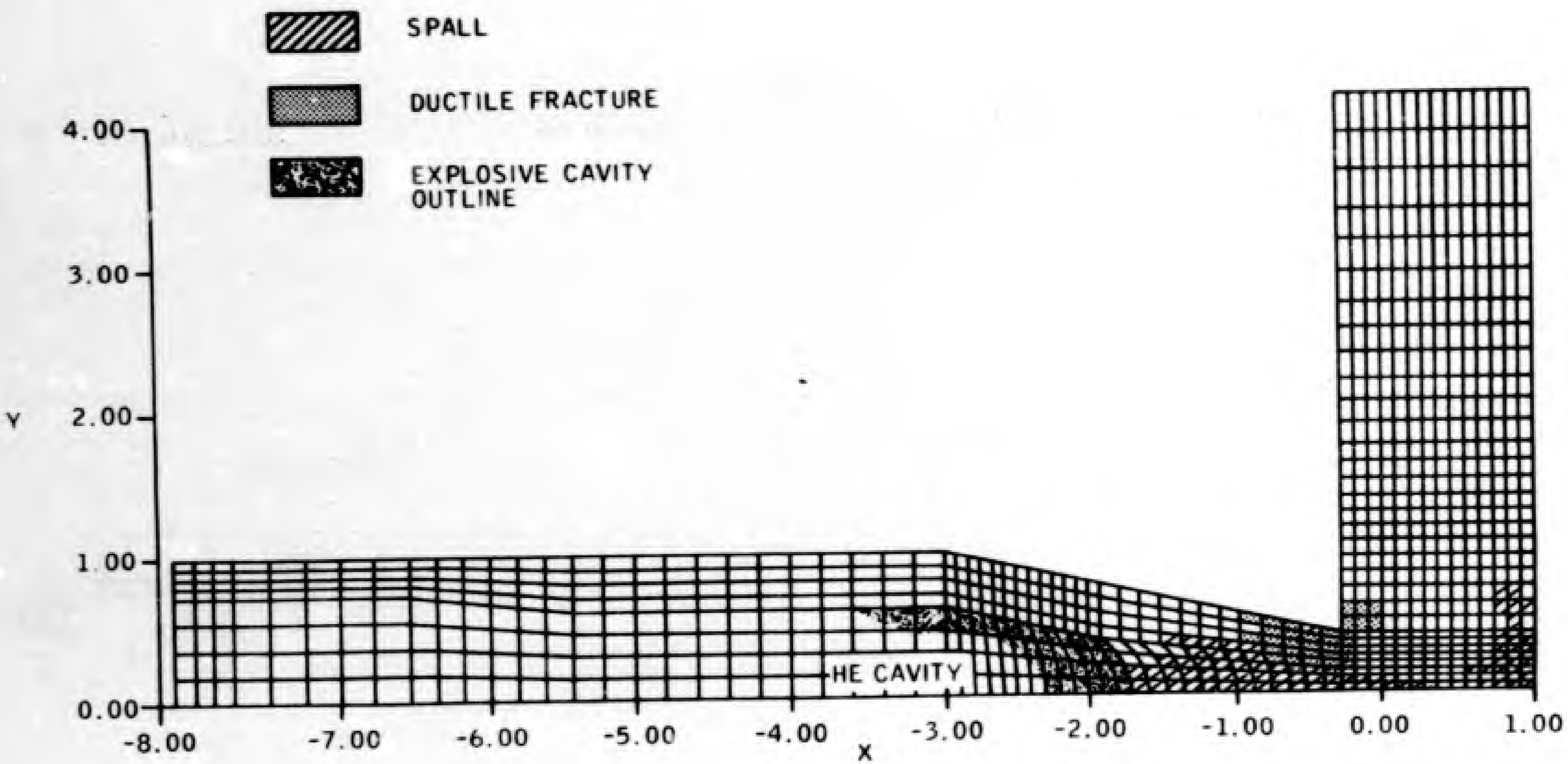

Figure 27. 1045 Material, Initial Cavity

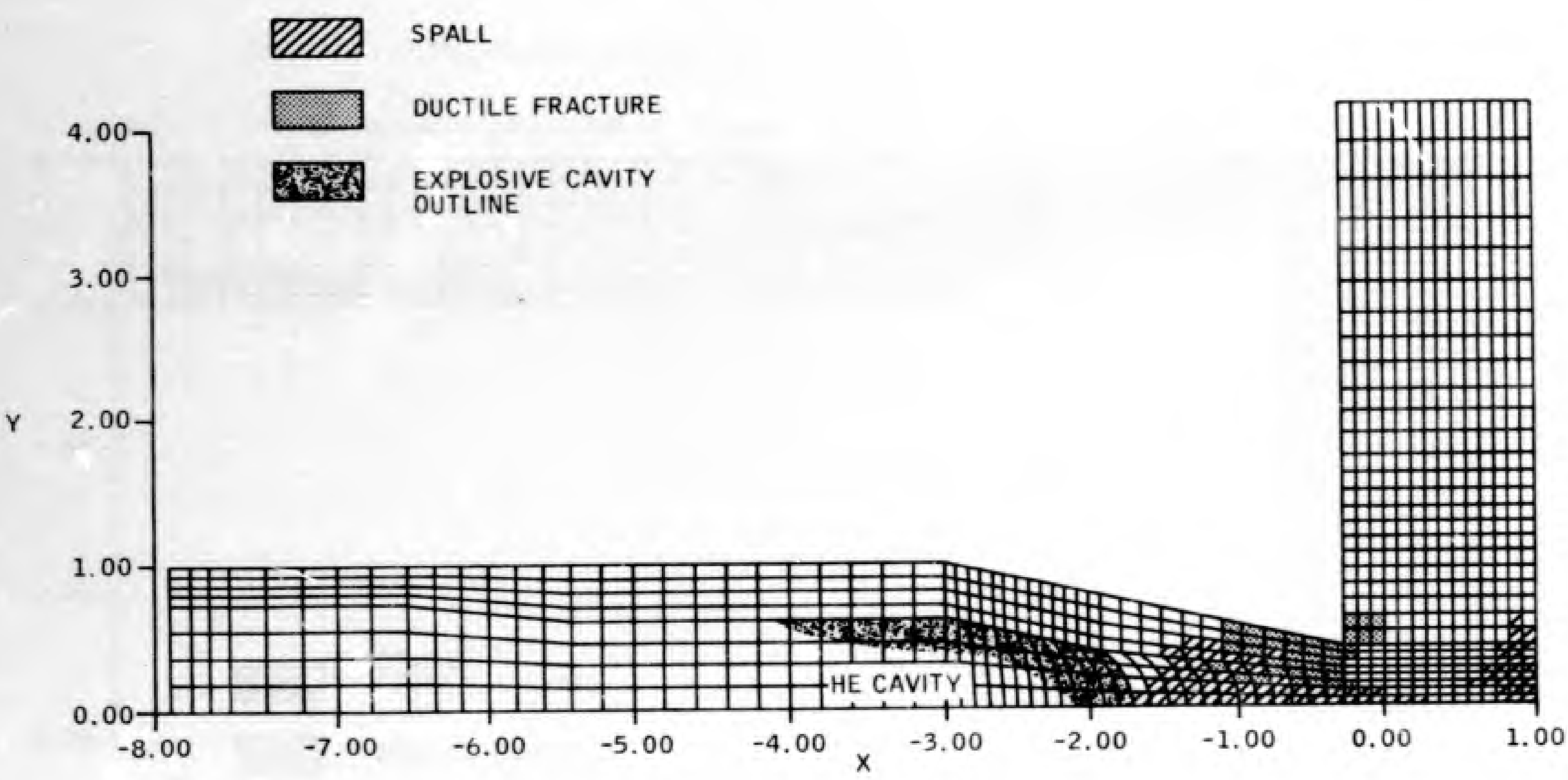

Figure 28. 52100 Material, Initial Cavity

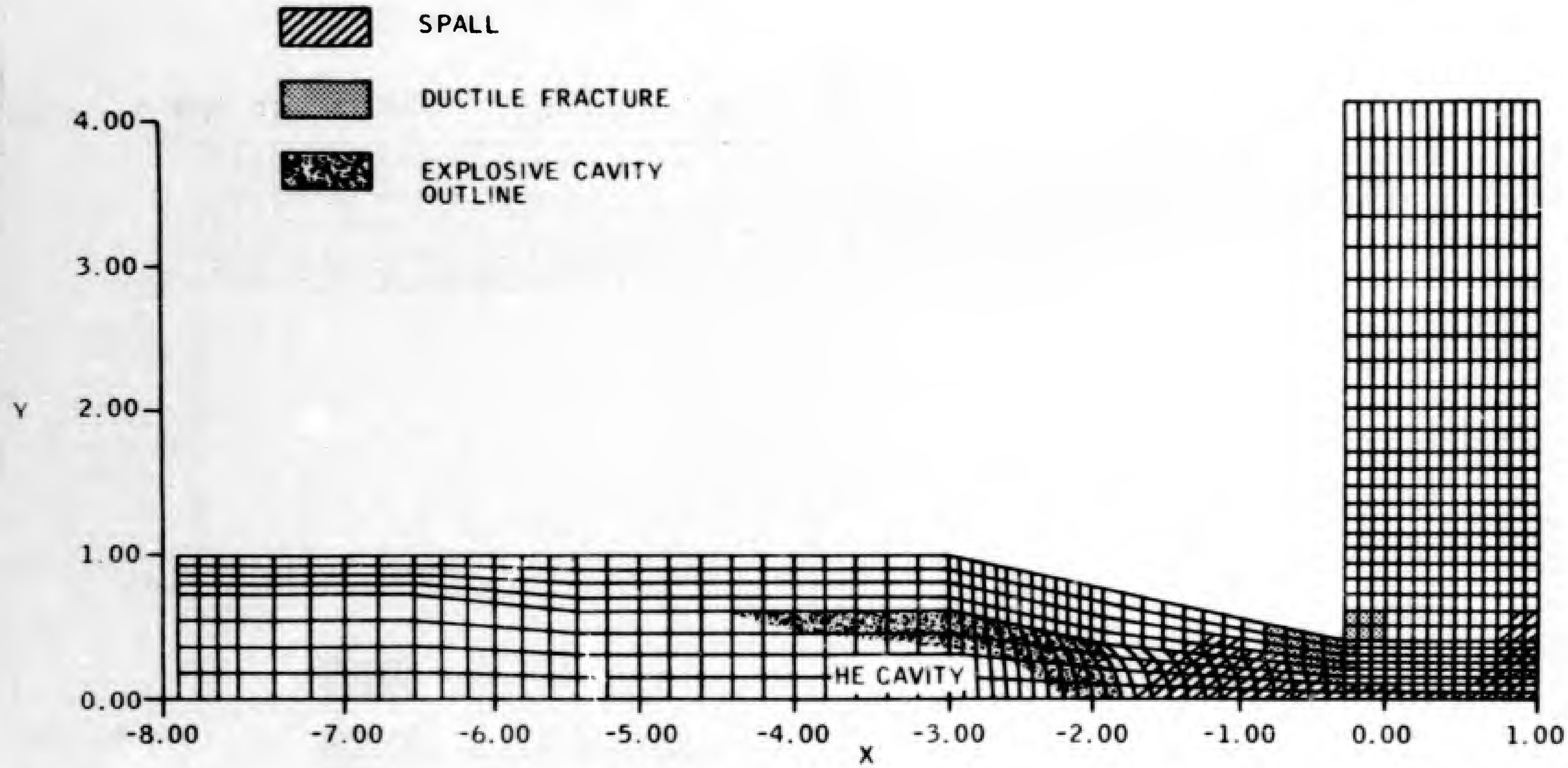

Figure 29. 1045 Material, Revised Cavity

Following are the results:

1. The forward surface of the explosive cavity fails in tension, causing the tip to break free as in Figure 14.

2. Changes made in the explosive cavity produce some improvement.

3. The 52100 steel is not as well suited as the 1045 material to the SAPHE application.

4. A liner of aluminum pressed in the end of the explosive cavity would reduce the tip breakage on 0-degree impact.

5. The shock transferred to the explosive is not sufficient to detonate the explosive if the body remains intact.

4. Effectiveness

The SAPHE (Semi-Armor Piercing High Explosive) round effectiveness was evaluated in terms of fragmentation effects against materiel and personnel targets. Incendiary effects were not evaluated due to the lack of a model for incendiary effectiveness. The present 20mm round, the M56A3, was also evaluated against the same targets for comparison purposes.

The fragmentation characteristics of the SAPHE round were estimated on a theoretical basis because data from fragmentation tests were not available. The fragment mass and spatial distributions were estimated by use of the scaling and distribution laws of Gurney-Sarmousakis and Mott. The nose portion of the round was assumed to break up into three fragments of equal weight. Initial fragment velocities were predicted from Gurney's formula. Fragmentation test results from the JMEM Weapon's Characteristics Report were used in evaluating the M56A3 effectiveness.

The targets investigated were trucks, armored personnel carriers, parked aircraft, and personnel. The results of these studies indicated that the 20mm projectile combining high explosive (HE) and antiarmor (AP) capabilities would enhance the effectiveness of the 20mm gun system against light materiel targets.

B. EXTERIOR BALLISTICS

When fired from an aircraft going 790 KTAS in a 30-degree dive against ground targets, the projectile shall have a computed downrange velocity at zero degree yaw, of at least 3,360 fps at a 2,000-foot slant range and 1,060 fps at a 9,000-foot slant range. Under the above conditions, the average time of flight should be approximately 1.4 seconds at 4,000 feet and should ballistically match the M56 round to within 1 mil out to 4,000 feet.

The minimum dispersion consistent with the other performance parameters is desired. The maximum dispersion of 10 projectiles fired single shot from a Mann barrel should not exceed a 1-mil mean radius.

The purpose of the exterior ballistics analysis was to ensure that the round would meet its ballistic goals and would be stable over its expected range of operating conditions. During the early design phase, a tradeoff had to be made between nose length and bourrelet length. A longer nose would mean a lower zero yaw drag and higher zero yaw performance; a shorter bourrelet would mean more barrel balloting and a higher initial angle of yaw, and thus higher induced drag, lower performance, and lower accuracy. The final compromise set the nose length at a minimum necessary to meet performance specifications (with an allowance for the drag estimation error). This maximized the bourrelet length, ensuring a very small tipoff at launch and high accuracy resulting from the clean launch. The selected configuration was a 3/4-power form with a truncated nose tip.

The estimated aerodynamic drag coefficient of the SAPHE round is given in Figure 30 and the SAPI drag coefficient, in Figure 31. As can be seen, the two estimated curves are nearly identical. As a result of the nearly identical external configurations of the two rounds, they have nearly identical trajectories. Trajectories computed using the estimated drag curve are presented in Figures 32 to 37.

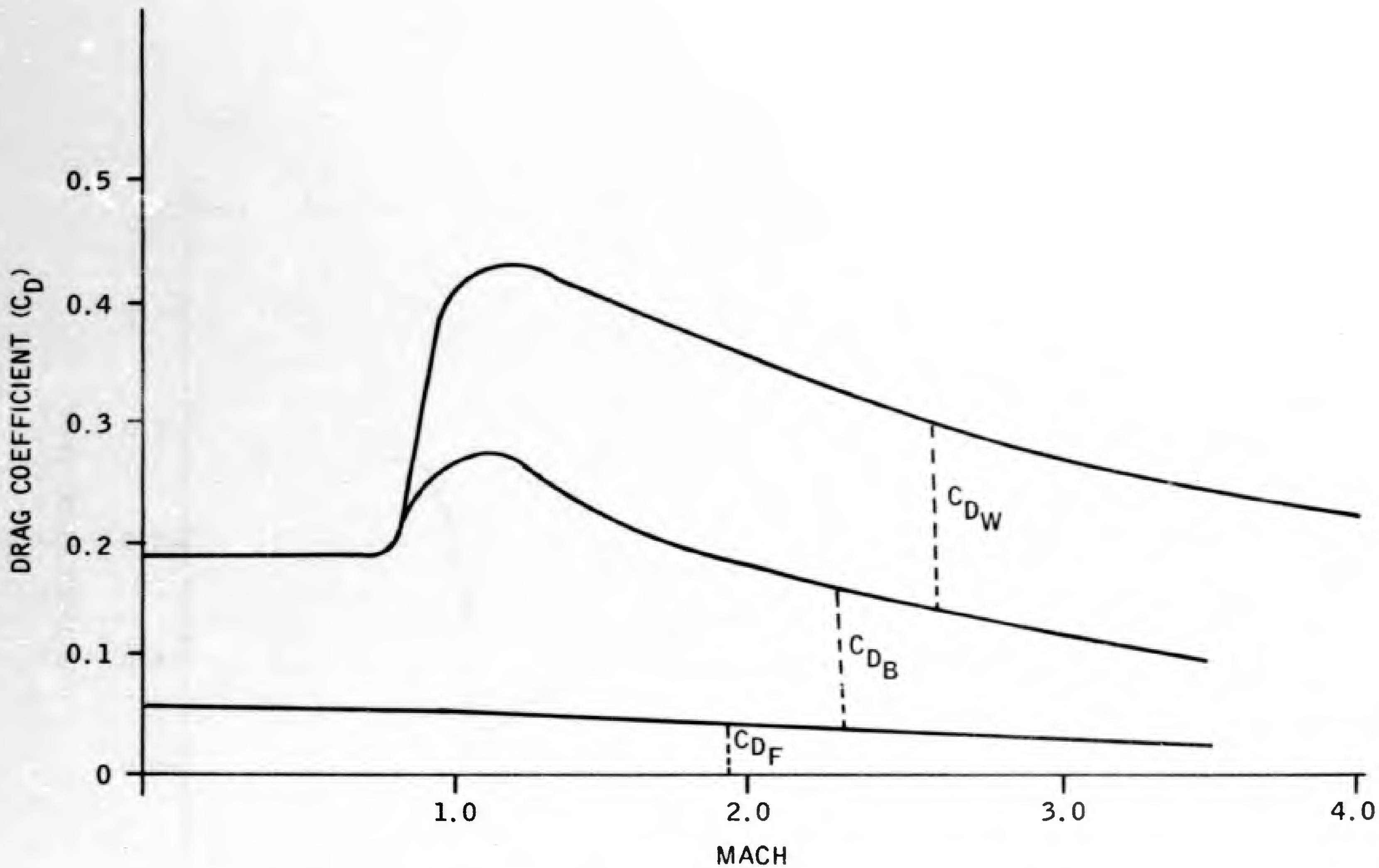

Figure 30. 20mm SAPHE Drag Coefficient, 1.2-Inch Bourrelet Length, 0.00338-Square-Foot Reference Area

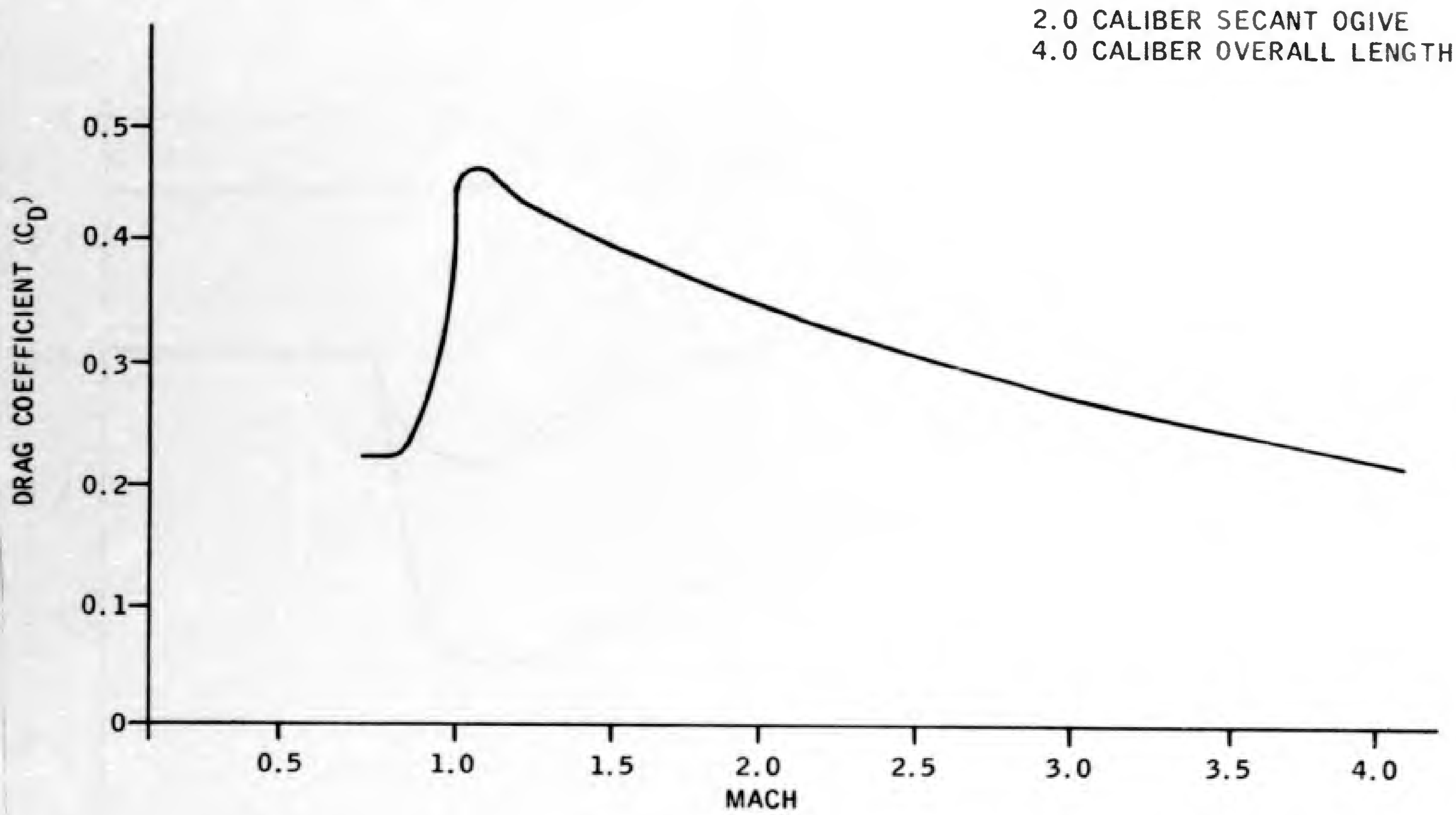

Figure 31. 20mm SAPI Drag Coefficient

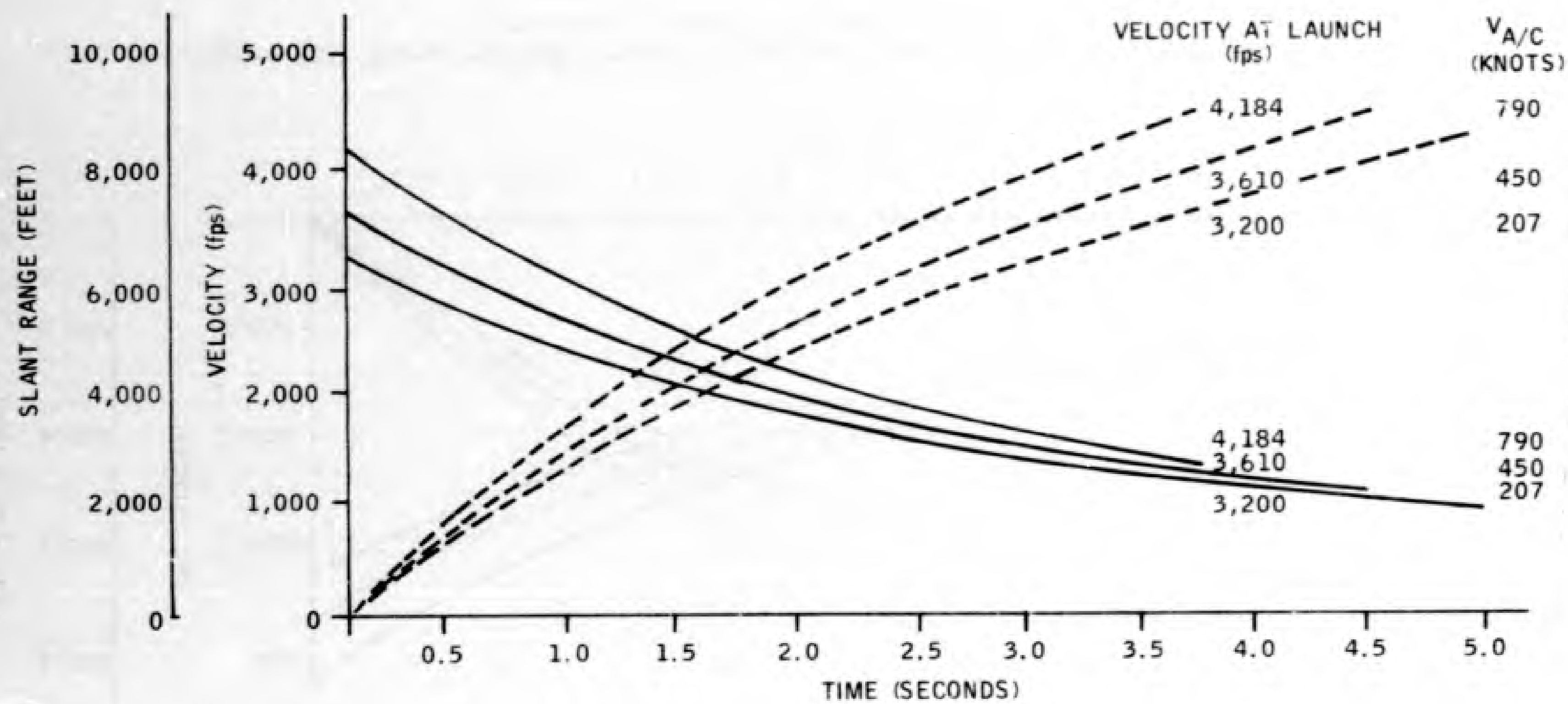

Figure 32. 20mm SAPHE Trajectories, Altitude at Launch (5,000 Feet), Attitude at Launch (30 Degrees)

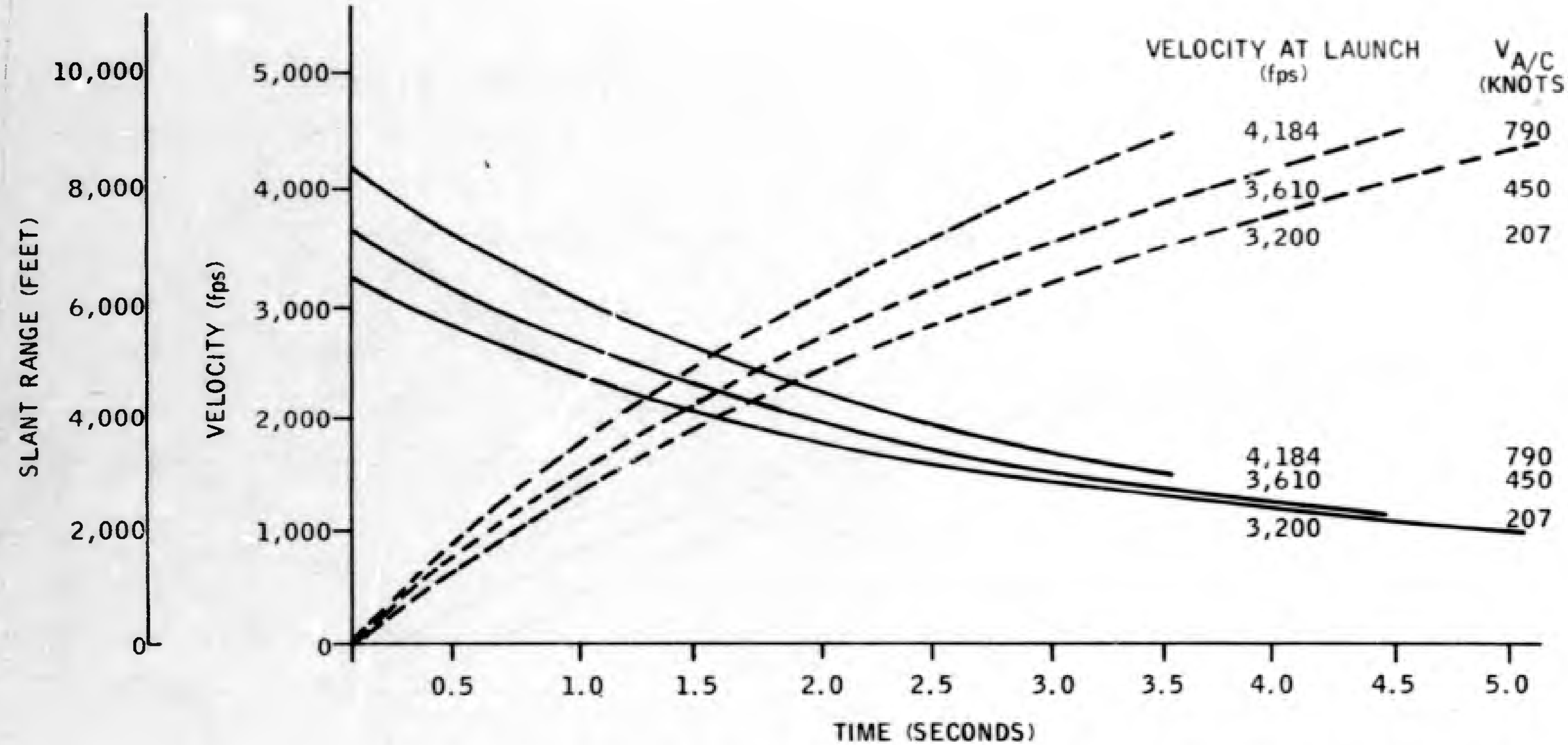

Figure 33. 20mm SAPHE Trajectories, Altitude at Launch (5,000 Feet), Attitude at Launch (15 Degrees)

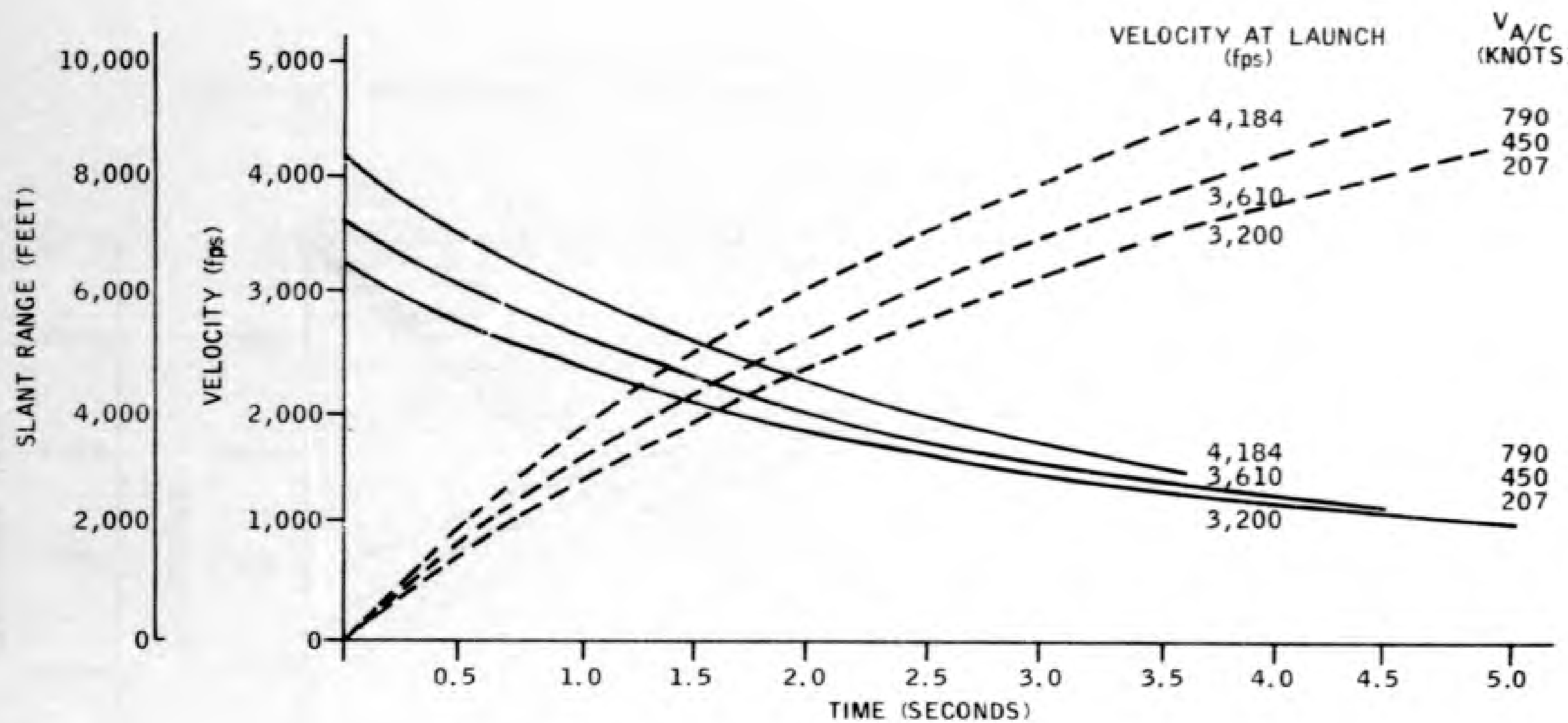

Figure 34. 20mm SAPHE Trajectories, Altitude at Launch (5,000 Feet), Attitude at Launch (0 Degrees)

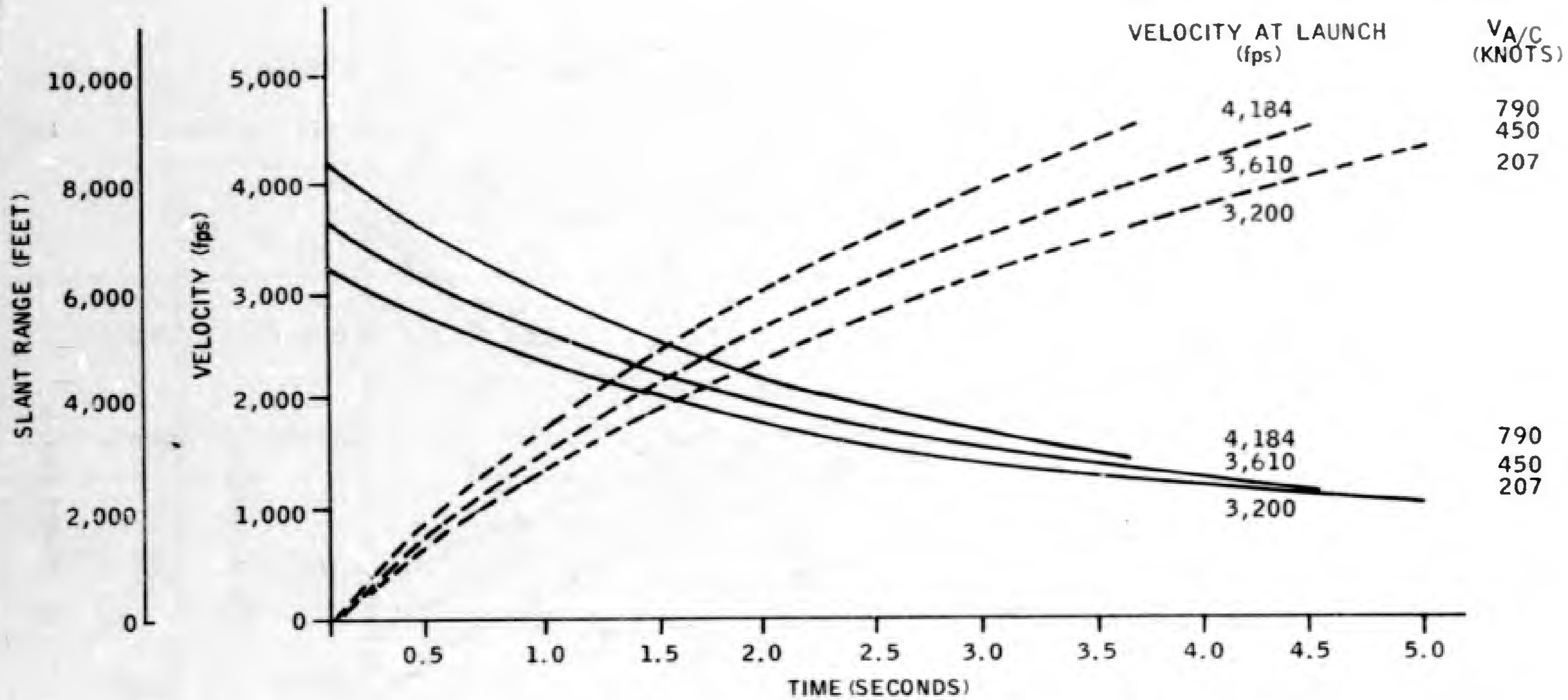

Figure 35. 20mm SAPHE Trajectories, Altitude at Launch (5,000 Feet), Attitude at Launch (-15 Degrees)

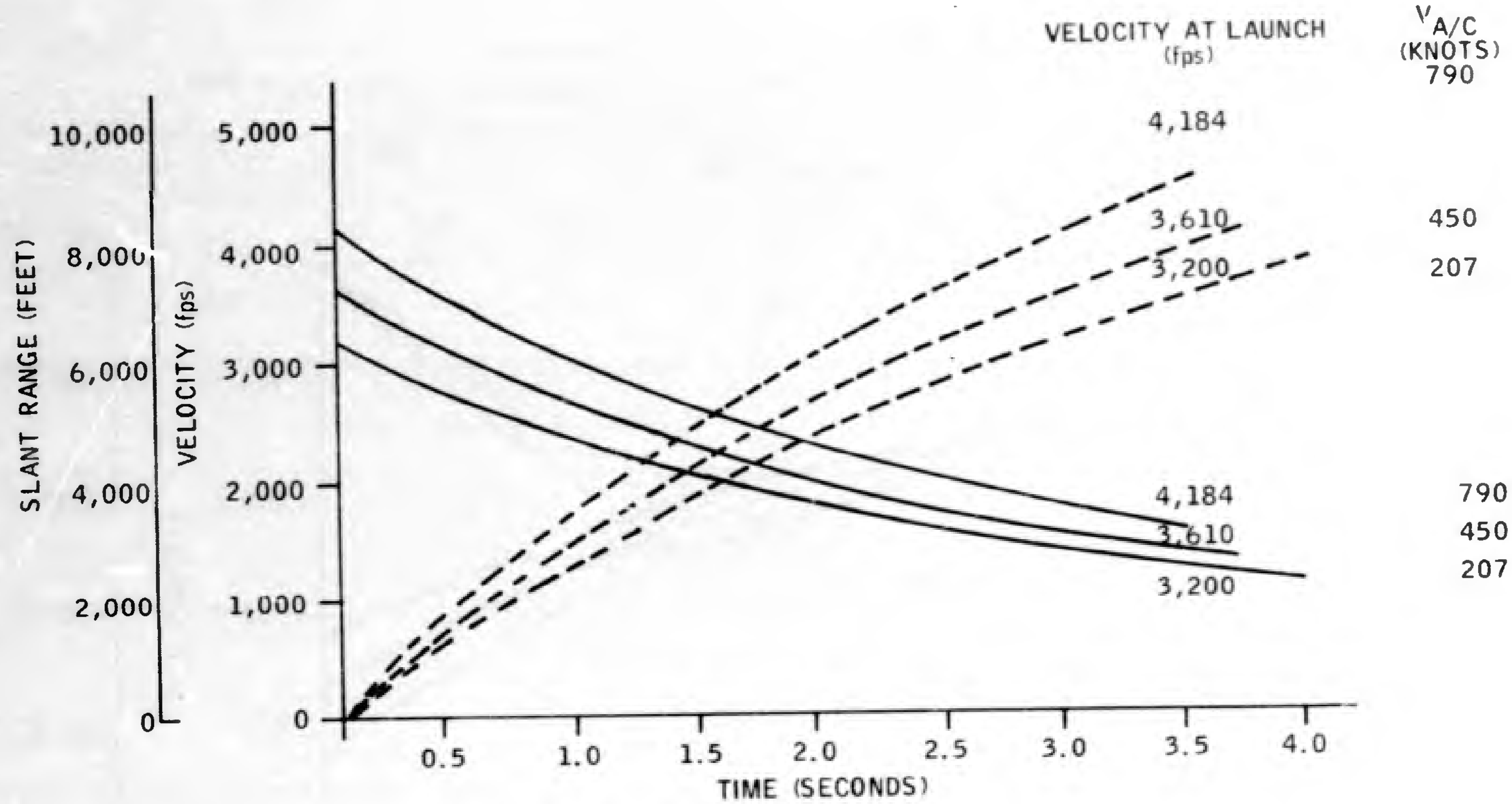

Figure 36. 20mm SAPHE Trajectories, Altitude at Launch (5,000 Feet), Attitude at Launch (-30 Degrees)

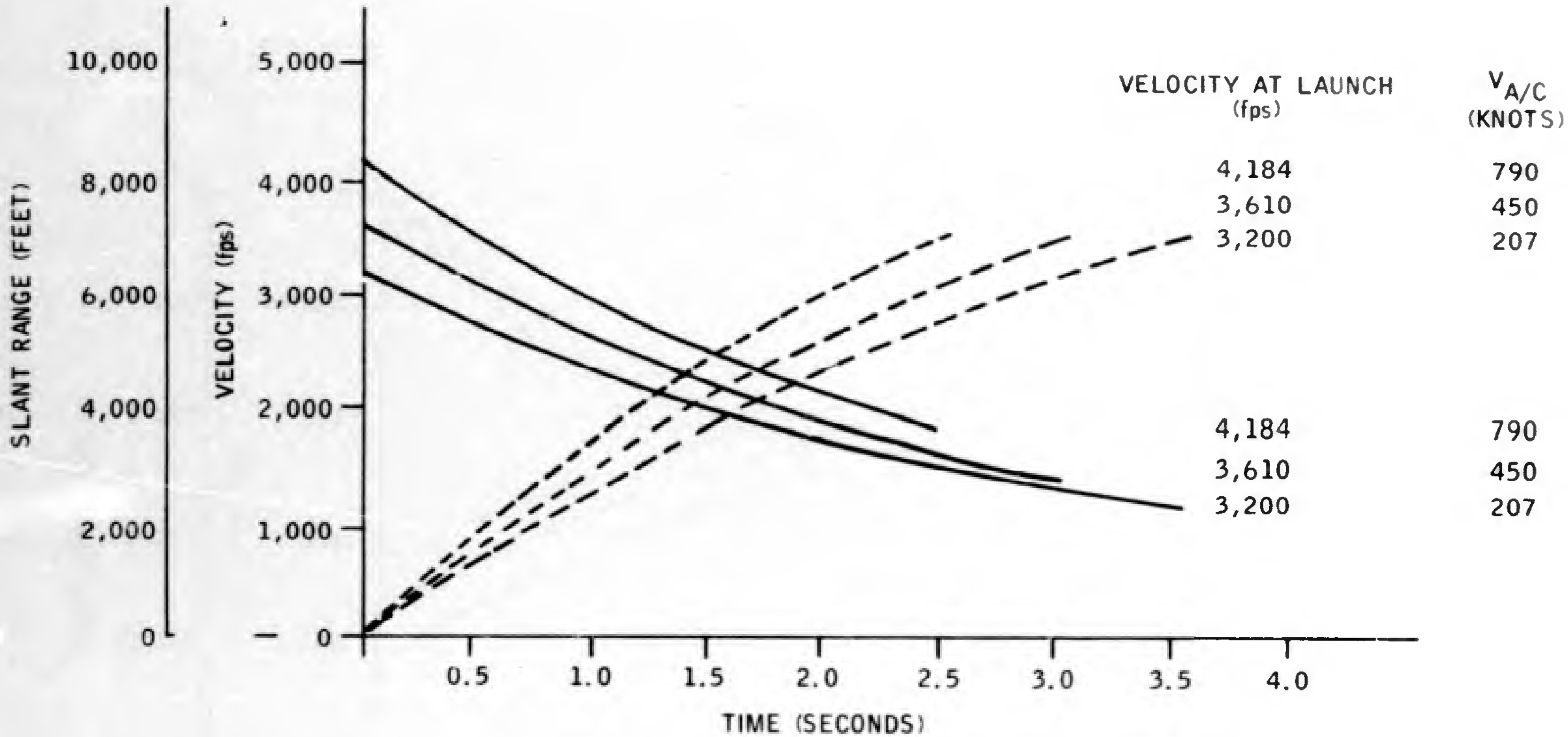

Figure 37. 20mm SAPHE Trajectories, Altitude at Launch (5,000 Feet), Attitude at Launch (-45 Degrees)

The normal force and center of pressure of the SAPHE round were estimated and are presented in Figures 38 and 39. These estimates were used to estimate the gyroscopic stability of the SAPHE round. The additional aerodynamics necessary for dynamic stability analysis were also estimated. Murphy's[2] stability criteria were used.

According to Murphy, the gyroscopic stability of a round is given by:

$$Sg = \frac{\left[\frac{Ix}{Iy}\left(\frac{pd}{V}\right)\right]^2}{4\left(\frac{\rho S d^3 C_{m\alpha}}{2\,Iy}\right)}$$

In addition, the dynamic stability of the round is

$$Sg = \frac{2\; C_{L_\alpha} + C_{mp_\alpha}/Ka^2}{C_{L_\alpha} - C_D - \frac{C_{mg} + C_{m\alpha}}{K_T^{\;2}}}$$

where:

Sg	=	gyroscopic stability parameter
Sd	=	dynamic stability parameter
Ix	=	roll moment of inertia
Iy	=	pitch moment of inertia
p	=	roll rate

2 Murphy, Charles H, "Free Flight Motion of Symmetric Missiles," BRL Report No 1216, dated July 1963.

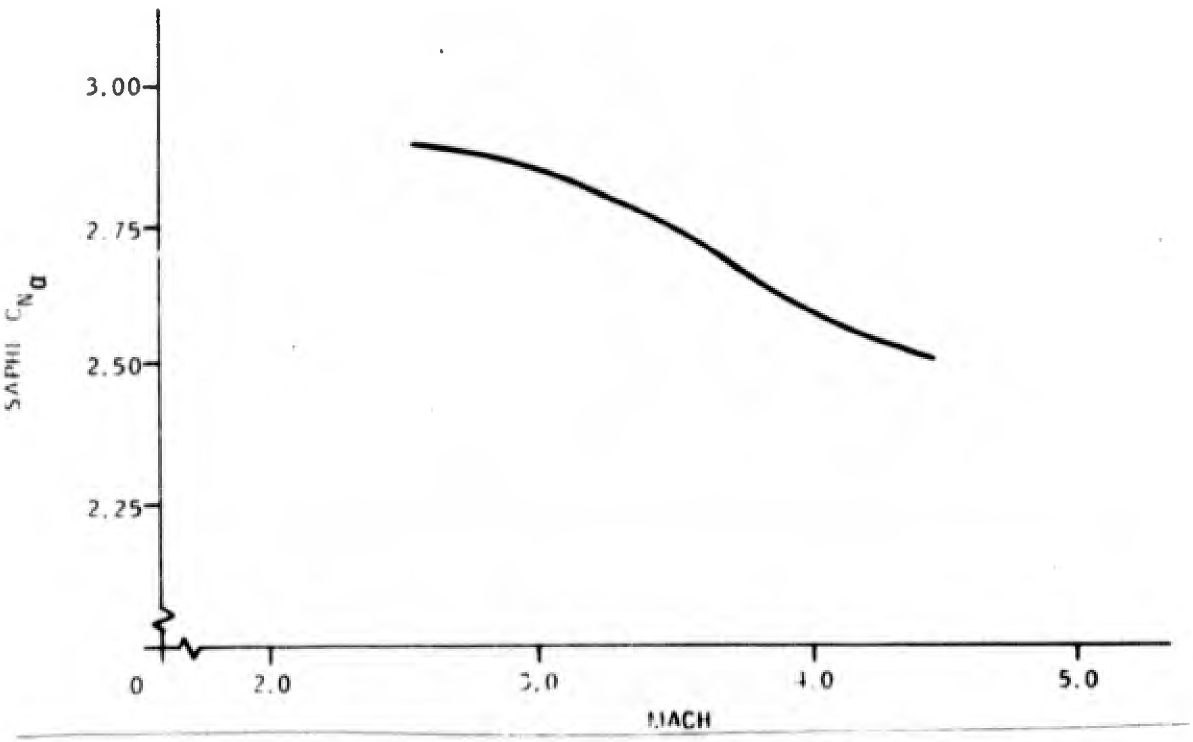

Figure 38. Trajectories Computed Using Estimated Drag Curve, C_{N_α} Versus Mach

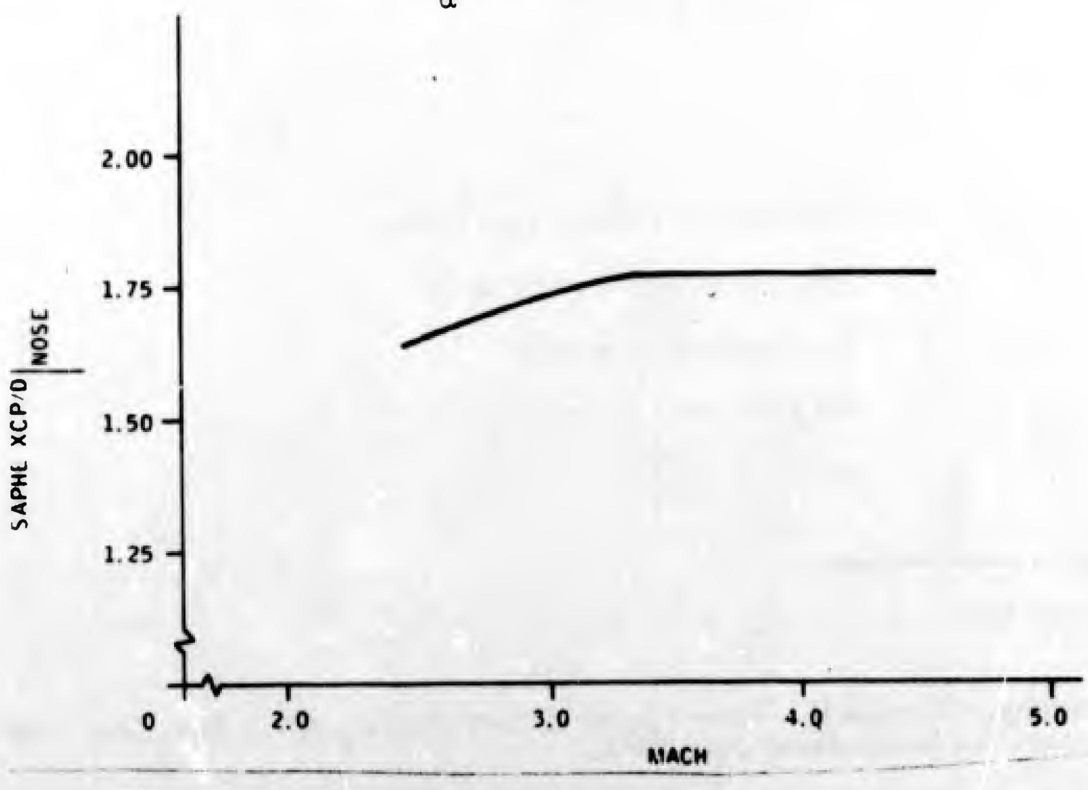

Figure 39. Trajectories Computed Using Estimated Drag Curve, $XCP/D|_{Nose}$ Versus Mach

d	=	reference diameter
V	=	projectile velocity
S	=	reference area
C_{m_α}	=	pitching moment coefficient
C_{L_α}	=	lift moment coefficient
C_D	=	drag coefficient
$C_{m_{p\alpha}}$	=	Magnus moment coefficient
$C_{m_\alpha} + C_{m_\alpha}$	=	pitch damping coefficients
Ka	=	axial radius of gyration
K_T	=	transverse radius of gyration
ρ	=	air density.

The conditions for stability are:

$$\frac{1}{S_g} < 1 \qquad \text{(gyroscopic)}$$

$$\frac{1}{S_g} < Sd(2-Sd) \qquad \text{(dynamic)}$$

Results of the aerodynamic stability analysis are given below for both the baseline SAPHE and the miniature alternate fuze version. The launch conditions included a sea-level launch from an aircraft flying at 790 knots in a standard atmosphere. The muzzle velocity was taken to be 2,850 fps from a barrel with a terminal twist of 7.05 degrees.

Projectile	Sd	Sg	Stable
Baseline	0.83	1.43	Yes
Miniature Fuze	0.76	1.85	Yes

The same analysis was applied for an air temperature of -65°:

Projectile	Sd	Sg	Stable
Baseline	0.78	1.12	Yes
Miniature Fuze	0.71	1.45	Yes

In standard air at 9,000-foot slant range, Sg of the baseline SAPHE grows to 7.35. The design of both versions is thus stable over the extremes of expected launch conditions.

C. PROPELLANT SYSTEM

The purpose of this study was to select a propellant to meet the pressure and velocity requirements of the 20mm SAPHE ammunition while having the requisite chemical and physical properties to survive military operating conditions. The SAPHE requirement is a propellant that will accelerate a 2,100-grain projectile to a minimum velocity of 2,850 fps at 78 feet from the muzzle, with the added requirement that the sample standard deviation shall not exceed 40 fps. In achieving this velocity, it is further specified that the peak pressure, measured by a copper crusher gage in the gun breech, will not exceed 60,500 psi as defined by the following equation:

$$P = \overline{X} + K(\overline{R}) < 60{,}500 \text{ psi}$$

Here $\overline{X}$ is the mean pressure from 20 tests, $\overline{R}$ is the average of the pressure ranges determined from four sets of five tests of the above 20 tests, and K is the constant 0.8.

The requirement of the propellant to survive military operating conditions was determined by subjecting the candidate propellant to several representative tests: (1) high temperature storage, (2) propellant temperature cycling, and (3) vibration. All propellants able to satisfy these criteria were considered for use and the candidate with the best overall performance was selected.

The selected SAPHE projectile design defined the volume for propellant to be 2.26 cubic inches, substantially less than that of the M55. The small volume dictated use of an inhibited propellant, since uninhibited propellants were not sufficiently progressive to limit the peak pressure while supplying the energy to accelerate the projectile.

The foregoing considerations were applied to a preliminary analytical screening of propellants and the following propellants selected as feasible candidates:

Canadian Industries Limited	Hercules	Olin-Mathieson
CIL 5268	6928-109	X2988
CIL 5222	6928-141	
CIL 1407C		
CIL 1377A		
CIL 1377B		
CIL 1377C		

These propellants were screened by gun tests as described below. For the propellant to produce the same test result from shot to shot, it must provide a gas-flow rate which is fixed in terms of mass-flow rate versus time and in terms of the gas chemical/physical properties. Variations in mass-flow rate may occur because the burning rate of the propellant varies or the surface area is altered by cracking of the propellant configuration, while variation in the gas properties may occur because the chemical composition of the propellant is altered. Both types of variation affect gun performance, but because of the other possible causes of gun performance, variation may not be recognized. Therefore, each new batch of propellant received was subjected to propellant bomb tests to detect these variations. Each propellant was subjected to charge sizing to determine the requisite SAPHE charge weight. Promising candidates were then subjected to one series of 20 tests at 70°F to assess pressure and velocity and standard deviations. These were followed by high and low temperature tests and a small number of storage tests. The tests of each propellant are summarized in Table VIII.

TABLE VIII. PROPELLANT GUN TEST SUMMARY

PROPELLANT	CHARGE SIZING	PRESSURE VELOCITY (+70°F)	HIGH TEMPERATURE (+160°F)	LOW TEMPERATURE (-65°F)	STORAGE AT HIGH TEMPERATURE (-65°F)	STORE (+160) CYCLED BACK TO +70°F
CIL 5222	9					
CIL 5268	9					
CIL 1407C	12	31	2	9		1
CIL 1377A	3					
CIL 1377B	6	27	8	11	2	1
CIL 1377C	3					
HERCULES 6928-109 (80/20 BLEND)	2					
HERCULES 6928-141 (80/20 BLEND)	2					
OLIN X2988	59	20	3	5	2	
TOTAL TESTS	105	78	13	25	2	2

FOR EVALUATION PURPOSES, MOST OF THE TEST ROUNDS EXCEPT THE CHARGE SIZING ROUNDS WERE ACCOMPANIED WITH REFERENCE ROUNDS. REFERENCE ROUNDS WERE M55 CARTRIDGES LOADED WITH EITHER OLIN WC 870 OR CIL 1377B.

1. Test Vehicle

To test the candidate propellants, a SAPHE D (Dummy Projectile), a high carbon steel unit, was designed to have essentially the same mass properties as the SAPHE. It was internally machined to arrive at a 2,100-grain weight.

The projectile assembly is shown in Figure 40. For internal ballistic studies, the characteristics of the projectiles which should be constant are (1) the assembled projectile intrusion depth into the case, (2) the diameter and length of the copper engraving band, (3) the crimp depth, and (4) the all-up weight of the projectile. From a set of 15 projectiles inspected, the following data were obtained.

Characteristic	High Value	Low Value
Intrusion Depth (inch)	0.842	0.836
Engraving Band Outside Diameter (inch)	0.826	0.825
Engraving Band Axial Length at Outside Diameter	0.1609	0.1575
Crimp Groove Depth (inch)	0.028	0.027
Projectile Weight (grams)	136.8	134.9

The case design was already fixed, but a sample check was made with respect to (1) volume of the case with projectile installed, (2) weight of the case, (3) the depth of the crimp groove, (4) the case length, and (5) depth inside the case. The range in dimensions for 100 cases was as follows:

Dimensions		High	Mean	Low
t	(inch)	0.0542	0.0505	0.0480
L1	(inches)	4.007	-	4.000
L2	(inches)	3.641	3.63	3.620
Weight	(grams)	123.5	121.8	119.0
Volume	(cubic centimeters)	37.10	36.82	36.55

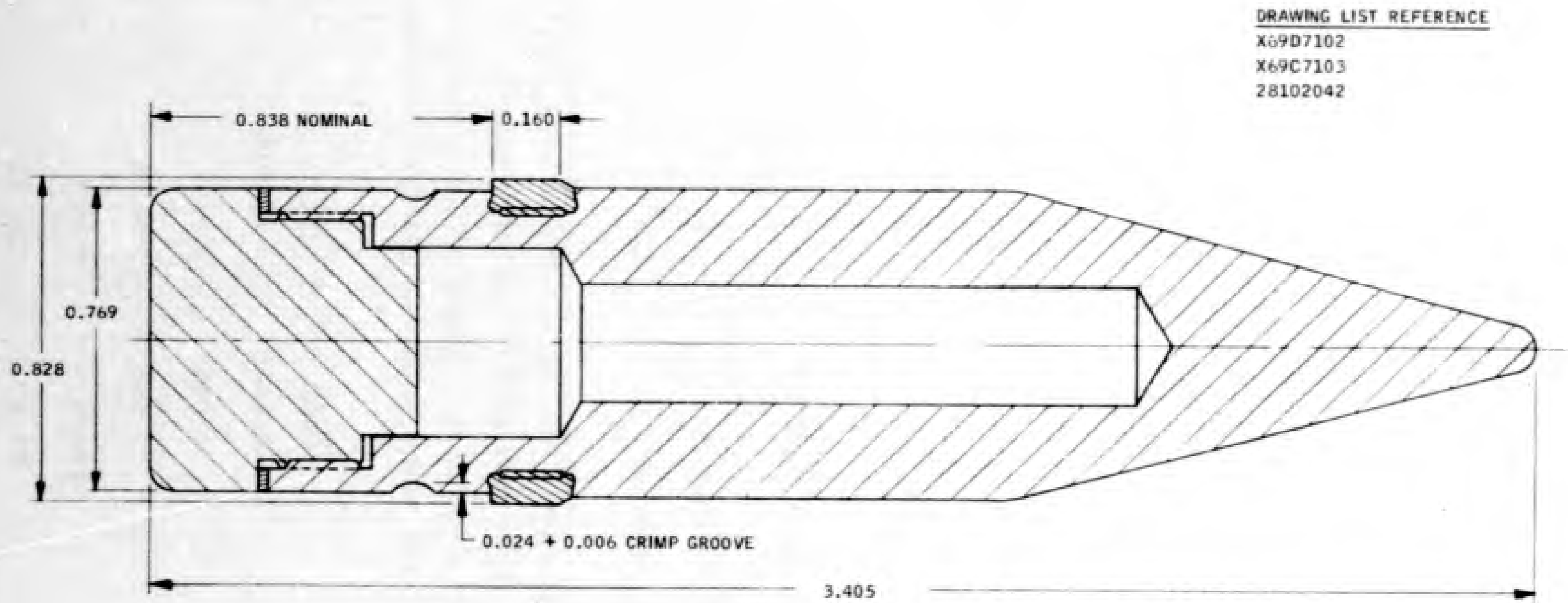

Figure 40. SAPHE Propellant Projectile (2, 100 Grains)

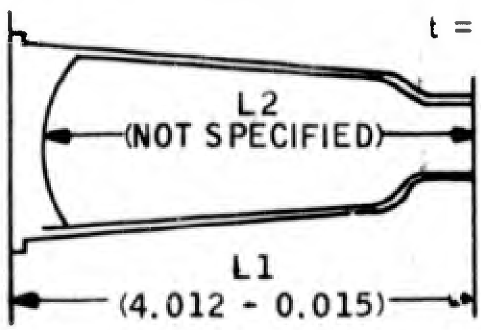

Results showed that case dimensions were within the specified dimensions. From a set of 15 pull tests on the crimped case and projectile, a force of 1,505 pounds with a standard deviation of 133 pounds was obtained; this is within military specifications.

2. Test Procedure

All gun tests were performed in the Hopkins indoor range with the instrumentation shown schematically in Figure 41. The gun was placed on a Frankfort mount and the SAPHE projectile fired through lumiline screens located 28 feet and 128 feet downrange. The gun firing circuit was a dc line to the breech cap and a piezoelectric gage was attached to the gun barrel several inches from the base of the plug. Some problems were encountered in trying to assess ignition from the traces because of the proximity of the firing circuit to the piezoelectric gage, but groundloop problems were minimized. The copper crusher attachment was located directly opposite the gage on the barrel and a muzzle coil was placed at the end of the barrel for action time determination. One yaw card was placed at about 130 feet downrange to monitor projectile yaw dispersion.

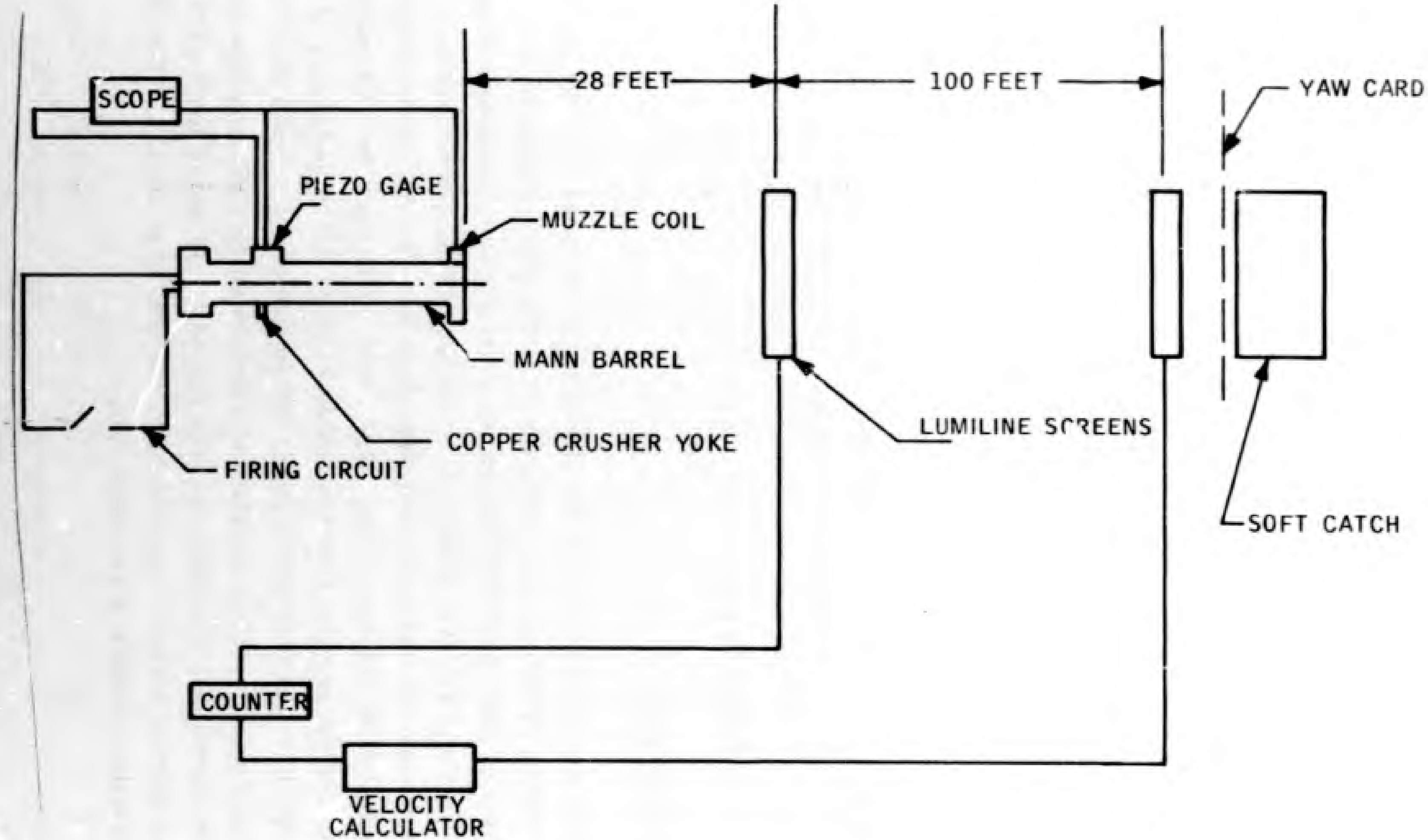

Figure 41. Propellant Test Range (Hopkins)

The distance between the lumiline screens (100 feet) divided by the number of seconds required for the projectile to pass from one to the other gave the average velocity at 78 feet. A velocity calculator also triggered by the screens was used as a secondary velocity-measuring method.

In determination of copper crusher pressure, each copper crusher was measured before and after each test with a super micrometer capable of measuring to the nearest millionth of an inch. The readings were taken to five significant figures and the difference of the before and after readings rounded off to four places and used for the tarage table value.

The output of the piezoelectric gage (Kistler) was fed to an oscilloscope to give a pressure-time trace as shown in Figure 42. A second trace initiated by the breech cap circuit oscillated when the projectile passed the muzzle coil at the end of the gun barrel. The time elapsed from the start of the trace to muzzle exit gave the gun action time.

The shape of the pressure trace at ignition was used to determine whether the pressure rise was smooth or rough or whether there were any unusual dips in the pressure as it rose to the peak. These results were reviewed for propellant selection but are not considered in detail in this report.

To retain a high level of accuracy with the piezoelectric gage pressure measurement, the gage was calibrated before and after each series of tests by applying pressure to it with a 100,000-psi hydraulic pressure generator. The voltage output of the gage amplifier and the scope traces taken at various pressure levels were recorded.

3. Pressure and Velocity Tests

The test results (included in Appendix II) indicated that CIL 1407C and 1377B and Olin X2988 satisfied the pressure and velocity requirements better than the other propellants. The results for these propellants are shown in Table IX.

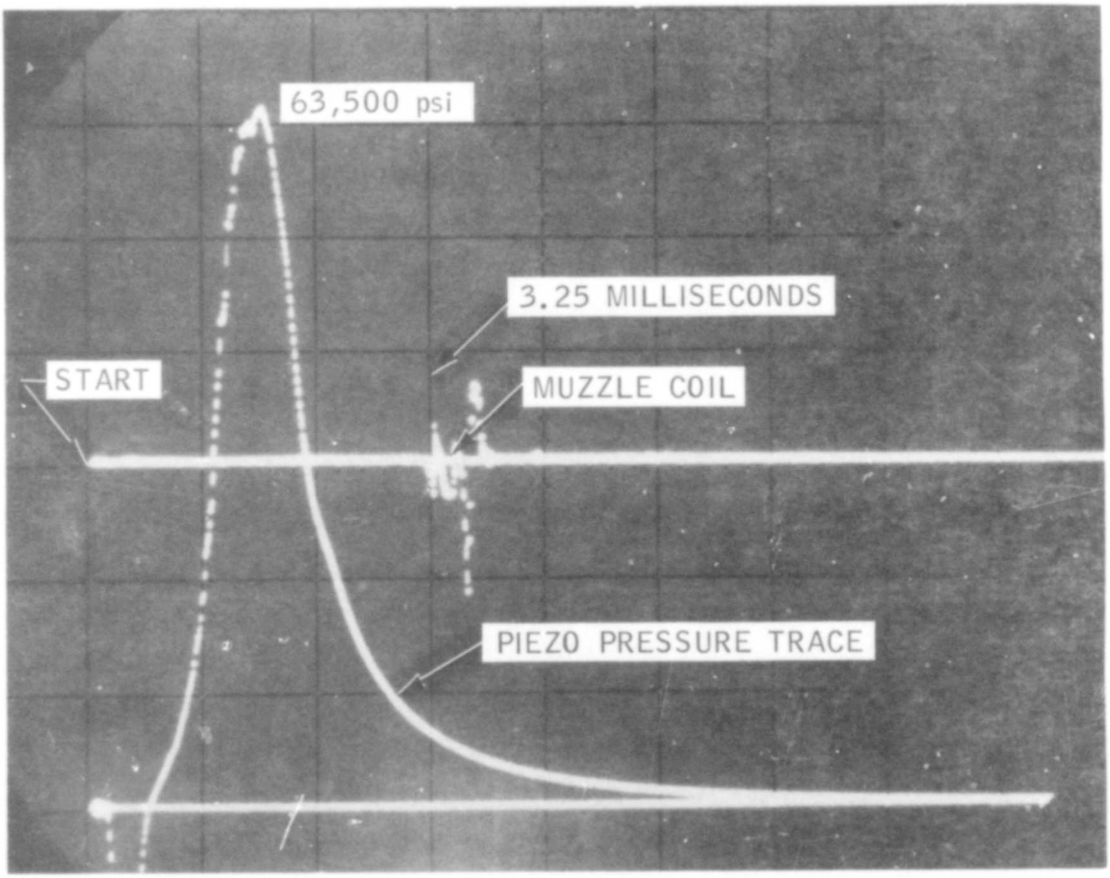

TEST ROUND NO. 7

3-11-70

36.0 GRAMS OLIN X2988

P_S - 63.5 KPSI

$P_{CRUSHER}$ - 53.0 KPSI, V - 2,891 fps

Figure 42. Representative Oscilloscope Trace

TABLE IX. RESULTS OF PRESSURE AND VELOCITY TESTING

TEST PARAMETER	TEMPERATURE		
	+160°F	70°F	-65°F
PROPELLANT 1377B (CHARGE WEIGHT = 35.0 GRAMS)			
MEAN VELOCITY (fps)	2,970.00	2,894.00	2,837.00
VELOCITY STANDARD DEVIATION (fps)	13.00	22.00	13.00
MEAN PRESSURE (PIEZO) (PSI)	67,700.00	59,800.00	54,960.00
MEAN PRESSURE (CRUSHER) (PSI)	58,000.00	50,600.00	45,900.00
PRESSURE STANDARD DEVIATION (CRUSHER) (PSI)	1,055.00	2,470.00	1,100.00
ACTION TIMES (MILLISECONDS)	2.98	3.01	3 18
NUMBER OF ROUNDS	3.00	20.00	5.00
PROPELLANT 1407C (CHARGE WEIGHT = 35.0 GRAMS)			
MEAN VELOCITY (fps)	2,946.00	2,891.00	2,831.00
VELOCITY STANDARD DEVIATION (fps)	---	16.00	6.00
MEAN PRESSURE (PIEZO) (PSI)	69,000.00	62,300.00	57,100.00
MEAN PRESSURE (CRUSHER) (PSI)	59,550.00	52,900.00	48,400.00
PRESSURE STANDARD DEVIATION (CRUSHER) (PSI)	---	1,867.00	570.00
ACTION TIME (MILLISECONDS)	3.00	2.99	3.17
NUMBER OF ROUNDS	2.00	20.00	5.00
PROPELLANT OLIN X2988 (CHARGE WEIGHT = 35.6 GRAMS)			
MEAN VELOCITY (fps)	2,908.00	2,875.00	2,836.00
VELOCITY STANDARD DEVIATION (fps)	11.00	9.00	11.00
MEAN PRESSURE (CRUSHER) (PSI)	53,400.00	50,600.00	51,700.00
PRESSURE STANDARD DEVIATION (PSI)	565.00	1,426.00	1,450.00
ACTION TIME (MILLISECONDS)	---	3.36	---
NUMBER OF ROUNDS	3.00	20.00	3.00

Photographs, dimensions and chemical and physical properties of CIL 1407C, 1377B and Olin X2988 are presented in Figures 43, 44, and 45. The CIL propellants are single perforation cylinders with the perforation diameter 0.0065 inch. The cylinder web thickness of 1407C is 0.020 inch and the thickness of 1377B is 0.024 inch. Both CIL propellants are coated with methyl centralite but differ in the percent of inhibitor (5.41 percent by weight for 1407C and 3.52 percent for 1377B). The Olin propellant has a 0.0225-inch web and is coated with 8.26 percent ethyl centralite.

Results for 1407C indicate a satisfactory mean velocity of 2,891 fps however, the pressures are about as high as they can go without exceeding limits imposed by the contract. The results show that the Olin propellant has satisfactory velocity-pressure results. The extreme variation is 5,500 psi, and the standard deviation is only 1,426 psi. The extreme variation in velocity is 39.0 fps with a standard deviation of 9.0 fps

To determine if the performance of the three candidate propellants was degraded at temperature extremes, samples of each were temperature-conditioned for 17 hours at either 160°F or -65°F and then fired. These results (Table IX) showed that the temperature characteristics of each of the propellants was satisfactory.

The candidate propellants were then stored at 160°F for eight days. One military specification (MIL-STD-810B) states that ammunition will be heated to 160°F for not less than 48 hours. Eight days was arbitrarily chosen. However, the cartridge cases had not been sealed to the projectile, so this test cannot be considered a standard test. It is, however, a comparative test, since each propellant was subjected to the same test conditions.

Two cartridges of CIL 1377B stored in this manner were fired at 160°F. The average results are shown in Table X. Because of the high pressures encountered with the CIL 1377B, 1407C was not tested at 160°F. Both the 1377B and 1407C were allowed to cool to 70° and a single round of each propellant was fired.

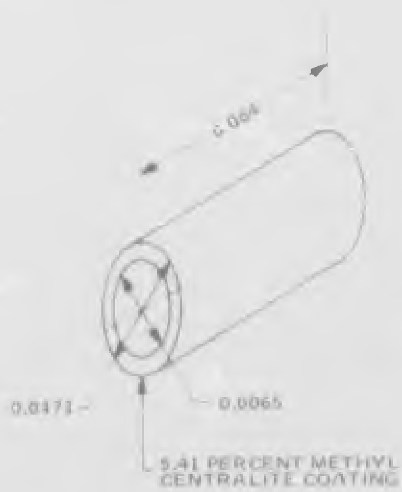

COMPOSITION	PERCENTAGE
METHYL CENTRALITE	5.41
DIPHENYLAMINE	0.84
POTASSIUM SULFATE	0.40
BASIC LEAD CARBONATE	0.78
NITROCELLULOSE	92.57
PROPERTIES	
STABILITY AT 134.5°C	50 MINUTES
EXPLOSION AT 134.5°C	5 HOURS
BULK DENSITY	0.94 gm/cc
BURNING SURFACE PER POUND	2,373 SQUARE INCHES

Figure 43. CIL 1407C Characteristics

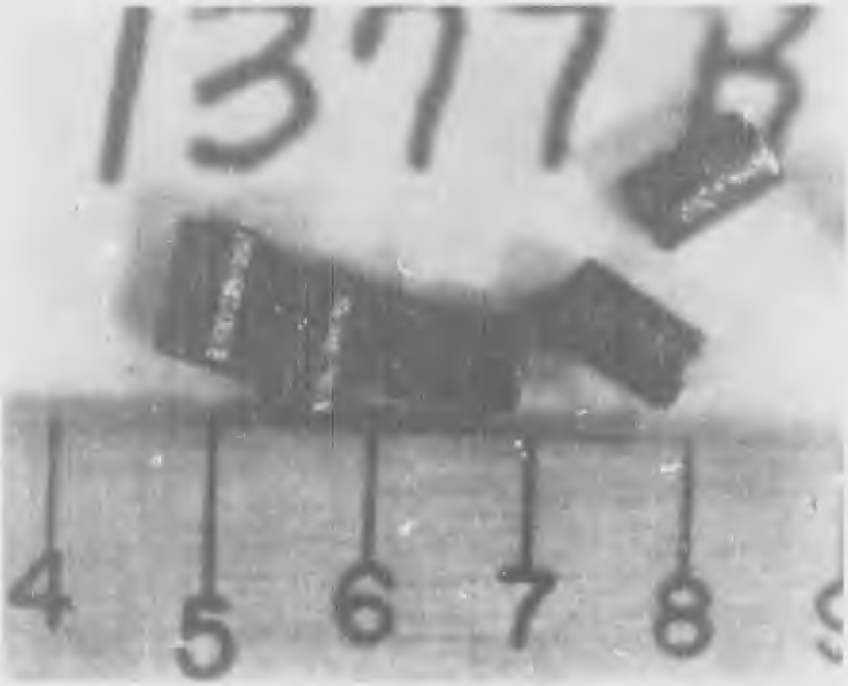

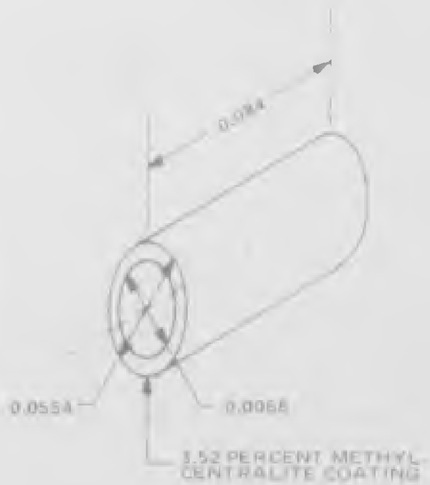

COMPOSITION	PERCENTAGE
METHYL CENTRALITE	3.52
DIPHENYLAMINE	0.87
POTASSIUM SULFATE	0.65
LEAD CARBONATE	0.83
NITROCELLULOSE	94.13
PROPERTIES	
STABILITY AT 134.5°C	40 MINUTES
EXPLOSION AT 134.5°C	5 HOURS
BULK DENSITY	0.96 gm/cc
BURNING SURFACE PER POUND	1,974 SQUARE INCHES

Figure 44. CIL 1377B Characteristics

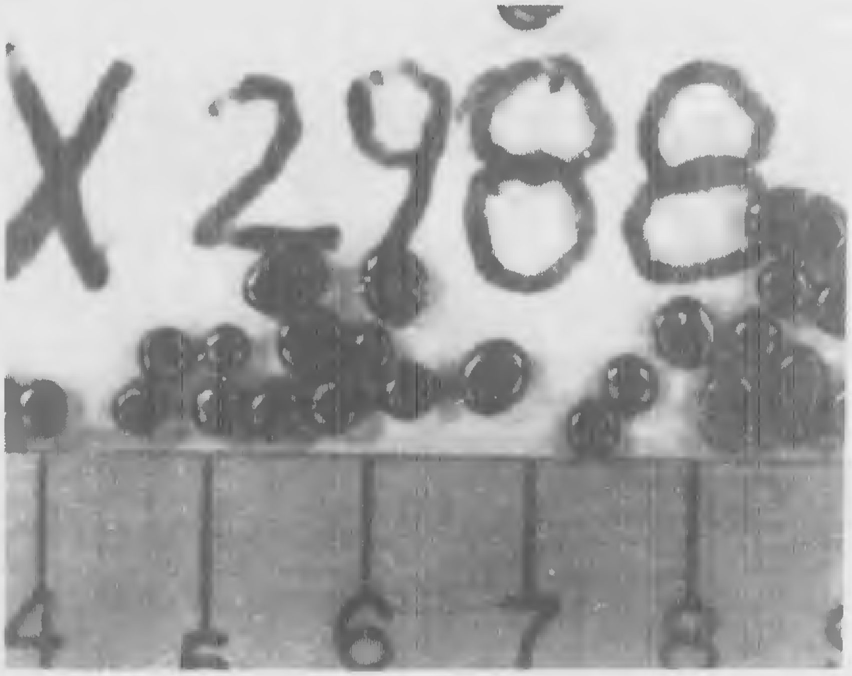

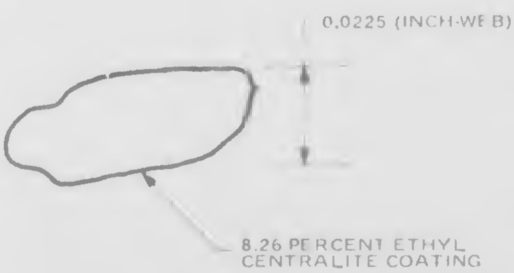

COMPOSITION	PERCENTAGE
NITROGLYCERINE	9.65
ETHYL CENTRALITE	8.26
DEPHENYLAMINE	1.00
NITROCELLULOSE	77.35
MISCELLANEOUS	3.74
PROPERTIES	
(EXPECTED) STABILITY AT 120.5°C	50-60 MINUTES
RUN FOR 300 MINUTES	(NO EXPLOSION)
BULK DENSITY	987 gm/cc

Figure 45. Olin X2988 Characteristics

TABLE X. HIGH TEMPERATURE STORAGE (8 DAYS)

Propellant	+160°F		Cooled to +70°F	
	Pressure (Crusher)	Velocity (fps)	Pressure (Crusher)	Velocity (fps)
1377B	60,400	3,007	62,100	3,002.6
1407C	–	–	59,000	2.952.0

These results suggest possible temperature instability of the propellant. The 1377B and 1407C were subsequently removed from additional rounds and weighed. The propellant charges were several tenths of a gram less than the 35.0-gram charges reportedly loaded. In several cases, this decrement amounted to about 1.0 percent of the total weight. It is interesting to note that 1.0 percent of the propellant by weight had been lost in drying of one- to two-gram samples of propellant in laboratory tests.

4. Conclusions

Primer ignition of propellants has been adequate to obtain consistent results. Ignition traces, however, have been somewhat erratic and merit some study to assess possible ignition difficulties with the highly inhibited propellants.

Propellant gas erosion of the gun does not appear excessive. The candidate propellants are so highly inhibited that the flame temperatures are low (<2,850°K) and reasonably nonerosive.

The CIL 1377B propellant appears to have the highest velocity capability if the pressure and velocity deviations could be decreased. The vendor stated that the standard deviations obtained for 1377B are larger than he has been getting with similar propellants and expressed the belief that future lots of the propellant would exhibit much less dispersion.

A disadvantage of 1377B is the possibility of unsatisfactory long-term storage. The vendor noted that CIL propellants have been subjected to short-duration tests at 150°F and that the Military-Standard-required 150°F storage over a period of 30 days may be too severe for the CIL propellants.

The CIL 1407C propellant showed less pressure-velocity variation but provided a higher average pressure and calculated $\overline{P}$ for the same velocity than CIL 1377B. The bulk loading density of CIL 1407C was lower than either of the candidates so that the charge weight would be lower by 1/2 to 1 gram.

The Olin X2988 showed a **smallest standard** deviation of pressure and velocity and had the highest bulk loading density, which should make it possible to load as much as 36.5 grams into the case instead of 35.5 grams for 1377B and 35.0 grams for 1407C.

a. Safety

The propellants under consideration are single and double base and can be handled according to existing codes. No safety hazards other than those normally defined for gun propellants is anticipated.

b. Reliability

The Olin propellant performed quite reliably in pressure/velocity tests when tested against the standard M55 round, which is an excellent reference round. In the series of 20 tests, the SAPHE round performed as well as the standard in terms of shot-to-shot pressure and velocity variations. The CIL propellant pressure and velocity deviations are about double those of X2988.

	GFE (Standard 20mm M55)		SAPHE D Propellant Round	
	$\overline{P}$	σ	$\overline{P}$	σ
Reference Pressure	51,000	1,500	--	--
Measured Pressure	51,0002	1,446	50,600	1,426
Reference Velocity	3,387	11	--	--
Measured Velocity	3,389	16	2,875	9

The 90 percent confidence levels on the copper-crusher pressure mean for each propellant, based upon 20 pressure/velocity tests, was calculated. The true mean pressure is expected to lie between the following minimum and maximum pressures at 90 percent confidence level:

Propellant	Minimum Pressure	Mean	Maximum Pressure
CIL 1377B	49,000	50,600	52,200
CIL 1407C	51,700	52,900	53,100
Olin X2988	49,500	50,600	51,500

The performance test data can also be used to estimate the maximum charge weight and maximum velocity for each propellant system. The charge weight establishment curves are presented in Figures 46, 47, and 48. To aid in charge weight determination, two 3-sigma limit lines have been added to these curves. If the standard deviation is assumed to vary negligibly with charge weight, it can be determined for a given sample of tests whether pressures will exceed the maximum of 60,500 psi (copper crusher) and whether velocities will fall below 2,850 fps. The results of this study are summarized in Table XI. In all cases, the maximum charge weight for the M103 case was exceeded before the pressure limit (70,500 piezo gage) was reached.

TABLE XI. MAXIMUM GUN PRESSURES AND MINIMUM PROJECTILE VELOCITIES EXPECTED FROM CIL AND OLIN PROPELLANT TEST SAMPLES

Propellant	Charge Weight (Grams)	Maximum Pressure (Psi)	Estimated Minimum Velocity (Fps)
CIL 1377B	35.5	58,000	2,870
CIL 1407C	35.0	57,500	2,845
Olin X2988	36.5	58,000	2,900

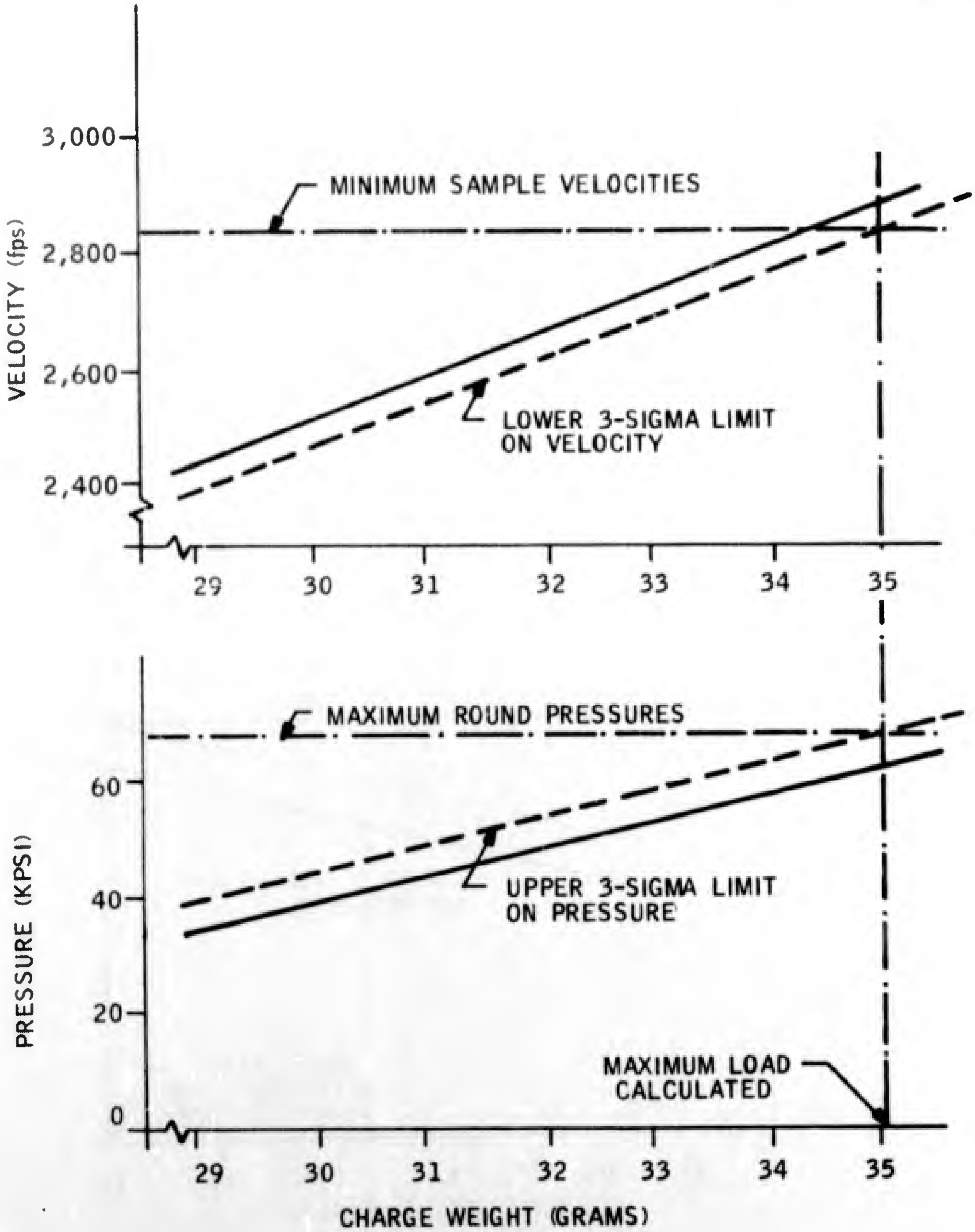

NOTE: PIEZO PRESSURES/VELOCITIES AVERAGE 78 FEET

Figure 46. Pressure and Velocity Versus Charge Weight for CIL 1407C

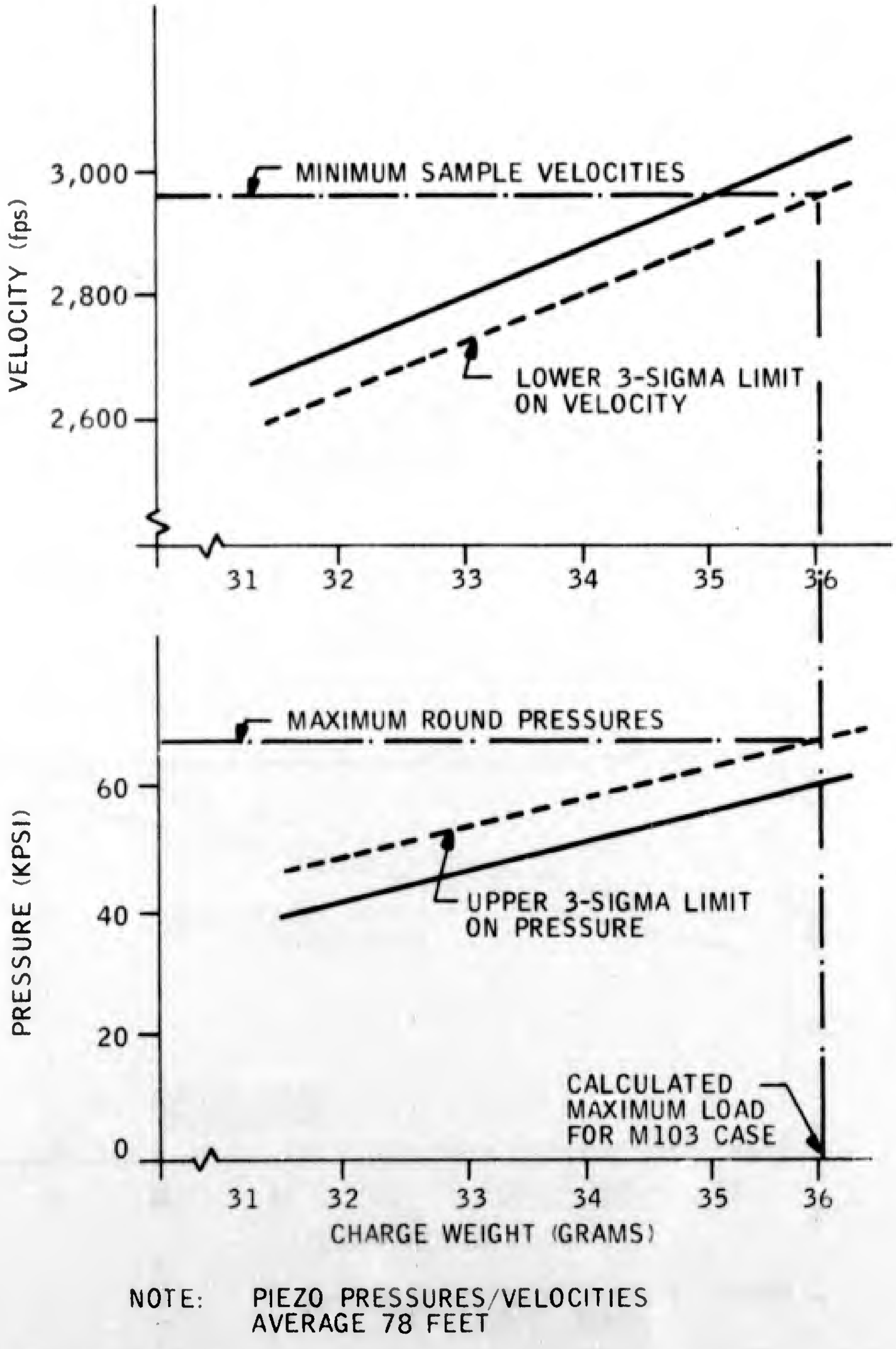

Figure 47. Pressure and Velocity Versus Charge Weight for CIL 1377B

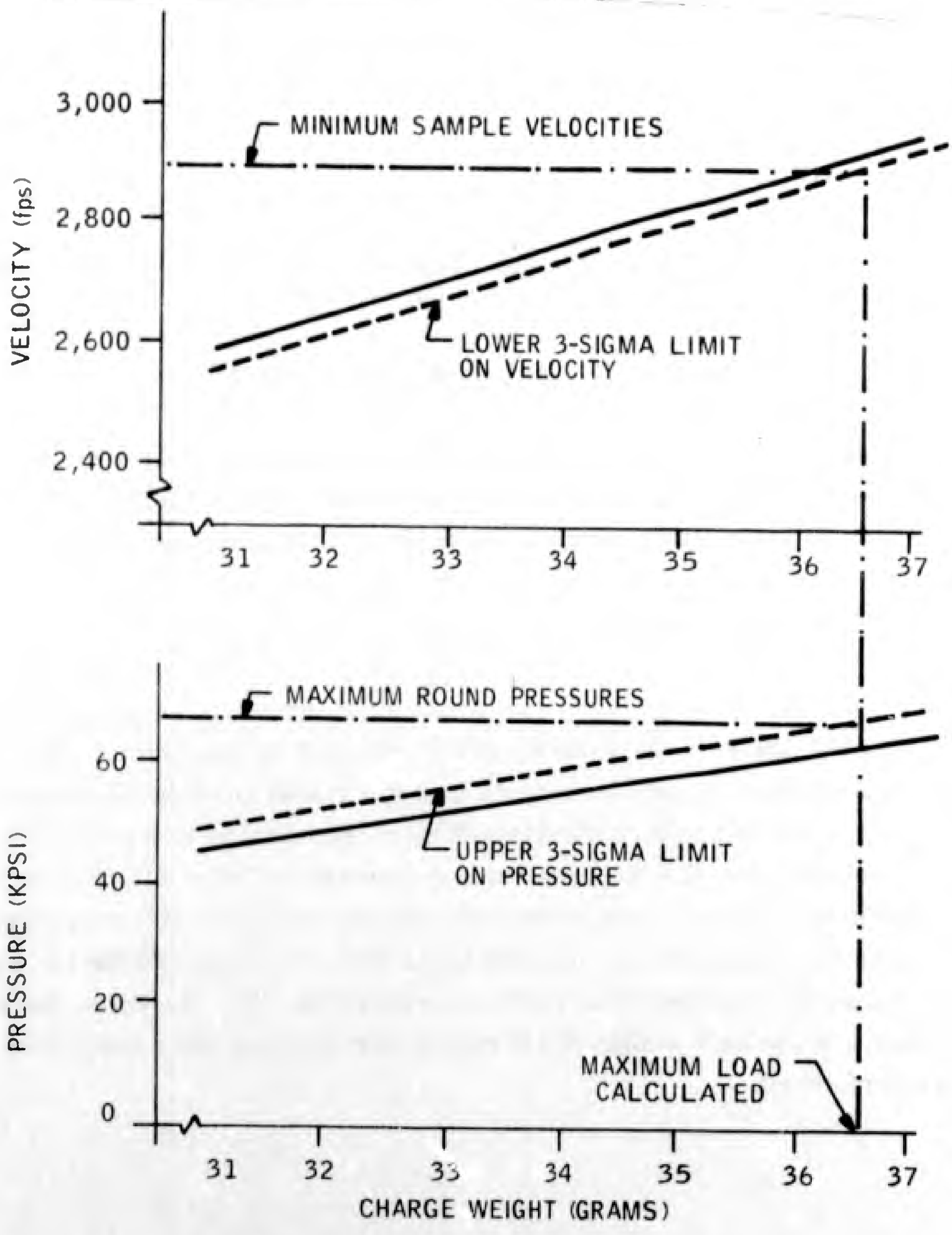

NOTE: PIEZO PRESSURES/VELOCITIES
AVERAGE 78 FEET

Figure 48. Pressure and Velocity Versus Charge Weight for Olin X2988

It was concluded that all three propellants would meet the requirements. X2988 was chosen over the other candidate propellants because of the following:

- It exhibited the least variation in pressure and velocity.
- Ball propellants have a known resistance to damage from rough handling, vibration, and temperature storage.

5. <u>Charge Sizing, Verification and Qualification Tests</u>

Propellant charge sizing, verification, and qualification tests were performed between March and June 1970 on two lots of Olin X2988. (Lot 1 propellant is designated X2988; Lot 2 propellant is designated X2988. 1).

a. Charge Sizing Tests

Lots 1 and 2 were subjected to charge sizing at three charge weights (550, 555, and 560 grains). Pressures, velocities, and action items were recorded with both piezoelectric and copper-crusher pressures obtained for Lot 1. Action times were obtained from oscilloscope traces for Lot 1 and by counters for Lot 2. Data are summarized in Table XII, and curves for pressure, velocity, and action time versus charge weight are presented in Figure 49. Included on the graph along with the sizing results for Lot 1 are data points obtained from previous tests of this lot. Based on these results, a propellant weight of 555 grains was selected and verification tests were performed.

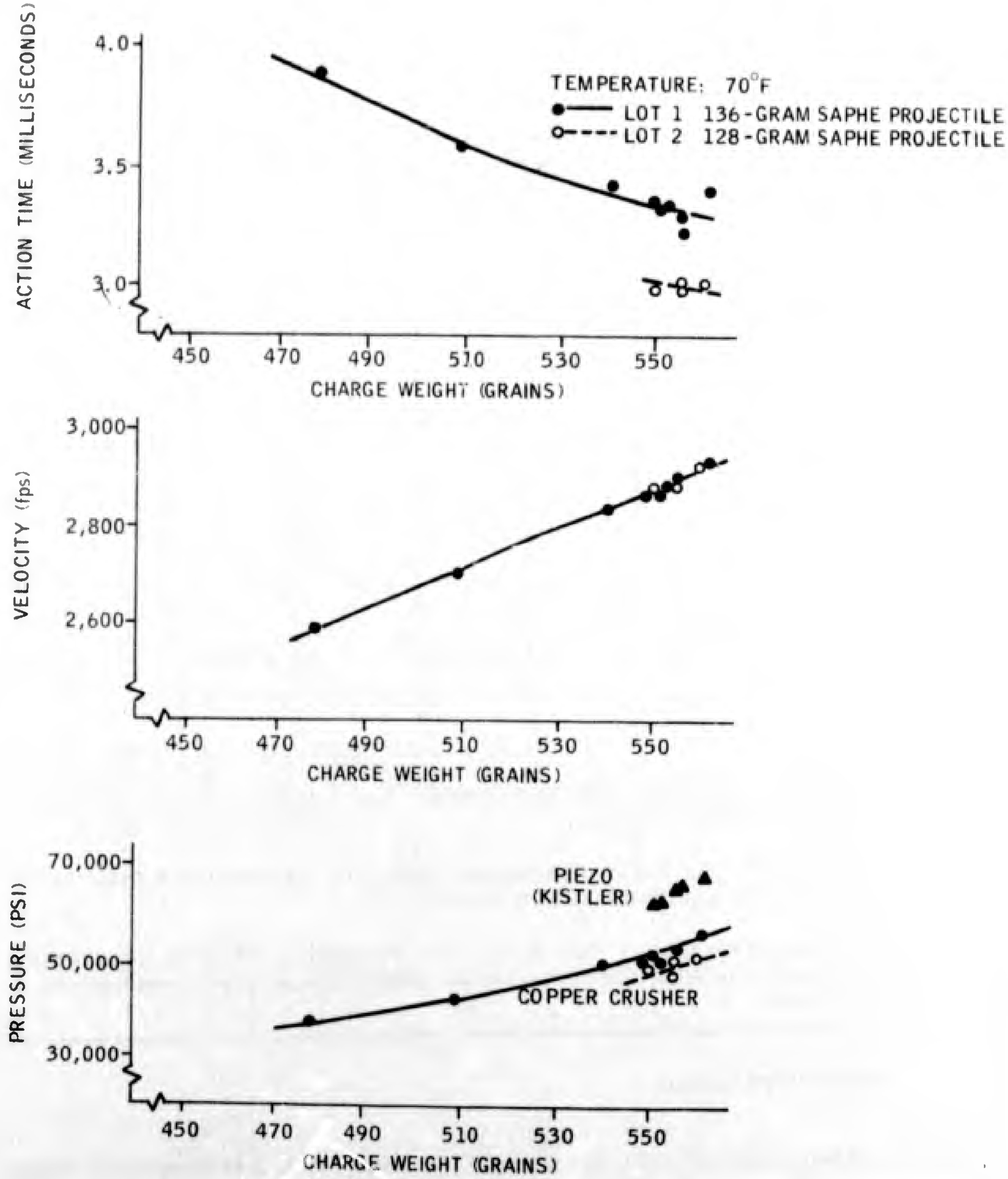

Figure 49. Action Time, Velocity and Pressure Versus Charge Weight (Olin X2988)

TABLE XII. SIZING TESTS[a] (LOTS 1 AND 2)

	Charge Weight (Grains)					
	550		555		560	
	Lot 1	Lot 2	Lot 1	Lot 2	Lot 1	Lot 2
Velocity (fps)[b]	2,876	2,886	2,894	2,897	2,928	2,931
Velocity Standard Deviation (fps)	15	38.4	8	17.5	16	18
Pressure (piezo) (kpsi)	61.9	NA	64.4	NA	67.6	NA
Pressure (crusher case) (kpsi)	49.7	49.2	51.4	50.8	54.2	51.1
Pressure Standard Deviation (crusher)	2.5	6.1	0.8	1.46	3.2	2.26
Action Time (milliseconds)	3.34	3.00	3.24	3.04	3.24	3.02
Action Time Standard Deviation (milliseconds)	c	0.014	c	0.024	c	0.062
Number of Rounds	5	5	5	5	5	5

a A 2,100-grain projectile was used for Lot 1 tests and a 1,970-grain projectile for Lot 2 tests.

b Corrected on the basis of pressure and velocity averages estimated from a set of standard 20mm rounds.

c Because action time scope data were extremely difficult to analyze, standard deviations estimated from these results were considered inaccurate.

b. Verification Rounds

Results of verification tests performed for Lots 1 and 2 at propellant loads of 555 grains are reported in Table XIII. In these tests, the copper crusher pressures obtained for the larger sample were different from those of the sizing tests. The Lot 1 average pressure rose about 3 kpsi to 54.7 kpsi. When the effects of pressure standard deviation and variations of pressure expected with temperature were considered, it was decided that the Lot 1 propellant loads should be reduced to 552 grains for the qualification tests discussed in subparagraph c. Average pressures for Lot 2 propellant dropped about 2 kpsi, to 48 kpsi. Average velocities and action time results for verification rounds generally agreed with those observed for the charge sizing tests.

TABLE XIII. VERIFICATION ROUNDS OF OLIN X2988 (LOT 1 AND LOT 2), 555 GRAINS, IN PGU-2/B (+70°F)

	Lot 1	Lot 2 [a]
Mean Velocity (corrected) (fps)	2,911	2,908
Velocity Range (fps)	2,868 to 2,912	2,860 to 2,921
Velocity Standard Deviation (fps)	8	20.6
Mean Peak Pressure (crusher), (kpsi)	54.7	48.0
Pressure Standard Deviation (kpsi)	1.6	2.2
Action Time (milliseconds)	3.3	3.0
Action Time Standard Deviation (milliseconds)	NA	0.055
$t + 4\sigma_t$	NA	3.22
Number of Rounds	10	10

[a] Tests performed with 1,970-grain

c. Qualification Pressure Velocity Tests

Samples of 20 rounds, each loaded with 552 grams of Lot 1 X2988, were evaluated at 165°F, 70°F, and -65°F. Results of these tests are summarized in Table XIV. The average peak pressures, velocity, action time, and action time plus four standard deviations have been plotted in Figure 50.

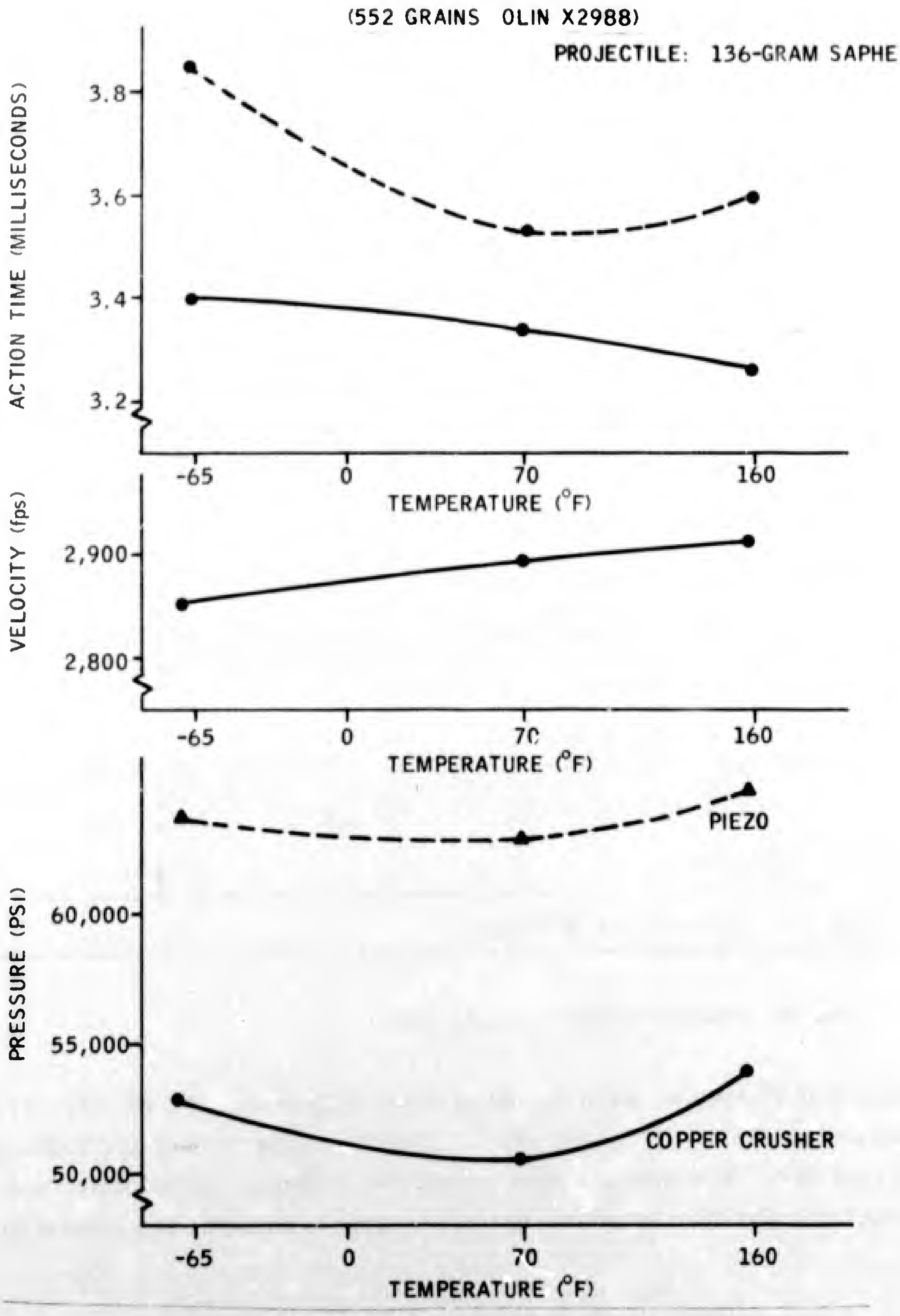

Figure 50. Action Time, Velocity, and Pressure Versus Temperature

Qualification test results indicate that Lot 1 propellant met the requirements specified for the 20mm PGU-2/B program.

TABLE XIV. PERFORMANCE OF OLIN X2988 (552 GRAINS) IN PGU-2/B

	+160°F	+70°F	-65°F
Mean velocity (corrected[a]) (fps)	2,915	2,891	2,852
Range of velocities (fps)	2,881 to 2,935	2,868 to 2,912	2,823 to 2,901
Velocity standard deviation (fps)	11	13	20
Mean peak pressure (piezo) (kpsi)	64.9	62.5	63.8
Mean pressure (corrected copper crusher) (kpsi)	54.5	52.3	54.4
Pressure standard deviation (crusher) (kpsi)	1.5	1.8	3.6
$\overline{P} + K(\overline{R})$ (crusher) (kpsi)	58.0	55.8	60.1
Action time (milliseconds)	3.27	3.34	3.40
Action time standard deviation (milliseconds)	0.08	0.05	0.11
$t + 4\sigma_t$	3.60	3.53	3.85
Number Rounds	20	20	20

[a] Mean velocities and pressures are corrected based upon velocities and pressure measured for selected reference rounds.

Copper crusher pressure averages for Lot 1 ranged between 52.3 and 54.5 kpsi over the temperature range (160° to -65°F). The high pressures measured were at the temperature extremes. Standard deviations of the pressures were also largest at the temperature extremes, with the greatest variations at -65°F, resulting in statistical parameter $\overline{P} + K(\overline{R})$ being 60.1 kpsi. From this it is concluded that X2988 meets the pressure requirements not only at ambient temperature but at the temperature extremes as well.

Velocities varied from 2,852 fps to 2,915 fps over the temperature range with a mean velocity at 70°F of 2,891 fps. If three standard deviations are considered to contain the population of velocities, the lowest velocity expected at 70°F would be 2,852 fps, which is above the minimum PGU-2/B velocity required (2,850 fps).

Action times were within the specified limits. The largest value of action time plus four standard deviations occurred at -65°F. and was 3.85 milliseconds below the upper limit of 4.0 milliseconds specified for 20mm ammunition.

d. Performance

Two lots of X2988 were subjected to performance test and found to meet the requirements. These are summarized in Table XV.

TABLE XV. PERFORMANCE TEST RESULTS, X2988 AND X2988.1

Requirement or Goal	Performance	
	Lot 1 (X2988)	Lot 2 (X2988.1)
Pressure (P + K(R)) ≤ 60,500	55.8	NA[a]
Velocity mean greater than 2,850 fps	2,891	2,908
Minimum velocity greater than 2,850 fps	2,868	2,860
Velocity range of 80 fps	2,868 to 2,912	2,860 to 2,921
(V ± 40 fps	(ΔV = 44)	(ΔV = 61)
Standard deviation of velocity 40 fps	13.0	21.0
Action time plus 4 standard deviations at -65°F. ≤ 4.0 milliseconds	3.85	NA
Number of tests	20	10

[a] Number of tests per sample was too small for estimate of this parameter.

D. SAFE/ARM AND FUZING SYSTEM

1. System Description

The SAPHE fuze must:

- Be safe before and during launch.
- Arm after launch.
- Be graze sensitive to 80-degree obliquity against 1/4-inch RHA.
- Be sensitive to impacts normal to a target.
- Delay function 0.21 millisecond.

Figure 51 shows the fuze before arming. The firing pin nests inside a rotor recess to lock the rotor prior to firing the round, while a crush washer supports the firing pin through the inertial weight. A rotor detent spring also locks the rotor in the out-of-line position.

Setback forces during launch permanently deform the setback washer under the combined weights of the firing pin, firing pin spring, and the inertia weight. With the setback washer deformed, the firing pin moves back and unlocks the rotor relative to the firing pin. Centrifugal force caused by projectile spin opens the rotor detent spring, removing the second restraint on rotor movement as in Figure 52. After forward acceleration terminates outside the bore, the last restraint (friction) on rotor movement is removed, and centrifugal and gyroscopic spin forces cause the rotor to align the detonator with the firing pin. During setback the tip of the firing pin does not entirely clear the rotor surface but remains in a slot in the rotor to allow the firing pin to track to the in-line position, i.e., the arming path is predetermined for more precise control of the arming function of the rotor.

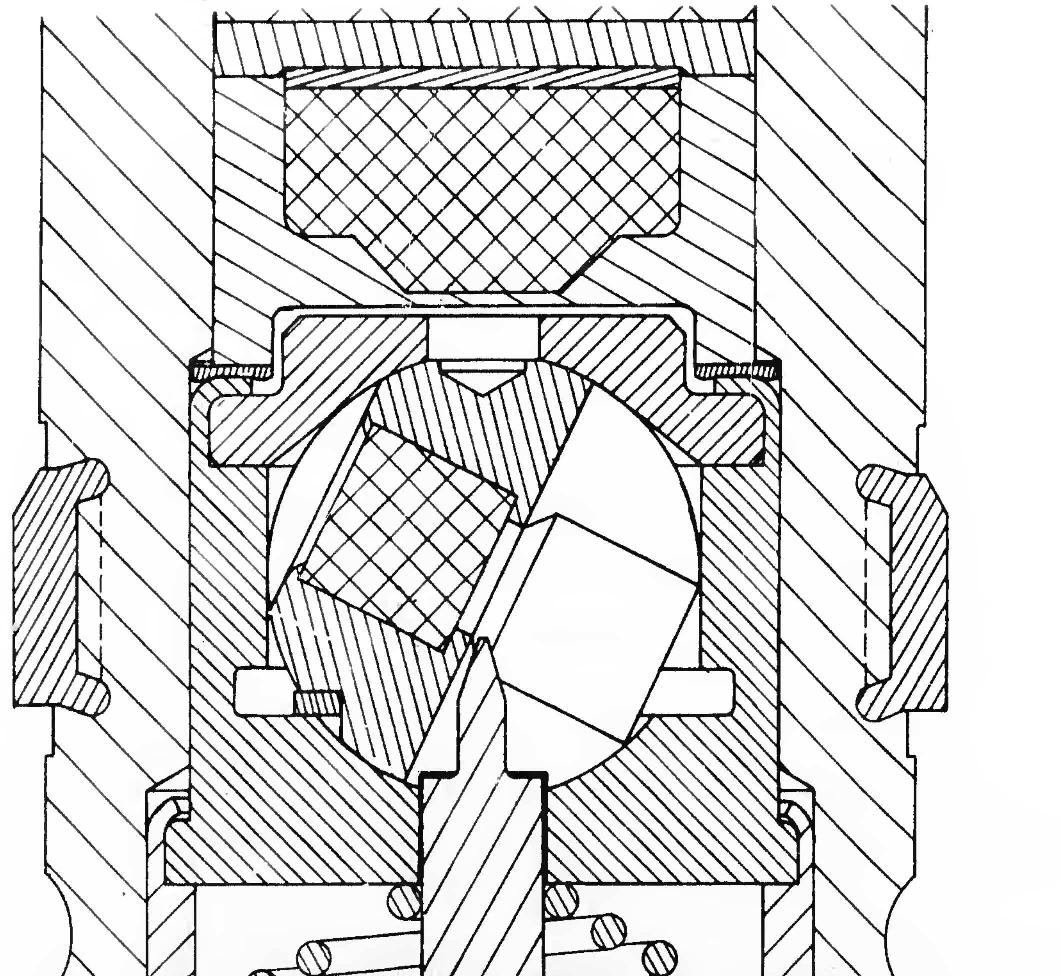

Figure 51. S&A Before Arming

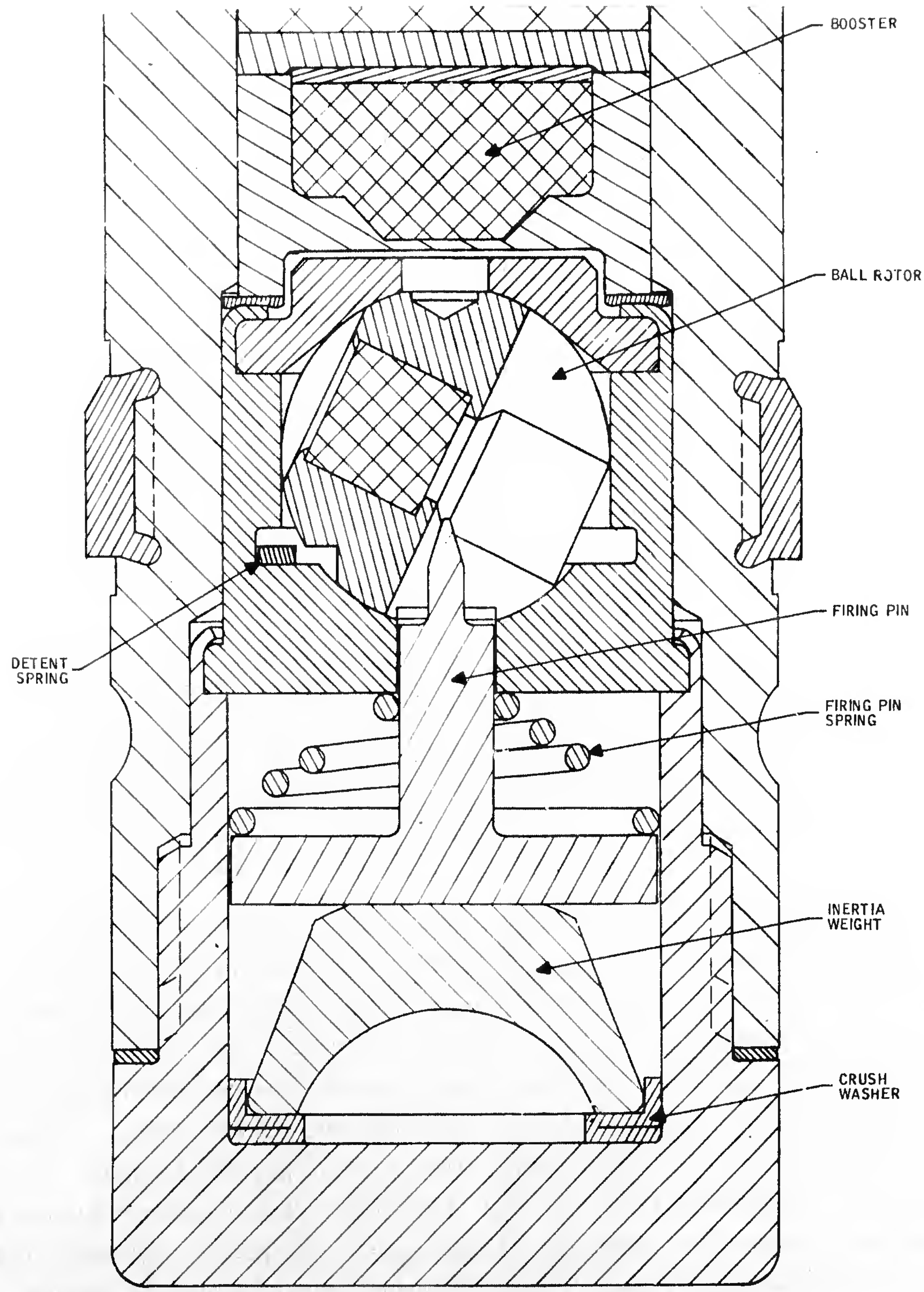

Figure 52. S&A System After Setback

For proper fuze functioning the inertia weight-firing pin combination must remain stable in flight (the inertia weight must not tip because of projectile spin, causing the firing pin to press into the detonator before impact) and yet must be sensitive to impacts at various obliquities. After setback the firing pin is constrained by the firing pin bias spring so that normal flight forces do not cause movement of the firing assembly.

Fuze function occurs in either of two ways. In normal impact of the projectile with a target the firing pin and inertia weight move forward under the force of deceleration, the firing pin penetrates the detonator, and warhead function is initiated. In oblique impact of the projectile with a target, a transverse component of force is added to the axial component and the inertia weight tips to drive the firing pin forward into the detonator as shown in Figure 53.

Two other fuzes were also investigated, one of smaller diameter to fit the thick wall warhead (see paragraph A) and one of shorter length so more explosive could be carried in the warhead. The fuze for the thick wall projectile is shown in Figure 54. Its operation is entirely similar to that of the fuze for the thin wall warhead.

Figure 55 shows the shorter alternate fuze before arming. Function is essentially the same as in the standard fuze except that the spring which holds the firing pin away from the detonator during flight is replaced by a system of 1/16-inch-diameter steel balls. On setback these move aft with the firing pin to a position opposite a groove in the inner fuze wall, and the spin-induced centrifugal force drives each ball into the groove so that the total is sufficient to guarantee a stabilizing force to prevent premature function. As both the destabilizing force and the stabilizing force supplied by this mechanism are proportional to the spin rate squared, the mechanism is self-compensating for spin decay. On either graze or normal impact, spin will decay and the inertia weight and firing pin can move forward to cause fuze function.

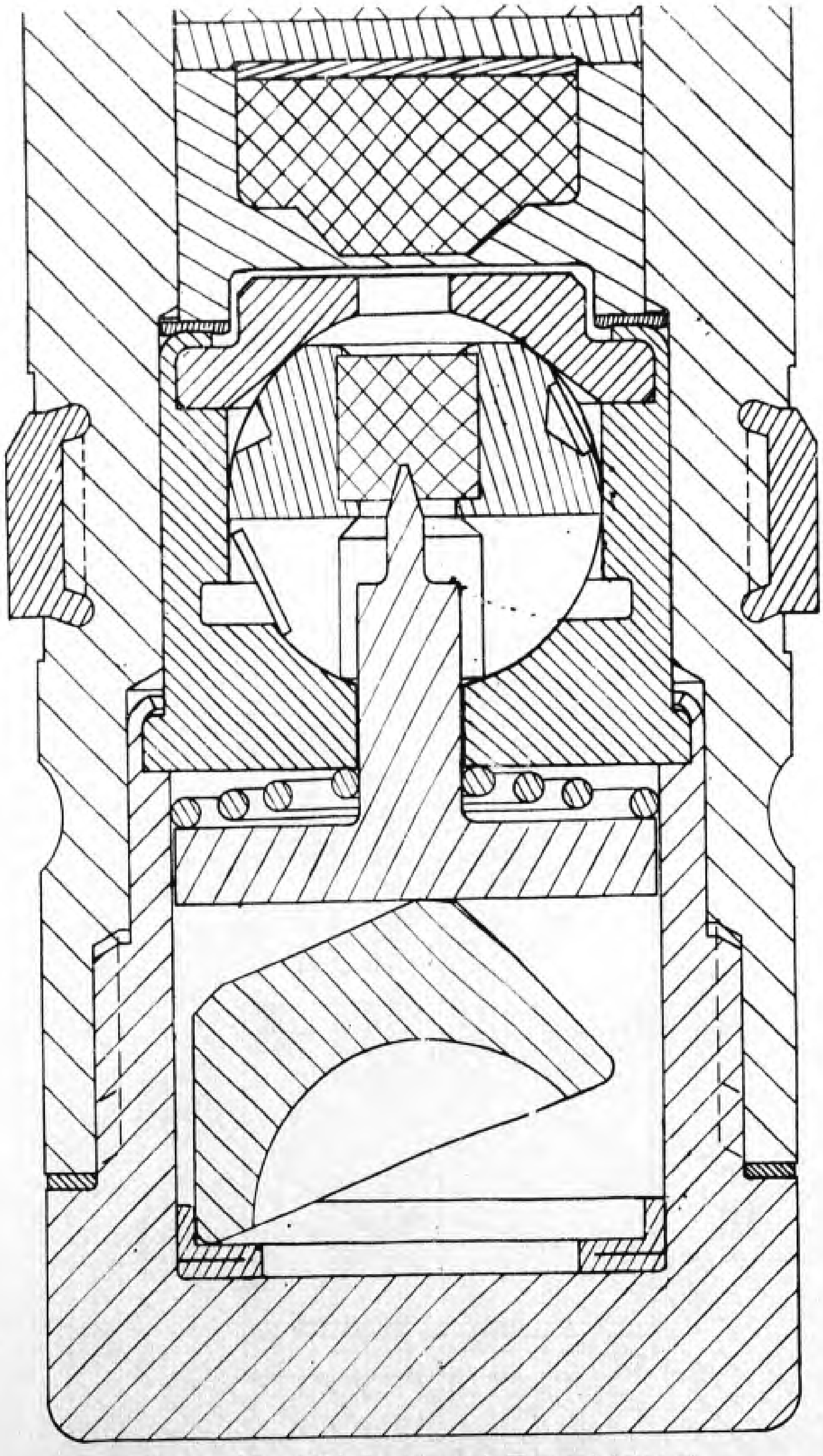

Figure 53. S&A System at Target Impact

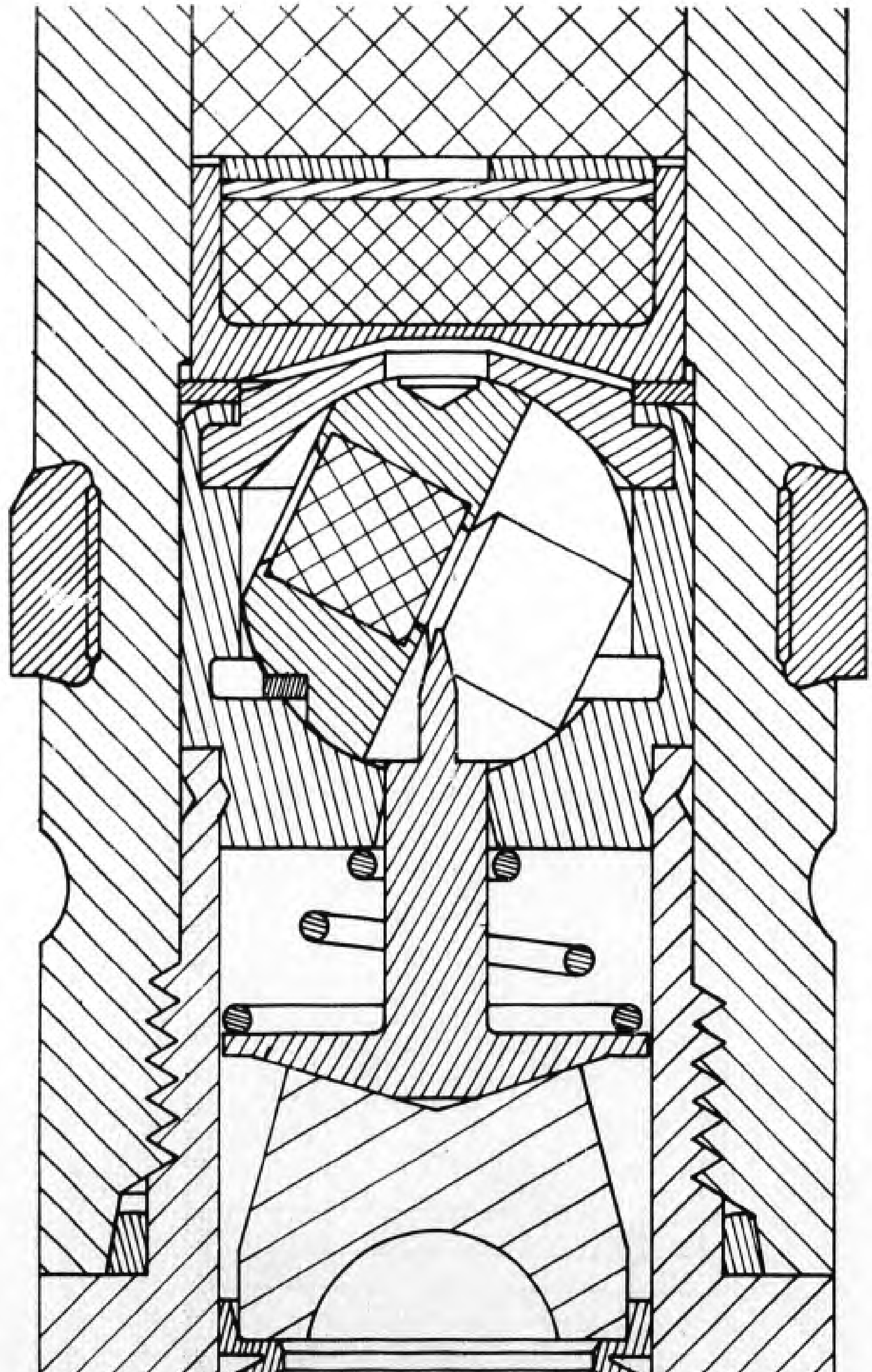

Figure 54. S&A for Thick-Wall Projectile

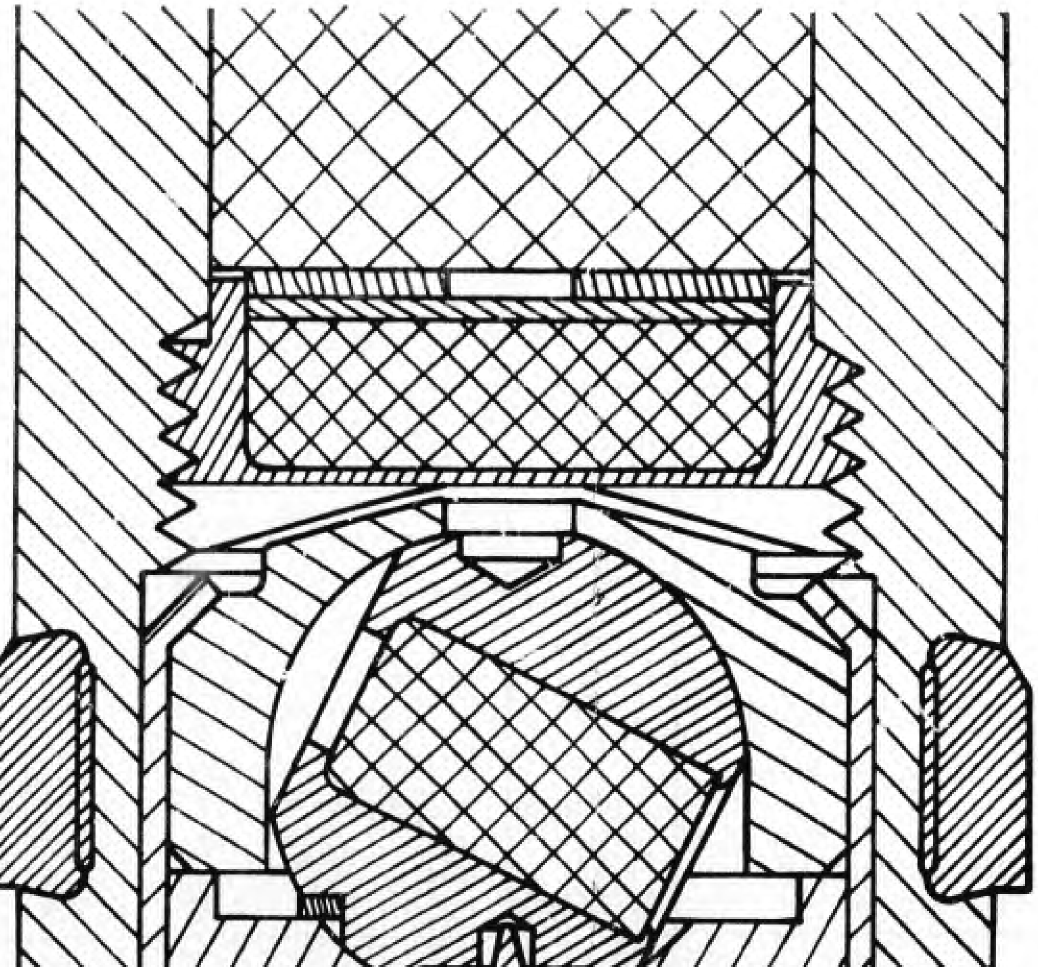

Figure 55. Short Fuze Before Arming

2. Analytic Results

a. Short Fuze

Table XVI shows the calculated mass data for the short fuze.

TABLE XVI. MASS DATA FOR SAPHE MINIATURE FUZE AND PROJECTILE WITH MINIATURE FUZE

Description	Fuze Alone	SAPHE With Miniature Alternate Fuze Short Version	Long Version
Round Length (inches)	--	3.180	3.405
Weight (pound)	0.0608	0.2612	0.2833
CG from Base (inches)	0.3963	1.1764	1.2950
Axial Moment of Inertia (lb.-in.^{2})	0.003096	0.02119	0.02309
Transverse Moment of Inertia (lb.-in.^{2})	0.005839	0.1612	0.2007

The short version of the SAPHE projectile (Figure 56) is one with a minimum length behind the rotating band, while the long version has a length equal to that of the SAPHE projectile with the standard fuze. Here the length savings of the miniature fuze has been used to increase the high explosive charge weight by 1.31 gram.

The axial force required to stabilize the inertia weight in flight is a function of:

- The eccentricity of the inertia weight center of gravity with respect to the projectile spin axis, ϵ (inches).
- The projectile spin rate, ω (1/second).

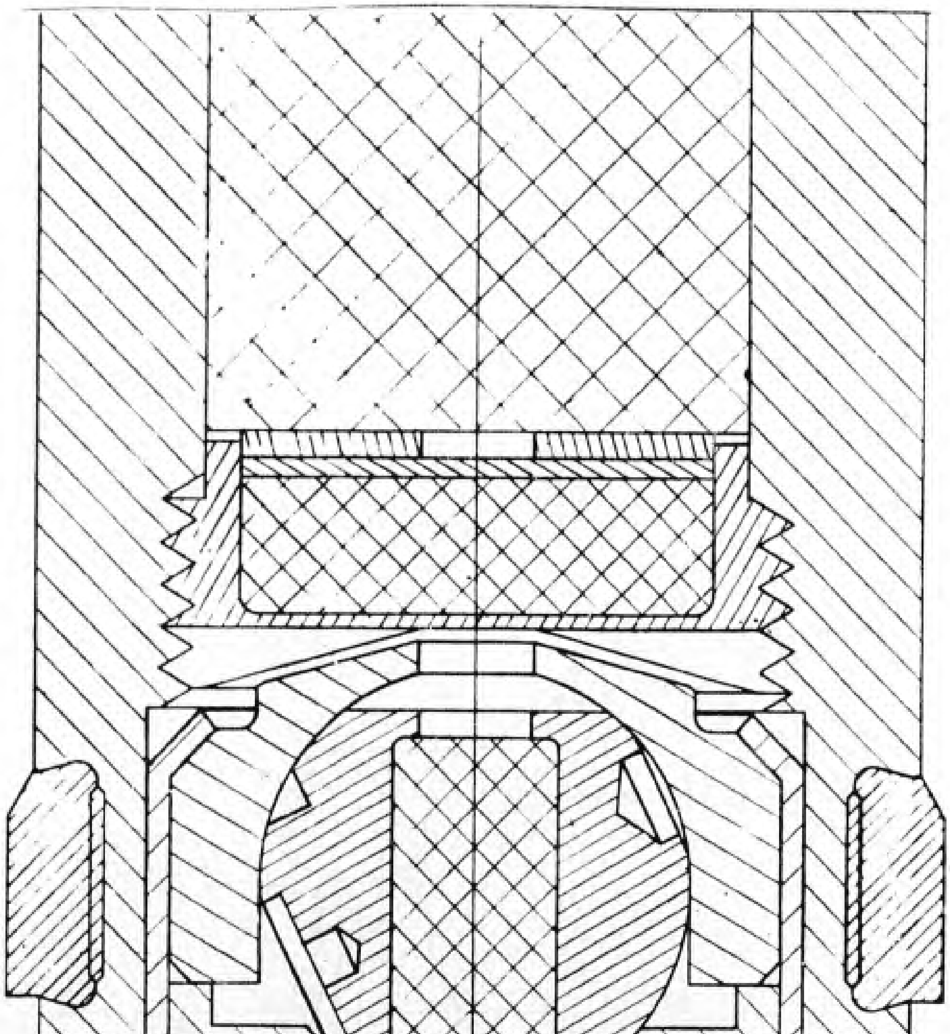

Figure 56. Short Fuze After Arming

- The axial distance from the weight pivot to the center of gravity, A_1 (inches).
- The transverse distance from the weight pivot to the center of gravity, A_2 (inches).
- The weight of the inertia weight, W (pounds).
- The deceleration of the projectile due to drag, g (g).

Figure 57 summarizes the geometry of the problem.

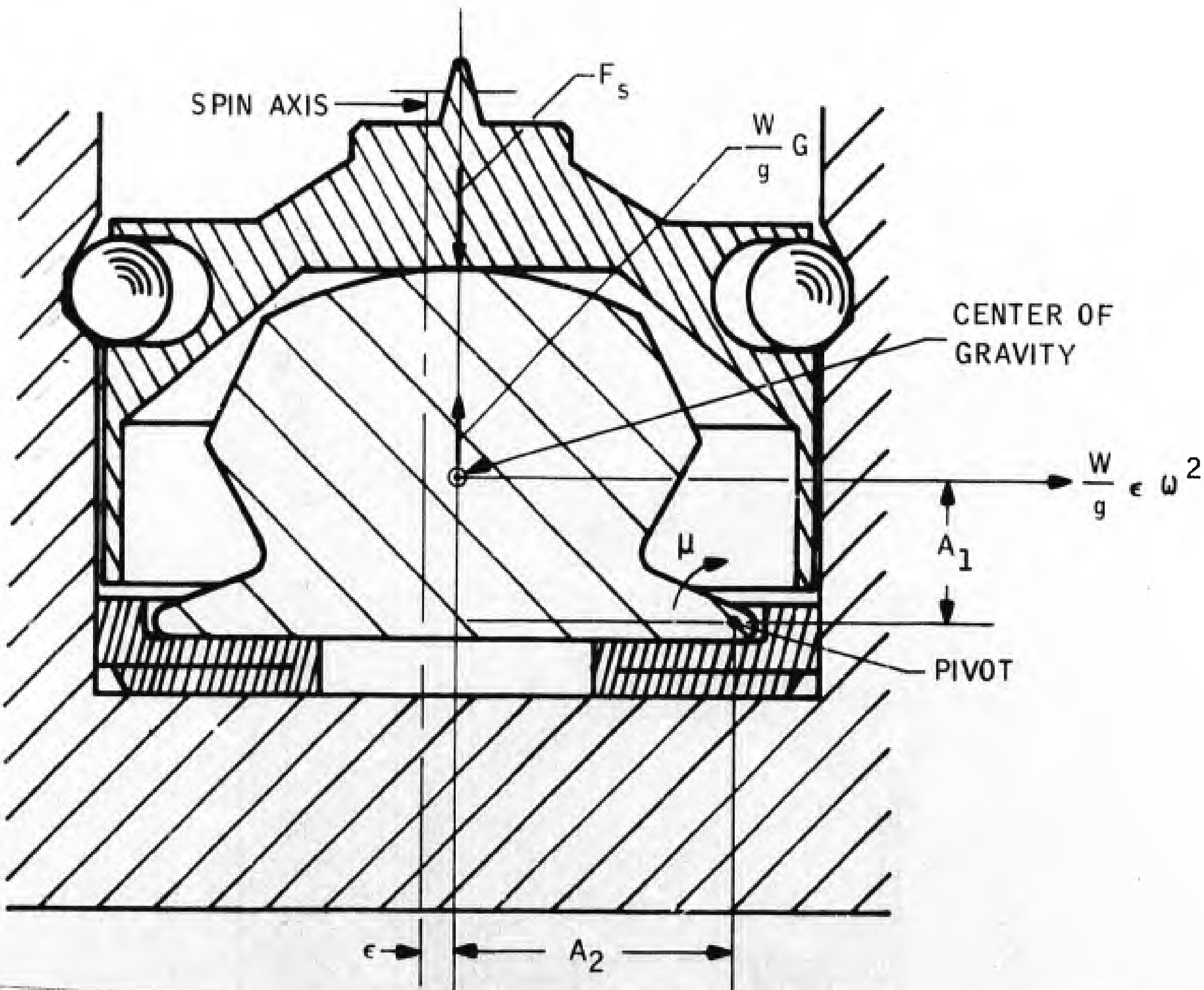

Figure 57. Inertia Weight Stability Model

The minimum stabilizing force, F_S, is that force necessary to maintain a zero moment about the weight pivot point.

$$M_p = -F_S A_2 + gWA_2 + (W\epsilon\omega^2 A_1)/g = 0$$

These parameters, calculated for two inertia weight designs, a prime weight concept (Figure 58) and a more easily stabilized modified weight concept (Figure 59), are summarized in Table XVII.

The value of ϵ was based on 0.008-inch tolerance and concentricity buildup, plus 0.004-inch estimated projectile spin axis displacement from projectile geometric axis.

The determination of the stabilizing force supplied to the inertia weight by the firing pin assembly is based on the centrifugal force applied to each ball by projectile spin. The variables considered are as follows:

- Projectile spin rate, ω (10720/seconds).
- Weight of each ball, W (0.362 X 10^{-4} pounds).
- Distance of ball from spin axis, R (0.0167 feet).
- Ramp angle of fuze wall at level of balls after setback, β (30°).

Figure 60 indicates the relationship between inertia and reaction forces. The solution is:

$$F_i = R_w{}^2 \frac{W}{g} = 2.16 \text{ pounds}$$

$$F_i - F_R \cos\beta = 0$$

$$F_S - F_R \sin\beta = 0$$

$$F_i - \sin\beta - F_S \cos\beta = 0$$

$$F_S = F_i \beta \tan = 1.25 \text{ pounds}$$

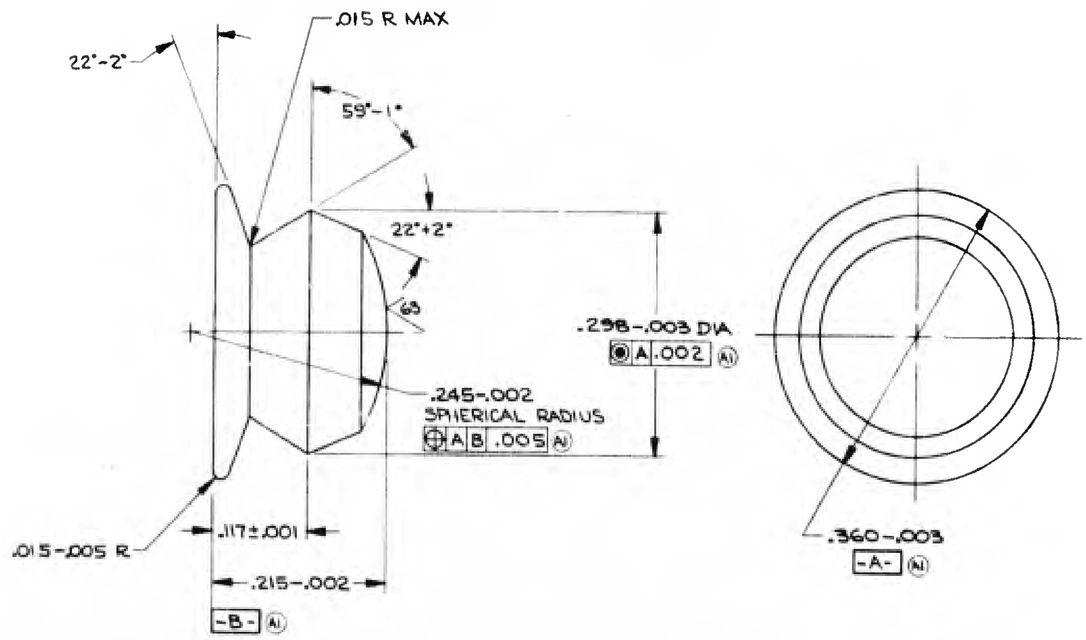

Figure 58. Inertia Weight, Drawing Number 28102861

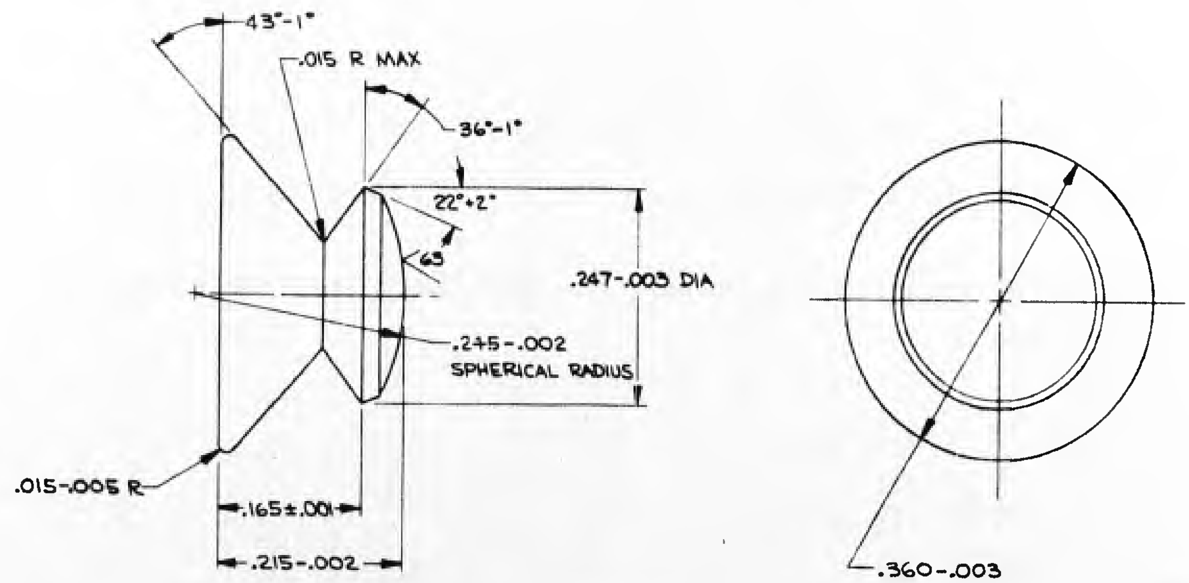

Figure 59. Inertia Weight, Drawing Number 28102862

TABLE XVII. WEIGHT STABILITY CALCULATIONS

	ε (Inch)	ω 1/(Seconds)	A_1 (Inch)	A_2 (Inch)	W (Pound)	G	F_S (Pounds)
Prime	0.012	10,720	0.0809	0.17	0.00334	47	5.84
Modified	0.012	10,720	0.0667	0.17	0.00274	47	3.96

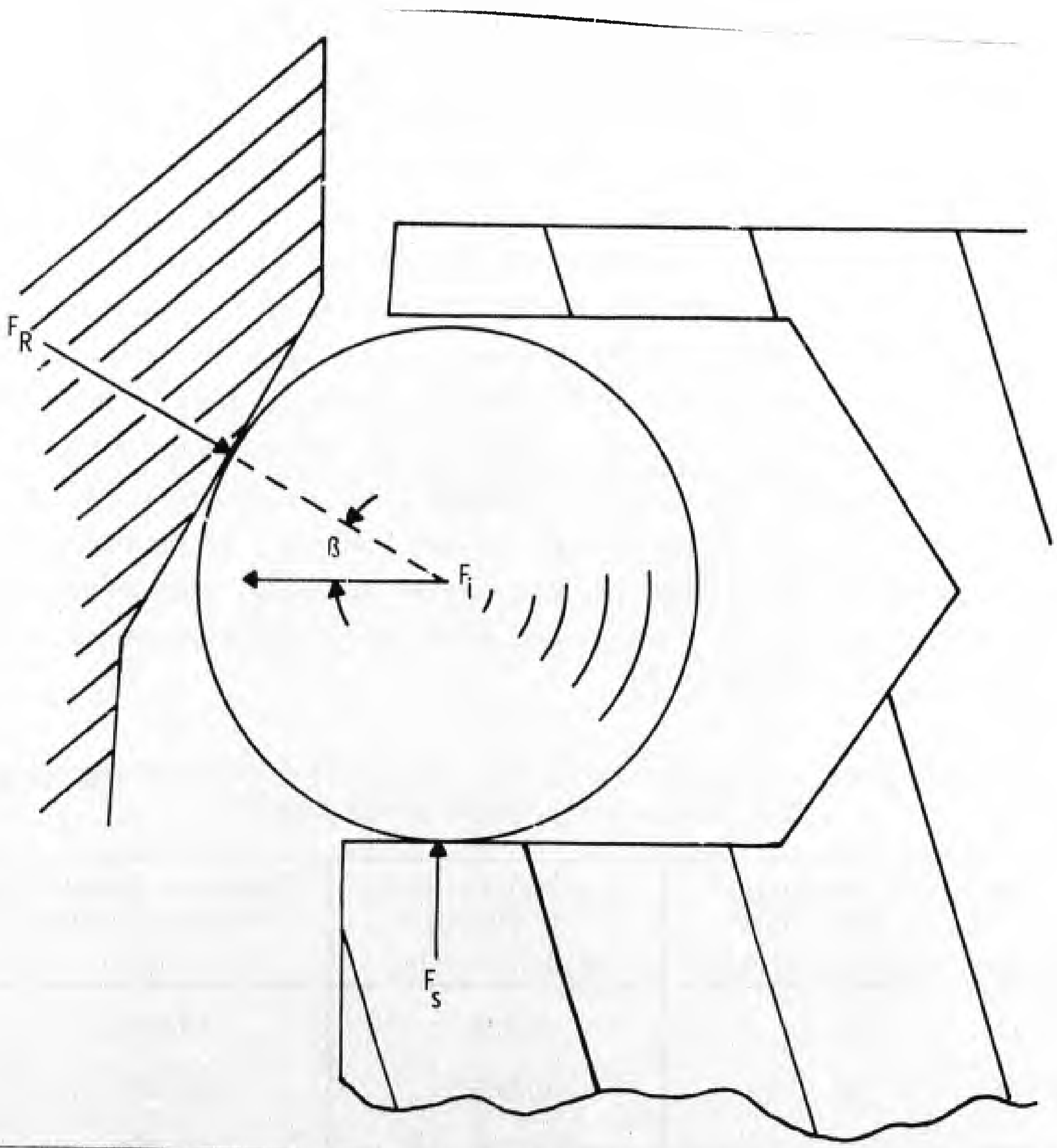

Figure 60. Forces Acting on Firing Pin Assembly Ball After Setback and Spinup

If N is the number of balls per firing pin, the total stabilizing force due to the firing pin is the product of N and F_S since each ball exerts a component of stabilizing force.

b. Graze Impact Function

A mathematical model of SAPHE fuze function on graze impact was developed. This capitalized on the marked similarity in the action of the fuzes under consideration for the SAPHE projectile. In this simulation the geometry, constraints, masses, and moments of inertia of the fuze components were combined with spring force and friction data as inputs to the equations of motion of the movable parts of the fuze. A step integration of these equations was used to simultaneously solve for the angular rate and acceleration of the tipping-inertia weight and the linear rate and acceleration of the firing pin. The driving force for this action was considered to arise from an idealized side acceleration time history for the fuze. This acceleration was calculated by assuming a collision between the projectile and target in which the projectile rebounded at an angle equal to the angle of incidence and at a velocity equal to the incident velocity. By varying the distance over which the projectile was considered to be in contact with the plate, a consistent set of constant acceleration levels and time durations was determined as shown in Table XVIII.

TABLE XVIII. ACCELERATION LEVELS AND TIME DURATION FOR FUZE FUNCTION SIMULATION

Assumed Length of Contact With Plate (Feet)	Assumed Length of Contact With Plate Project Lengths	Time Duration of Acceleration (Milliseconds)	Levels of Acceleration (Assumed Constant) (g)
1.41	5	0.706	15,300
1.13	4	0.565	19,100
0.85	3	0.424	28,500
0.566	2	0.283	38,200

This set of accelerations and time durations was used with the mathematical model to predict the energy available to the detonator at the end of the firing pin stroke. Each of the following four fuzes was analyzed in this fashion: 1) the thin wall standard fuze, 2) the thick wall standard fuze, 3) the miniature alternate fuze, and 4) the miniature alternate fuze with a modified inertia weight. Figure 61 shows the results of this comparison in terms of the energy available to the detonator at the end of the firing pin stroke.

The curve for the miniature fuze with a modified weight reflects the prediction that the function of this fuze is not complete at the termination of the side acceleration. The calculations indicate that in this case the firing pin is not in contact with the inertia weight at the end of its stroke. Therefore, the energy delivered to the detonator is the kinetic energy of the firing pin alone rather than the energy of the inertia weight and firing pin together as in the cases of the other fuzes.

Any one of the data points of Figure 61 reflects sufficient energy input to activate the detonator, as the estimated minimum energy for detonator activation is 0.047 in.-lb. Theoretically, then, the fuze designs will function properly under graze impact conditions.

3. Part Development

a. Inertia Weight

The previous feasibility study of the inertia weight used a mass weight of 0.0035 pound which proved to be impact sensitive to two sheets of 0.050-inch-thick cold rolled steel and to armor plate at 80 degrees obliquity. This weight is shown in Figure 62. Increasing the weight to 0.006 pound made the weight sensitive to one sheet of 0.050-inch-thick cold rolled steel but insensitive to armor plate at 80 degrees. The mass was added by filling the cavity in the base with solder.

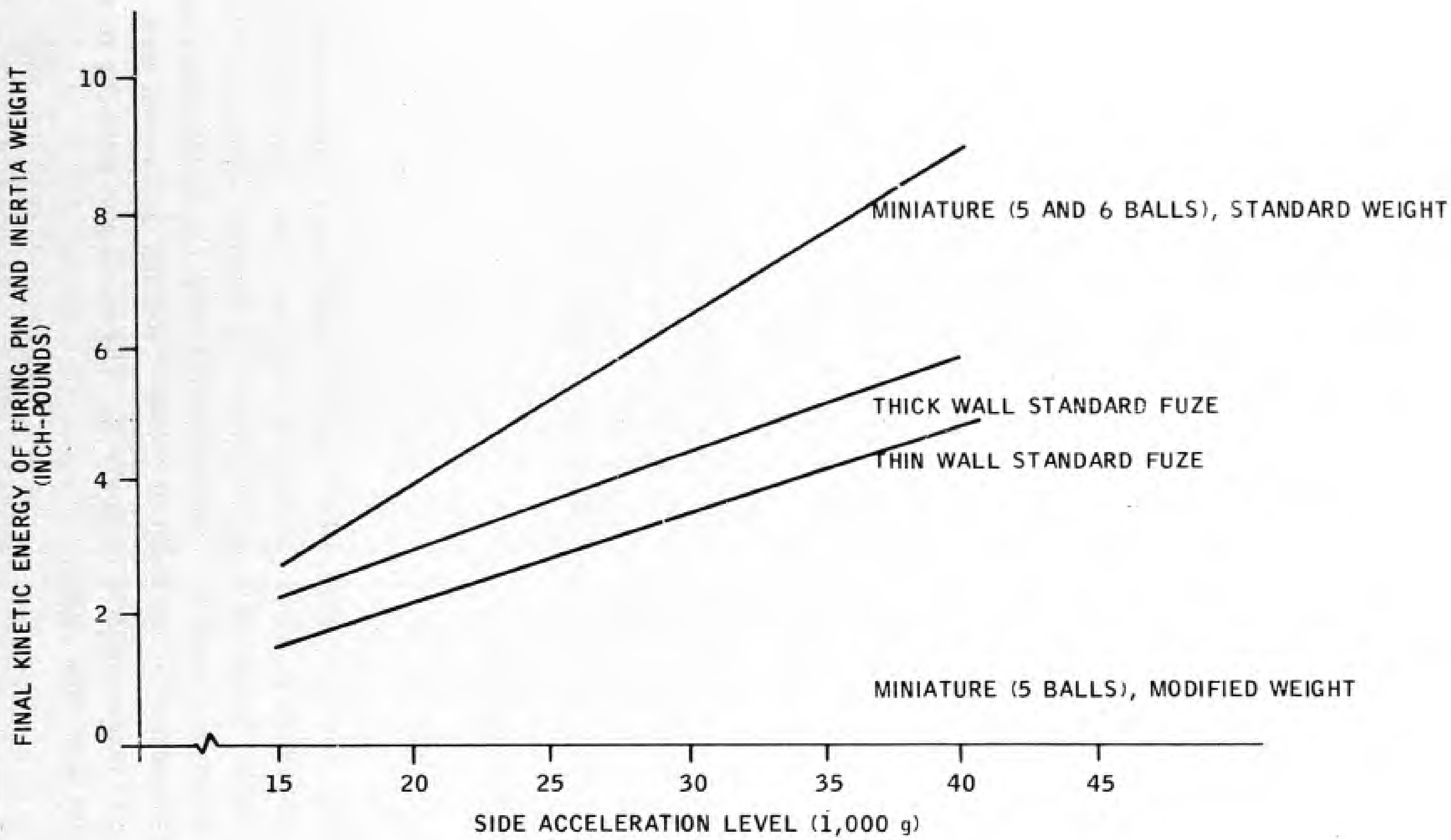

Figure 61. Energy Available to Detonator as a Function of Side Acceleration Level (Coefficient of Friction = 0.15)

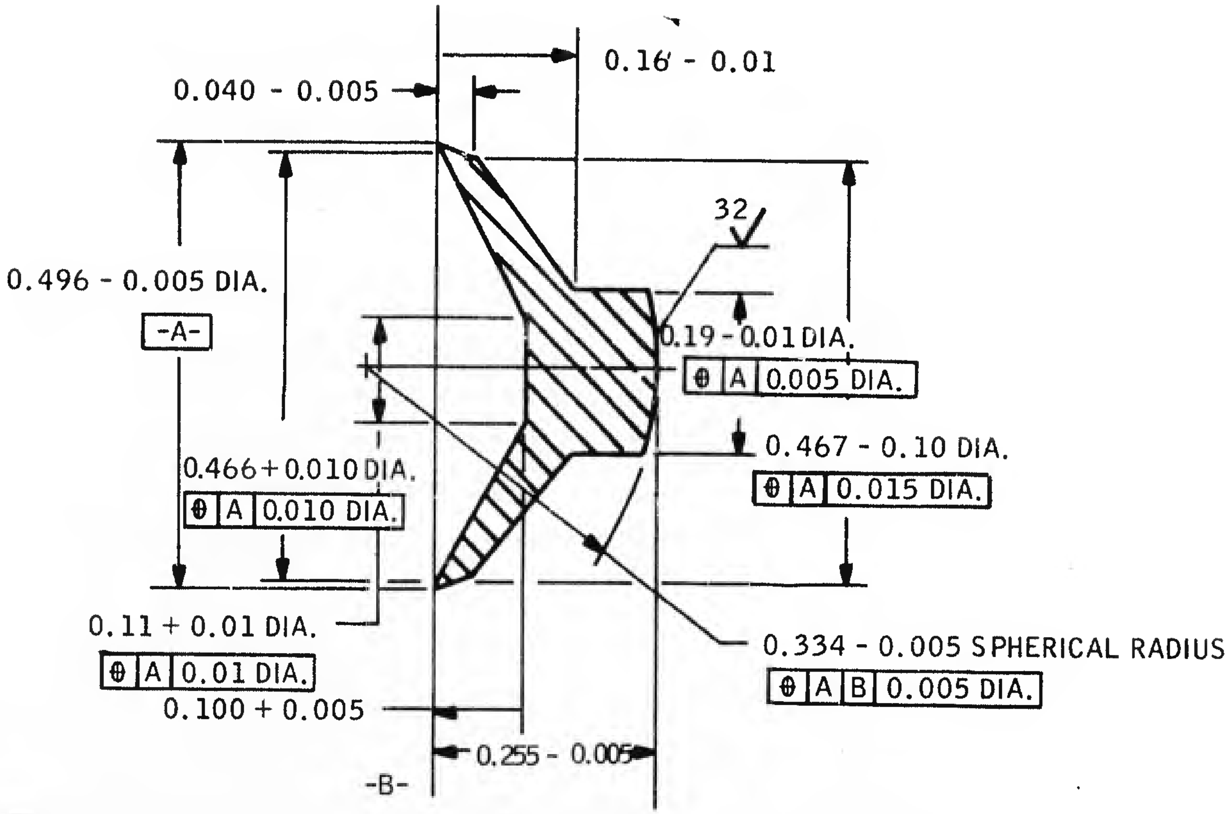

Figure 62. Inertia Weight = 0.0035 Pound

The inertia weight designs were analyzed as follows. The stability characteristic (susceptibility to tipping) of the inertia weight was assumed to be a function of the ratio of axial to transverse moments of inertia (I_{xx}/I_{BB}). On the basis of this assumption, a ratio of less than unity for the weight provides good graze sensitivity, but a ratio of greater than unity is less sensitive to graze because the axial moment, being larger than the transverse, causes a large gyroscopic moment that resists tipping to the angle required.

Based on these characteristics, a new inertia weight design was proposed, but it was found to lack a fixed pivot point for tilting on impact. The clearance between the weight and the fuze wall was minimal, 0.004 inch, and the pivot point changed as the weight increased its tilt angle.

A retainer cup for the inertia weight was introduced to provide adequate clearance for the weight in all tilt orientations. The wall of this cup was approximately 0.020-inch-thick and dictated a change in the maximum diameter of the weight to 0.460 inch.

The new weight (Figure 63) was capable of tilting 23 degrees and moving the firing pin forward 0.105 inch, but Production Engineering advised that a spherical cavity would be easier to produce in the weight, and the necessity of increased projectile wall thickness caused a further shrinkage in weight diameter. The load bearing area of the weight was also increased as a result of the design change. The design shown in Figure 64 has the following characteristics:

Weight = 0.0062 pound

C.G. = 0.119 inch from base

$I_{xx} = 0.132 \times 10^{-4}$ lb.-in.^{2}

$\frac{I_{xx}}{I_{BB}} = 0.073$

As the ratio of I_{xx} to I_{BB} is considerably less than one, it was anticipated that the weight would have good graze sensitivity.

The compressive strength of the weight was tested to establish its adequacy to withstand setback in a Tinius-Olsen loader at 2,000 pounds with no observed deformation. The combined force of the firing pin, spring, and inertia weight during setback is 1,004 pounds. The weight is thus capable of maximum setback without yielding.

The weight, when nested inside its crush washer cup, is capable of maximum tilt of 23 degrees inside the fuze cavity, sufficient to move the firing pin 0.105 inch forward from the full setback position to a 0.030-inch penetration of the firing pin into the detonator. Maximum penetration required

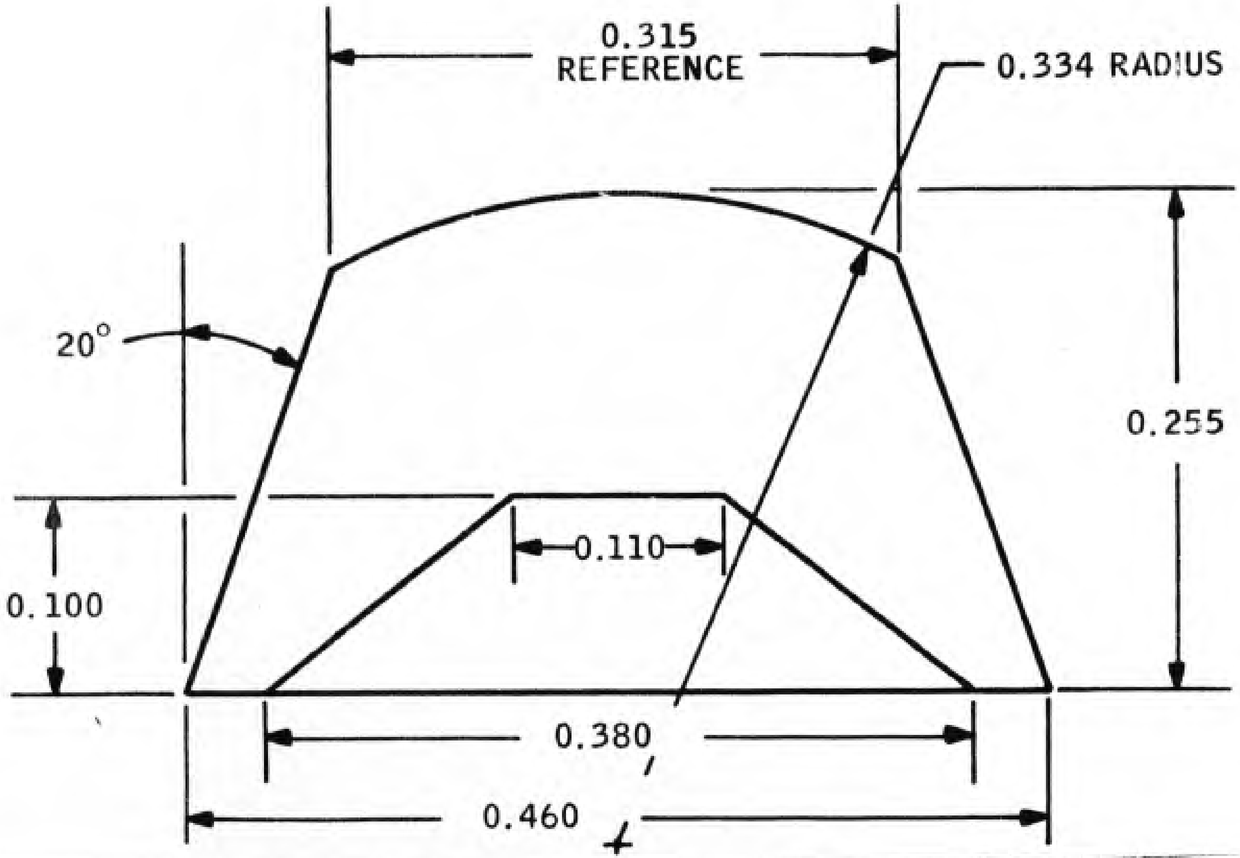

Figure 63. Redesigned Inertia Weight

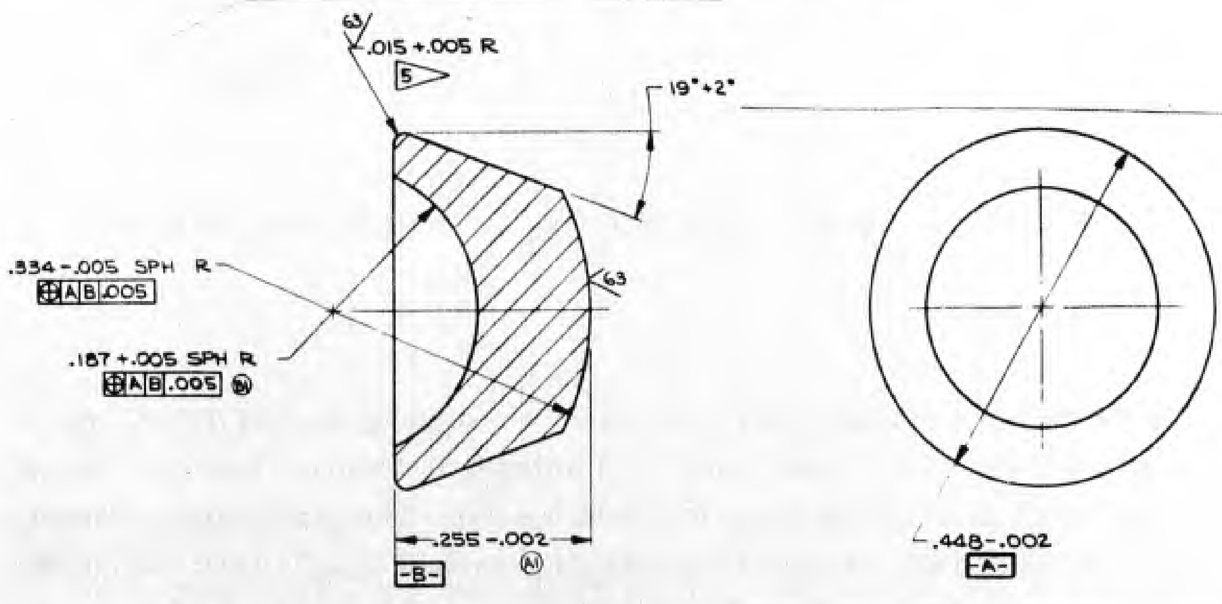

Figure 64. Inertia Weight, Drawing Number 28102037

of the M55 detonator for function is considered to be 0. 016 inch. It was concluded that the weight had sufficient structural integrity to survive launch acceleration and sufficient freedom of motion to ensure fuze function after graze impact.

Further fuze developments for improved sensitivity against light targets dictated the need for a lighter bias spring against the firing pin. The inertia weight was modified by truncating the forward spherical surface to produce a semiflat configuration (Figure 65).

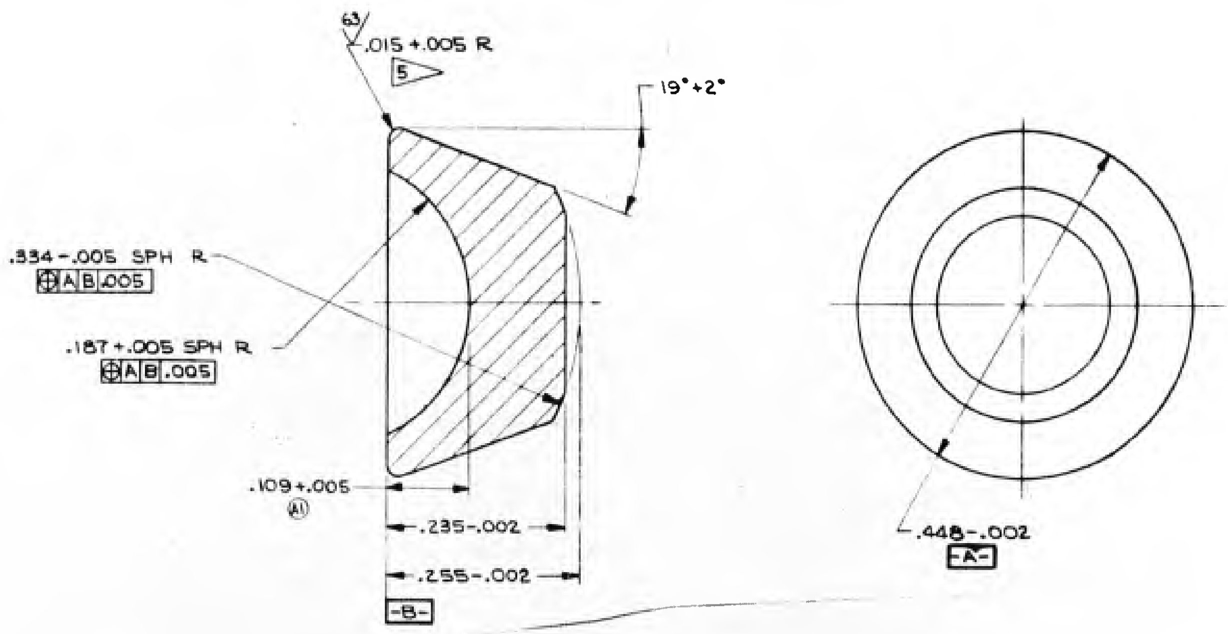

Figure 65. Semiflat Configuration, Drawing Number 28103278

b. Ball Rotor

The M505 ball rotor was used as a guide in designing the SAPHE ball rotor shown in Figure 66. A slot was added to the ball rotor for precise control of the arming path of the rotor by the firing pin. The gyroscopic precession of the rotor to align its spin axes with its principal axes is used to arm the fuze.

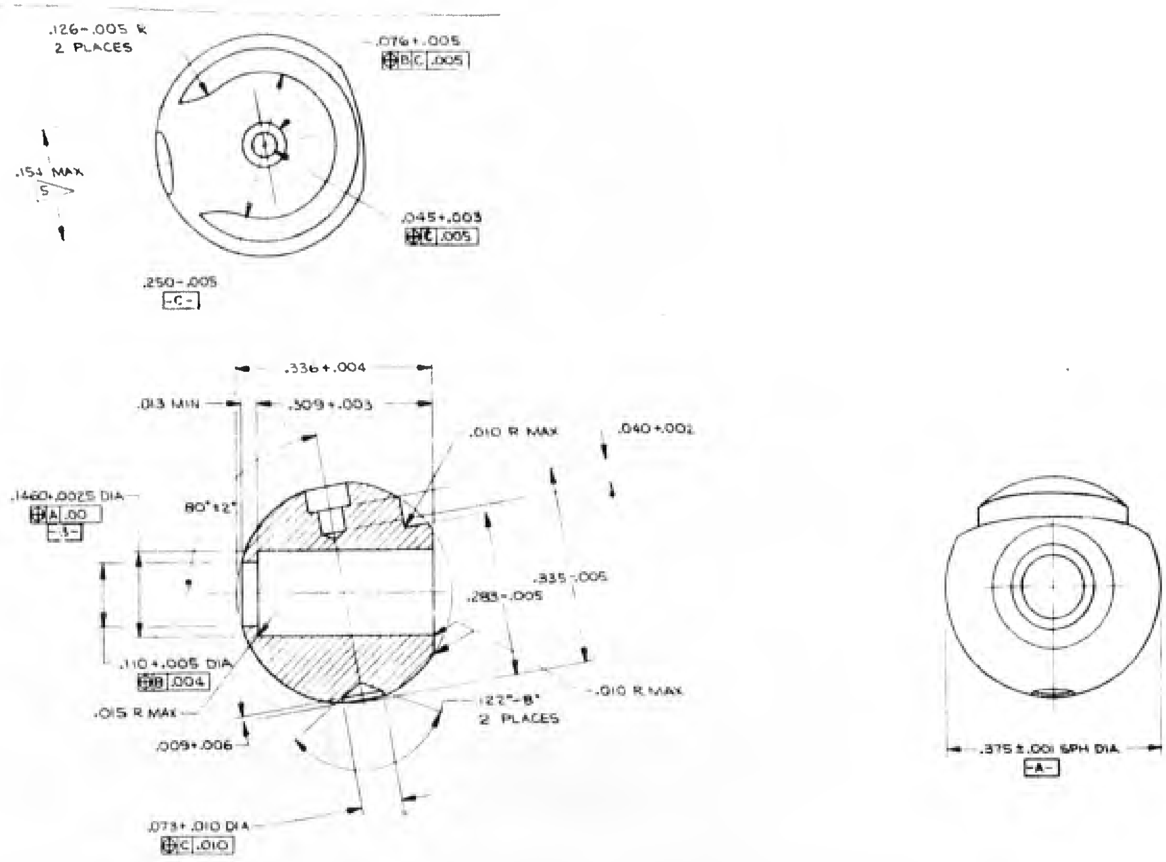

Figure 66. Rotor, Drawing Number 28102202

By use of a solid ball rotor as a foundation, a mathematical model was developed for the slotted ball rotor. The chief modification was inclusion of the interaction between the ball and the firing pin.

The impingement and the sliding of the firing pin against the cylindrical cavity wall of the rotor is the dominant energy dissipation mechanism of the slotted ball rotor; the friction between the outside of the ball and its spherical housing is considered minor.

Arming times as a function of offset fell in the range of 5 to 11 milliseconds for the SAPHE offset tolerance band. This was increased to 30 milliseconds when the normal force between the firing pin and the cylindrical cavity wall was reduced by a factor of 100. Thus, the slotted ball rotor is not unduly sensitive to the key parameters, offset and normal force (nor by inference friction, since it behaves like offset). As a consequence, it is possible that the slotted ball rotor has less arming range flexibility than the solid ball rotor.

Momentary arming does exist after the firing pin emerges from the slot; however, the duration of 25 microseconds is extremely brief. Very likely this threat can be completely eliminated by reducing the angle at which the firing pin can function the detonation by about one degree. The possibility of the firing pin being recaptured by the slot exists but has not been treated in this analytical study.

To test arming function, ball rotors were mechanically spun in an air-motor mounted fixture which simulates the fuze rotor housings. A rotor detent spring (C-ring) was used in each test to act as a trigger. The tests are described in Table XIX.

The spin fixture used in these tests prevented the rotor detent spring from completely releasing the ball rotor, and when the fixture spin was stopped, the rotor detent spring would close back on the ball. Orientation of the ball after arming could not be definitely established.

A new fixture was made of a rear and front rotor housing and the rotor detent spring was modified by decreasing its outside diameter for full opening. The new fixture also permitted observation of rotor arming during the spin process.

The results were as follows:

Test No. 1	at	872 rps	- partially armed rotor.
	at	1, 082 cps	- fully armed rotor.
Test No. 2	at	790 rps	- partially armed rotor.
	at	990 rps	- fully armed rotor.
	at	1, 100 rps	- rotor remained armed.
Test No. 3	at	790 rps	- partially armed rotor.
	at	1, 090 rps	- fully armed rotor.

TABLE XIX. ARMING FUNCTION TEST RESULTS

TEST NUMBER	ROTOR WITH INERT DETONATOR	ROTOR WITHOUT INERT DETONATOR	SPRING (rps)	RESULTS
1		X	1,220	ROTOR ARMED.
2		X	1,320	ROTOR ARMED.
3	X		1,364	ROTOR ARMED.
4	X		1,390	ROTOR ARMED.
5	X		1,375	ROTOR ARMED.
6	X		1,180	ROTOR DETENT SPRING OPENED.
			1,390	ROTOR ARMED.
7	X		1,125	ROTOR DETENT SPRING OPENED.
			1,400	ROTOR ARMED.
8	X		1,120	ROTOR DETENT SPRING PARTIALLY OPENED.
			1,400	NOT ARMED.
9	X		1,100	ROTOR DETENT SPRING PARTIALLY OPENED.
			1,400	NOT ARMED.

It was concluded that the slotted ball rotor arms at a spin rate of 1, 100 rps (66, 000 rpm) and rotates to a proper orientation for axial alignment of the detonator with the firing pin. After alignment, the rotor remains in a stable orientation.

c. Firing Pin

Preliminary investigations of the SAPHE base detonating fuze resulted in a firing pin shown in Figure 67, with the incorporation of a slotted ball rotor into the design. The firing pin was modified to provide the guide pin necessary for slotted ball rotor arming performance. The modified firing pin has a weight of 0, 0022 pound.

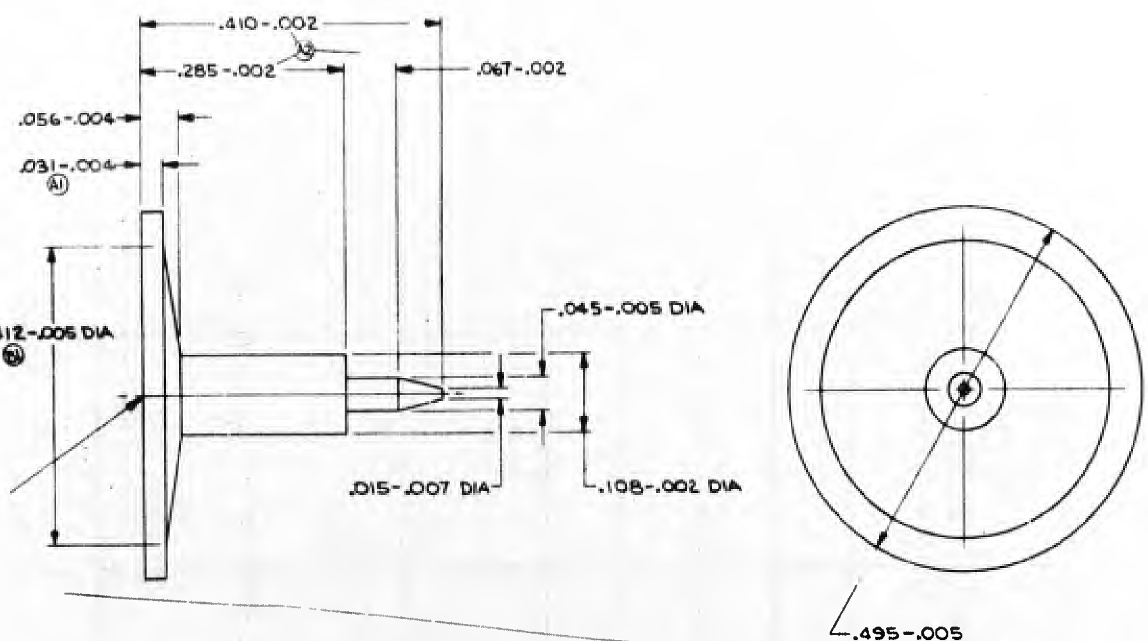

Figure 67. Firing Pin, Drawing Number 28102036

A static load test was conducted on the firing pin resting on the spherical crown of an inertia weight to establish what effect, if any, brinelling would have on the flange surface. The results are shown in Table XX.

TABLE XX. LOAD TEST OF FIRING PIN

Load Applied (Pounds)	Impression Depth (Inch)
404	0.0002
502	0.0002
600	0.0003
700	0.0004
725	0.0003
1,000	0.0005

Both the firing pin and the weight were made of 17-4 PH material in R_c 37 condition and appear to be capable of withstanding the setback forces of 122,000 g with no significant deformation of either part.

The load on the interface should be 366 pounds, and the impression made in the firing flange surface, even at 1,000 pounds, is not considered detrimental to the fuze sensitivity. Flight tests and bench tests made with a dummy detonator proved the design of the firing pin.

Latter modifications to the fuze required a firing pin with greater flange thickness to be used with an improved inertia weight support surface. This firing pin (Figure 68) survived gun firings with no damage.

d. Firing Pin Spring

The firing pin spring must provide a proper holding force to the inertia weight during flight to prevent premature detonation. Theoretical force requirements were calculated for various inertia weight configurations (Table XXI).

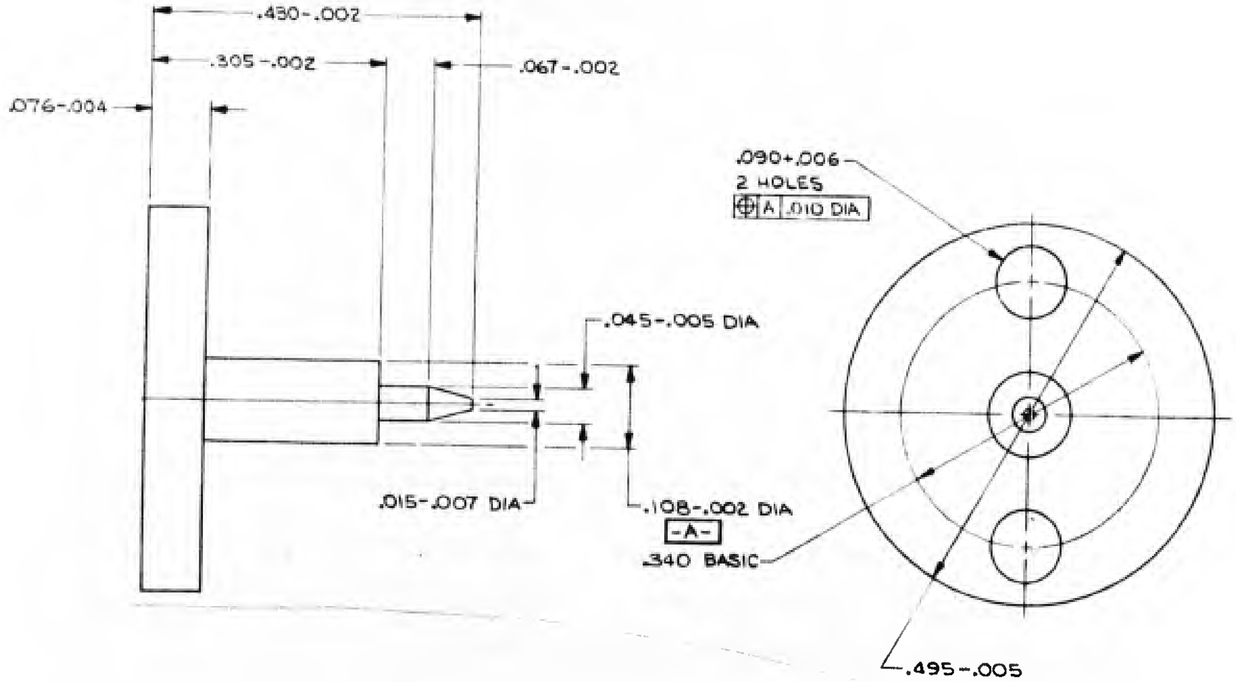

Figure 68. Firing Pin with Increased Flange Thickness, Drawing Number 28103277, Rev. A

TABLE XXI. SPRING FORCES FOR WEIGHT 0.012-INCH OFF CENTER

	Thin Wall	Thick Wall	Thick Wall	Initial Design (Actual)
Rotational Velocity (rpm)	0.0057	0.0057	0.0054	0.0035
120,000 rpm	15.10	9.10	8.64	6.96
100,000	10.7	6.45	6.10	4.96
80,000	7.02	4.20	3.97	3.23

Gun firing tests were performed on baseline fuzes with assorted springs of varying strengths with the results shown in Table XXII. (Flash X-ray pictures were used to aid analysis.)

TABLE XXII. GUN TESTS OF FIRING PIN SPRINGS

Spring Force Measured at 0.170-Inch Height (Pounds)	Velocity (Fps)	Rotational Velocity (Rpm)	Comment
7.7	2,760	99,600	No X-ray
7.5	2,930	106,000	Weight is proper
7.6	--	--	No X-ray
7.5	2,910	105,000	Full weight tilt
9.8	2,940	106,000	Weight is proper
10.1	--	--	No X-ray
10.0	2,940	106,000	Weight is proper
9.9	2,945	106,000	Weight is proper

It was concluded that the actual spring force required to hold the weight stable was less than a theoretical force value probably because the inertia weight did not realize the assumed offset of 0.012 inch.

The baseline fuze system requires a minimum spring force of 8.0 pounds for inertia weight stability when the projectile is fired from a standard twist barrel at 2,900 fps.

Later modifications to the inertia weight produced a semiflat forward surface which in return required a reduced spring force of 5.5 pounds (at 0.120-inch height) for inertia weight stability.

e. Crush Washer

The initial design of the crush washer was synthesized by assuming the washer to be a Bellville washer. To provide a fixed pivot point to the inertia weight, a retention cup was found necessary to separate the base of the weight from the fuze wall. A shallow wall cup was made an integral part of the setback washer to accomplish this purpose (Figure 69). The cup tended to support the inertia weight and provided a proper pivot contact point during the weight tilting action. General calculations for Bellville washers were used to establish washer dimensions.

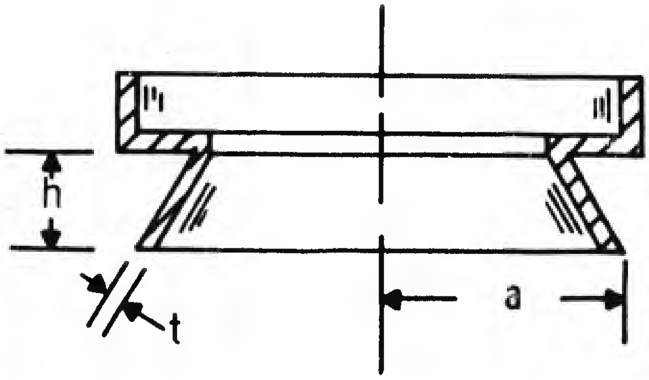

Figure 69. Setback Washer Shallow Wall Cup

For a Bellville washer, the maximum load P is given by

$$P = \frac{E\,ht^3}{0.37\,(1-\mu^2)\,a^2}$$

P = Load (pound)

E = Modulus of elasticity

t = Thickness (inch)

h = Inside height (inch)

μ = Poisson's ratio

0.37 = Constitutent

a = Radius (inch)

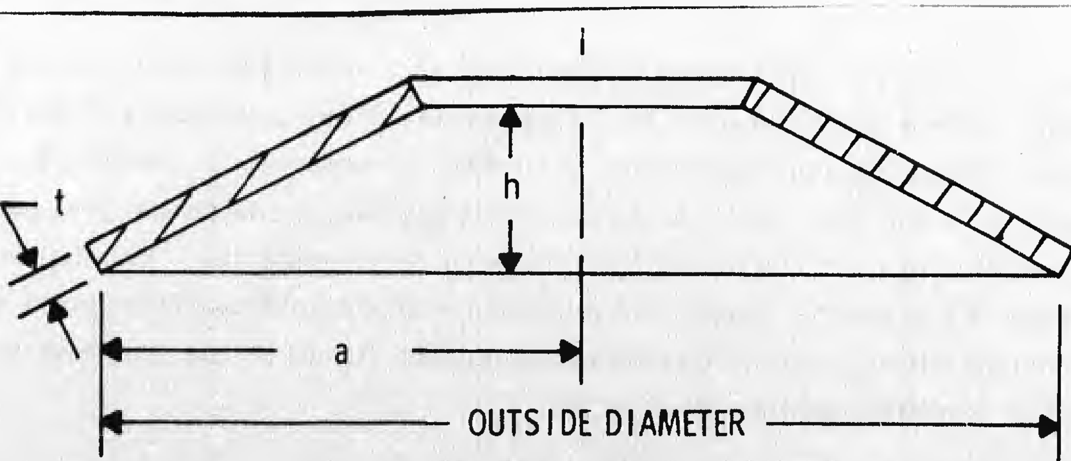

For an aluminum washer with a 0.025-inch height, a 0.480-inch outer diameter, and a desired function force of 140 pounds, the thickness was calculated to be 0.022 inch.

Test parts designed by this analysis were statically tested.

Test Results	Height Before (Inches)	Height After (Inches)	Load Applied (Pounds)
Unit No. 1	---	0.090	650
Unit No. 2	0.108	0.0925	673
Unit No. 3	0.107	0.092	651
Unit No. 4	0.108	0.093	688

The securing web between the cup and washer proved too substantial for proper yielding, and the washer failed in tension at a diameter approximating the web outside diameter, as shown in Figure 70. The above crushing loads are approximately five times the desired crushing load of 140 pounds, which is equivalent to a 15,000 g acceleration.

Separate test samples of Bellville washers (Figure 71) were fabricated of both 0.020-inch-thick material and 0.015-inch-thick material to establish the yield values of the washers without a securing web.

Bellville washers without a cup tested as follows:

0.015-inch-thick, 0.030-inch-height; 32 pounds to crush

0.020-inch-thick, 0.030-inch-height; 50 pounds to crush

Thus, the Bellville equation proved inapplicable; therefore, the washer was developed empirically.

After several iterations, the design illustrated in Figure 72 was tested. The washer thicknesses, 0.015 inch and 0.020 inch, were used for the Bellville washer portion of the item. Plots obtained from the Tinius-Olsen

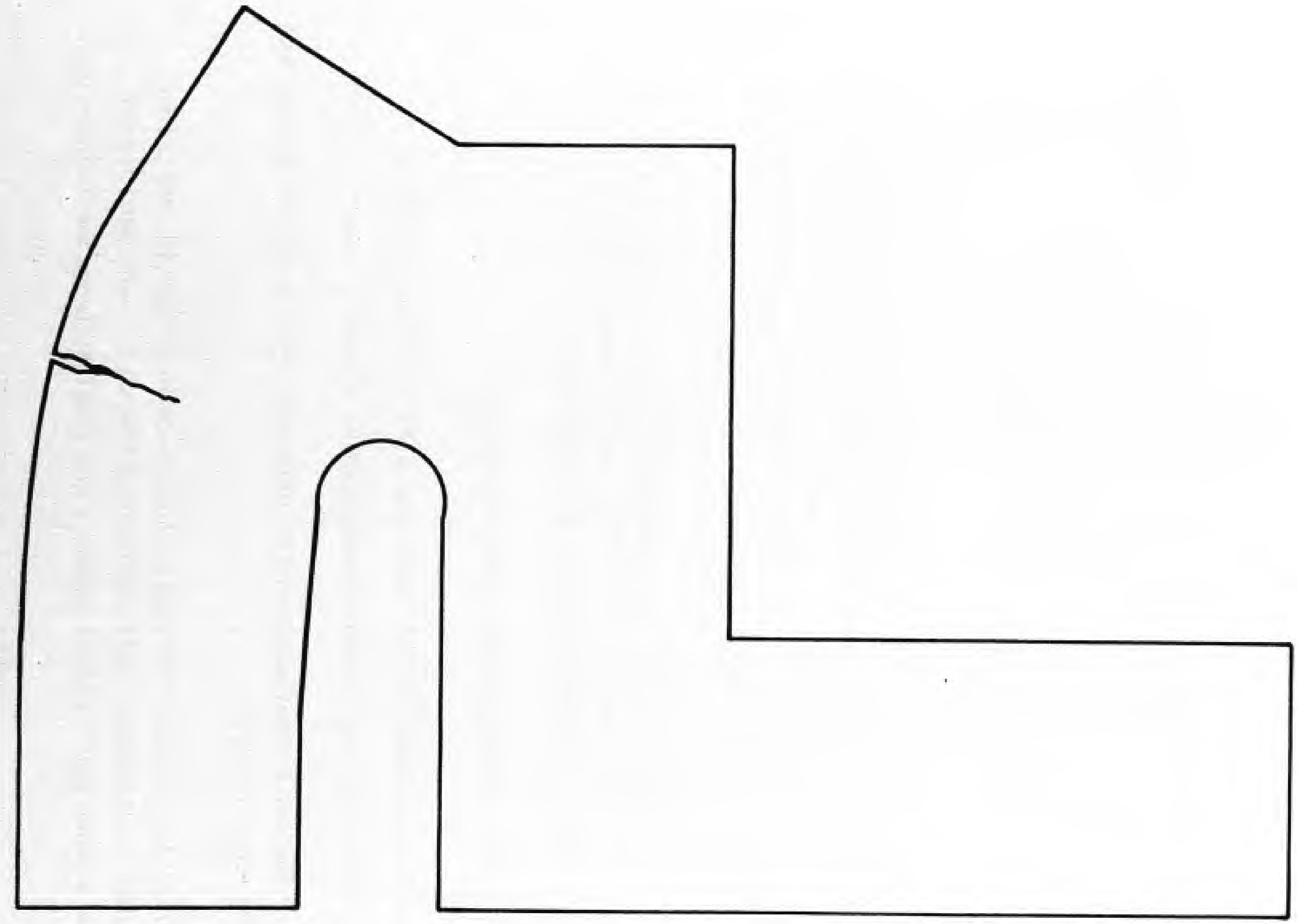

Figure 70. Cross Section Showing Failure Mode of Bellville Washer

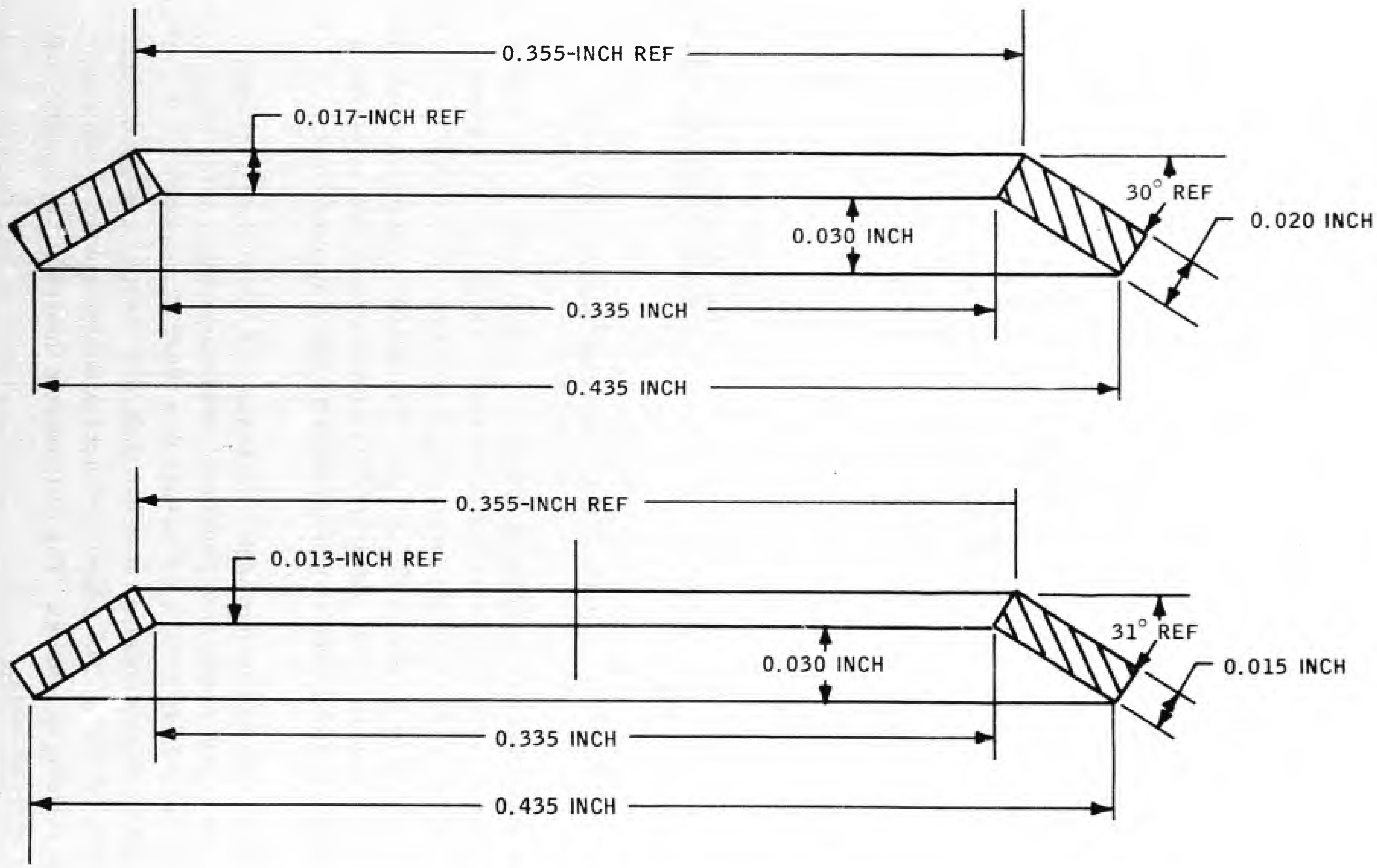

Figure 71. Separate Test Samples of Bellville Washers

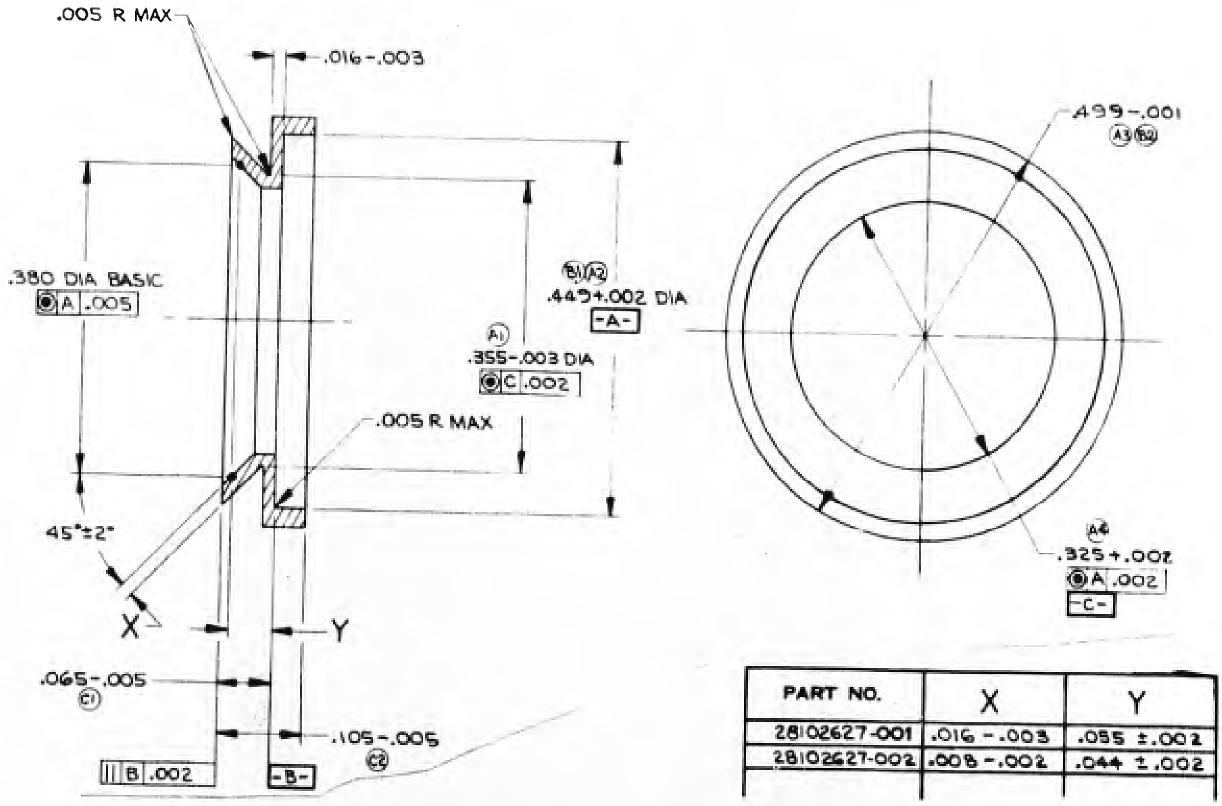

PART NO.	X	Y
28102627-001	.016 -.003	.055 ±.002
28102627-002	.008 -.002	.044 ±.002

Figure 72. Crush Washer, Drawing Number 28102627

testing machine are presented in Figures 73 and 74. The crush washer design with a washer thickness of 0.015 inch deflects to a permanent height of 0.038 inch from an initial height of 0.085 inch (change in height of 0.047 inch) when loaded to 750 pounds. The washer requires a minimum load of 250 pounds before yielding (250 pounds is equivalent to 27,800 g acceleration, 750 pounds is equivalent to 83,000 g acceleration).

The setback washer design with a thickness of 0.020 inch deflects and fractures at the washer/cup junction to cause separation of the washer from the cup and deformation of the washer to a nearly flat condition. The change in height is from 0.085 inch to 0.040 inch or a change in height of approximately 0.045 inch. The washer requires a minimum load of 395 pounds before yielding (44,000 g). The final washer thickness was selected as a result of these tests.

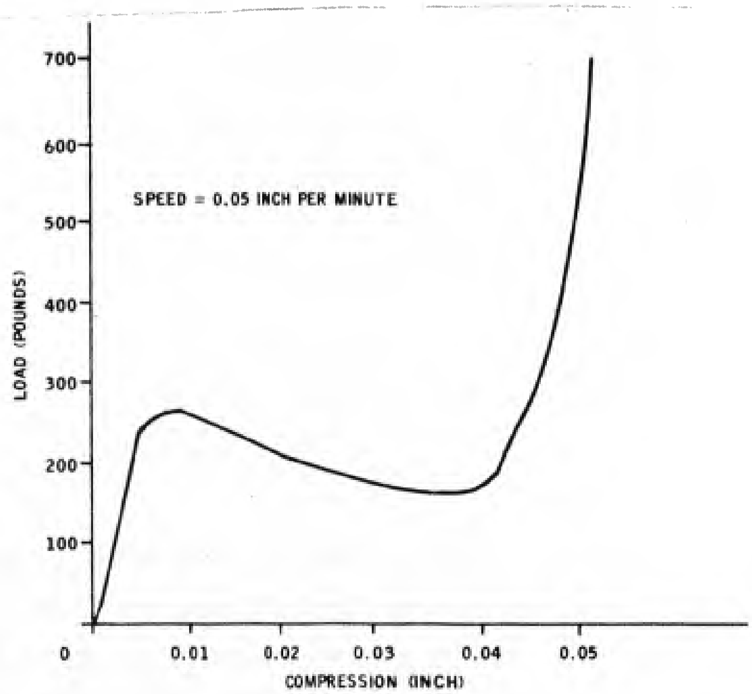

Figure 73. Tinius-Olsen Tester Results, Crush Washer

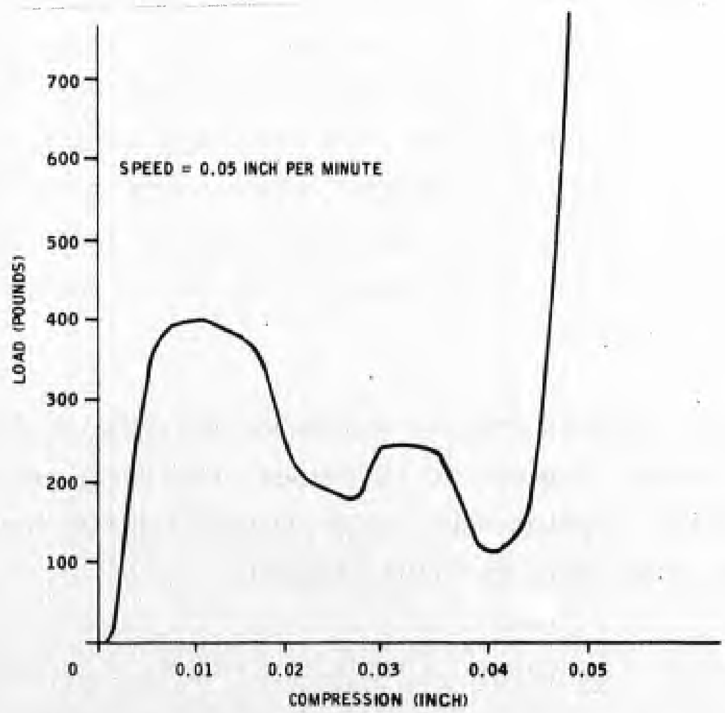

Figure 74. Tinius-Olsen Tester Results, Setback Washer

E. EXPLOSIVE TRAIN

The explosive train transforms the mechanical energy of the fuze into reliable in-line initiation of the projectile explosive and provides out-of-line safety for the fuze. The scope of the effort was limited to establishing explosive train reliability and safety.

1. Component Selection

a. High Explosive

High explosive LCA-1 was wet-mix mulled. This tends to grind aluminum into wax-coated RDX, which creates two advantages: 1) increased density versus pressing pressure, and 2) more uniformity in each round and from round to round because the constitutents do not segregate during handling. This explosive provides good incendiary effect as well as brisance for shattering warhead walls and is presently used in high-volume production of 20mm projectiles. No attempt was made during this program to select an optimum explosive. The explosive will be pelletized and reconsolidated in the projectile in accordance with current loading plant practice. High density (1.93 gm/cc) has been achieved within normal pressing limits. The scope of the program did not include optimization of the projectile explosive. A survey of explosives may offer alternates to LCA-1 which will increase projectile effectiveness.

The initial design required that the explosive height be machined into tolerance. As loading experience increased, machining was eliminated through adjustment of pellet size or by pressing the last increment to a specified height rather than specified density.

b. Booster

Explosive PBXN-5 per MIL-E-81111 was selected because it:

- Exhibits the desired high degree of control and uniformity of sensitivity needed for both safety and reliability.

- Can be loaded to high density, which creates a high degree of output while maintaining initiation sensitivity and rapid growth to detonation.
- Meets the explosive requirements of MIL-STD-1316, MIL-STD-332, and Fuze Safety Criteria, U. S. Air Force, dated November 1968.

PBXN-5 appeared to be a logical choice.

The cup depth was specified to obtain reliable function of the projectile explosive based on previous explosive train experience, and the wall thickness was selected so that loading operations could be handled without extensive confinement tooling on the threaded outside diameter. The detonator face of the cup was changed to improve the gap-jumping capability of the detonator-booster interface. The cup was designed to reduce costly loading and reduce fixturing. Elimination of the threaded outside diameter further simplifies the cup design, reducing loading costs and increasing explosive content. The booster was supported directly by the fuze front housing rather than by the threaded outside wall.

Optimization of the booster size was not undertaken in the present program. Results of the booster-to-HE Bruceton tests indicated that the booster explosive could be reduced. If the booster size is reduced, the projectile explosive can be increased, resulting in some increase in effectiveness.

c. Detonator

The M55 detonator was selected because it has the required stab-input sensitivity and the desired small size. High production usage will result in low cost.

Detonators with output charges greater than the M55 or with shaped end output would probably increase reliability. However, actual reliability level did not indicate that any changes were necessary.

2. Test Results

The test setups for the Bruceton tests of the explosive train are shown in Figures 75 and 76. The results are as follows:

a. Detonator to Booster

Initial Booster Cup Design

24 shots
$\overline{X}$ = 0.32 inch σ = 0.0445 inch
Point estimates 99.9% at 1.82-inch gap
99.9% reliability at 90% confidence at 0.092-inch
99.9% reliability at 83% confidence at max gap (0.114 inch)

Revised Booster Cup Design

5 shots
$\overline{X}$ = 0.4 inches

It was concluded from these five tests that the mean did not shift and that a repetition of the first test was unnecessary.

b. Booster to Main Charge

Vary aluminum thickness

$\overline{X}$ = 0.109 inch σ = 0.0044 inch

Point estimate 99.9% reliability 0.097 inch

99.9% reliability at 90% confidence 0.086 inch.

c. HE Quantity

Baseline - 5.2 grams

Miniature - 6.5 grams

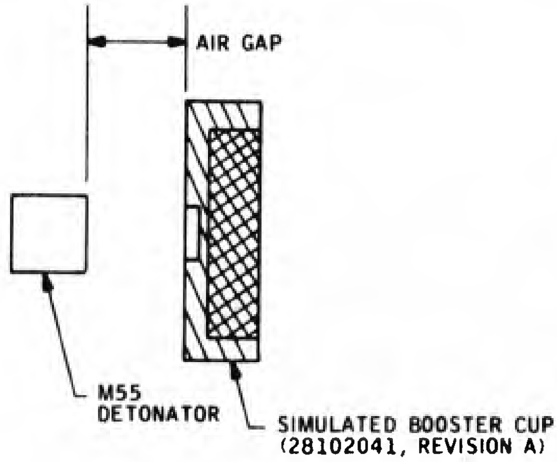

Initial Detonator-Booster
Bruceton Components

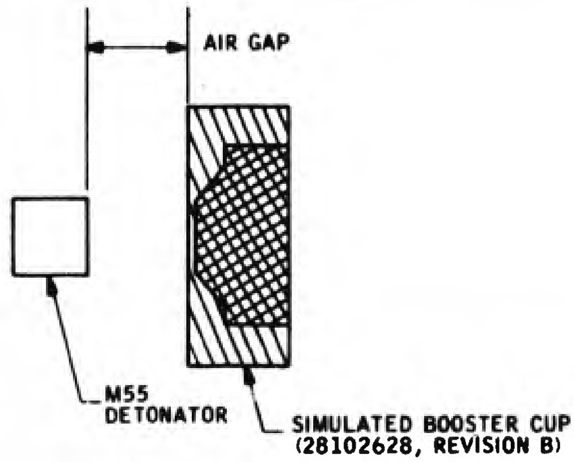

Revised Detonator-Booster
Bruceton Components

Figure 75. Test Components Used in Bruceton Tests (Detonator to Booster)

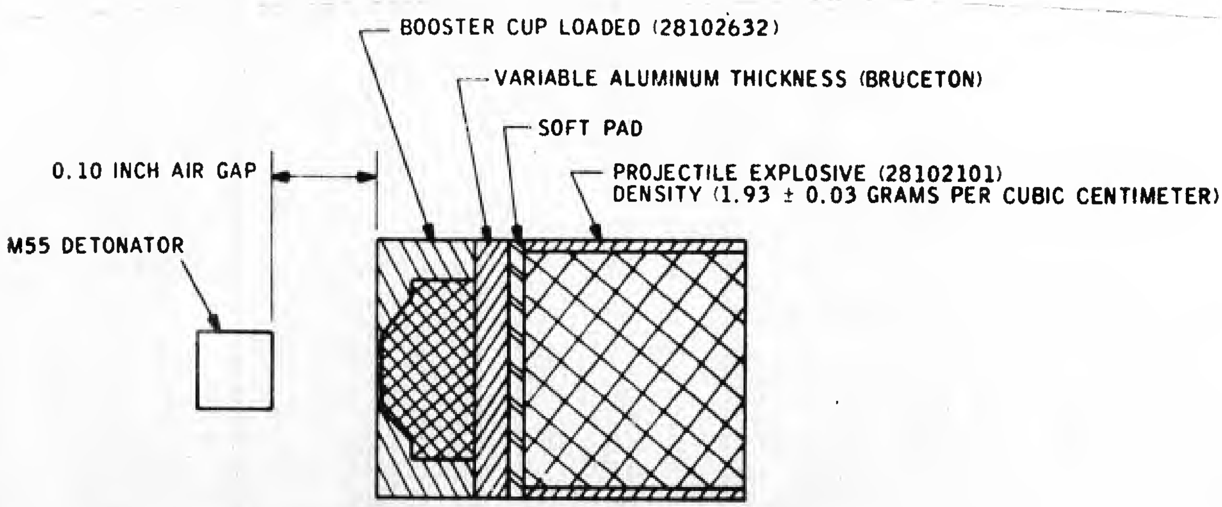

BOOSTER-MAIN CHARGE BRUCETON TEST

Figure 76. Test Components Used in Bruceton Tests (Detonator to Bruceton Revised Booster Cup Design Test)

SECTION IV

SYSTEM TESTS

A. FUNCTION AND SENSITIVITY

During early testing of the fuze, a 7.8-pound spring (at setback height) was used for gun tests. Because this weight was found to be marginally stable, a weight offset condition of 0.0085 inch was indicated. A 9.0-pound spring was then obtained for the first live round tests against various targets.

Initial testing of projectiles with the baseline fuze containing the 9.0-pound bias spring and the spherically faced inertia weight produced the results shown in Table XXIII.

TABLE XXIII. BUILD NO. 7, 117 UNITS (NO. 1001-1117)

Velocity	Target	Impact Angle (Degrees)	Successes	Percentage
3,000 fps	1/4-Inch RHA	0	9/9	100
		60	9/9	100
		80	8/18	45[a]
3,000 fps	1/2-Inch MS	0	9/9	100
		60	9/9	100
3,000 fps	1/2-Inch RHA	30	2/2	100
		45	2/3	100
3,000 fps	0.053-Inch MS	0	0/3	0
		45	0/4	0
3,000 fps	0.057-Inch MS	0	0/1	0
3,000 fps	0.100-Inch MS	0	4/5	80
		45	0/6	0
		80	3/4	75
800 fps	1/4-Inch RHA	0	0/5	0

[a] These failures were traced to hairline fractures in the projectile body, caused by heat treatment. The body failures caused fuze separation before the firing pin could reach the detonator.

As shown by the last entry in Table XXIII, the crush washer was found too rigid for the acceleration at 800-fps muzzle velocity and the rotor detent spring too strong for positive opening at spin speeds produced by the 800-fps velocity. To eliminate these causes of failure, the crush washer was pre-crushed before assembly into the low-velocity test units, muzzle velocity was increased, and the spring force reduced to 6 pounds. The results of ensuing tests are shown in Table XXIV.

TABLE XXIV. BUILD NO. 7 (PRECRUSHED WASHER)

Velocity	Target	Impact Angle (Degrees)	Successes	Percentage
1, 200 fps	1/4-In. RHA	0	9/9	100
		60	10/10	100
		80	5/5	100
	1/2-In. MS	0	9/9	100

Tables XXIII and XXIV show that performance of the fuze against light targets of mild steel did not meet the design goal. Improved sensitivity was required, and the inertia weight was redesigned to have a semiflat forward surface. This design permitted use of a lighter spring thereby reducing the impact force necessary to overcome the spring tension. The decrease in inertia weight mass was compensated for by increasing the firing pin flange thickness.

Build No. 8 contained the new weight/firing pin combination and used a 5.5-pound spring.[3] Results of Build No. 8 tests are shown in Table XXV.

---

[3]Load measured at setback height of 0.170 inch.

TABLE XXV. BUILD NO. 8 (ROUNDS 1118-1143)

Velocity	Target	Impact Angle (Degrees)	Successes	Percentage
3000 fps	1/4-Inch RHA	80	9/9	100
	0.048-Inch MS	0	0/2	0
	0.053-Inch MS	0	0/2	0
	0.057-Inch MS	0	3/9	33
	0.085-Inch MS	0	1/2	50
	0.104-Inch MS	0	1/1	100

Flash X-ray observation indicated that the spring coils might be stacking and preventing full travel of the firing pin toward the detonator. The spring was modified by removing one-third of the largest coil. Since the truncation was made to an inactive coil, the spring rate remained unchanged. The test results are shown in Table XXVI.

TABLE XXVI. BUILD NO. 10 (ROUNDS 1149-1163)

Velocity	Target	Impact Angle (Degrees)	Successes	Percentage
3,000 fps	0.048-Inch MS	0	1/5	20
	0.053-Inch MS	0	1/3	33
	0.057-Inch MS	0	4/5	80[a]
	0.075-Inch MS	0	2/2	100

[a] The four units which functioned against this target thickness had tumbled after passing through the target. The tumbling caused the inertia weight to tip with respect to the projectile, causing fuze function.

Five additional units were further modified by reducing the firing pin flange volume to reduce the weight and, in effect, to increase the spring load length for reduced spring force. The test results are shown in Table XXVII.

TABLE XXVII. BUILD NO. 11 (ROUNDS 1164-1168)

Velocity	Target	Impact Angle (Degrees)	Successes	Percentage
3,000 fps	0.038-Inch MS	0	1/5	20

Consideration was given to the effect of the projectile nosecap on fuze sensitivity against light targets. If the nose were less efficient as a perforator, an increase in velocity loss (i.e., an improved deceleration pulse) of the projectile could be achieved for improved fuze function. The nosecaps were accordingly removed from 12 projectiles to expose the relatively blunt body, and these were tested with the results shown in Table XXVIII.

TABLE XXVIII. BUILD NO. 11 (ROUNDS 1169-1187)

Velocity	Target	Impact Angle (Degrees)	Successes	Percentage
3,000 fps	0.048-Inch MS	0	7/7 (no caps)	100
	0.057-Inch MS	0	5/5 (no caps)	100
	0.057-Inch MS	0	4/8 (standard)	50

Since the nose cap was essential to efficient armor penetration, a compromise was to remove only the tip of the nose cap, to present a flat surface to the target while retaining the armor-piercing capability. No degradation in flight stability was found to result from this alteration. Tests of units thus modified were conducted, with the results shown in Table XXIX.

TABLE XXIX. BUILD NO. 12 (ROUNDS 1189-1204)

Velocity	Target	Impact Angle (Degrees)	Successes	Percentage
3,000 fps	0.052-Inch MS	0	0/7	0
	0.057-Inch MS	0	1/4	25
	0.061-Inch MS	0	5/5	100

Flash X-ray examination disclosed less tumbling after target penetration in these tests, and this fact would account for the reduced function rate in comparison with the round-nosed units.

Twenty units were assembled with the smallest coil of the bias spring reduced in diameter to permit improved nesting of the spring during firing pin travel. The test results of these units are shown in Table XXX.

TABLE XXX. BUILD NO. 14 (ROUNDS 1205-1224)

Velocity	Target	Impact Angle (Degrees)	Successes	Percentage
3, 000 fps	0. 052-Inch MS	0	0/2	0
	0. 057-Inch MS	0	9/18	50

The large flange of the firing pin could produce a damping effect during firing pin travel because air compressed by forward travel of the firing pin could produce a negative force against the flange, amounting to as much as 6 pounds. To prevent this reaction, two holes were drilled in the flange through which the air could vent during firing pin travel. A new spring of 6. 0 ± 0. 3 pounds was also introduced. Six units with these modifications (Build No. 15) and nine units with no vent holes (Build No. 16) were tested, with the results shown in Table XXXI.

TABLE XXXI. BUILD NO. 15 AND 16 (ROUNDS 1225-1238)

Velocity	Target	Impact Angle (Degrees)	Successes	Percentage
3, 000 fps	0. 052-Inch MS	0	0/2	0
	0. 057-Inch MS	0	0/4	0
3, 000 fps	0. 061-Inch MS	0	0/1	0
	0. 073-Inch MS	0	0/5	0
	0. 105-Inch MS	0	2/2	100

The new spring had been designed with 0.037-inch-diameter wire to reduce the stresses in the spring for long-term storage life. However, the spring rate of the new spring proved far too high, providing a 13-pound actual force at a 0.060-inch height (detonation) as compared with an 8-pound force of the 5.5-pound spring at the same height. The calculated load of the new spring was 10.0 pounds. This spring was rejected as unworkable for fuze function against light armor.

Three special test lots were assembled to retest the value of venting the firing pin flange. The 5.5-pound spring was used in these units. Lot 17 contained the vented firing pin, Lot 18 contained the vented firing pin and an inverted spring position (large coil in reverse direction), and Lot 19 contained an inverted spring but no vents. The test results are shown in Table XXXII.

TABLE XXXII. BUILD NO. 17, 18, AND 19 (ROUNDS 1239-1268)

Velocity	Target	Impact Angle (Degrees)	Successes	Percentage
3,000 fps	0.052-Inch MS 0.057-Inch MS	0 0	1/5 4/5	20 80
3,000 fps	0.048-Inch MS 0.052-Inch MS	0 0	2/5 5/5	40 100
3,000 fps	0.052-Inch MS 0.057-Inch MS	0 0	2/5 4/5	40 80

Lot acceptance testing was performed on units representing the 800 delivery units. These units contained fuzes with the 5.5-pound spring and the vented firing pin. The results are shown in Table XXXIII.

TABLE XXXIII. LOT ACCEPTANCE TEST RESULTS, UNITS CONTAINING 5.5-POUND SPRING AND VENTED FIRING PIN

Velocity	Target	Impact Angle (Degrees)	Successes	Percentage
3,000 fps	1/4-Inch RHA	60	5/5	100
		80	7/7	100
	0.057-Inch MS	0	2/11	18
	0.061-Inch MS	0	20/29	69
	0.080-Inch MS	0	11/11	100

It was concluded that:

1. The PGU-2/B baseline fuze meets the design requirements against targets of 1/4-inch RHA at obliquities of 0 to 80 degrees.

2. The PGU-2/B fuze does not meet the sensitivity requirements against targets of 18-gage mild steel. Although 100 percent function of fuzes has been attained on 0.052-inch mild steel sheet, the bias spring used in the successful tests was unsuitable for 20-year storage.

B. ACCURACY AND DISPERSION

Thirty projectiles were fired from a Mann barrel, 10 each at three different targets. The results are shown in Table XXXIV.

TABLE XXXIV. ACCURACY AND DISPERSION

Range: 500 yards
Temperature: 84°F
1 Mil = 18 inches

Humidity: 30 percent
Wind: 5 - 10 miles per hour from the South

Target Number	Number of Shots	Mean Radius (Inches)	Mean Vertical Distance (Inches)	Mean Horizontal Distance (Inches)
1	10	13.2	10.6	6.0
2	10	9.8	8.0	4.7
3	10	10.6	8.2	5.7
	Average	11.2 0.62 mil		

The mean radius is less than 1 mil. Histograms of horizontal and vertical deviations show nonnormal distribution in the vertical plane, possibly caused by the flexibility of the firing fixture in that plane.

C. ENVIRONMENTAL

The rounds were tested for resistance to jolt, jumble, 10-foot drop, rough handling, and aircraft vibration tests. Results are shown in Table XXXV.

TABLE XXXV. RESULTS OF ENVIRONMENTAL TESTS

Test	Quantity Tested	Quantity Passed
Jolt, MIL-STD-331, Test 101	9	9
Jumble, MIL-STD-331, Test 102	9	9
10-foot drop, MIL-STD-331, Test 111 (Modified)	15	15
Rough Handling, MIL-STD-331, Test 114	15	15
Aircraft Vibration, MIL-STD-810B, Test Method 514, Category (b) Procedure I, Curve D, Time Schedule I	15	15

D. OVERPRESSURE

1. Projectile

The projectile with functioning fuze was tested for resistance to gun firing with chamber pressures of 67, 500 psi ± 2, 500 psi (copper crusher). The actual test conditions are shown in Table XXXVI.

TABLE XXXVI. FIRING RESISTANCE TEST RESULTS

Round	Pressure (Psi)	Velocity (Fps)
1	76, 000	3, 010
2	69, 000	(No reading)
3	(No reading)	3, 034
4	76, 500	3, 017
5	80, 600	3, 027

No projectile damage resulted from the tests.

2. Fuze Components

Seven projectiles of 4340 steel (heat-treated to R_c 45) were properly banded and filled with a simulation explosive of Filler E (density 1. 72 gm/cc). A 2024 T-4 aluminum booster cup with Filler E and a functioning fuze were assembled into each projectile.

Each projectile was fired from a standard-twist Mann barrel into a target of cotton waste material for soft-catch retrieval. Each projectile was disassembled after the test and analyzed for parts damage. All units were X-rayed before and after testing. The test data are shown in Table XXXVII.

TABLE XXXVII. SOFT-CATCH TEST RESULTS

Unit No.	Chamber Pressure
4	53, 000
5	56, 000
6	56, 000
7	71, 450
8	65, 550
9	67, 850
10	70, 800

The results were as follows:

1. Simulated Setback Washer – The inside edge of the cup portion of the washer had a series of shave-outs as if the weight had made repeated passes at the edge around its periphery.

2. Inertia Weight – Impact marks were apparent on the peripheries of the major diameter and the minor diameter. The peen marks indicate each weight bounced and spun around during the projectiles tumbling in the cottom waste material. There was some galling on the periphery of each weight crown caused by the spinning weight during deceleration in the waste material.

3. Firing Pin – The spring support flange of the firing pin was permanently deformed into a dish of 0.002-inch depth. Dishing was caused by the bias spring setback load coupled with the internal setback load on the flange itself during the gun firing.

4. Bias Spring – No damage.

5. Simulated Rotor and Housing Assembly – There were spring marks on the rear surface of the slug around the firing pin hole indicating a high energy input of the weight to the firing pin.

6. Booster Cup – Each booster cup failed in tension and shear with the Filler E loading the cup to deflect it against the rotor housing. The cup was not able to withstand the setback load of the Filler E.

It was concluded that the fuze components tested also can survive the high accelerations. However, the support flange of each firing pin was permanently deflected 0.001 to 0.002 inch because of setback acceleration. The booster cups on each projectile failed under the setback acceleration of the Filler E material and did not sustain the load. The test was then repeated with booster cups of 7075-T6 aluminum. These units survived without damage.

X-ray examination of units in flight showed inertia weights in all units in proper position for target impact. Latter firing pin design and inertia weight design resulted in firing pins with sufficient structure to survive all gun firing setback accelerations.

E. ARMING DISTANCE

The following were additional requirements of the contract: (1) The fuze must arm only when it has exited safely from the gun barrel, and (2) The explosive train of the warhead must not be completed until the delivery aircraft is outside the lethal envelope of the warhead.

Impact safe distance test results to date are shown in Table XXXVIII.

TABLE XXXVIII. IMPACT SAFE DISTANCE RESULTS

Target Distance (Inches)	18	21	24	27	31	39
Percent Function	0	20	50	40	20	10
Test Quantity (76)	5	11	29	10	9	5

The minimum fuze arming distance after muzzle exit is 21 inches. The maximum distance is unknown.

F. SAFETY

Another contract requirement was that the effectiveness of the interrupter shall be determined by the techniques of MIL-STD-331.

The total quantity tested was 220. In about half of the units tested, the front rotor housing was cracked. Four booster cups were penetrated by gases or fragments. The boosters were not detonated, and there was no damage to the booster explosive.

The unit has passed the detonator safety test. However, several cracks in the front rotor housing were found, indicating a minimum design safety margin. Strengthening of the front rotor housing is recommended in future effort.

G. SHORT FUZE

Two series of test firings were performed with the shorter alternate fuze. The first series of four rounds included ball rotors with dummy detonators and modified Belleville springs to maintain inertia weight stability. In all cases, the inertia weight was not held stable by the spring as determined by examination of in-flight flash X-rays and by examination of the soft-caught hardware. However, it was possible to conclude that the ball rotors armed properly before impact with soft catch based on the condition of the ball rotors which were gouged and pricked along an arming path. This is attribtued to the firing pins being repeatedly driven into the rotors by the motion of the inertia weights. Moreover, two of the dummy detonators had been holed and chewed by a sharp object, presumably the firing-pin tip. This could not have occurred with an unarmed rotor. The third dummy detonator was not holed, probably because the firing pin tip had been battered flat on the ball before the arming was complete. One projectile was not recovered.

The second series of ten projectiles included the ball system of maintaining in-flight inertia weight stability, but did not include ball rotors.

Two parameters were varied to properly bracket the performance of the ball-containing firing pin designed to maintain inertia weight stability. The number of balls per unit was varied from three to seven to vary the stabilizing force supplied to the inertia weight, and the required stabilizing force was varied by including a modified inertia weight with a lower center of gravity and less mass. It was therefore more easily stabilized than the original inertia weight design.

For each weight design, a range of balls per unit was picked which would ensure some successes and some failures so that the exact stabilizing capability, as well as the feasibility of the system, could be established.

Table XXXIX presents the results of this testing. Success or failure of each unit was determined through in-flight flash X-rays taken 25 meters from the muzzle. A satisfactory correlation exists between predicted stability and the test results.

An examination of the soft-caught projectiles and fuzes revealed nothing that would refute the conclusions drawn from the X-rays.

The hardware tests revealed that the fuze-projectile combination has ample strength to withstand the gun environment. The cartridge cases were loaded for 65 to 70 kpsi peak chamber pressure and no evidence of structural failure was found.

In every case the firing pins were found in a fully forward position, indicating that the soft-catch environment was sufficient to cause a full firing pin stroke. A deep impression in the walls of the piston-like firing pins was caused by the fully tipped inertia weights. This damage, which in no way represents a malfunction, attests to violent interaction between inertia weight and firing pin and to the associated probability of the function of a live fuze even in the relatively gentle soft catch environment.

The stability of the projectiles themselves was determined to be satisfactory within the limits of the test setup. The Celotex® panel at the front of the soft catch showed that the projectiles had struck with little or no yaw. The soft catch was located 100 meters from the muzzle in the first test series and at 25 meters in the second test series.

To summarize, the first test series established the arming capability of the miniature alternate fuze ball-rotor design. The second test series established:

TABLE XXXIX. FIELD TEST OF INERTIA WEIGHT STABILIZING SYSTEM
(4-5 FEBRUARY 1970)

UNIT NO.	WEIGHT TYPE	CALCULATED STABILIZING FORCE REQUIRED (POUNDS)	NO. OF BALLS IN UNIT	CALCULATED STABILIZING FORCE SUPPLIED (POUNDS)	ANTICIPATED RESULTS	TEST RESULT
201	PRIME	5.84	4	4.96	WEIGHT TIPPED IN FLIGHT.	WEIGHT TIPPED IN FLIGHT.
202	PRIME	5.84	5	6.2	WEIGHT STABLE IN FLIGHT.	WEIGHT STABLE IN FLIGHT.
203	PRIME	5.84	5	6.2	WEIGHT STABLE IN FLIGHT.	NO X-RAY.
204	PRIME	5.84	6	7.44	WEIGHT STABLE IN FLIGHT.	WEIGHT STABLE IN FLIGHT.
205	PRIME	5.84	6	7.44	WEIGHT STABLE IN FLIGHT.	WEIGHT STABLE IN FLIGHT.
206	PRIME	5.84	7	8.68	WEIGHT STABLE IN FLIGHT.	WEIGHT STABLE IN FLIGHT.
207	MODIFIED	3.96	3	3.72	WEIGHT TIPPED IN FLIGHT.	WEIGHT TIPPED IN FLIGHT.
208	MODIFIED	3.96	4	4.96	WEIGHT STABLE IN FLIGHT.	WEIGHT TIPPED IN FLIGHT.
209	MODIFIED	3.96	5	6.2	WEIGHT STABLE IN FLIGHT.	WEIGHT STABLE IN FLIGHT.
210	MODIFIED	3.96	6	7.44	WEIGHT STABLE IN FLIGHT.	WEIGHT STABLE IN FLIGHT.

1. Performance of an inertia weight stabilizing system.

2. Structural integrity of the fuze-projectile combination.

3. Capability for firing pin movement on collision with a soft target.

4. Stability of projectiles to the initial tipoff effects of launch.

Together, the two test series established proper fuze operation in flight but did not establish:

1. Graze sensitivity.

2. Normal impact sensitivity.

3. Function delay.

SECTION V

SAFETY AND RELIABILITY

The design safety for the 20mm Semi-Armor Piercing High Explosive (SAPHE) fuze concepts was numerically evaluated. Safety Fault Tree Diagrams were constructed and evaluated by use of event probabilities based on contractor test experience, where possible, and on engineering judgement when actual test data was nonexistent or insufficient.

The estimated safety failure rate of the PGU-2/B is 0.174×10^{-6}. This is nearly 5.75 times better than the Safety Design Goal of one safety failure per million units. No single element failure mode of the fuze exists which will result in a premature or inadvertent function of the cartridge.

The probability of a safety failure during the manufacture-through-usage life cycle of the 20mm SAPHE miniaturized fuze has been calculated to be 0.409×10^{-6} (one safety failure per each 2.4 million units). The design goal for safety probability is 1.0×10^{-6} (one safety failure per each 1.0 million units). Detailed analyses are included as Appendix III. Table XL summarizes the safety data.

Table XLI compares the calculated performance of the SAPHE with the design goals. The launch conditions were taken to be 5,000 feet above sea level, with an aircraft velocity of 790 KTAS and a quadrant angle of 30 degrees below horizontal. The projectile muzzle velocity was assumed to be 2,850 fps.

TABLE XL. 20MM SAFETY FAILURE RATES

LIFE CYCLE PHASE	PRIMARY FUZE DESIGN	MINIATURE FUZE DESIGN
FUZE DURING ASSEMBLY OR SHIPPING	0.167×10^{-6}	0.381×10^{-6}
FUZE OR ROUND DURING LOADING, TRANSIT, OR STORAGE	0.00166×10^{-6}	0.00281×10^{-6}
FUZE OR ROUND DURING USE	0.00473×10^{-6}	0.0256×10^{-6}
TOTAL	0.174×10^{-6}	0.409×10^{-6}

TABLE XLI. CALCULATED PERFORMANCE VERSUS DESIGN GOALS

Item	Goal	Calculated Performance
Velocity at 2, 000-foot slant range	>3360	3, 460
Velocity at 9, 000-foot slant range	>1060	1, 360
Time of flight to 4, 000-foot slant range	~1. 4 seconds	1. 38
Ballistic match with SAPI	Same	Excellent
Ballistic match with M56	1 mil at 4, 000 feet	1 mil at 2, 500 feet
Maximum range, ground launch	M56	M56, 12, 000 feet SAPHE, 16, 000 feet

The SAPHE projectile thus meets and exceeds the performance standards set forth in the contract and was shown to be stable.

Experimental Results

Preliminary free-flight drag coefficient data determined by the Arnold Engineering Development Center at Tullahoma, Tennessee, are compared to the predicted drag data for a muzzle velocity of 2,920 fps in Figure 77. The experimental drag data of Figure 77 were used to compute PGU-2/B trajectories for the launch conditions specified in the requirements (790 KTAS aircraft in a 30-degree dive). These trajectories are presented in Figures 78 and 79. Table XLII summarizes the performance data.

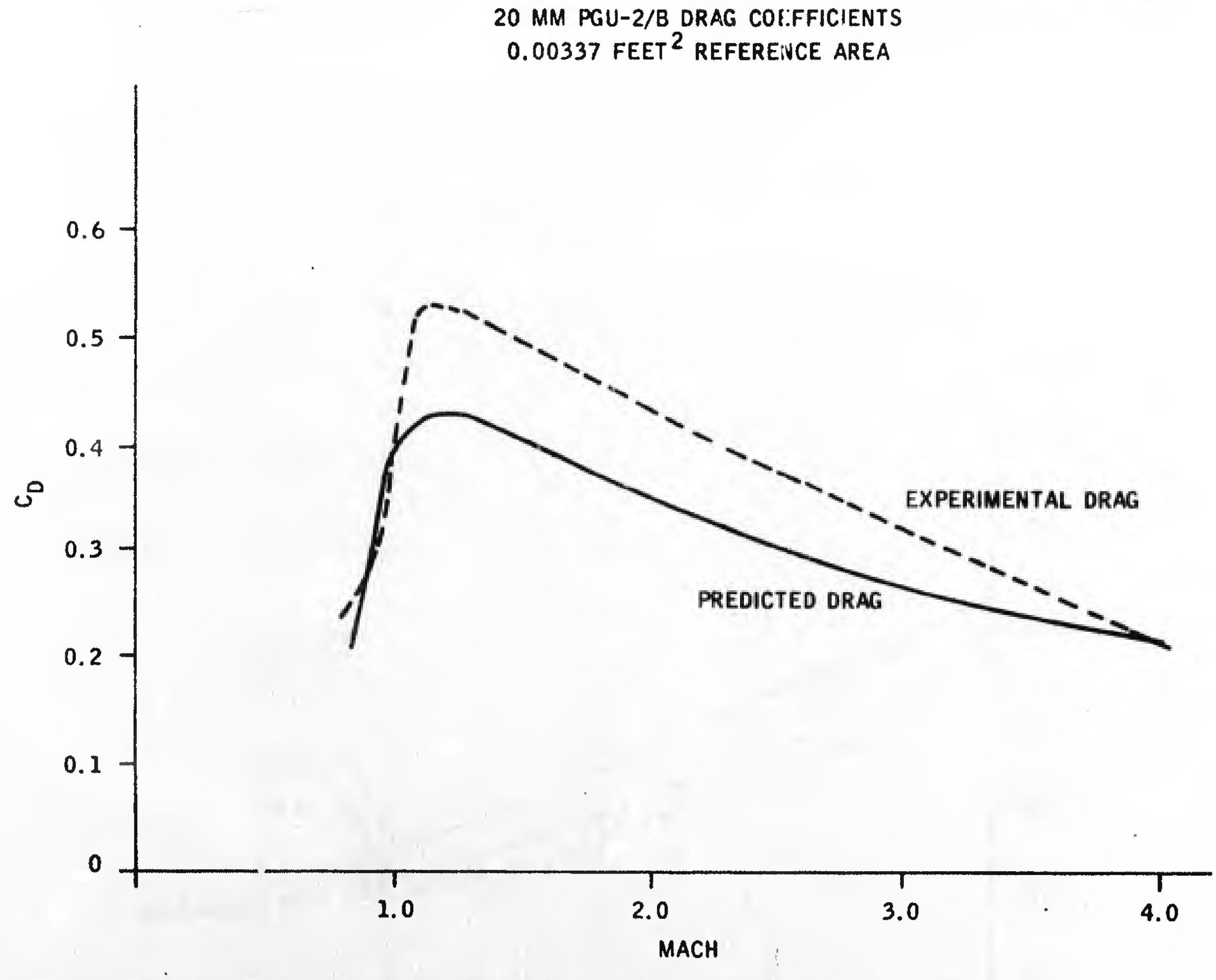

Figure 77. Comparison of Experimental and Predicted Drag Coefficient Data

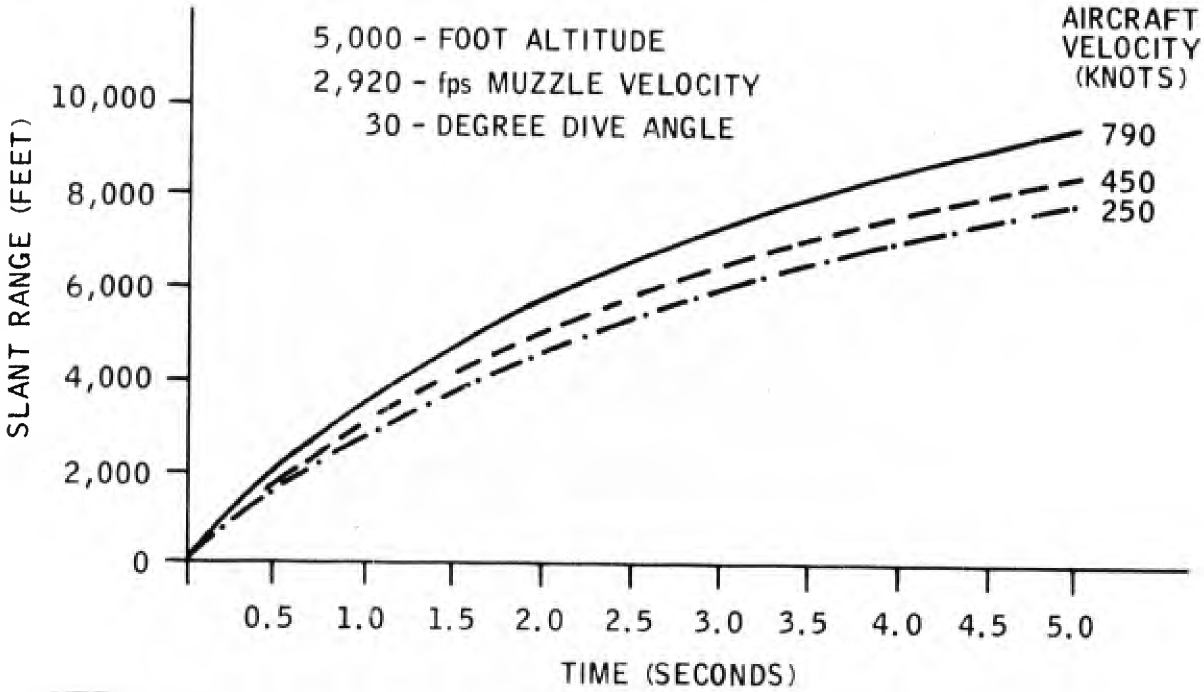

Figure 78. PGU-2/B, Time Versus Slant Range Using Experimental Drag Data

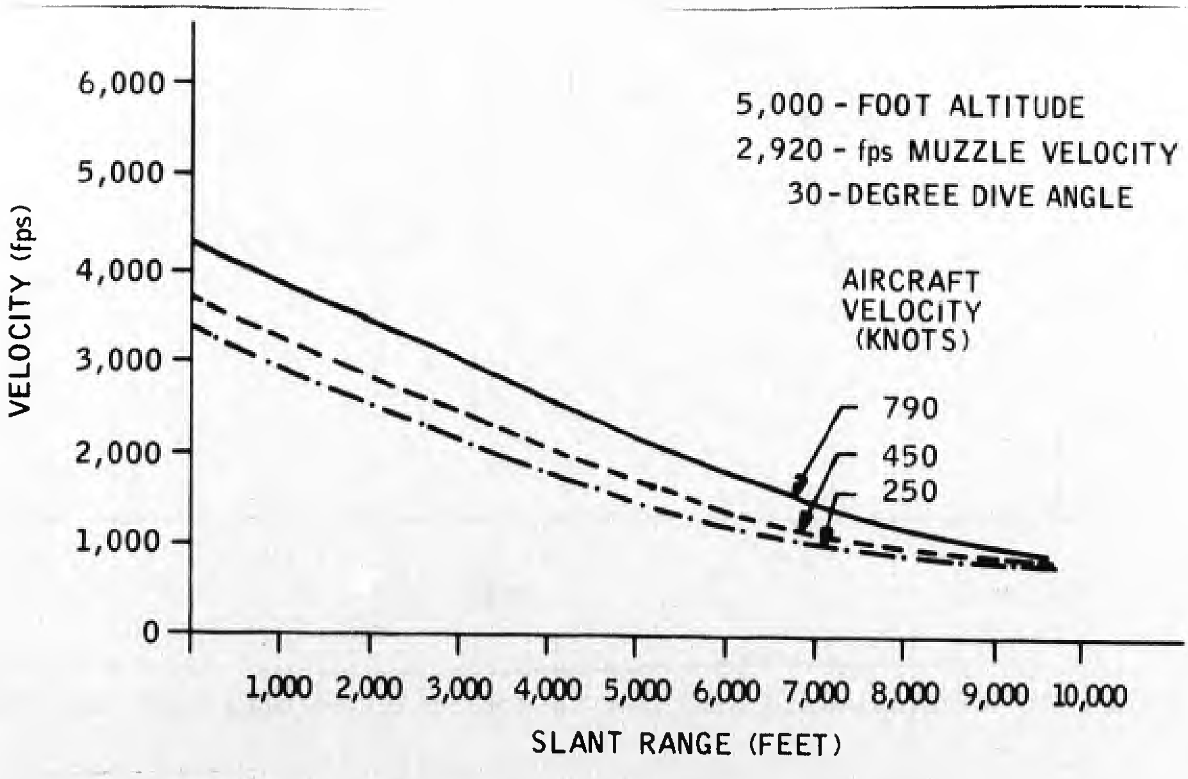

Figure 79. PGU-2/B, Velocity Versus Slant Range Using Experimental Drag Data

TABLE XLII. SUMMARY OF PERFORMANCE DATA

	Requirement	Predicted	Experimental
Velocity at 2, 000-foot slant range	3, 360 fps	3, 460 fps	3, 460 fps
Velocity at 9, 000-foot slant range	1. 060 fps	1, 360 fps	970 fps
Time of flight to 4, 000-foot slant range	1. 4 seconds	1. 38 seconds	1. 19 seconds
PGU-2/B trajectory match with M56 to 4, 000-feet	1 mil	1/4 mil	1/4 mil

These data show that the round can be expected to meet the trajectory requirements.

SECTION VI

IMPROVED ARMING DELAY

A. OBJECTIVE

During development of the PGU-2/B (SAPHE) projectile, it was observed that all projectiles armed momentarily at a muzzle distance of about 2 feet. This effect was attributed to overshoot as the firing pin left the slot, causing a momentary in-line position before the rotor started its normal spiral path to the armed position.

The contract was then modified to add an acceptable arming delay to the fuze. The basic objective of the program was to achieve a safe-separation distance of at least 6 meters, with an all-arm distance of 50 meters. The design goal was a safe-separation of 15 meters, if this proved possible without degradation of function or sensitivity of the projectile.

B. REDESIGN

To provide the required safe separation of the fuze, six parts were redesigned or changed: the rotor, setback spring, firing pin, crush washer, detonator, and rear rotor housing. These changes and the reasons for them are discussed in this section.

1. Rotor

To allow three degrees of freedom in rotor operation, a full ball rotor, shown in Figure 80, was substituted for the slotted rotor. This rotor was basically the M505 fuze rotor with a cage angle of 80 degrees. It normally used a detonator with an outside diameter (OD) of 0.147 inch but was adapted to the minature detonator (OD of 0.087 inch) by use of a steel adapter sleeve (Figure 81).

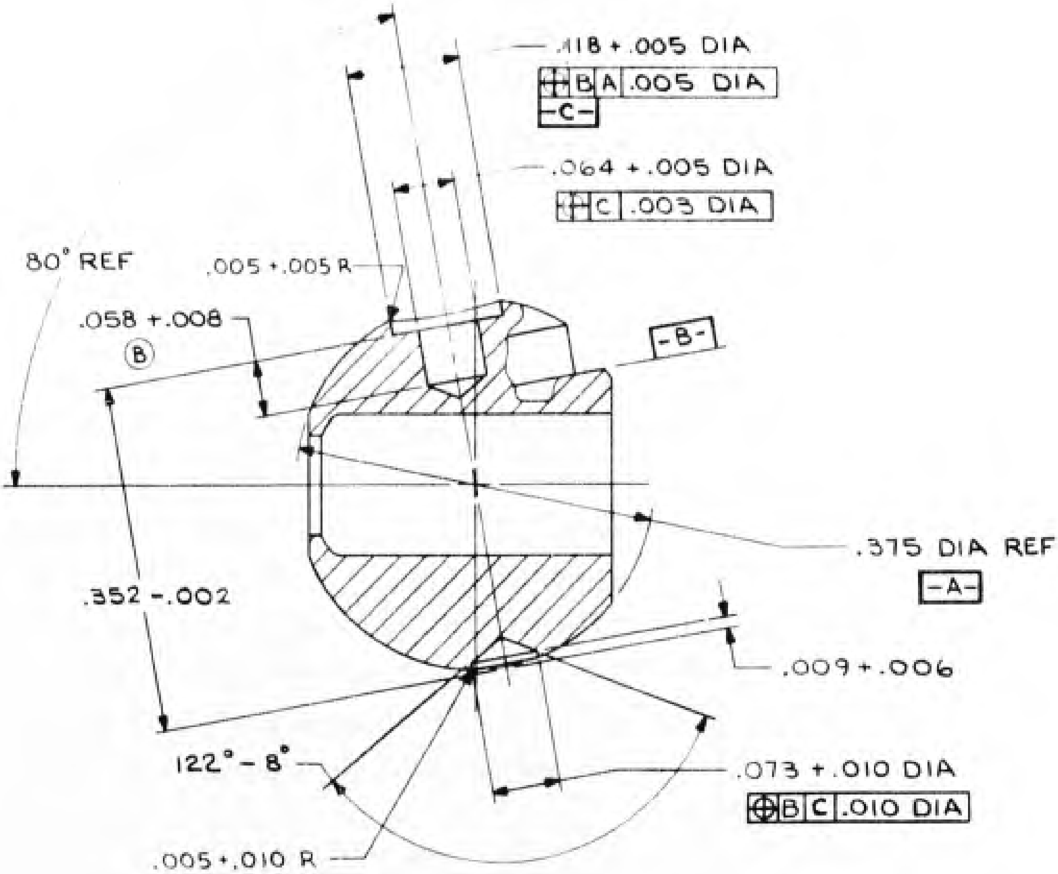

Figure 80. Modified Ball, Drawing Number 28009120

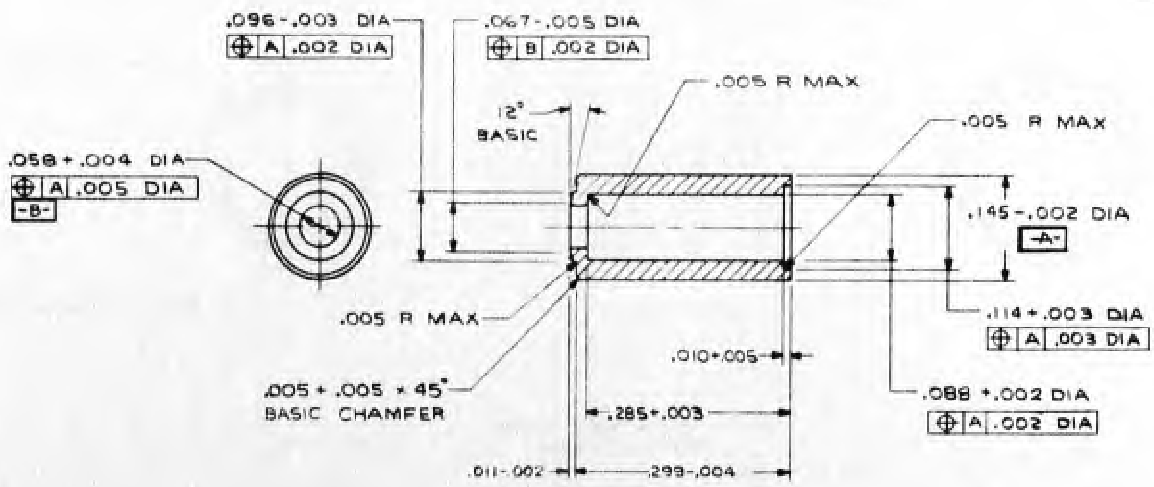

Figure 81. Detonator Sleeve, Drawing Number 28009118

The design change also offered increased out-of-line safety because the rotor cage angle was increased from 64 degrees in the existing fuze to 80 degrees. In case of inadvertent detonator function, the discharge would be directed into the strong side wall of the projectile.

2. Setback Spring

A stronger setback spring would provide increased insurance against a premature function caused by instability of the inertia weight, and the new fuze required a firing pin that could be completely withdrawn from the rotor. This required a reduction in storage volume for the spring which was already overstressed in storage in the standard SAPHE. A new spring would ideally have increased material volume for reduced torsional stresses and a reduced spring rate for greater sensitivity of the fuze against light targets, but would have provided a 6.0-pound force. To accomplish this a hybrid helical spring was designed for low stresses in storage and a low spring rate. This spring is illustrated in Figure 82.

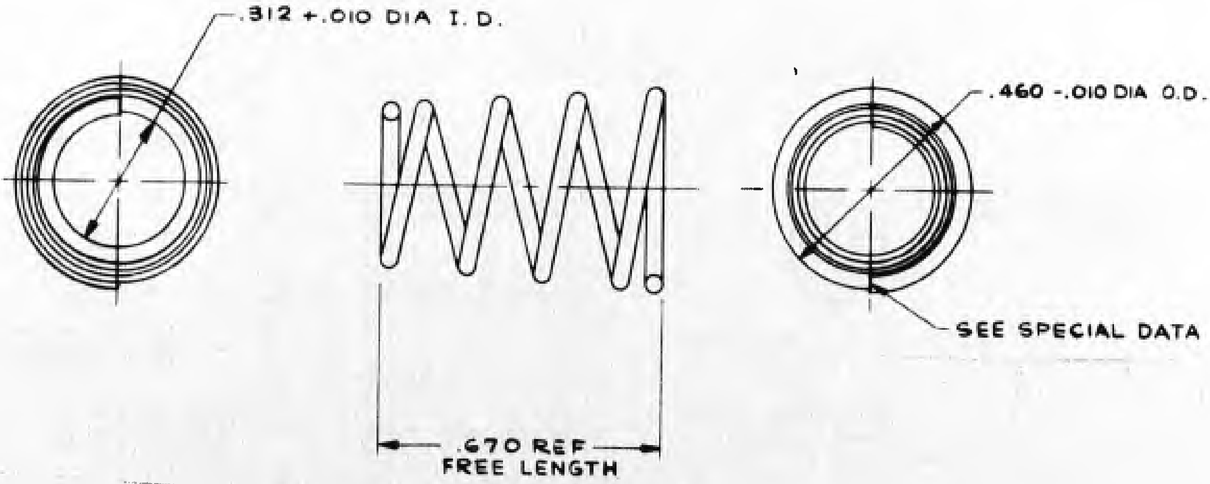

Figure 82. Setback Spring, Drawing Number 28009141

3. Firing Pin

The firing pin, redesigned to permit use of the hybrid helical spring, is shown in Figure 83. It weighed 0.0047 pound and was able to support all coils of the spring on setback. The increased mass of the pin would increase fuze sensitivity against thin plates on normal impact.

4. Crush Washer

So that the firing pin could be completely withdrawn from the rotor, the crush washer was modified to allow a setback distance of 0.085 inch. The modified washer (Figure 84) required a minimum load of 270 pounds before yielding. As the combined weight of the firing pin, inertia weight and setback spring is 0.012 pound, the yield load of 270 pounds is equivalent to approximately 22,000 g's. Results of compression tests (Figures 85 and 86) yielded the following data:

Unit No.	Overall Height before Test	Height after Test	Maximum Load at Yield (Pounds)	Maximum Applied Load (Pounds)
1	0.1665	0.075	271	826
2	0.1655	0.0755	282	828

5. Detonator

The change of the M55 detonator to the 20mm VADS (Honeywell No. 531680) was made to:

1. Change the ratio of moments of inertia to reduce the ball driving torque.
2. Increase the arming angle by effectively reducing the entry angle for the firing pin to reach the detonator.
3. Bridge the gap from firing pin to booster caused by full withdrawal of the firing pin.

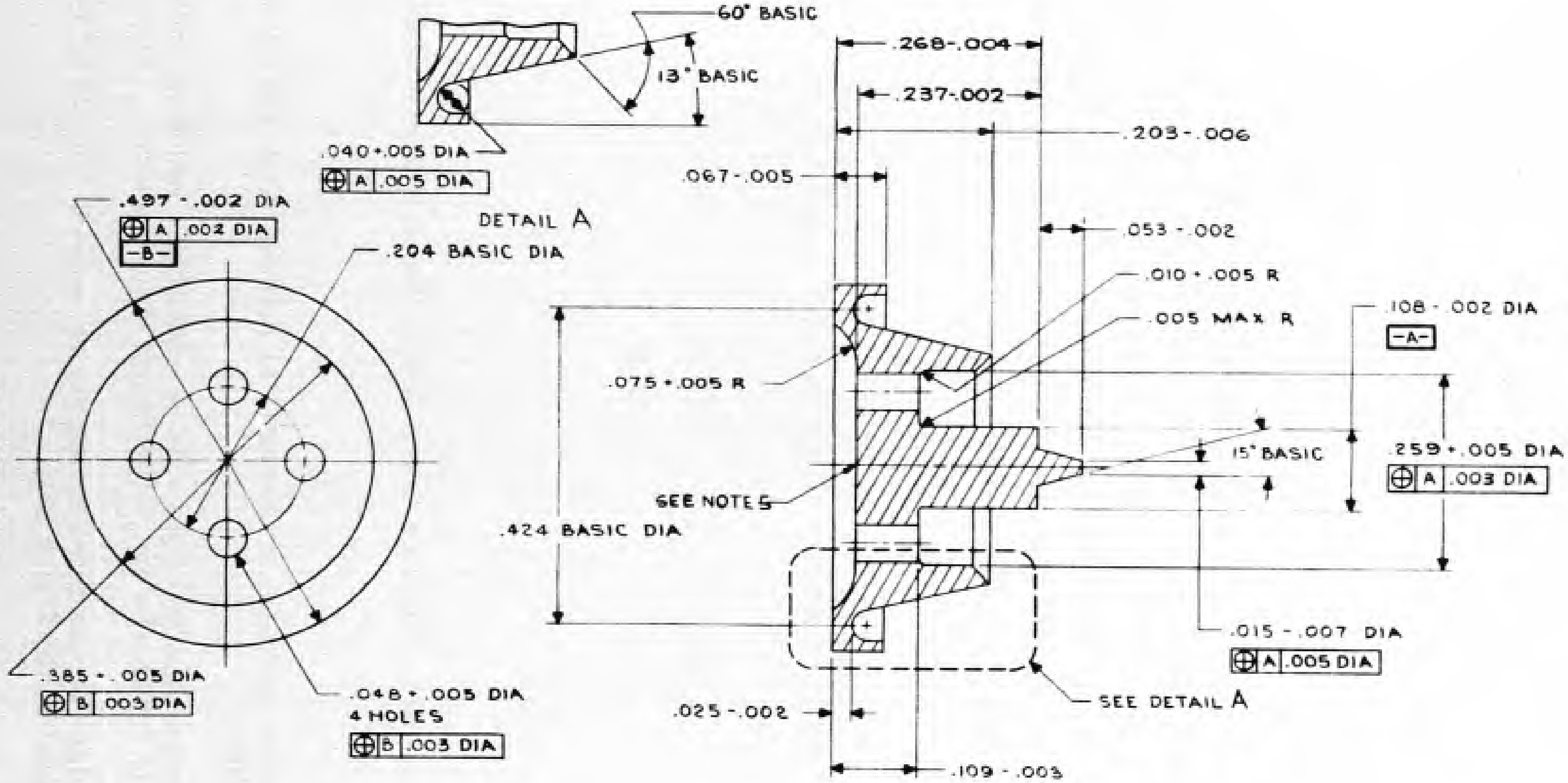

Figure 83. Firing Pin, Drawing Number 28009124

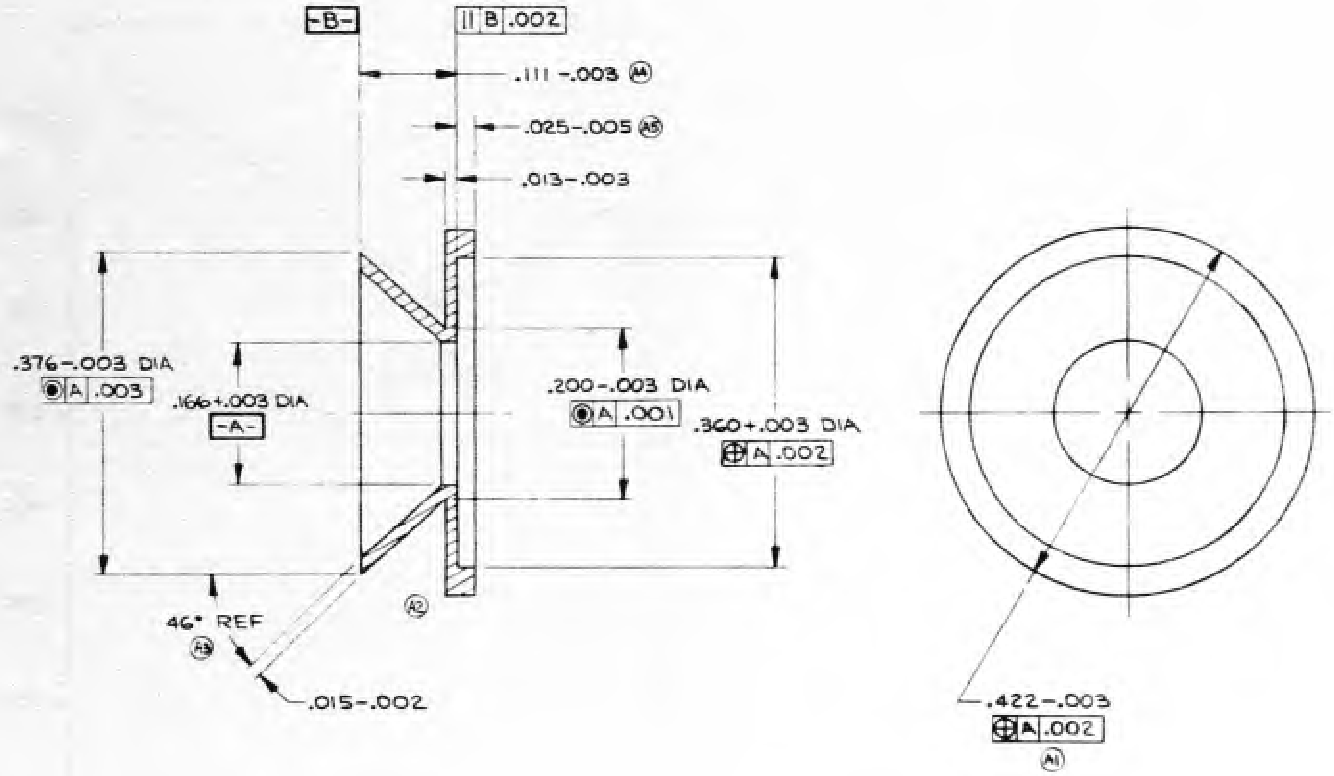

Figure 84. Crush Washer, Drawing Number 28102863

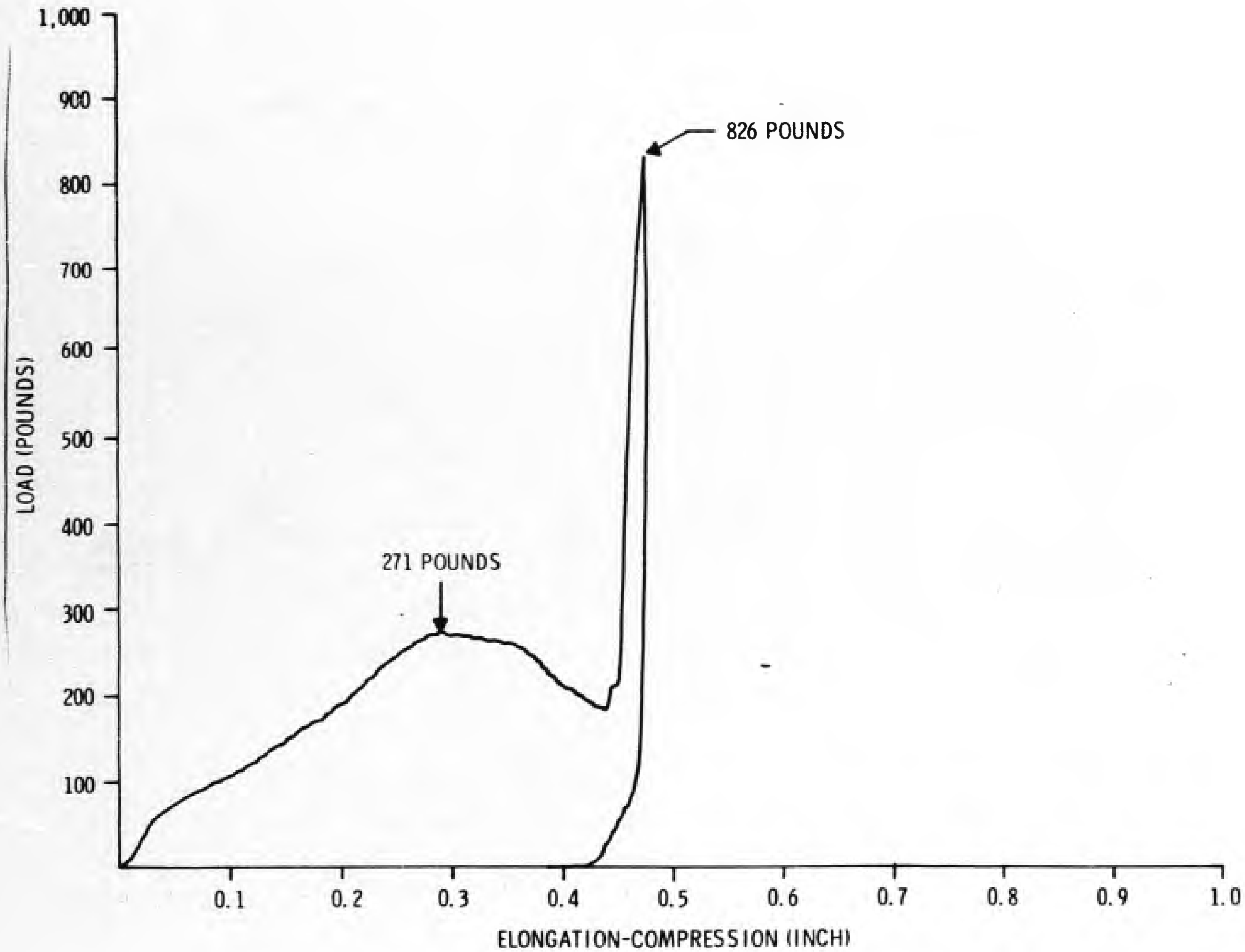

Figure 85. Results of Compression Tests (Unit 1)

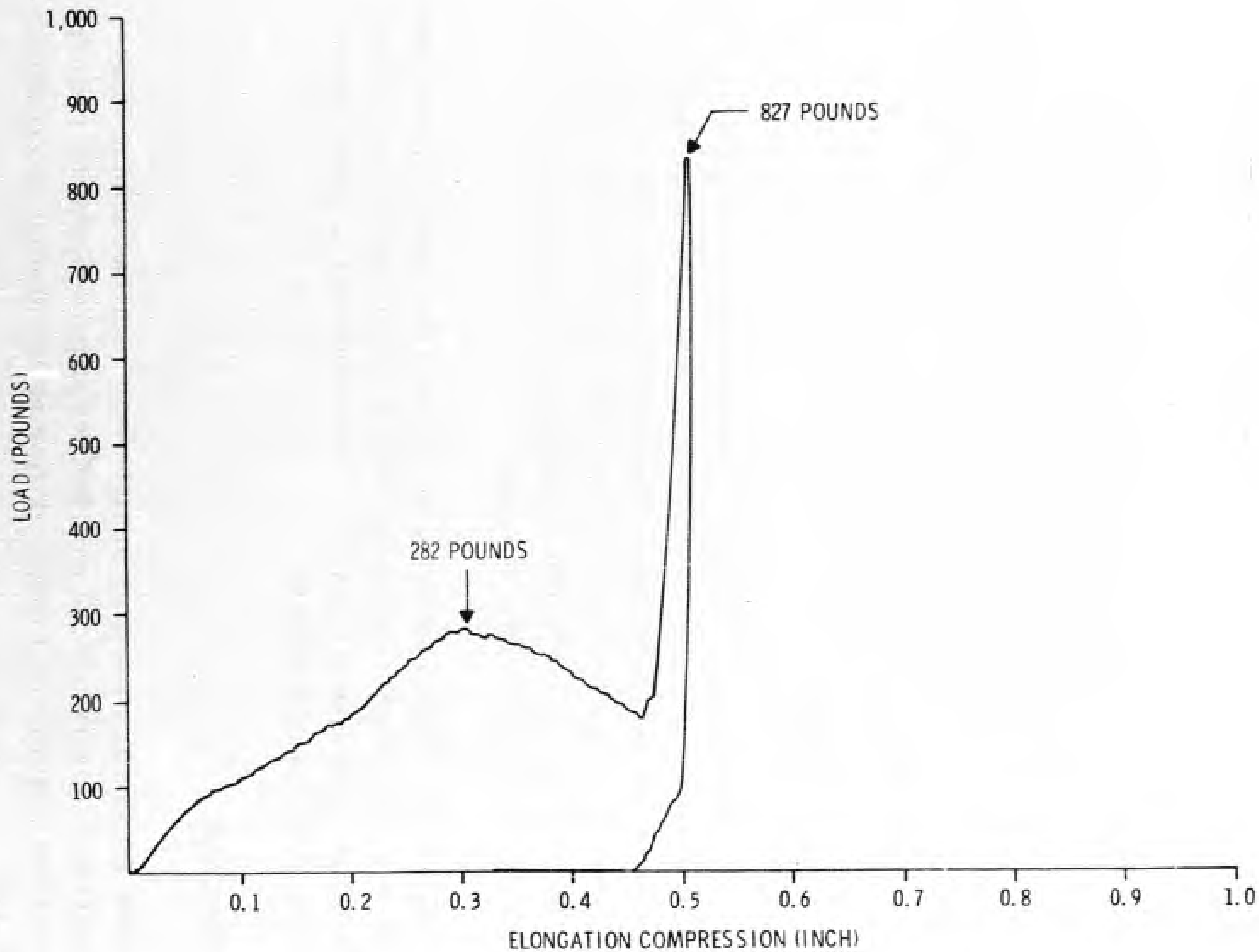

Figure 86. Results of Compression Tests (Unit 2)

Preliminary tests of the detonator output across air gaps to a booster at 7 degrees off axis indicated that the detonator functioned across an air gap from 0.025 to 0.350 inch. The test setup is illustrated in Figure 87. In a second testing technique, the air gap was maintained constant and the web thickness of the booster was varied.

High order detonations occurred in the boosters in all cases where the air gap was a maximum of 0.145 inch and effective web thickness of the booster was 0.017 inch maximum (0.012 + 0.005 inch). Since the normal air gap in the fuze would be 0.103 inch (0.088 min., 0.1175 max.), it was concluded that the miniature detonator would be acceptable, and it was incorporated into the SAPHE fuze design.

6. Rear Rotor Housing

The rear rotor housing was modified as shown in Figure 88 by increasing the thickness between its ball cavity and the after end of the housing to permit complete withdrawal of the firing pin from the rotor. The underside was also provided with a U-groove to retain the first coil of the hybrid bias spring. Six vent holes, 0.050 inch in diameter, were added to permit gas escape with accidental detonator function.

Static load testing indicated failure could occur with a load of 4,800 pounds. Maximum load that could occur during setback acceleration was calculated to be less than 2,400 pounds. A typical load curve from a Tinius Olsen load testing is shown in Figure 89.

C. ANALYSIS

Fuze graze sensitivity, thin plate impact sensitivity, and arming delay were analyzed to ensure that the modified design would meet the required and/or desired arming delay without degrading the function or sensitivity of the round.

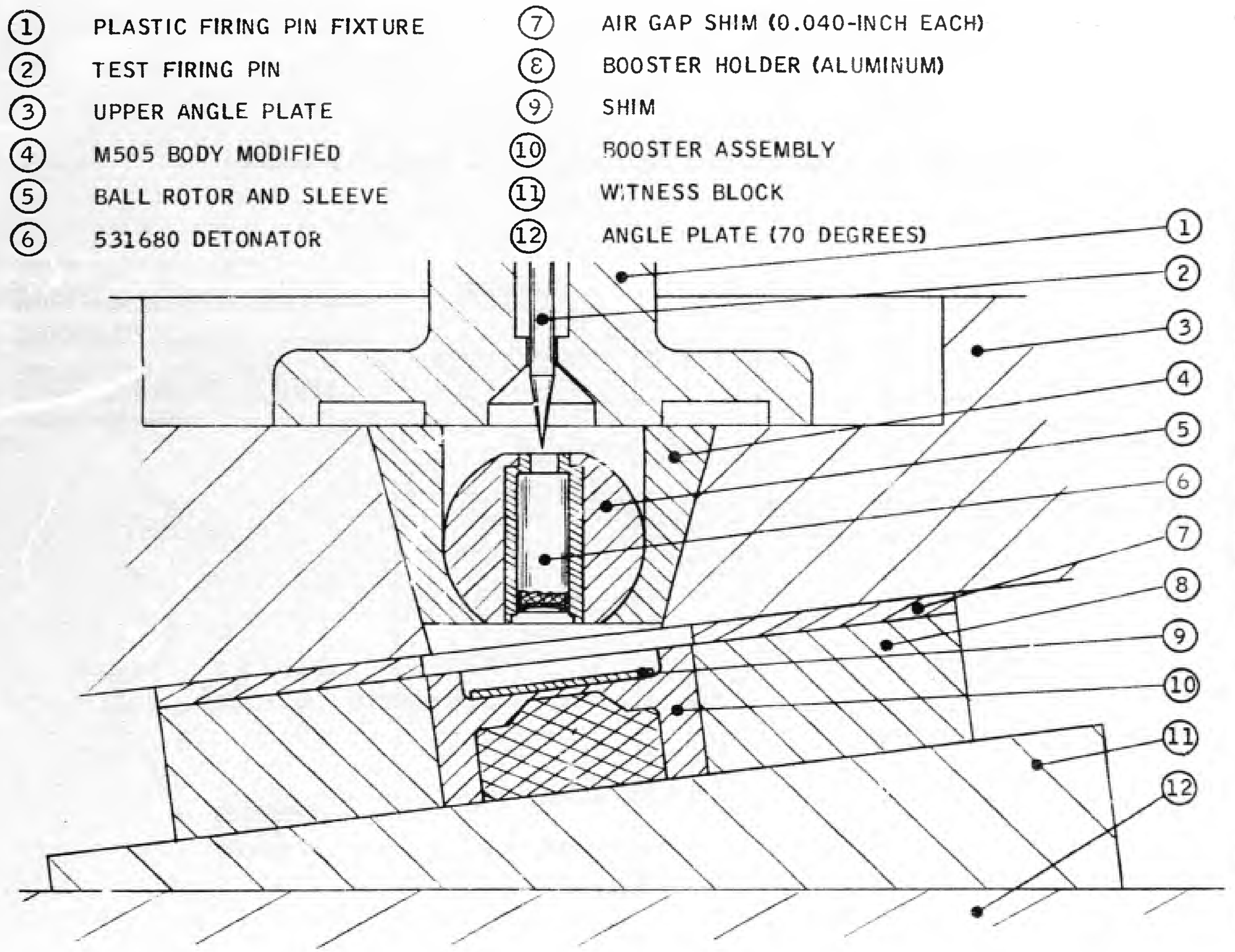

Figure 87. Fixture for Explosive Train Testing

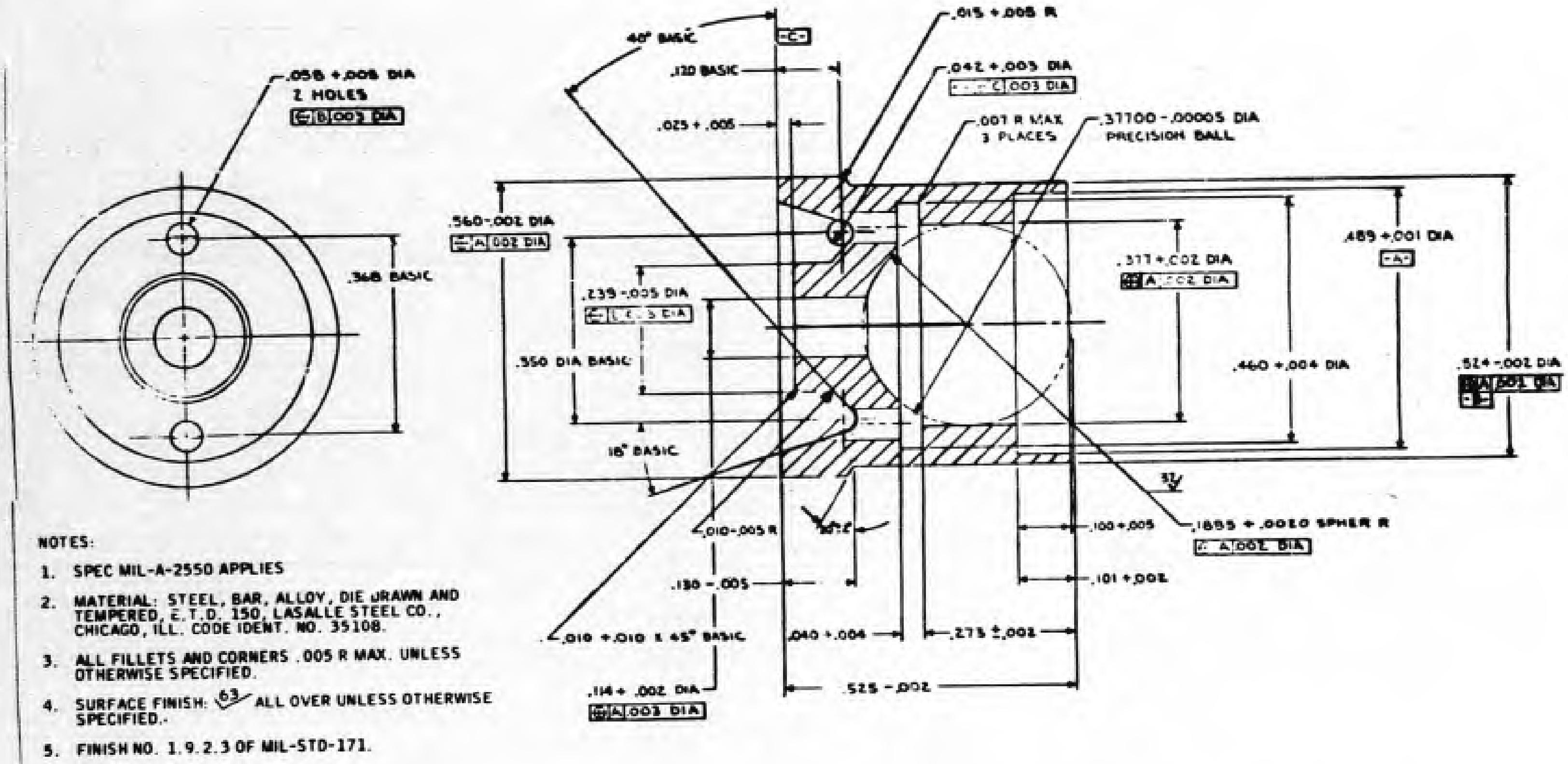

Figure 88. Rear Rotor Housing, Drawing Number 28009131

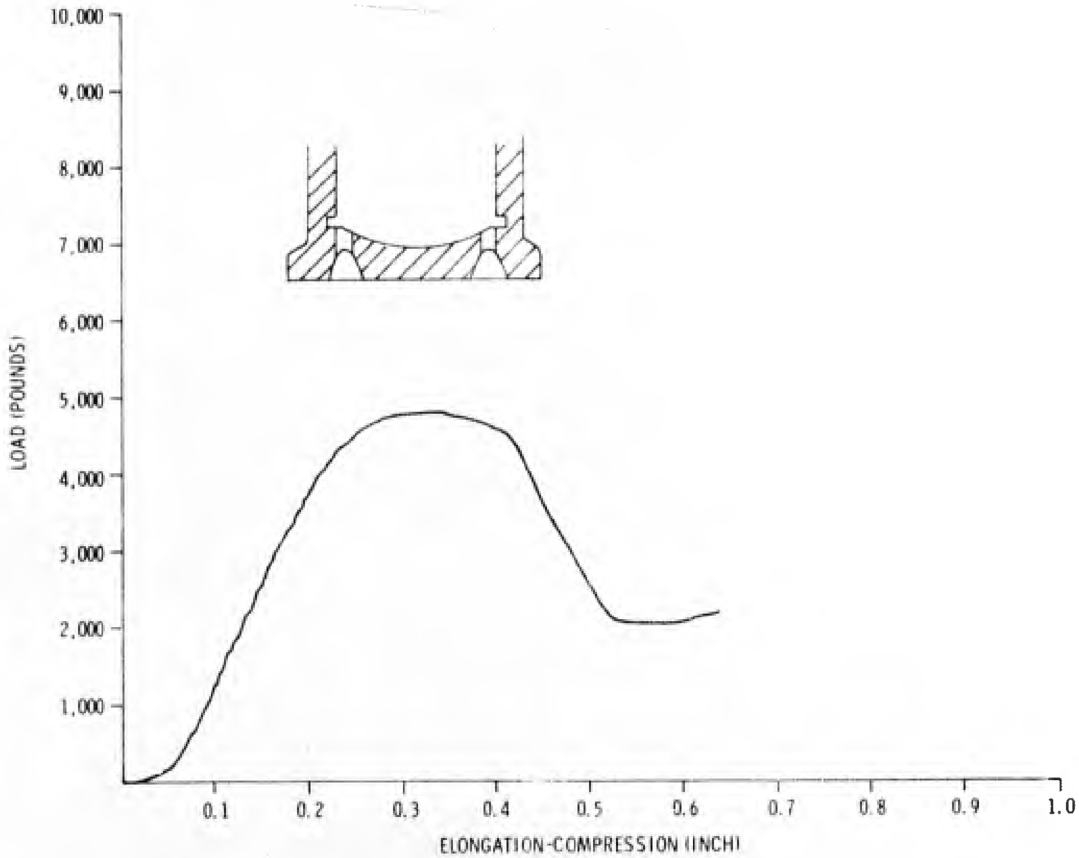

Figure 89. Typical Curve for 0.080-Inch Groove Depth and Six 0.050-Inch Holes

A graze sensitivity math model was used to predict action time (time from impact to firing pin contact with detonator), firing pin final velocity, and energy input to the detonator. Figures 90 and 91 depict the anticipated changes due to alteration in spring characteristics, firing pin weight and firing pin travel. Firing pin velocity and input energy available to the detonator is less for the modified fuze than for the standard fuze under any given level of side acceleration. It must be noted, however, that the input energy required is less than 0.06 inch-pound, and order of magnitude less than that available under the anticipated conditions of an 80-degree obliquity impact against hard steel targets. The standard SAPHE meets the required 100 percent function against 1/4-inch armor at 80-degree obliquity, and the modified fuze should also meet or exceed this requirement.

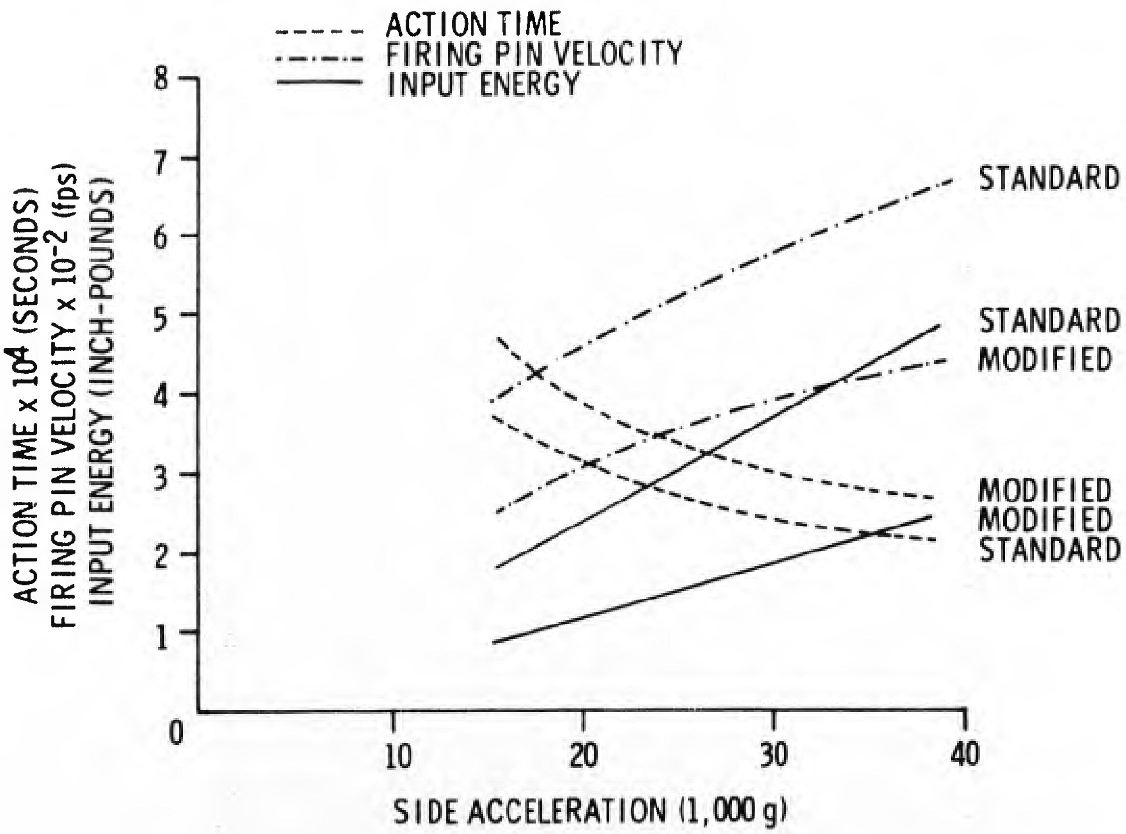

Figure 90. Graze Sensitivity of Standard and Modified SAPHE Fuzes

A very simple math model was used to calculate the energy available to initiate the detonator under various levels of deceleration against thin steel targets at normal obliquity. As the standard SAPHE attains an 85 percent proper function rate against 16-gage mild steel, and does not function reliably against 18-gage mild steel, the average deceleration encountered against the former target is probably just sufficient to supply the 3/4 to 1 inch-ounce energy required to function the detonator as a function of the average deceleration level encountered on normal impact. An 800-g level of deceleration is probably representative of the 16-gage mild steel target. In this range of average deceleration, the modified SAPHE should be more sensitive than the standard SAPHE. This means that the modified SAPHE should function reliably against thinner targets.

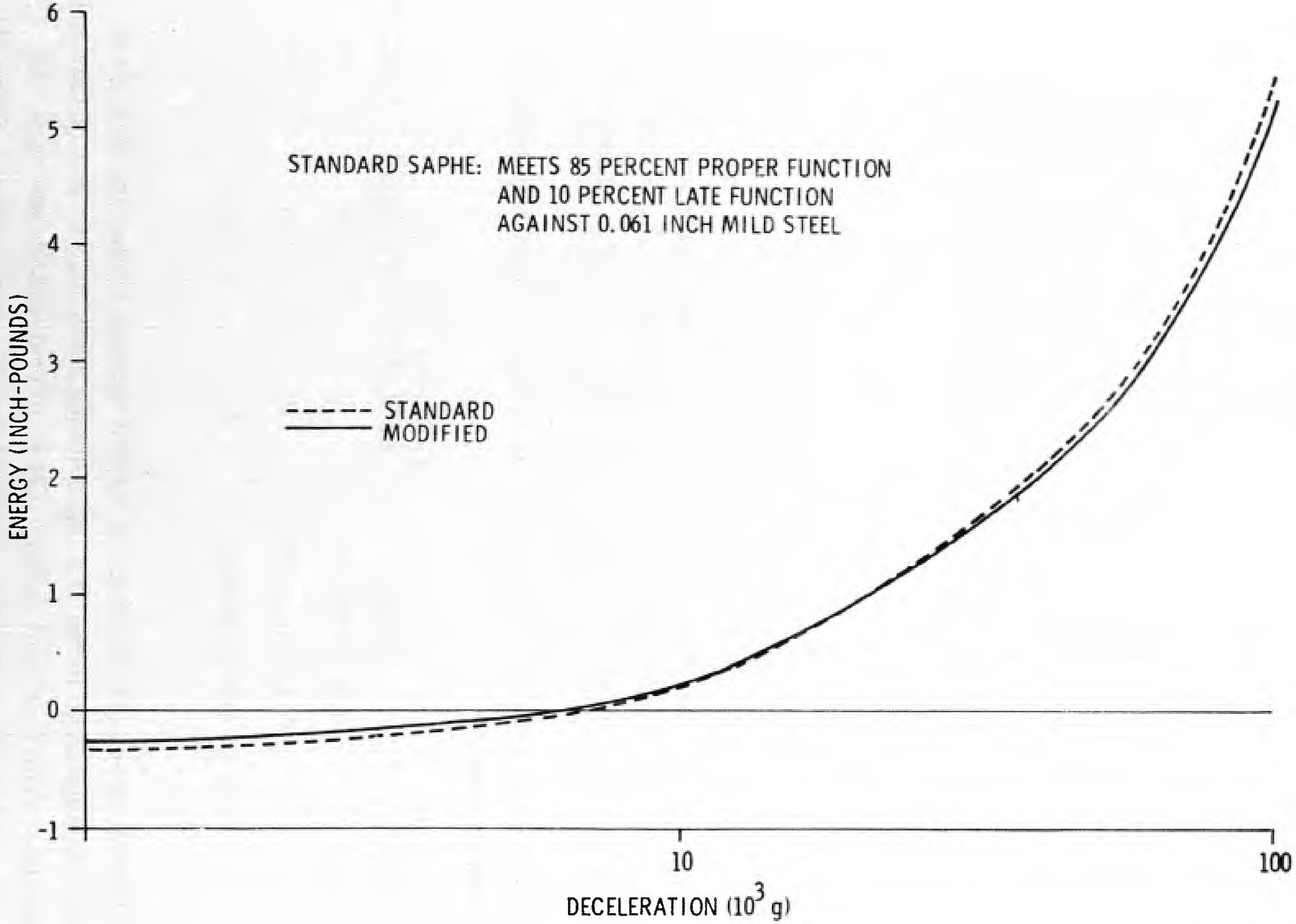

Figure 91. Energy Available to the Detonator on Normal Impact

Ball rotor arming delay is a function of several variables, among them friction coefficient (μ), rotor offset from the spin axis (ϵ), and the azimuth angle (ψ_o') of the detonator axis with respect to the offset direction. Figures 92 and 93 depict the arming delay of the modified SAPHE ball rotor. These predictions were made with the six-degree-of-freedom ball rotor math model. Figure 92 is the arming delay for unlubricated balls and Figure 93 for lubricated balls. The chosen friction values reflect friction test results obtained in another program; the offset values anticipated for the modified SAPHE are in the 0.003- to 0.007-inch range. Figure 92 indicates that the required safe separation distances (6 to 50 meters) should be met without friction control.

D. DEVELOPMENT

Nineteen of the new design PGU-2/B projectiles were gun-tested against 0.100-inch mild steel targets at contractor's test range. The results (Figure 94) showed that the new design was capable of meeting the arming delay requirements. (The twentieth test, Figure 94, was against a 0.049-inch-thick mild steel target to test sensitivity; no function occurred.)

Initial sensitivity testing of projectiles with the modified fuze produced the following results:

Approximate Velocity	Target	Obliquity (Degrees)	Successes	Percentage
2,900	0.062-inch MS	0	0/8	0
	0.110-inch MS	0	1/5	20
	1/4-inch RHA	80	0/4	0

The failures were attributed to the hybrid springs containing five coils, whereas springs used in the arming distance tests had a total of four coils per spring. (The four-coil spring was an overstressed spring in the assembly, but had been readily available for the arming test.) Since all

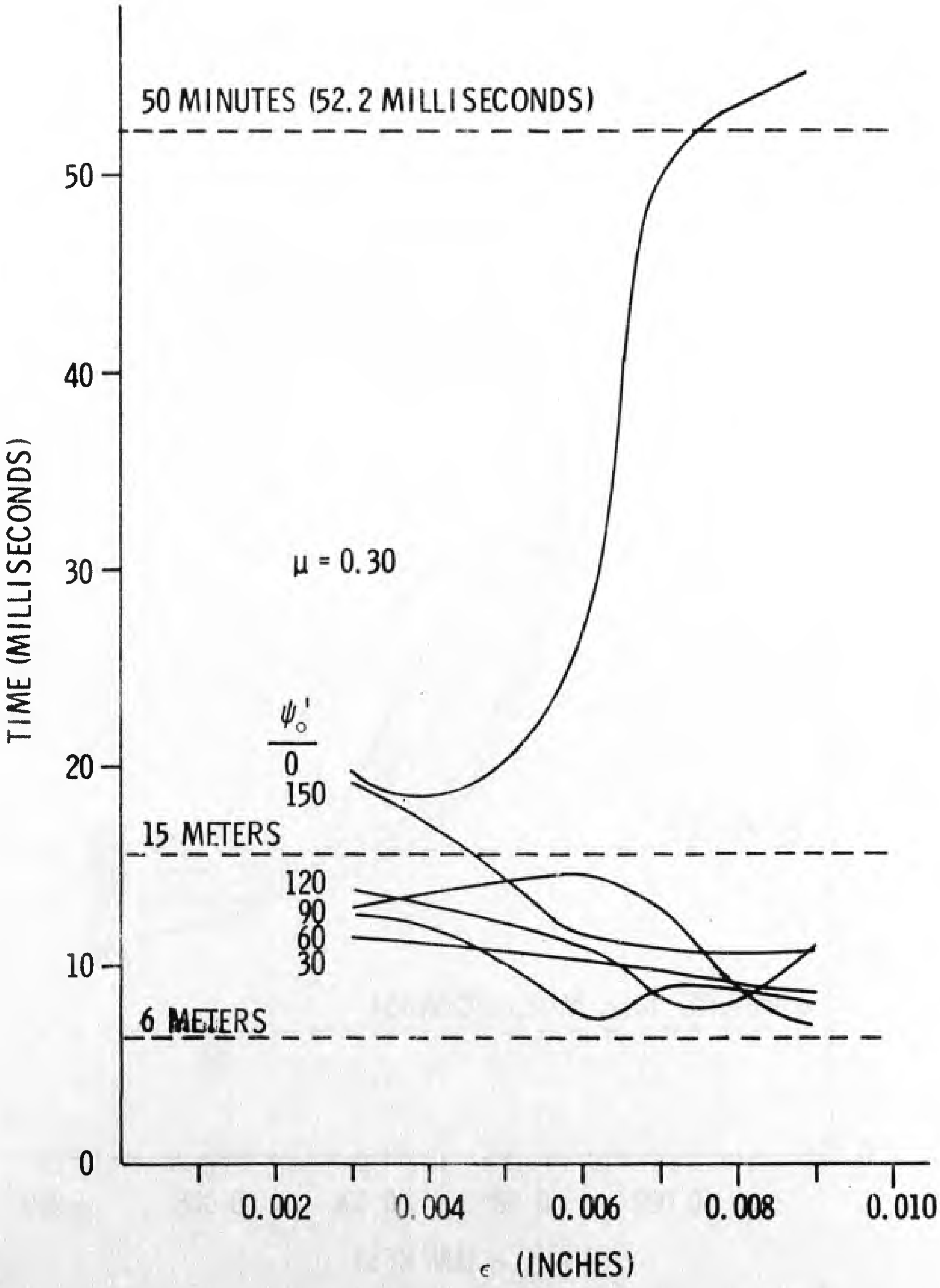

Figure 92. Time to Arm an Unlubricated Ball Rotor of the Modified SAPHE Design

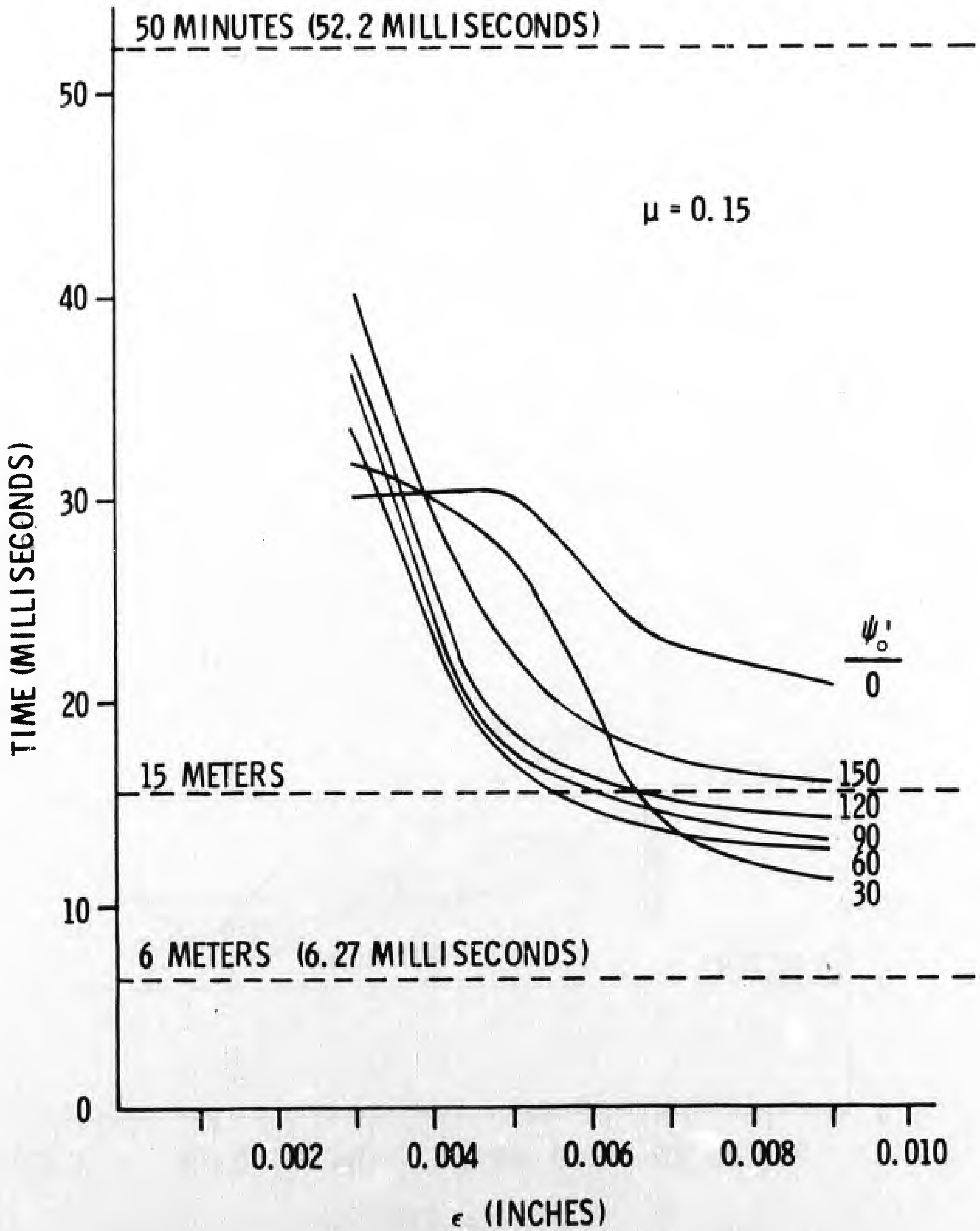

Figure 93. Time Required to Arm a Lubricated Ball Rotor of the Modified SAPHE Design

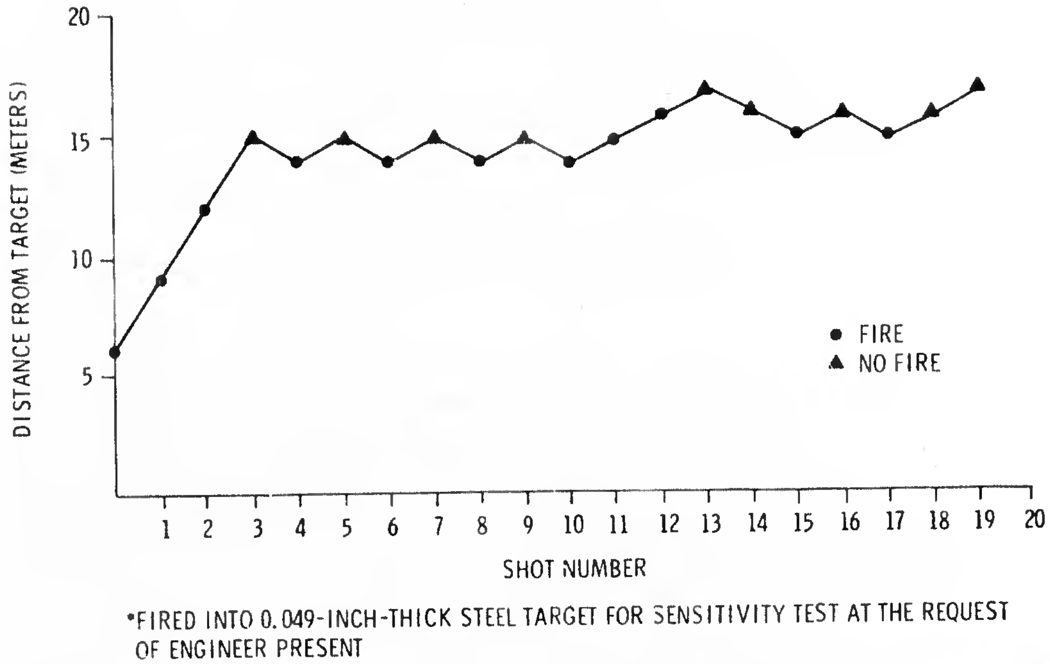

Figure 94. SAPHE Bruceton Test, 17 September 1971

projectiles were destroyed by impact against backup plates, no positive causes could be established other than the possibility that spring coil hangup or stacking prevented full forward travel of the firing pin into the detonator.

There had been three projectiles remaining from this lot that were not tested, and a repeat test was conducted to confirm or deny the conclusions from the first test. This test group included the three reserve units from above plus six inert projectiles with inert fuzes. Flash X-ray was employed to establish arming and function of the fuzes. In addition, the six inert units were retrieved from cotton waste material for fuze analysis after testing. The six soft catch units contained two of each type of three springs supplied from separate vendors. Results are shown below:

Velocity		Obliquity (Degrees)	Successes	Percentage
2,900	0.102-inch MS	0	1/3	33
	0.102-inch MS	0	Soft catch	

Analysis of the soft-catch retrieved units showed that the setback springs had been deformed from a truncated cone shape to a barrel shape with coils No. 2, 3, and 4 having permanently expanded beyond the outside diameter of the largest coil. This same shape existed on all springs, including those with four coils previously tested. Internal markings in the fuze gave evidence of a coil having been obstructed by the protrusion at the interface of the rear housing and the base plug.

X-ray observation confirmed that the active spring coils expanded to give the spring a barrel shape, and in most cases either No. 2 or No. 3 coil was obstructed from further forward movement by protrusion of the rear housing. The condition would cause the stacking of two coils and prevent firing pin travel to the detonator.

Six units were modified to remove the protrusion that obstructed the hybrid helical spring, and six units were built with a new firing pin, a modified inertia weight, and a conical spring similar to that in the standard SAPHE. The firing pin was changed (as shown in Figure 95) to function with a conical spring, and the firing pins had four 3/32-inch-diameter vent holes in the flange. The inertia weight was changed (as shown in Figure 96) by making the front surface flat. This reduced the mass of the weight from 0.0056 pound to 0.0049 pound, thus permitting use of a lighter spring. The new spring (Figure 97) gave a stabilizing force of 4 pounds.

Test results were as follows:

Hybrid Spring Units

Velocity		Obliquity (Degrees)	Successes	Percentage
2,900	16 gauge MS	0	0/4	0
	14 gauge MS	0	2/2	100

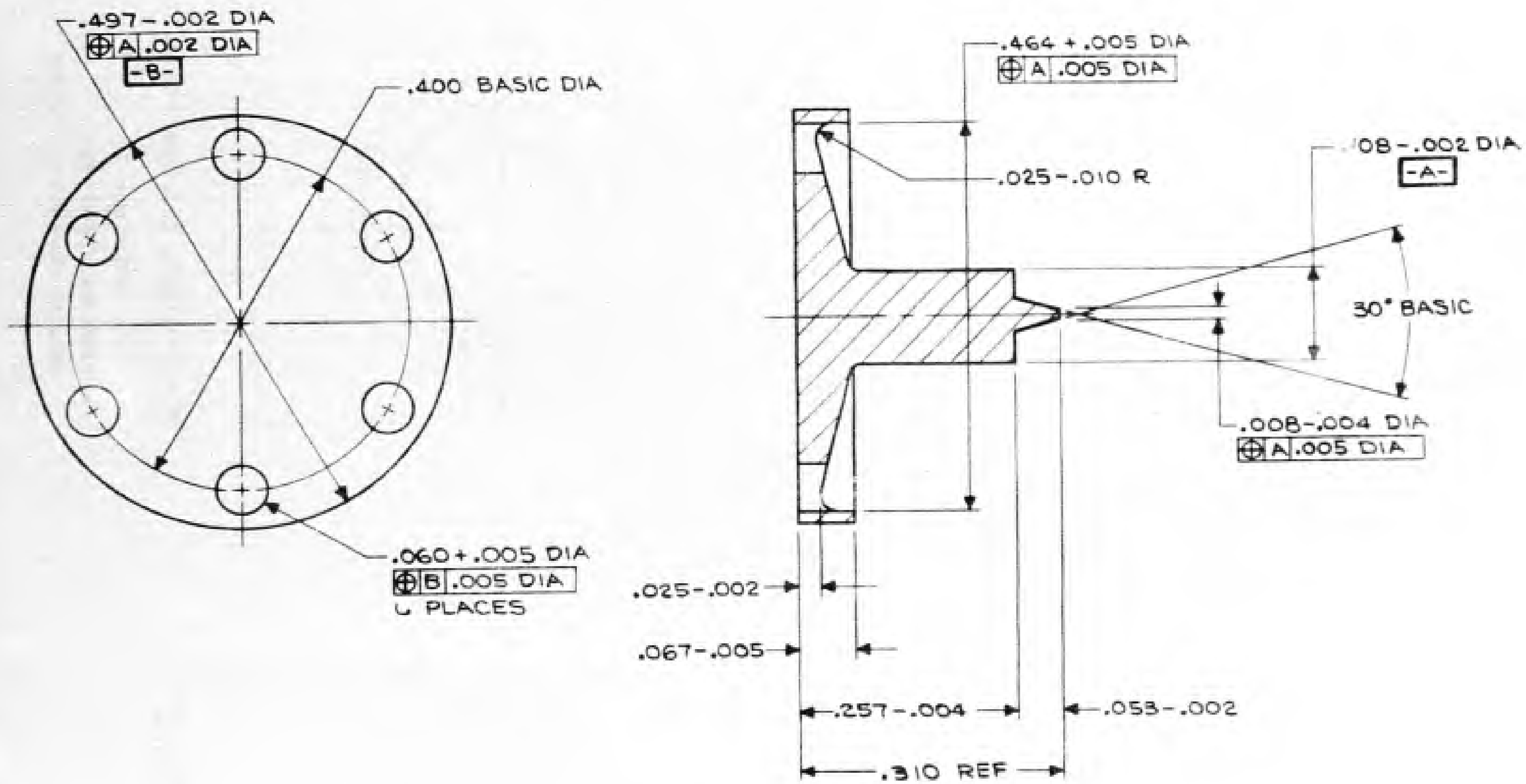

Figure 95. Firing Pin, Drawing Number 28009655

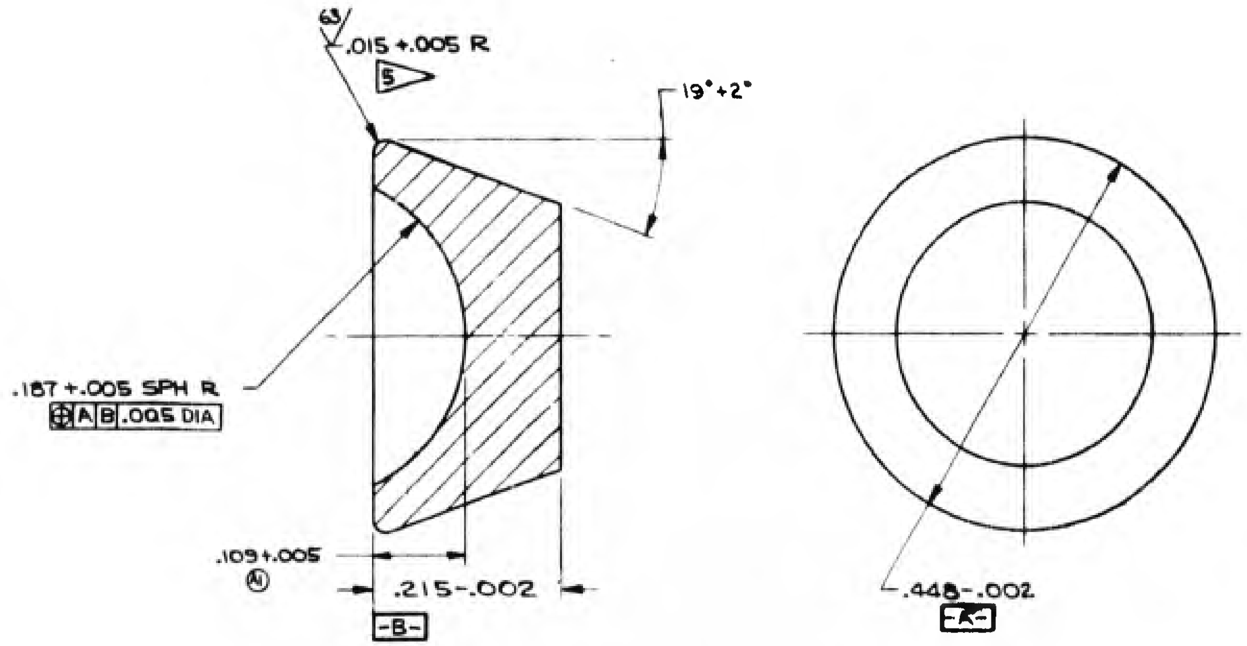

Figure 96. Inertia Weight, Drawing Number 28103276

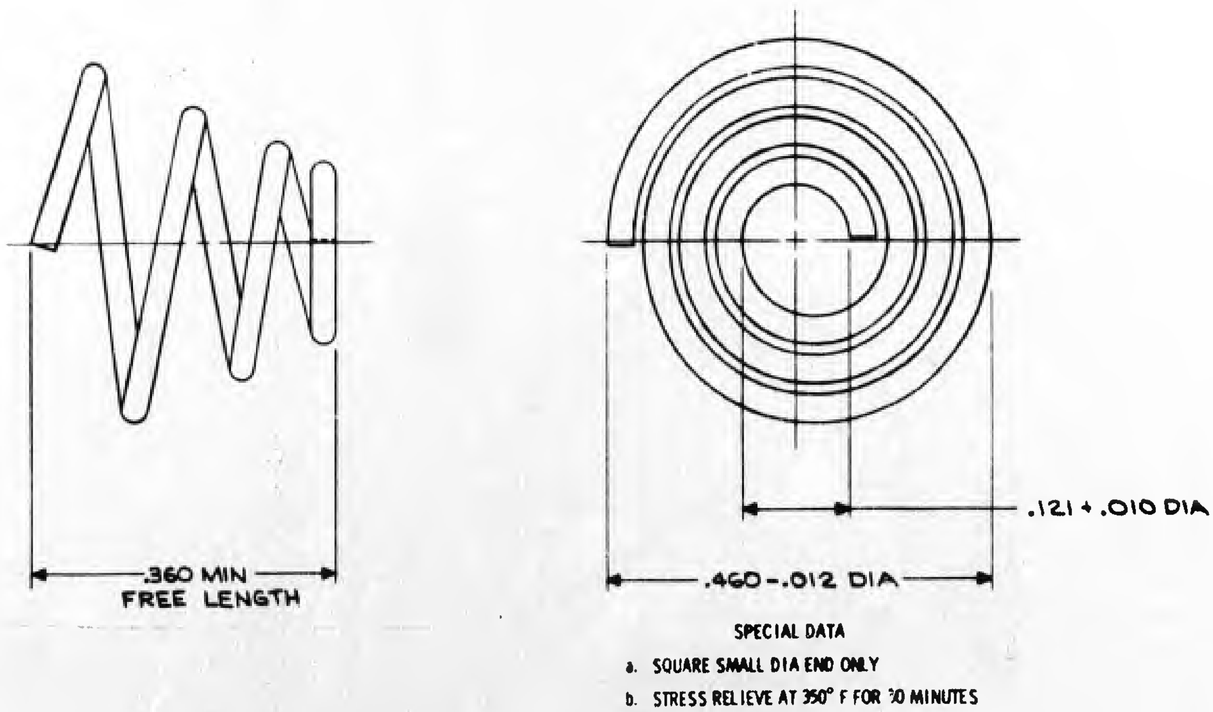

Figure 97. Setback Spring, Drawing Number 28009939

Conical Spring Units

Velocity	Target	Obliquity (Degrees)	Successes	Percentage
2,900	16 gauge MS	0	0/2	0
	14 gauge MS	0	2/4*	50

* One of the four units had an incorrectly selected hybrid spring and could not function (this unit had vent holes). The two successful units had firing pin flanges with four holes in each.

Static X-rays showed that in some cases the large coil of the conical spring had not nested properly in the firing pin flange. The springs had been readily available from contractor inventory and had the large coil slightly oversize (approximately 0.020-inch). However, failure could not be positively attributed to this condition.

Eight new fuzes were built with the flat weight and new firing pin, but with each conical spring having 1/2 coil clipped from the major diameter to ensure proper nesting. Six fuzes were also built with a significant modification. These units consisted of the standard SAPHE inertia weight with a semiflat forward surface and a firing pin held by six 1/16-inch diameter balls to replace the setback spring. This fuze is illustrated in Figure 98. Test results were as follows:

Velocity	Target	Obliquity (Degrees)	Successes	Percentage
		Conical Spring Units		
2,900	16 gauge	0	0/2	0
	14 gauge	0	0/3	0
	12 gauge	0	1/2	50
		Ball Lock Units		
2,900	16 gauge	0	0/2	0
	14 gauge	0	0/2	0
	12 gauge	0	0/1	0

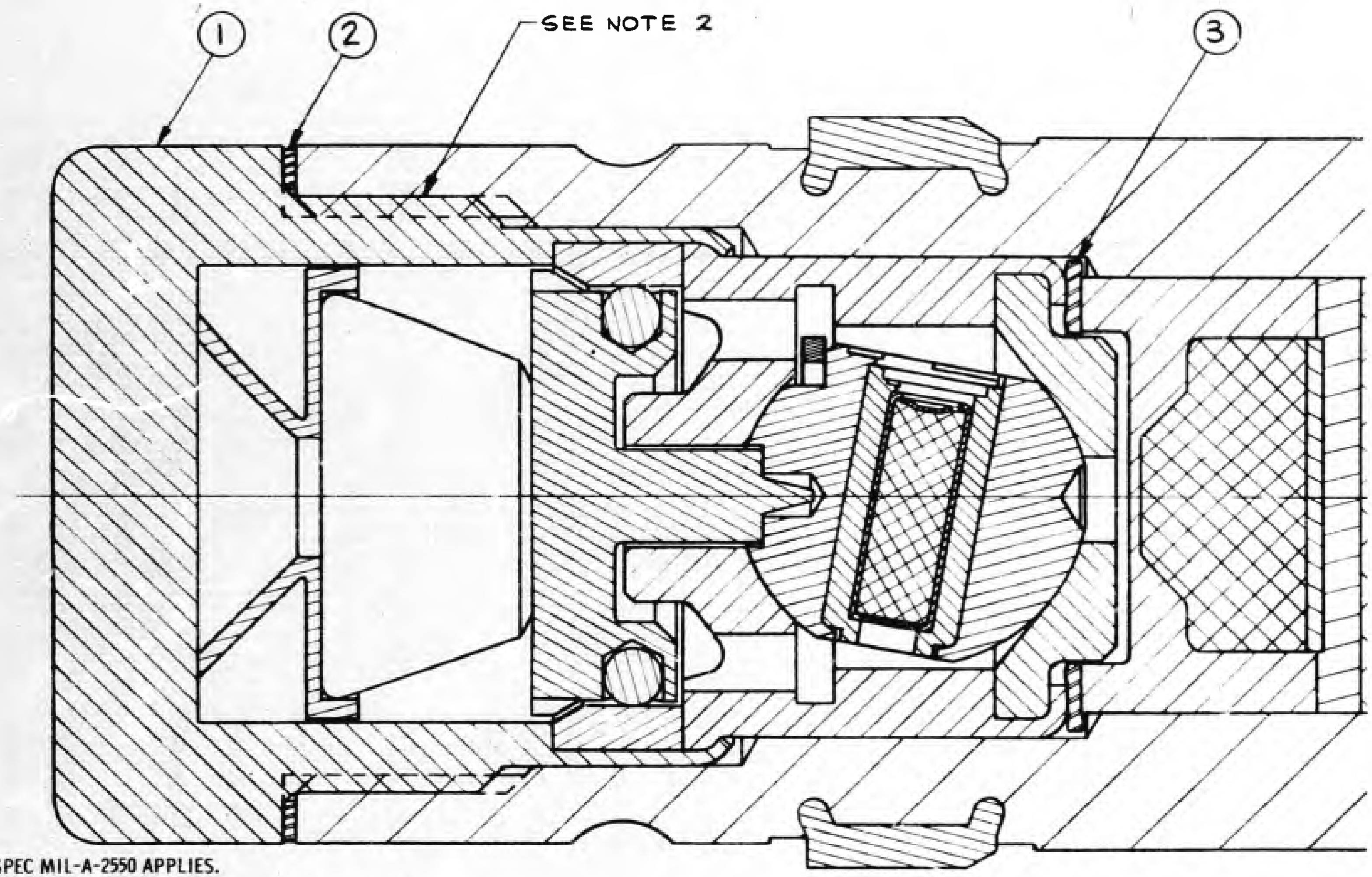

NOTES:

1 - SPEC MIL-A-2550 APPLIES.

2 - THREAD SEALANT MATERIAL: ADHESIVE, SEALANT, CELLULOSE NITRATE, TYPE II, PER MIL-A-82484.

3 - WHERE DAMAGED, RETOUCH EXTERIOR SURFACE PER 28102981-001 AS APPROPRIATE.

Figure 98. 20mm PGU-2/B Projectile, Drawing Number 28009562

Analysis established that 8 of the 12 units tested had improper rotor adaptor sleeves for the miniature detonator, preventing the firing pin tip from reaching the detonator.

X-rays of fuzes after target impact indicated that four of the seven spring system fuzes had firing pins in far enough forward to have reached a properly placed detonator and must have impacted into the obstructing detonator sleeve. One unit indicated insufficient travel of firing pin, one had no X-ray, and one functioned properly. Four of the ball/lock fuzes also had firing pins sufficiently forward for firing, while one additional unit had no X-ray.

A new test lot was built. This consisted of both spring system fuzes and ball/lock fuzes. Diameters of the firing pin and the number of vent holes in the flange of the spring units were also varied.

The miniature detonator had previously been used with firing pin tips of $0.008 \begin{smallmatrix} +0.000 \\ -0.004 \end{smallmatrix}$ inch diameter. All SAPHE firing pins had a tip diameter of $0.015 \begin{smallmatrix} +0.000 \\ -0.007 \end{smallmatrix}$ inch. Testing of the modified SAPHE fuze with the miniature detonator and reduced diameter firing pin tip configurations would yield information on detonator/firing pin relationships for improved sensitivity.

Test results were as follows:

Velocities: 2, 900 fps
Obliquities: 0 degree

Ball Lock Fuze

Target MS	Successes		X-ray Analysis *	
	0.015	0.008	0.015	0.008
18 gage	1/2	1/3	2/2	2/3
16 gage	1/2	2/3	2/2	3/3
14 gage	1/1	-	1/1	-
Total	3/5	3/6	5/5	5/5

Spring System

	0.015	0.008	0.015	0.008
18 gage	0/2	2/3	0/2	2/3
16 gage	1/3	0/2	1/3	2/2
14 gage	1/1	-	1/1	-
1/4 RHA 80 degrees	1/1	1/1	1/1	1/1
Total	3/7	3/6	3/7	3/6

* X-ray observation again indicated that firing pin travel on units that failed to function was sufficient to have penetrated detonators in several cases.

Further analysis of the test results showed that firing pin flanges with six vent holes were superior to firing pins with four vent holes as shown below:

	Successes	
	6 holes	4 holes
18 gage	2/2	0/3
16 gage	3/3*	0/2
14 gage	-	1/1

* Successes include X-ray observations of forward travel of firing pins.

The X-ray photographs also gave evidence that four of the successfully fired units were low order explosions in each main charge, while boosters were intact or undamaged. This would indicate possible detonator-to-booster insensitivity. In previous air gap tests the miniature detonator had occasionally punched a hole through the booster cup and explosive fill without initiating the explosive at air gaps of 0. 130 to 0. 150 inch and through barriers of 0. 020 to 0. 025 inch. The Miznay Shardin profile of the detonator evidently produced a very small diameter jet that fired into a relatively larger diamemeter receiver area, resulting in a dissipation of energy into the large area without properly supporting the shock wave.

This detonator was initially designed for effectively jumping air gaps of 0. 200 to 0. 400 inch, so that the air gap range (0. 090 inch to 0. 120 inch) of the modified SAPHE was not in its most efficient range.

To improve the efficiency of the relatively thin jet, a booster of different proportions was fabricated and tested by Stresau Laboratories. This booster had an improved explosive column diameter in relation to the jet diameter (Figure 99) and was inserted into the high explosive column where all surfaces of the booster would be an interface with the HE except at the receiver end of the detonator. This configuration did not provide proper initiation.

The explosive train was then investigated by Stresau Laboratories whose report is included as Appendix IV. The investigation showed that a loading pressure of 55, 000 psi, used by contractor to consolidate the boosters, reduced sensitivity, and a loading pressure of approximately 37, 000 psi produced the most reliable transmission of detonation. Stresau then supplied contractor with 250 boosters loaded with PBXN-5 consolidated at 38, 000 psi, and fuzes were fabricated for a new series of tests. Fuzes were the same as the test fuzes prior to the explosive train problem. All firing pin flanges contained six 1/32-inch holes equally spaced near the flange periphery. Test results were:

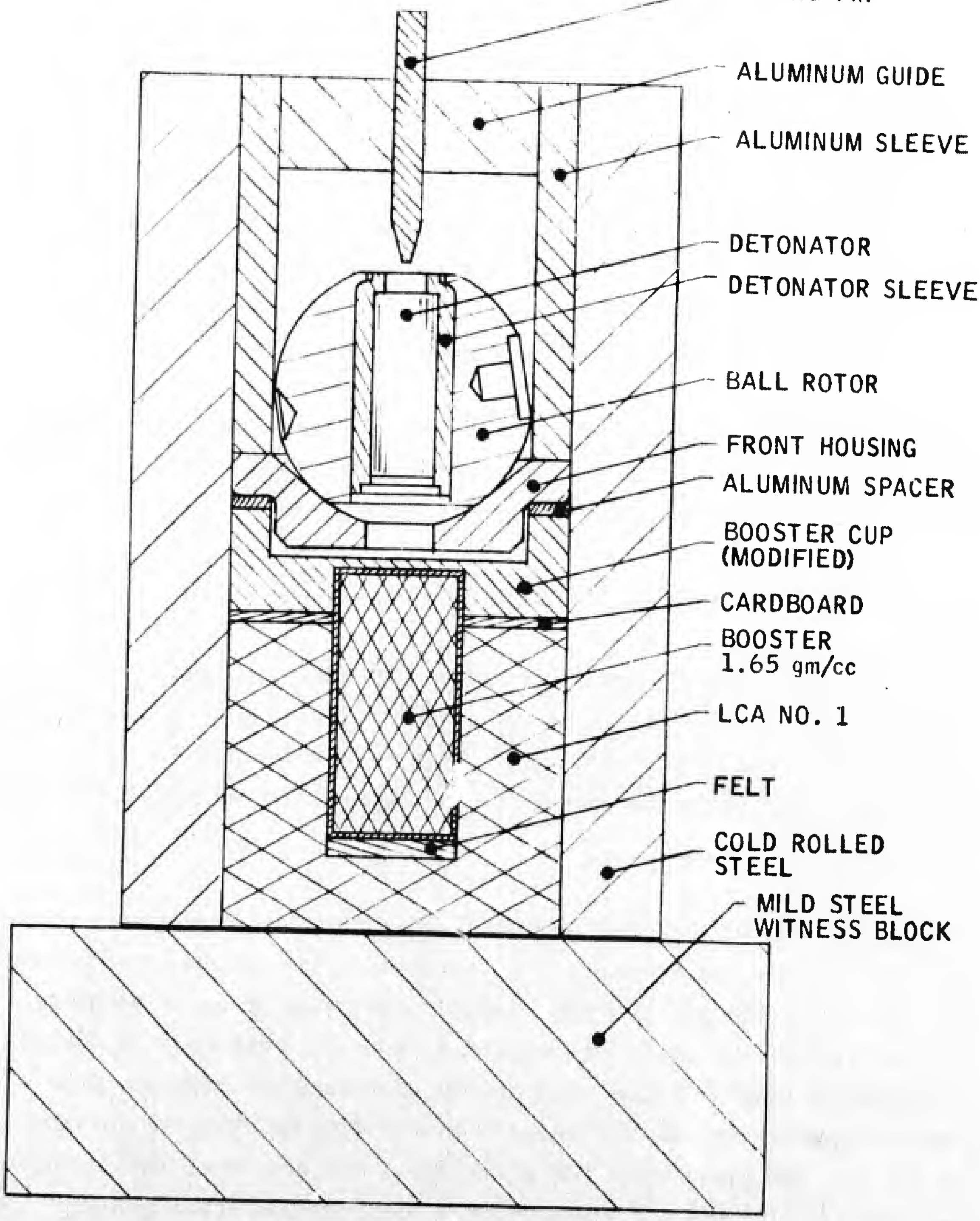

Figure 99. Test Fixture for Small L/D Booster

	Successes	
16 gage	5/5	(1 was low order)
18 gage	6/6	(1 was low order)
1/4 - 80 degrees	2/2	(1 was possible low order)

As low order initiation was still in evidence, it was decided to improve friction control by lubricating the rotor for a more positive alignment and better explosive propagation. Accordingly, 25 fuzes were modified by applying a lubricant (McLube 1720) to each ball rotor. Low density boosters were also used. Test results were:

	Successes	
18 gage	4/5	
16 gage	7/8	(2 possible low order)
1/4 - 80 degrees	5/10	(4 of 10 additional units had fuze separation on oblique target. 1 of 10 was a dud.)

As the McLube lubricant did not accomplish the expected improvement in explosive propagation, it was postulated that the problem may have been the eclipse of the detonator output by the front rotor housing. (See Figure 100.) It was therefore decided to increase the diameter of the front rotor housing hole by 40 percent to prevent eclipsing of the jet if the rotor did not reach perfect alignment.

Unlubricated rotors were assembled into fuzes; the rotor housing hole was 0.140 inch diameter. Test results in arming against a 12-gage target were as follows:

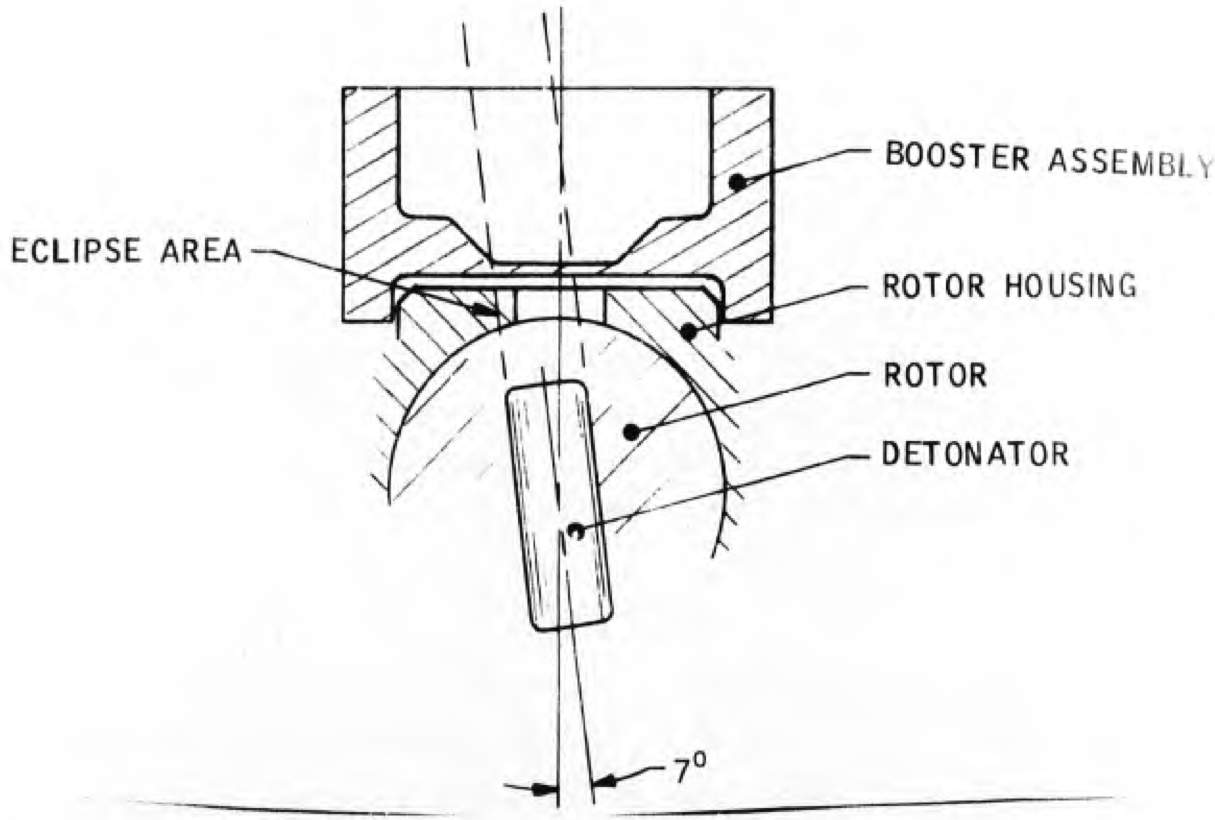

Figure 100. Eclipse Condition With Rotor Alignment 7 Degrees Off Axis

6 meters	1/8 successes	
15 meters	6/8 successes	(1) low order
25 meters	6/8 successes	
35 meters	6/8 successes	(1) low order
50 meters	7/8 successes	

As low order detonation was still a problem, for the next test the rotor contact areas were lubricated with Emralon, and the larger front housing hole and Stresau loaded boosters were used in units fired against 12-gage targets at 50 meters. There were 10 out of 10 successes.

As functions appeared proper at 50 meters, testing for arming delay at 6 meters with lubricated parts was considered essential, and fuzes were assembled containing Emralon lubricated parts, enlarged front housing holes, and Stresau boosters. Three of the 10 functioned at 6 meters, one low order, showing that arming delay had not been accomplished nor was propagation of explosive completely reliable. However, it was considered that improved arming delay could be accomplished by better lubrication and surface treatment of ball contact areas. Ten fuzes were assembled with polished and molykoted (molybdenum disulfide) surfaces and a clipped C-ring to ensure a more positive opening of the rotor detent spring (C-ring). The modified C-ring is shown in Figure 101.

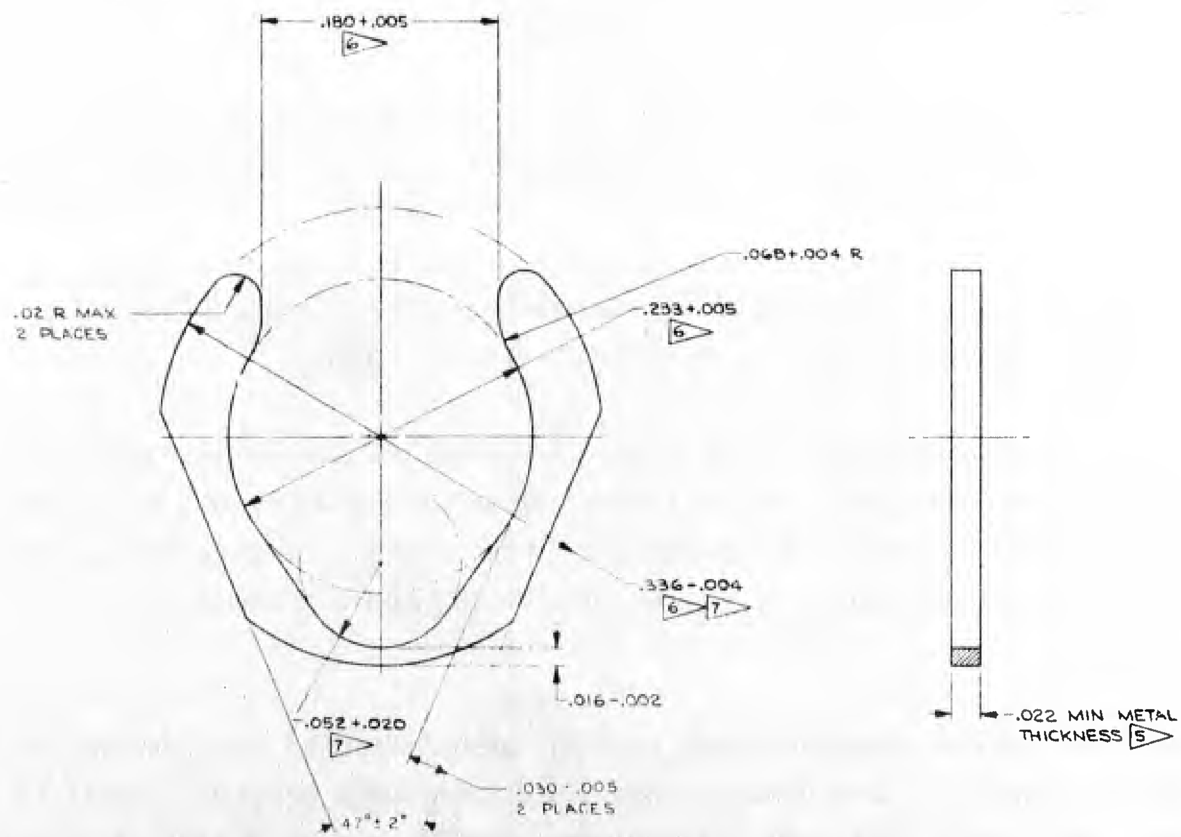

Figure 101. Rotor Detent Spring, Drawing Number 28009934

The ten fuzes were assembled into rounds with Stresau boosters and tested at 6 meters with no functions. It was concluded that molykote lubrication improved arming delay.

A confirmation test on identical fuzes—except with a standard SAPHE C-ring in place of the clipped C-ring to establish the C-ring contribution to arming characteristics—resulted in one out of ten functioning at 6 meters. This confirmed that lubrication contributes to arming delay.

In an attempt to find an alternate detonator, detonators were fabricated by a local vendor with the full diameter of the M55 but the same length as the miniature detonator (Figure 102A). The detonator had an internal sleeve to reduce the explosive column but retain the larger output of the M55.

In laboratory tests, three functioned high order, but in the remaining two the booster fill blew out with no significant energy output. Apparently, NOL was forced under the aluminum sleeve and expelled it, breaking up the RDX so that it did not initiate. The detonator was then modified by chamfering both ends of the tube to prevent this and to improve transition of the shock wave into the larger diameter of RDX fill (Figure 102B).

Tests of the modified detonator in the out-of-line position showed that the output was too powerful. A third detonator was designed by decreasing the column length of the RD 1333 to reduce output strength (Figure 102C). This detonator failed to initiate a booster consistently and was therefore abandoned.

As shown earlier, boosters could be made more sensitive to the output of the miniature detonator if the pressed fill density were reduced. Boosters were accordingly made with a density of 1.65 g/cc and fuzes using the miniature detonator assembled into test rounds. The results were as follows:

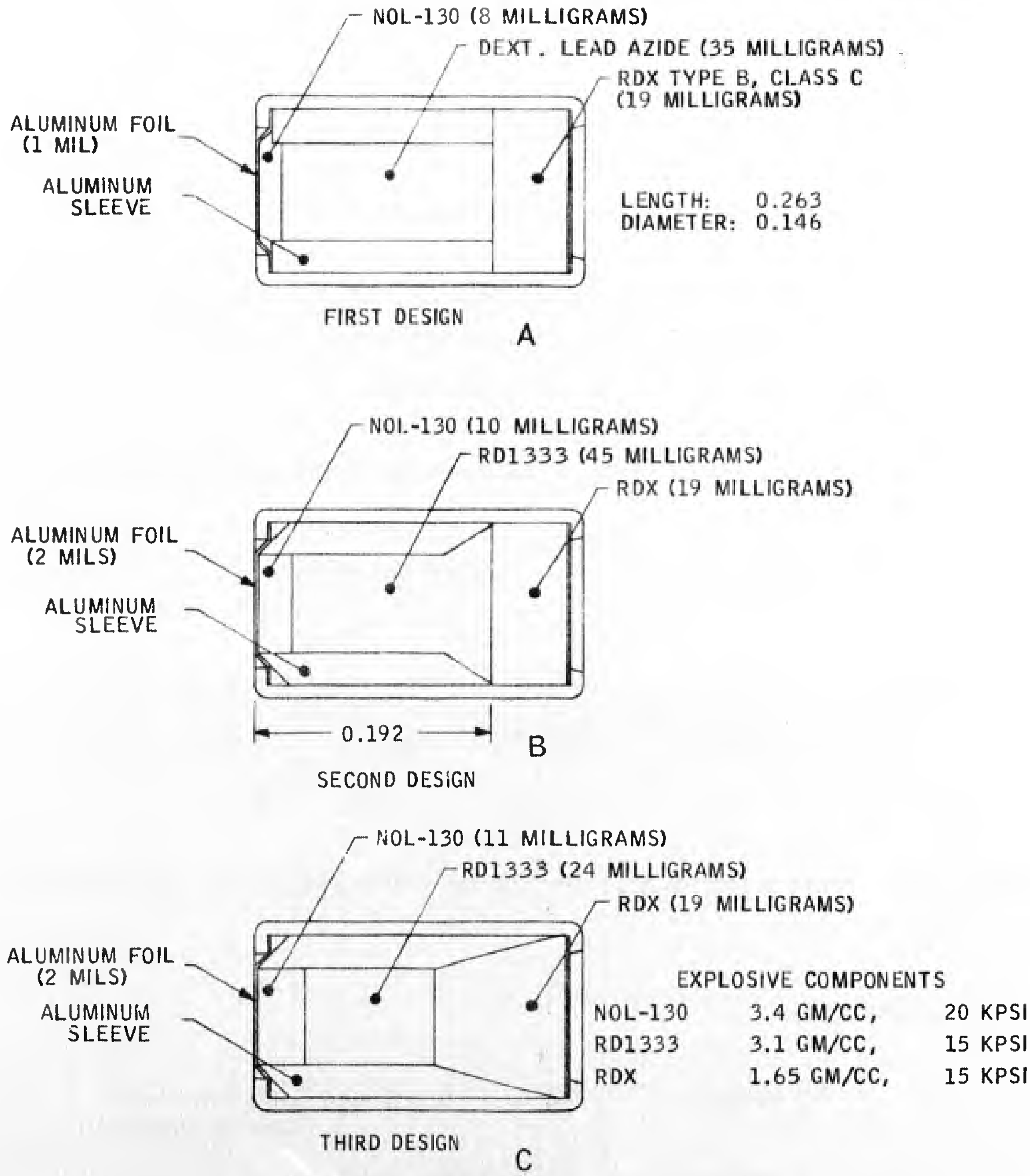

Figure 102. 20mm SAPHE Detonator Evolution

50 meters	8/10	5/8 possible low order
6 meters	2/10	
10 meters	10/10	6/10 possible low order

60 percent of those units which functioned were low order.

Space Ordnance Systems (SOS) of California had a detonator readily available that had similar characteristics to the miniature detonator except that the end plate had a spherical concave surface of 0.150-inch radius rather than 0.090-inch radius. This modification would tend to broaden the output jet for more efficient propagation of the explosive.

When tested against a dent plate, this detonator compared with the others as follows:

	Dent Dimensions	
	Diameter (Inch)	Depth at Center (Inch)
SOS	0.095	0.020
Miniature-Detonator	0.083	0.025
M55	0.170	0.009

Twenty-five fuzes were then assembled with SOS detonators and standard boosters.

Test results were:

50 meters	13 of 14 functioned (One low order) (One no function)
6 meters	4 of 10 functioned

It was apparent that arming delay of the fuze and proper explosive train propagation were not accomplished. Further engineering effort on the SAPHE 20mm fuze was suspended pending results of 30mm SAPHE fuze arming tests and further explosive train work.

APPENDIX I
RELATED FUZE PROGRAMS

This appendix is included in this report to summarize related fuze arming delay development activities on the 20mm SAPHE and M505A3 (modified) fuze programs. The 30mm SAPHE projectile is currently being developed by the contractor as a candidate for the GAU-8/A gun system, and the M505A3 fuze is being modified and tested under an independent development program to investigate ball rotor arming delay characteristics. Test data obtained from these programs have shown the feasibility of obtaining increased nonarming distances by preventing rotor movement until the projectile is in free flight. The results of the more significant tests are summarized below.

A. 30MM SAPHE

The baseline 30mm SAPHE fuze (Figure I-1) is basically a modification of the 20mm SAPHE fuze. Differences are:

1. The 30mm fuze front rotor housing is integral with the side walls of the ball rotor cavity instead of a two-piece forward configuration in the 20mm.
2. The 30mm fuze contains two M55 detonators instead of one in the 20mm baseline fuze or a miniature detonator in the modified fuze.
3. The 30mm fuze firing mechanism contains a sliding mass instead of a tipping mass.

Arming delay tests of the 30mm fuze compared the interaction of the ball rotor and its detent spring (C-ring) on the nonarming performance at 6 meters range. The results were as follows:

- With normal C-ring clearance (see Figure I-2A), 7 of 34 fired
- Without C-ring, 10 of 14 fired
- With reduced C-ring clearance (see Figure I-2B), 1 of 20 fired.

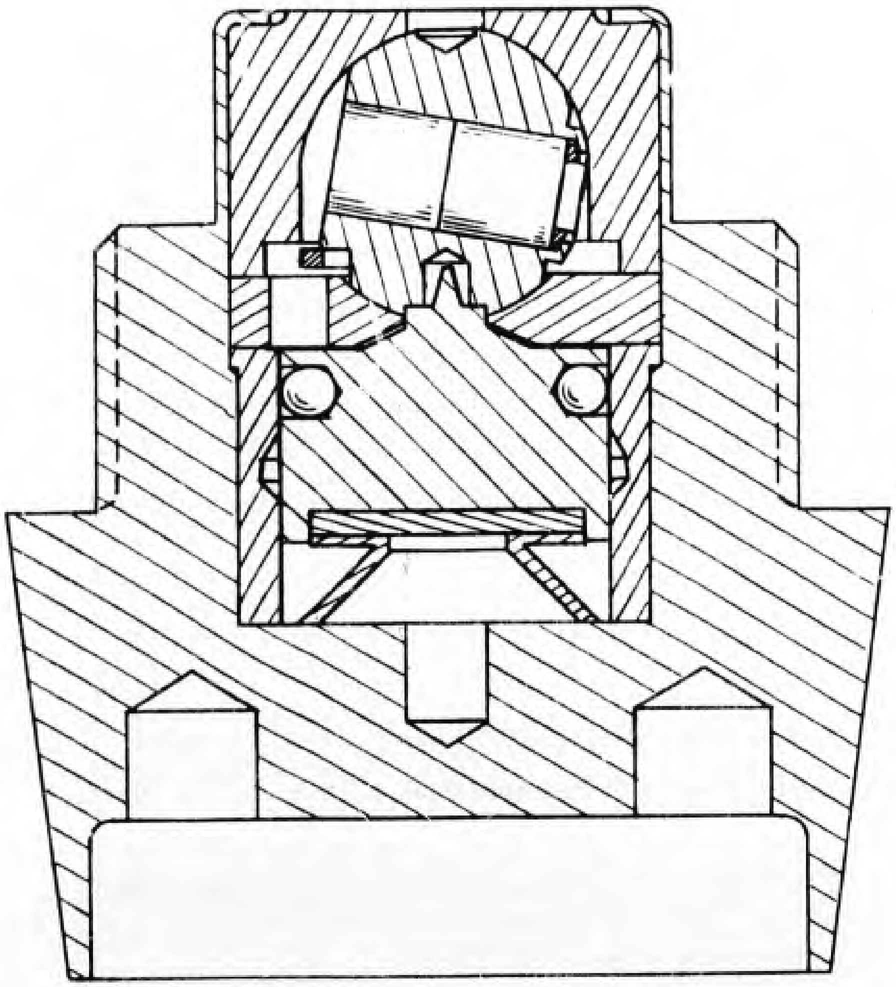

Figure I-1. Baseline 30mm SAPHE Fuze

These results show a significant difference between the fuzes that contain reduced C-ring clearance and the fuzes without C-rings or normal clearance. The conclusion is that without a C-ring or reduced clearance, the rotor begins to move before leaving the muzzle, resulting in earlier arming. Where the clearance is reduced, setback causes the ball to clamp the C-ring and prevent it from opening. This, in turn, prevents rotor movement until free flight is achieved.

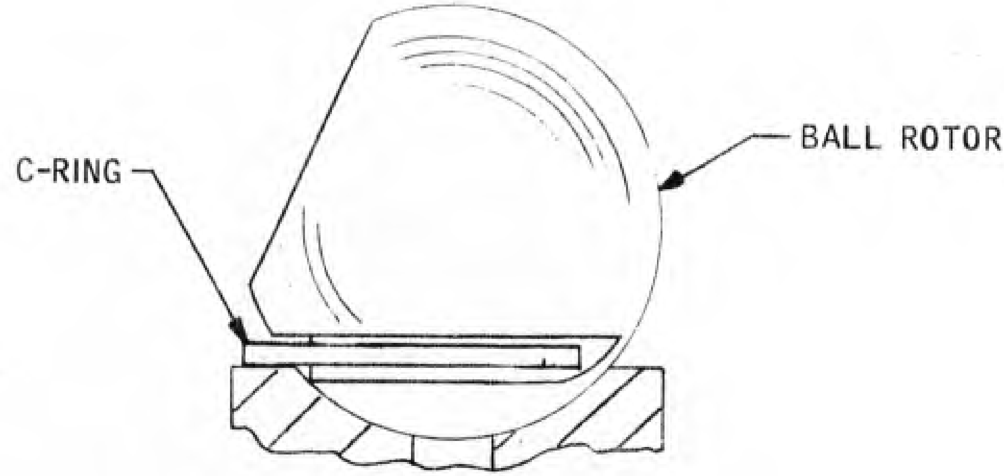

A. NORMAL SAPHE FUZE C-RING CLEARANCE CONDITION

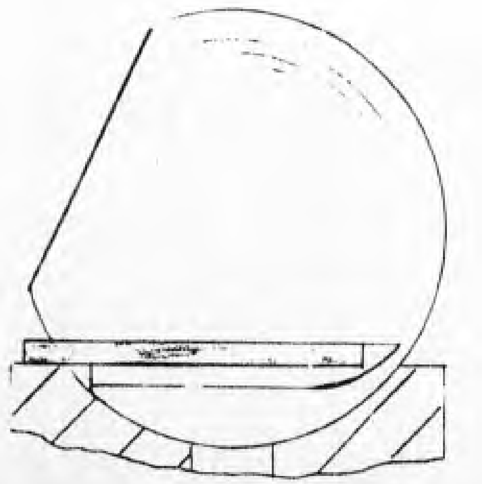

B. REDUCED C-RING CLEARANCE CONDITION

Figure I-2. Ball Rotor Showing C-Ring Clearance

An alternate method of locking the ball rotor during setback is shown in Figure I-3. In this system, a ball prevents movement of the rotor during setback. After setback the locking ball is cammed away to free the rotor. This feature is also adaptable to the 20mm SAPHE fuze.

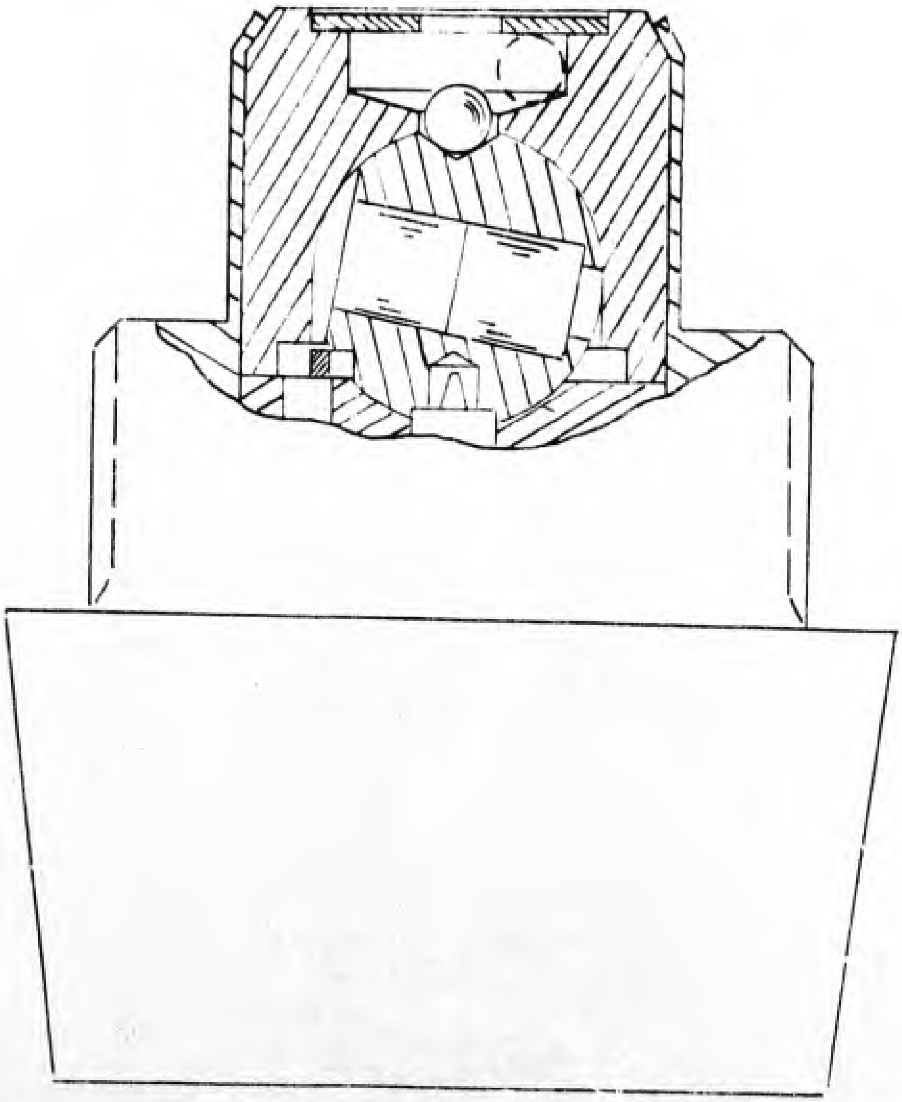

Figure I-3. 30mm SAPHE Fuze With Setback Rotor Lock

B. MODIFIED M505A3 FUZE

Contractor independent development activities have included tests of modified M505A3 fuzes to investigate ball rotor arming characteristics. The modified M505A3 fuze shown in Figure I-4 includes, essentially, the same changes as in the 20mm SAPHE fuze (miniature detonator and lubricated ball rotor and cavity) except that the clearance between the ball rotor and C-ring is near zero. The results of tests of the modified M505A3 fuzes were:

First Test - 27 fuzes tested by Bruceton method:

- Mean arming distance - 17.8 meters
- Standard deviation - 1.9 meters.

Confirmation Test

- 15 of 15 fired at 65 meters
- 20 fuzes tested by Bruceton method
  - Mean arming distance - 21.6 meters
  - Standard deviation - 6.3 meters
- 0 of 10 fired at 9 meters
- 0 of 10 fired at 12 meters
- 0 of 10 fired at 15 meters.

These results show a considerably longer minimum arming distance than demonstrated for the 20mm SAPHE fuze because of the changed C-ring clearance.

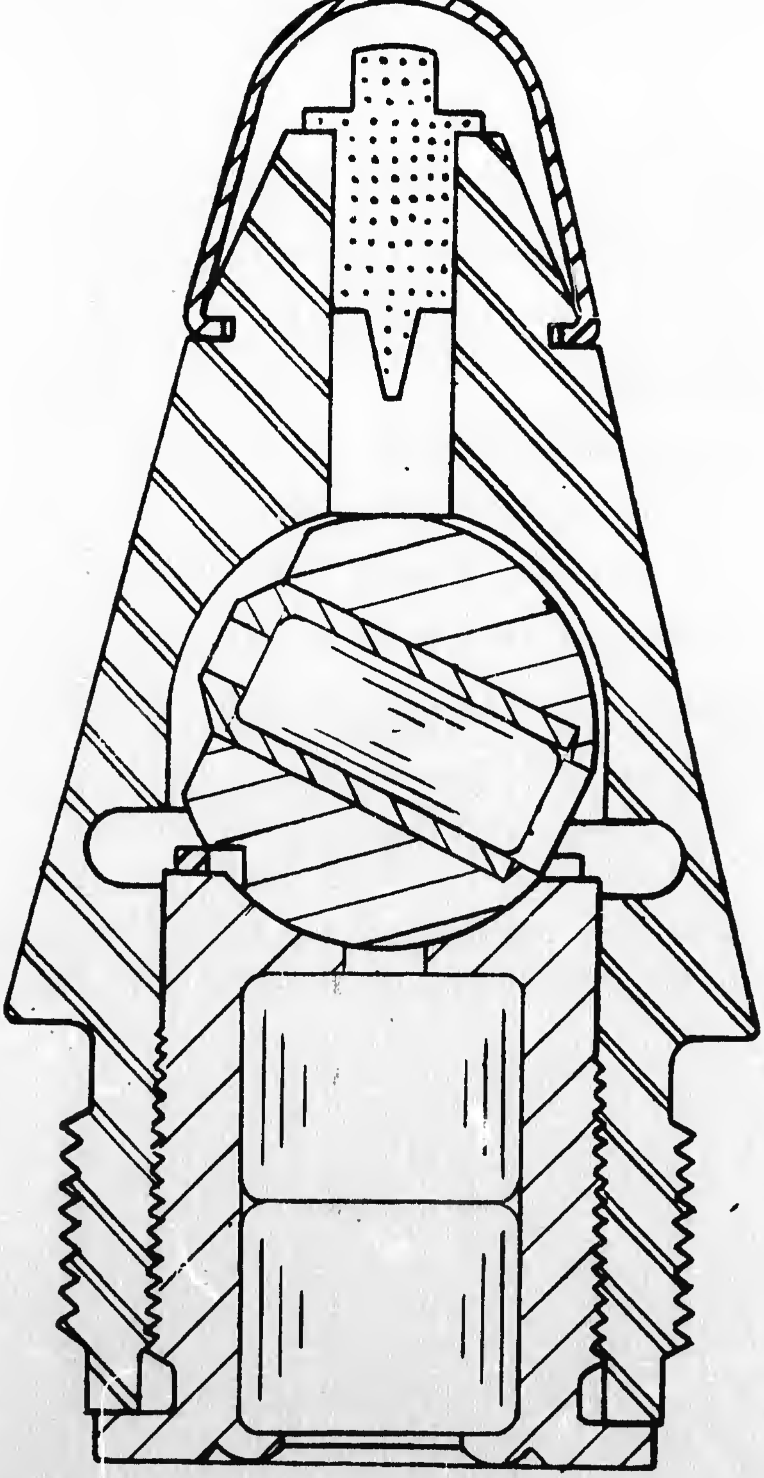

Figure I-4. M505A3 Fuze With Miniature Detonator

APPENDIX II

20MM SAPHE PROPELLANT EVALUATION

A. SUMMARY

Eight propellants were subjected to test evaluation in the 20mm SAPHE gun to select a candidate propellant that would provide sufficient energy to deliver the requisite round performance.

Pertinent Data

- 2,100-grain projectile (20mm diameter)
- 55-inch-length barrel
- 2,850 fps minimum muzzle velocity (higher desired)
- 2.26 ± 0.011 cubic inches chamber volume (measured from five of Lot No. 2 cases)
- 58,000 psi maximum average pressure
- 60,000 psi maximum peak pressure
- -65 to 165°F environmental temperature
- 1,505 ± 134 pounds cartridge separation force (measured from 15 pull tests)
- Range (1,350 to 1,800 pounds)

Consistent with the program objective of using available propellants, off-the-shelf lots of propellant were obtained from two major suppliers, Canadian Industries Limited and Hercules.

Propellants gun tested included six methyl centralite inhibited CIL propellants (CIL 5222, 5268, 1407C, 1377A, 1377B, 1377C) and two Hercules (6928.109 and 6928.141). Both Hercules propellants are 80 percent by weight inhibited grains (5 percent ethyl centralite) and 20 percent uninhibited. Properties on CIL propellants are listed in Table II-1, and nominal data for Hercules propellant are listed in Table II-2. Primarily, inhibited propellants were

TABLE II-1. CANADIAN INDUSTRIES LIMITED (SINGLE BASE) PROPELLANT PROPERTIES

	CIL 5222	CIL 5268	CIL 1407	CIL 1377		
				A	B	C
PROPELLANT COMPOSITION (PERCENTAGE)						
METHYL CENTRALITE	3.44	5.56	5.41	2.17	3.52	5.44
DIPHENYLAMINE	0.88	0.85	0.84	0.82	0.87	0.88
POT SULFATE	0.70	0.44	0.40	0.86	0.83	0.83
LEAD CARBONATE	0.85	0.78	0.78	95.38	94.13	92.29
NITROCELLULOSE	94.13	92.37	92.57	95.38	94.13	92.29
GEOMETRIC CONFIGURATION						
OUTSIDE DIAMETER (INCH)	0.0429	0.0499	0.0471	0.0557	0.0554	0.0562
INSIDE DIAMETER (INCH)	0.0064	0.0066	0.0065	0.007	0.0068	0.0068
LENGTH (INCH)	0.067	0.0837	0.0643	0.0827	0.0834	0.0833
WEB (INCH)	0.0216	0.0183	0.0203	0.0244	0.0241	0.0247
FORCE CONSTANT	333,400	326,000	---	---	---	---
FLAME TEMPERATURE (°F)	2,823	2,700	---	---	---	---
BURNING RATE (NOMINAL)						
COEFFICIENT	---	0.002	---	---	---	---
EXPONENT	---	0.74	---	---	---	---
HEAT OF COMBUSTION (CALORIES PER GRAM)	738	700	---	---	---	---

TABLE II-2. HERCULES PROPELLANTS

COMPOSITION	6928.109 (80/20 BLEND) DOUBLE BASE	6928.141 DOUBLE BASE
GEOMETRIC CONFIGURATION		
OUTSIDE DIAMETER (INCH)	0.060	---
INSIDE DIAMETER (INCH)	0.0225	---
LENGTH (INCH)	0.083	---
WEB (INCH)	0.0225	0.0425
FORCE CONSTANT		
$\left(\frac{\text{POUND-FEET}}{\text{POUND}}\right)$	357,000	---
FLAME TEMPERATURE ($^{\circ}$K)	3,100	3,065 TO 3,100
MOLES PER GRAM	0.0414	---
BURNING RATE		
COEFFICIENT	0.00064	---
EXPONENT	0.89	
INHIBITED COATING (PERCENTAGE)	5.0	5.0

used because high propellant burning rate progressivity is required to provide the projectile velocity of 2,850 fps.

In November 1969, nine tests (Table II-3) each were performed on CIL 5222, 5268, and 1407. In December 1969, a second set of three tests on 1407C was made. This series also included three tests of 1377A, six tests of 1377B, three tests of 1377C, and two tests each on Hercules 6928.109 and 6928.141.

CIL 1377B was found to provide sufficient energy to produce 2,850 fps projectile velocity with maximum peak pressure of 58,000 psi (Piezo data) at ambient temperature. Because all pressure data was obtained with Piezo gages, it was not known what would be observed with the copper crushers specified in the contract. Information sources indicated that, for these propellants, the Piezo gage would read about 10,000 psi higher than the copper crusher.

It was uncertain whether 1407C met pressure and velocity requirements. In the first test series, the requisite velocity and peak pressure was achieved with a 35.0-gram charge; however, in the December tests, a peak Piezo gage pressure of 64,750 psi was obtained for the same charge weight.

The other CIL propellants (5222, 5268, and 1377A and C) did not appear to perform as well as the 1407C and 1377B.

The Hercules propellants appeared to bracket the pressure requirements. Test data presented in Table II-4 show pressure peaks of 68,000 psi for 6928.109 and 23,000 psi for 6928.141. Velocities of 2,750 fps were achieved with the 6928.109, which were good considering the low charge weight. It was felt that slightly larger web thicknesses would decrease peak pressures and allow increases in charge weight sufficient to obtain the 2,850 fps velocity desired.

At that time, 2,100-grain projectiles were being used. Using lighter projectiles would require a new propellant. Previous experience with 1407C

TABLE II-3. 20MM SAPHE PROPELLANT TEST RESULTS, 27 POUNDS, 20 NOVEMBER 1969

PROPELLANT	CHARGE WEIGHT (GRAMS)	NUMBER OF ROUNDS	AVERAGE PEAK PRESSURE [a] (psi)	AVERAGE VELOCITY (fps)	IGNITION DELAY (MILLISECOND) [b]
CIL 5222	25.75	3	c	2,393	c
	30.75	3	39,100	2,454	0.90
	35.75	3	63,800	2,930	0.60
1407C	29.0	3	29,600	2,401	0.65
	32.0	3	40,800	2,594	0.40
	35.0	3	57,000	2,846	0.25
CIL 5268	27.0	3	28,100	2,455	0.80
	30.0	3	39,300	2,556	0.60
	33.0	3	52,200	c	0.47

NOTES:

[a] PRESSURES RECORDED ARE PIEZO ONLY; COPPER CRUSHER MATERIALS HAD NOT ARRIVED AT TIME OF FIRING.

[b] IGNITION DELAYS WERE DETERMINED FROM BEST ESTIMATE OF ZERO TIME IN PRESSURE TIME TRACES.

[c] INSTRUMENTATION FAILURE.

TABLE II-4. 20MM SAPHE PROPELLANT TEST RESULTS, 19 ROUNDS
4 DECEMBER 1969

PROPELLANT	NUMBER OF ROUNDS	CHARGE WEIGHT (GRAMS)	AVERAGE PEAK PRESSURE	AVERAGE VELOCITY	APPROXIMATE IGNITION DELAY (MILLISECOND)
CIL 1407C	3	35.0	64,750	2,910	0.23
1377A	3	31.0	54,100	2,733	0.27
1377B	3	31.5	42,200	2,623	0.18
1377B	3	34.5	56,400	2,851	0.37
1377C	3	35.5 (MAXIMUM)	46,500	2,755	0.43
HERCULES					
6928.109	2	27.5	67,050	2,750	1.7
6928.141 [a]	1	27.5	23,000	2,050	1.0
6928.141 [a]	1	25.0	23,500	2,100	1.6

[a] UNBURNED PROPELLANT LEFT.

indicates sufficient weight of this propellant cannot be loaded into the SAPHE case to meet velocity requirements with a 121-gram projectile.

B. RESULTS

1. Test Firing Results (20 November 1969)

Test firings of CIL propellants 5222, 1407C and 5268 were performed using the 20mm SAPHE (136-gram) projectile in the M103 case and the M52A3B1 primer.

Oscilloscope pressure traces and downrange velocities via velocity screens were obtained. Pressure and velocity versus charge weight data are graphically presented in Figures II-1 through II-3.

By extrapolation of the velocity curves to 2,850 fps, a charge weight could be selected and a peak pressure could be predicted from the pressure curve for each propellant.

Extrapolating the velocity curve in Figure I-1 for CIL 5222 indicated a 34.5-gram charge would provide the required velocity but peak pressure would be about 59,000 psi. This propellant could meet SAPHE requirements.

The 1407C propellant data for the 35-gram charge weight provided a 58,000-psi average pressure and 2,850-fps velocity.

The CIL 5268, however, projected a high peak pressure of 63,000 psi for the 2,850-fps velocity.

Without copper crusher data, it would be difficult to say whether or not these candidates meet SAPHE requirements.

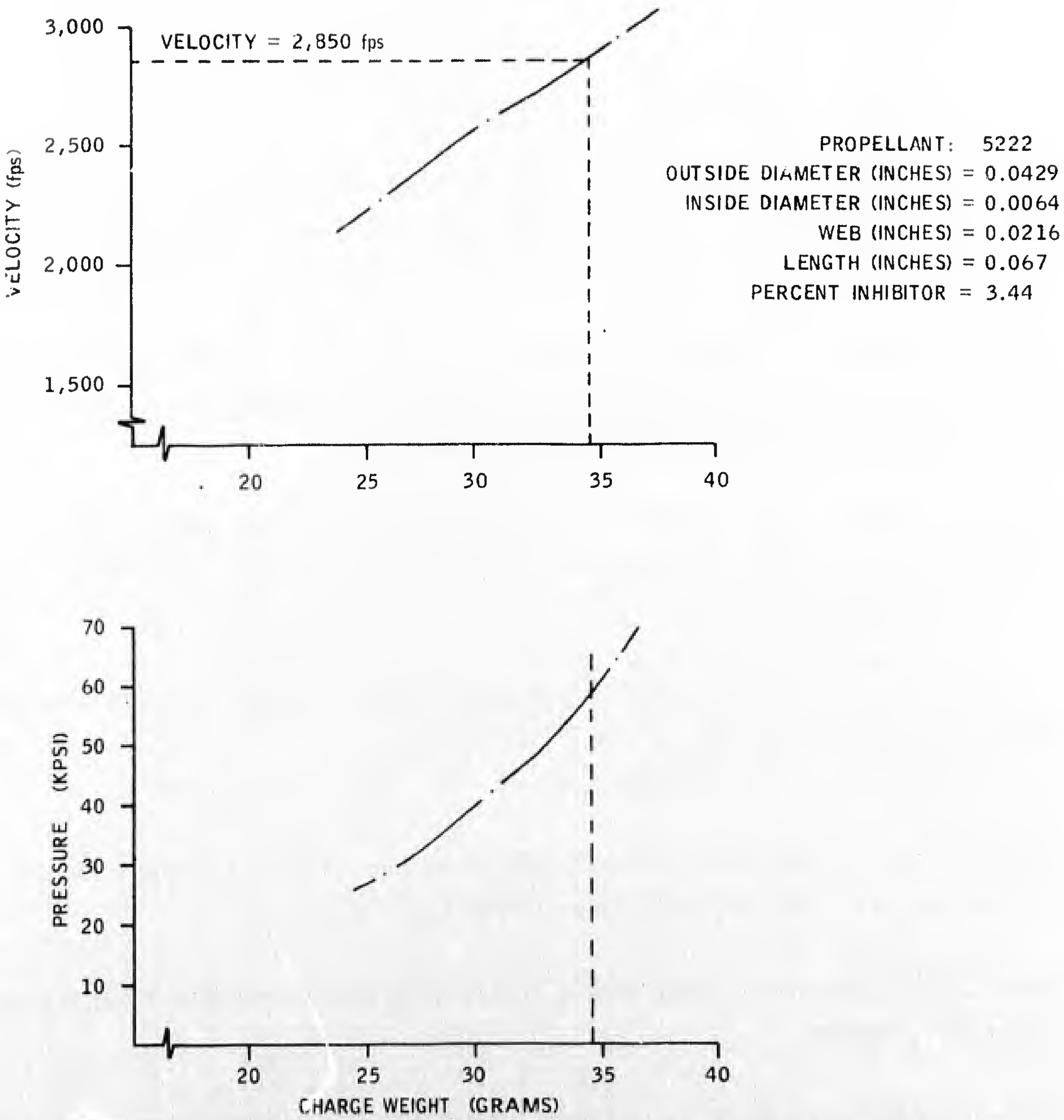

Figure II-1. Pressure and Velocity Versus Charge Weight for CIL 5222

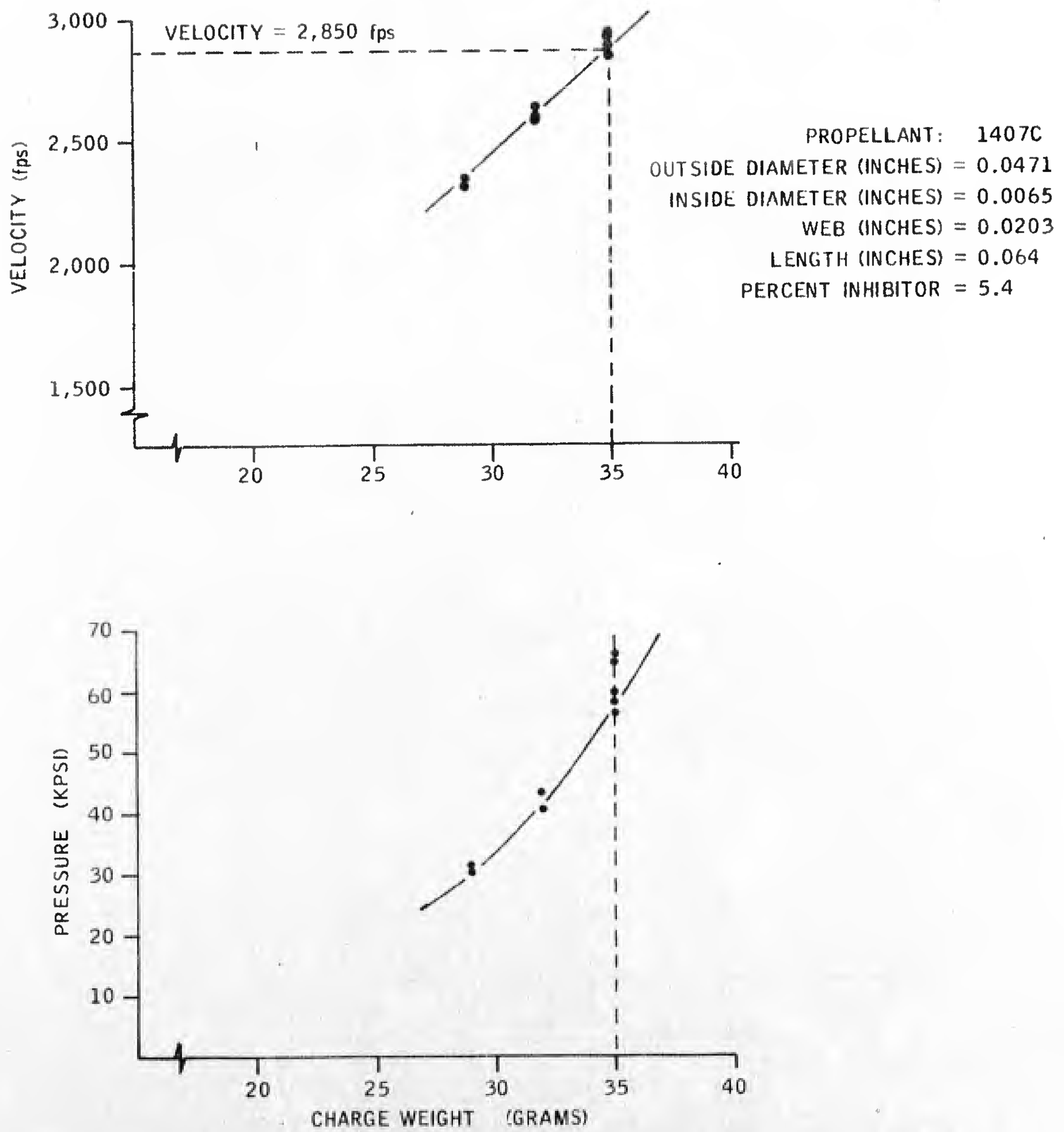

Figure I-2. Pressure and Velocity Versus Charge Weight for CIL 1407C

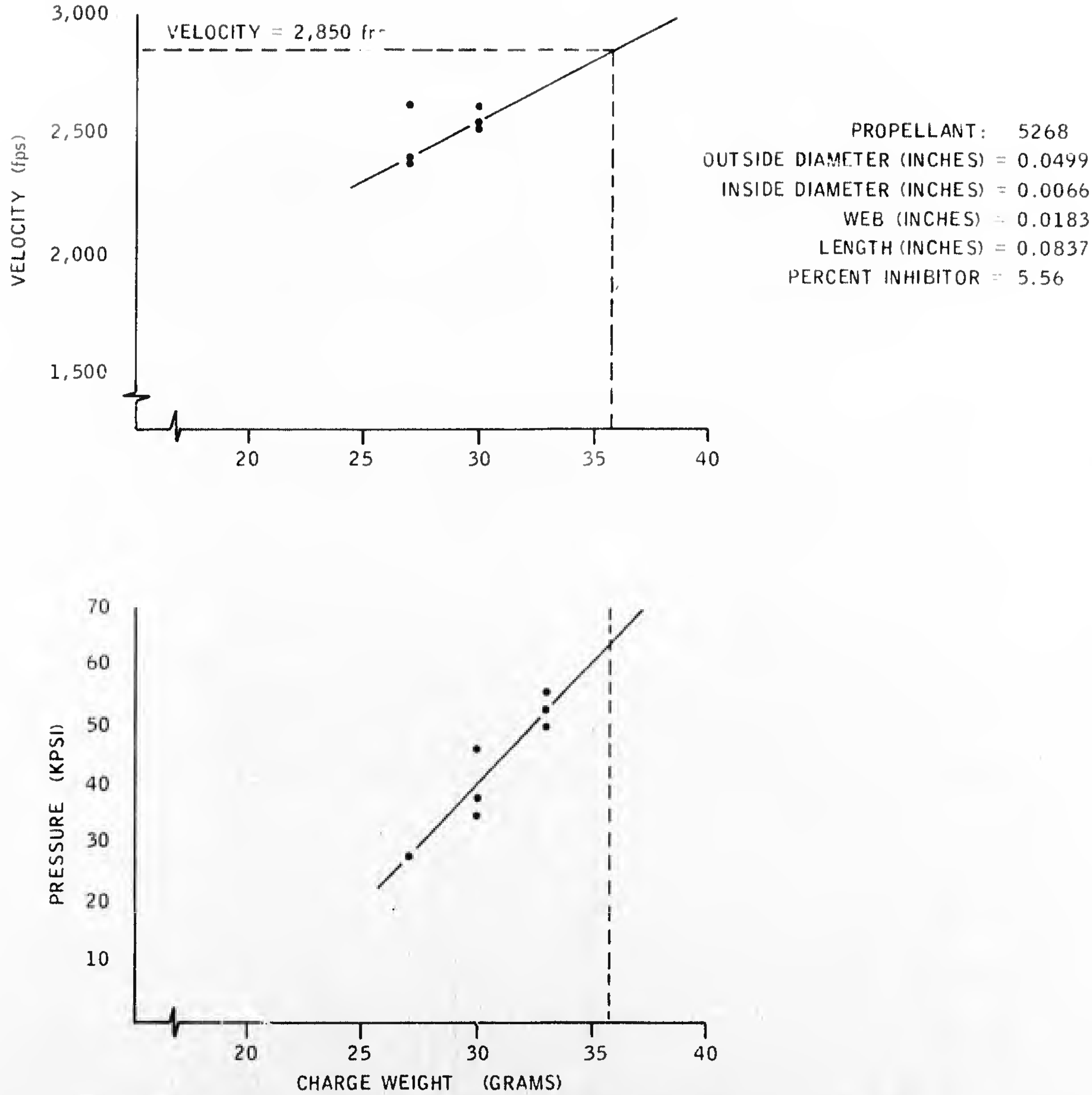

Figure II-3. Pressure and Velocity Versus Charge Weight for CIL 5268

2. Test Firing Results (4 December 1969)

Test firings using similar projectiles and cases were conducted to evaluate CIL propellants 1407C, 1377 A, B, and C, and Hercules (80/20 blend inhibited/uninhibited) propellant series 6928.109 and 6928.141. Measured peak pressures and velocities are presented as a function of charge weights in Figures I-2 and I-4 for 1407 and 1377, respectively. Results are summarized in Table II-4.

Peak pressures for 35-gram charges of 1407C were measured again. This time higher peak pressures (64,750 psi) and velocities (2,910-fps) were obtained. Differences between the November and December tests have not been resolved. It was noted early in this series that the shell was being rotated slightly in some instances, resulting in misalignment of the pressure gage with the hole drilled in the cartridge case. Precautions were taken to correct this alignment problem. This possible difference in testing, however, would not account for the increased velocity (2,850 to 2,910 fps) observed in the December tests compared with those in November.

Twelve rounds of 1377 propellant were fired. Pressure and velocities plotted as functions of charge weight are presented in Figure II-4.

A 31-gram charge of CIL 1377A provided a pressure of 54,000 psi at a velocity of 2,733 fps. Two charge weights (31.5 and 34.5 grams) of the 1377B were fired and provided average peak pressures of 42,000 psi and 56,400 psi. Corresponding velocities were 2,623 and 2,851 fps. The 1377C was loaded at maximum charge weight for the case volume (35.5 grams), and test results showed peak pressures of 46,500 psi and velocities of 2,755 fps.

In summation, CIL 1377A appeared to be a bit fast and, assuming velocity and pressure versus charge weight curves to parallel those of 1377B, a charge weight of 32.0 grams would be necessary to obtain 2,850 fps projectile velocity and peak pressure of 62,000 psi. A charge of 34.5 grams 1377B appeared to provide the velocity of 2,850 fps with average pressure

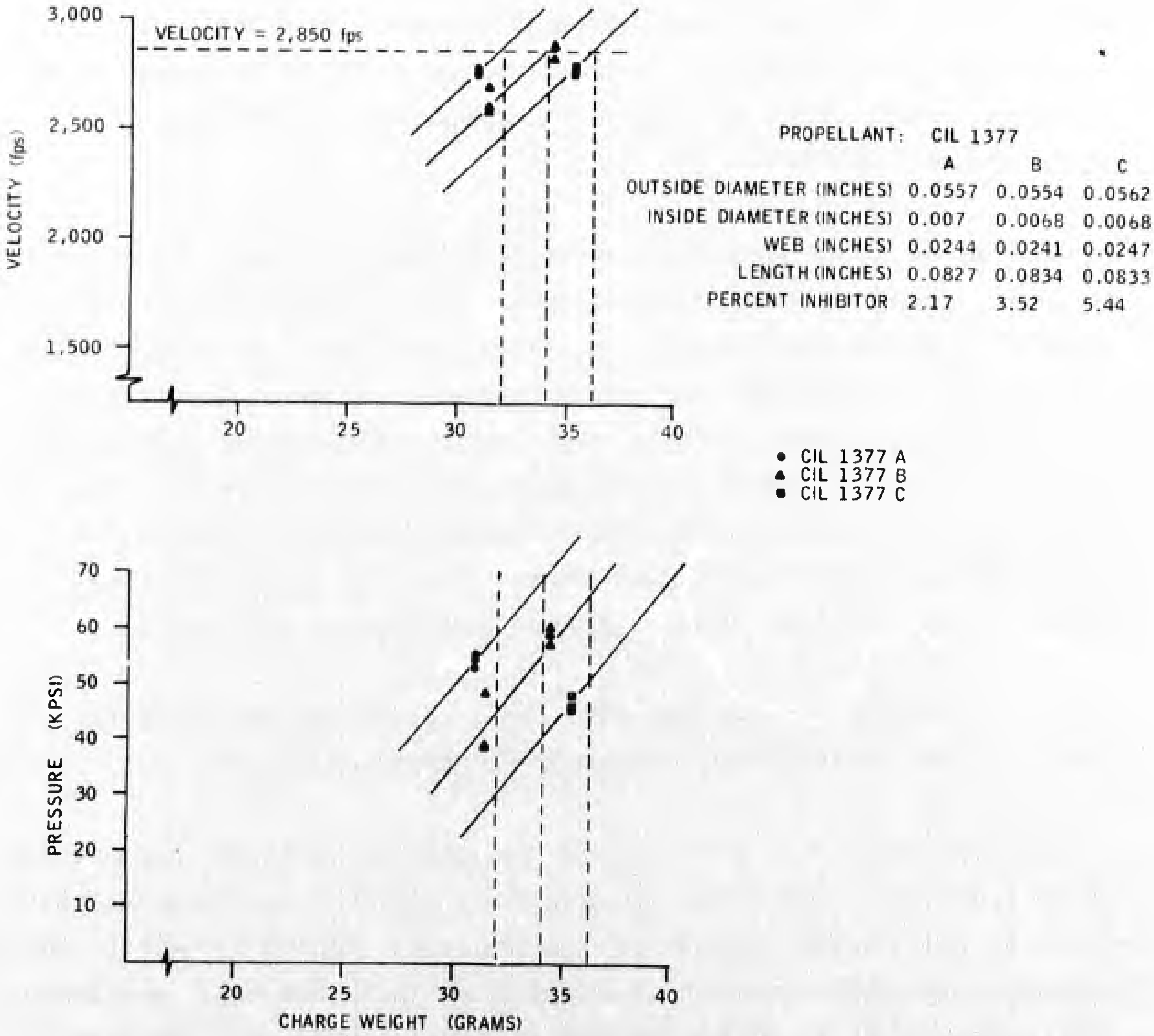

PROPELLANT: CIL 1377	A	B	C
OUTSIDE DIAMETER (INCHES)	0.0557	0.0554	0.0562
INSIDE DIAMETER (INCHES)	0.007	0.0068	0.0068
WEB (INCHES)	0.0244	0.0241	0.0247
LENGTH (INCHES)	0.0827	0.0834	0.0833
PERCENT INHIBITOR	2.17	3.52	5.44

Figure II-4. Pressure and Velocity Versus Charge Weight for CIL 1377

of about 56,400 psi, clearly meeting SAPHE requirements. In the case of 1377C, the maximum load did not meet the velocity requirement.

With Hercules propellant, 27.5 grams of 6928.109 blend was too fast, providing a peak pressure of 67,000 psi and velocity of 2,750 fps. This suggested that a slight increase in web propellant thickness would decrease the peak and allow increases in the charge weight needed to provide the required 2,850-fps velocity.

The 6928.141 results were not extremely useful since the quantity of unburned propellant could not be determined. A larger charge weight could result in the propellant burning more fully.

C. CONCLUSIONS

1. A plot (Figure II-5) constructed from test data shows the effect of propellant web thickness on peak pressure for various inhibitor contents and charge weights.

- Note that the inhibitor level can be decreased from 5 to 3 percent by increasing the web thickness from 0.018 inch as with 5268 or 0.02 inch as with 1407C to 0.024 inches as with 1377 and the same peak pressures can be retained.
- Computer program studies not presented indicated propellant may be incompletely burned if web thicknesses increase much above 0.027 inch. This is shown as an apex limit line in Figure II-5.
- From past experience, maximum loading of CIL propellants is 35.5 grams. Using lower charge weights for a volumetric loading density will provide reproducible gun performance over the temperature range.
- A CIL propellant with web thickness of 0.024 to 0.027 inch and an inhibitor content of 2.5 to 3.5 percent is expected to provide minimum weight/minimum inhibitor level propellant both characteristics that still meet SAPHE peak pressure and velocity requirements.

2. Note that a change in projectile weight from 136 grams to 121 grams would require selection of new propellants.

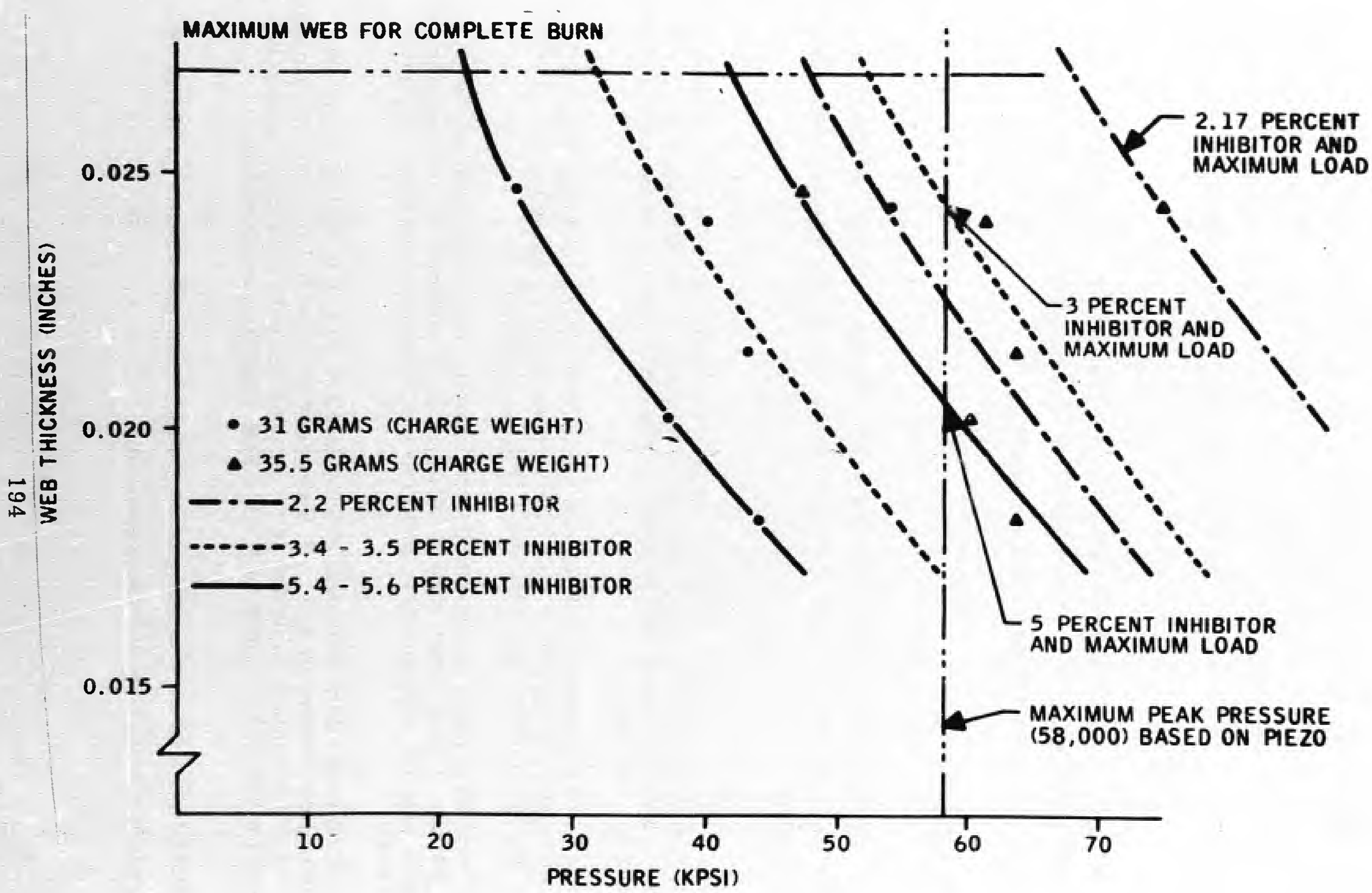

Figure II-5. Web Thickness Versus Peak Pressure for CIL Propellants With Varied Inhibitor Contact

D. RECOMMENDATIONS

1. Establish procedures for propellant procurement, loading, and testing that provides reproducible test results.

2. Select projectile weight.

3. Determine effect of inhibitor concentration on gun performance over temperature range.

4. Determine best loading density to obtain consistent gun performance.

5. Obtain copper crusher data and identify causes for differences in pressure and velocity data.

APPENDIX III

20MM SAPHE SAFETY ANALYSES

A. 20MM SAPHE SAFETY ANALYSIS (W6635)
Contract Number F08635-70-C-0009

1. References

1. Contract No. F08635-70-C-0009, Annex No. 4, Safety Engineering Annex.

2. Honeywell Inc. Memo dated 11 March 1969, J. P. Streff, "20mm SAPHE Safety Analysis," E8002.

2. Introduction

In compliance with Reference 1, a numerical evaluation of design safety for the 20mm Semi-Armor Piercing High Explosive (SAPHE) cartridge was conducted. The safety fault tree diagrams presented in Reference 2 were expanded for purposes of this evaluation. The safety numerics were determined using contractor experience data, or estimated values based on engineering judgement, for the probability of occurrence for each event presented in the diagrams. The 20mm SAPHE primary concept was reviewed for compliance with the contractor safety goals presented in Reference 2.

3. Conclusion

The estimated safety failure rate of the primary design concept for the 20mm SAPHE Cartridge is 0.174×10^{-6}. This is nearly 5.75 times better than the design goal of one safety failure per million units. No single element failure mode of the fuze exists which will result in a premature, or inadvertent, function of the cartridge.

Five of ten contractor safety goals are completely satisfied by the present 20mm SAPHE fuze design. It is anticipated that the design will comply with an additional three safety goals following completion of the applicable MIL-STD-331 tests. The fail safe goal is partially satisfied by the present design, but the assembly design goal is not satisfied. Future design modifications could result in partial or complete compliance with the fail safe and assembly design safety goals.

4. Procedure

Safety Numerical Evaluation -- The safety fault tree diagrams presented in Reference 2 were reviewed for applicability to the 20mm SAPHE concept illustrated in Figure III-1 and the function description presented in paragraph A.5 of this Appendix. These safety diagrams were expanded to include additional failure modes or assembly defects associated with the fuze. These revised safety diagrams are included in paragraph A.6. Mathematical equations were written for each diagram and evaluated, using the probabilities presented in Table III-1.

The probability values presented in Table III-1 are based on actual contractor experience or engineering judgment, as noted. The contractor experience probabilities have been taken from actual data associated with similar elements employed in the safing and arming mechanisms of other fuzes. These fuzes were assembled by the contractor on automated assembly machines, and it was assumed that the 20mm SAPHE fuze would also be assembled on automated assembly machines when high-volume production is required. The safety numerical evaluation has been oriented to that product.

The evaluation of the premature, or inadvertent, function probability considered all phases of the ammunition life cycle as shown in Figure III-2. The probability of a premature function is presented in Table III-2.

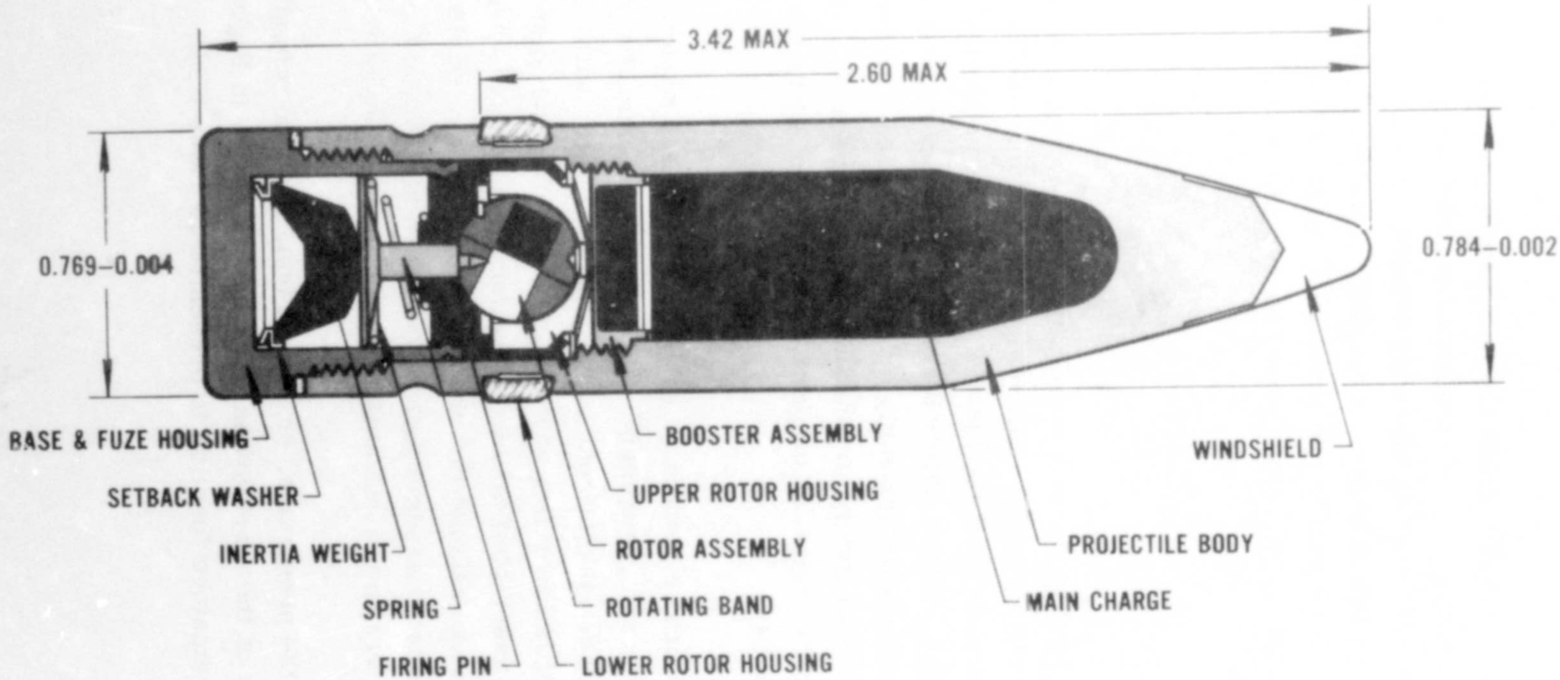

Figure III-1. 20mm SAPHE Primary Concept

TABLE III-1. EVENT PROBABILITY[a]

IDENTIFICATION CODE	FAULT TREE ENTRY (OR EVENT)	PROBABILITY[b] (PER MILLION)	DATA SOURCE
B_I 1	HANDLING ENVIRONMENTS CAUSE ROTOR TO ALIGN	0.99[c]	1,2
A_I 3	C-RING MISSING	7.0	3
A_I 4	C-RING MALFORMED	36.0	3
A_I 5	C-RING DAMAGED	7.0	3
A_I 6	C-RING MISASSEMBLED	22.0	3
A_I 7	C-RING GUIDE MALFORMED	58.0	3
A_I 8	C-RING GUIDE MISSING	38.0	3
A_I 9	C-RING GUIDE DAMAGED	884.0	3
D_I 4 , D_{III} 9	SETBACK WASHER MISSING	18.0	3
D_I 12	HANDLING ENVIRONMENTS FORCE DETONATOR AFT	0.99[c]	1
D_I 13	FIRING PIN SPRING FORCES FIRING PIN AFT	0.9999[c]	1
D_I 14	HANDLING ENVIRONMENTS FORCE FIRING PIN AFT	0.99[c]	1
D_I 15 , D_I 16 , E_I 10 , F_I 10	FIRING PIN SPRING MISSING	18.0	3
D_I 17	HANDLING ENVIRONMENTS PLUS INERTIA WEIGHT FORCE FIRING PIN FORWARD (NO SPRING PRESENT)	0.99[c]	1
D_I 18	HANDLING ENVIRONMENTS PLUS INERTIA WEIGHT FORCE FIRING PIN FORWARD (SPRING PRESENT)	0.99[c]	1
D_I 19	DETONATOR HOUSING DAMAGED	16.0	3
D_I 20	DETONATOR HOUSING MALFORMED	28.0	3
E_I 4	INERTIA WEIGHT MISSING	18.0	3
E_I 9	HANDLING ENVIRONMENTS PLUS SETBACK WASHER FORCE FIRING PIN FORWARD (NO SPRING PRESENT)	0.99[c]	1
E_I 11	HANDLING ENVIRONMENTS PLUS SETBACK WASHER FORCE FIRING PIN FORWARD (SPRING PRESENT)	0.99[c]	1
F_I 4	FIRING PIN MALFORMED	126.0	3
F_I 9	HANDLING ENVIRONMENTS PLUS INERTIA WEIGHT AND SETBACK WASHER FORCE FIRING PIN FORWARD (NO SPRING PRESENT)	0.99[c]	1
F_I 11	HANDLING ENVIRONMENTS PLUS INERTIA WEIGHT AND SETBACK WASHER FORCE FIRING PIN FORWARD (SPRING PRESENT)	0.99[c]	1
A_{II} 3	INSPECTION ERROR (MANUAL/VISUAL)	0.01[c]	3
A_{II} 5	HANDLING ENVIRONMENTS CAUSE DETONATOR TO BE INITIATED HIGH ORDER	0.99[c]	1
C_{III} 7	PROPELLANT CHARGE FAULTY	0.0001[c]	1
C_{III} 8	SETBACK OCCURS (NORMAL FUNCTION)	0.9995[c]	1
C_{III} 9	SPIN SUFFICIENT TO MOVE ROTOR (IN THE BORE)	0.99[c]	1
D_{III} 4	FUZE BASE MATERIAL DEFECTIVE (POROUS)	1.0	1
D_{III} 5	PROPELLANT GASES ENTER FUZE FORCING FIRING PIN FORWARD (FUZE BASE POROUS)	1.0[c]	1
D_{III} 6	BALLOTING OF PROJECTILE IN THE BORE OCCURS	0.1[c]	1
D_{III} 8	DETONATOR INITIATED DUE TO SETBACK FORCES (DETONATOR IMPARTS FIRING PIN)	0.99[c]	1
D_{III} 10	INERTIA WEIGHT MISASSEMBLED	13.0	3

[a]PROBABILITY OF OCCURRENCE BASED ON CONTRACTOR EXPERIENCE FOR SIMILAR EVENTS.

[b]PROBABILITY OF OCCURRENCE ESTIMATED.

[c]PROBABILITY OF OCCURRENCE NOT PER MILLION.

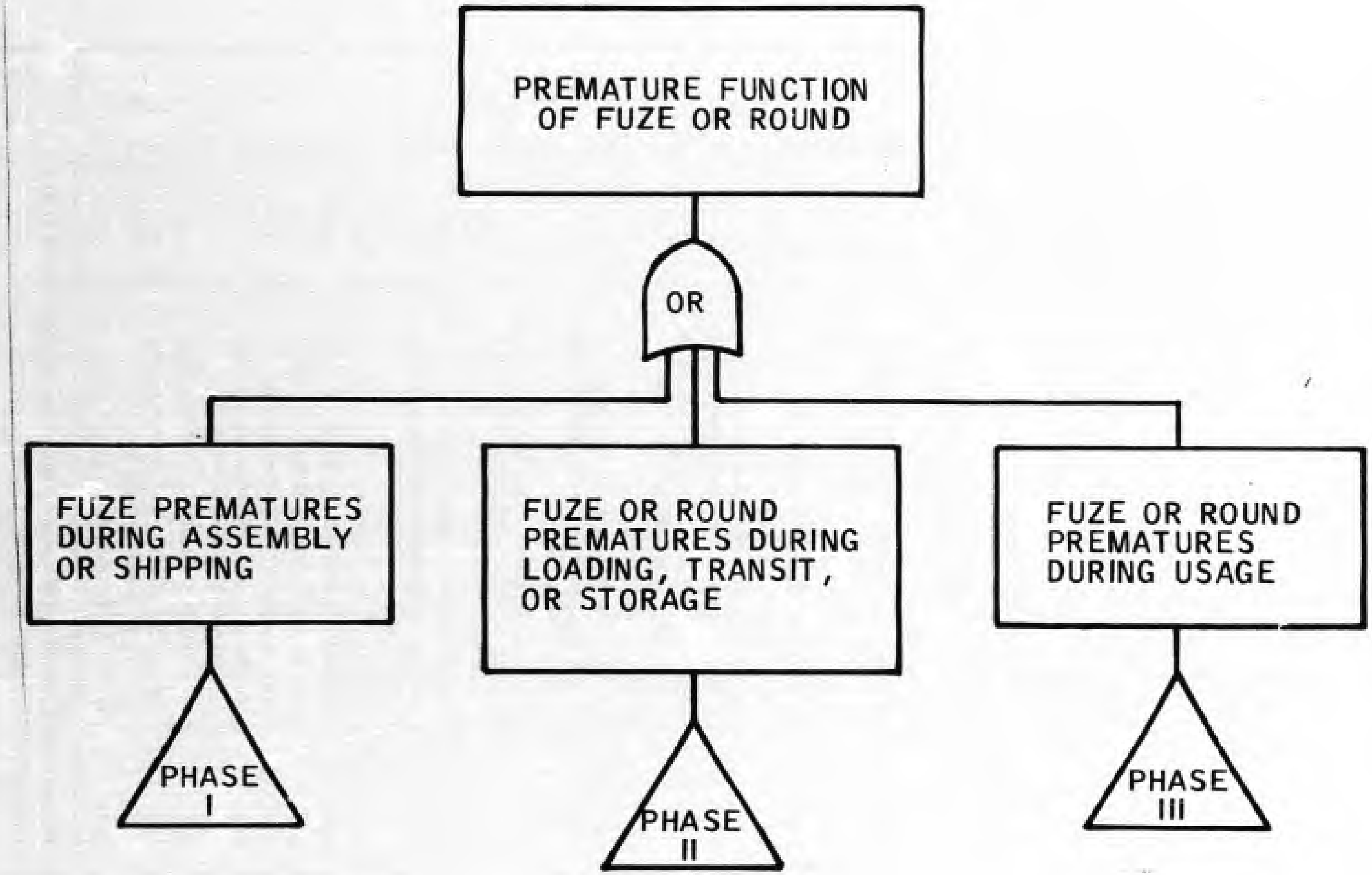

Figure III-2. Premature Function Probability Diagram

TABLE III-2. PREMATURE FUNCTION PROBABILITY

Life Cycle Phase	Premature Probability (Per Million)	Occurrence Rate (One Per x Million Units)
I	0.1670	5.99
II	0.0017	588.2
III	0.0050	200.0
Totals	0.174	5.75

The premature probability of 0.174×10^{-6} is nearly 5.75 times better than the goal (1.0×10^{-6}).

Safety Goal Compliance -- The compliance of the 20mm SAPHE fuze design with the contractor safety goals discussed in Reference 2 was reviewed and the results are given in Table III-3. The present design completely satisfies five of the ten goals listed. Three additional goals will be satisfied upon completion of the applicable MIL-STD-331 tests. The present design does not totally comply with two goals, fail safe and assembly design.

The fail safe goal requires:

- The fuze return to, or remain in, the safe state if the arming sequence is initiated and subsequently interrupted before completion.
- The fuze return to the safe state if arming is complete but the explosive function is not initiated at the target.

The 20mm SAPHE fuze must experience both setback and spin to complete the arming cycle. If the setback forces are sufficient to allow crushing of the washer, the fuze cannot return to the original safe state. If spin is initiated and then interrupted, the rotor will not necessarily return to the original safe state. The rotor will not necessarily advance to the armed state either, but will most likely remain in that position which it held at the time of spin interruption.

TABLE III-3. CONTRACTOR SAFETY GOAL COMPLIANCE

SAFETY GOAL	COMPLETE COMPLIANCE	PARTIAL COMPLIANCE	DOES NOT COMPLY	REMARKS
FUZE DESIGN	X			
EXPLOSIVE TRAIN SAFETY				TO BE DEMONSTRATED BY MIL-STD-331 TESTING.
INTERRUPTER LOCK FEATURES	X			
ARMING ENERGY	X			
SAFETY SYSTEM	X			
ARMED FUZE INDICATION OR INSTALLATION PRECLUSION	X			
FAIL SAFE		X		
ASSEMBLY DESIGN			X	
FUZE EXPLOSIVE HAZARD				TO BE DEMONSTRATED BY MIL-STD-331 TESTING.
ENVIRONMENTAL SAFETY				TO BE DEMONSTRATED BY MIL-STD-331 TESTING.

The assembly design goal requires:

- It be impossible to assemble the fuze in a manner that would function when one of the safing features is missing.
- It be impossible to assemble the fuze if any of the safing features are improperly incorporated so that its function is subverted.
- It be physically impossible to assemble a fuze in the armed state.
- Fuze assembly and/or final inspection shall confirm that all safing features are functional.

The 20mm SAPHE fuze design makes ultimate function possible when one safing feature is missing (missing C-ring does not preclude detonator impact by the firing pin). Also, the fuze could be assembled without the setback washer (allowing the firing pin to be focused aft by the firing pin spring), or without the C-ring (allowing loss of the safing feature associated with spin). A defective C-ring could prevent assembly of the rotor into the fuze, but a rotor without a C-ring could be installed into the fuze. Visual inspection of the fuze will result in detection of an armed fuze, but not necessarily in detection of a fuze that is missing a safing feature and that could subsequently become armed. Strategic assignment of automatic inspection stations during fuze assembly will greatly reduce the likelihood of assembling a fuze in the unsafe state. If final inspection includes radiograph or X-ray of the fuze, confirmation that all safing features are incorporated would be possible.

5. 20mm SAPHE Function Description

The following is a description of 20mm SAPHE function.

1. The setback washer is crushed due to setback forces, allowing the inertia-weight and firing pin to move aft, freeing the first safing feature of the fuze.
2. Acceleration of the projectile causes the rotor to set back on the C-ring and/or the lower rotor housing, restricting rotor movement.

(a) Deceleration of the projectile frees the rotor from the setback force, allowing rotor movement in the nonaligned orientation.

(b) Projectile spin causes the C-ring to open, disengaging the rotor and freeing the second safing feature of the fuze.

3. Projectile spin causes the freed rotor to seek the in-line orientation.

FUZE IS ARMED

4. Upon forward or graze impact, the inertia-weight drives the firing pin forward, overcoming firing pin spring force and driving the firing pin into the channel of the rotor leading to the detonator.

5. The firing pin impacts the detonator which is rigidly mounted in the rotor, and the detonator is initiated.

6. The detonator initiates the booster charge.

7. The booster charge initiates the main charge.

FUNCTION

6. <u>20mm SAPHE Safety Fault Tree Diagrams and Evaluation</u>

This section provides an analysis of the flow of events required to produce a potential hazard. These events are put in an AND/OR relationship which allows Boolean Algebra to be applied. The following logic symbols apply to Figures III-3 through III-12.

A logical AND relation; an AND gate.

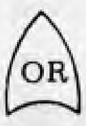

A logical OR relation; an OR gate.


An event or situation caused by subsequent contributing events or situations.

PHASE I

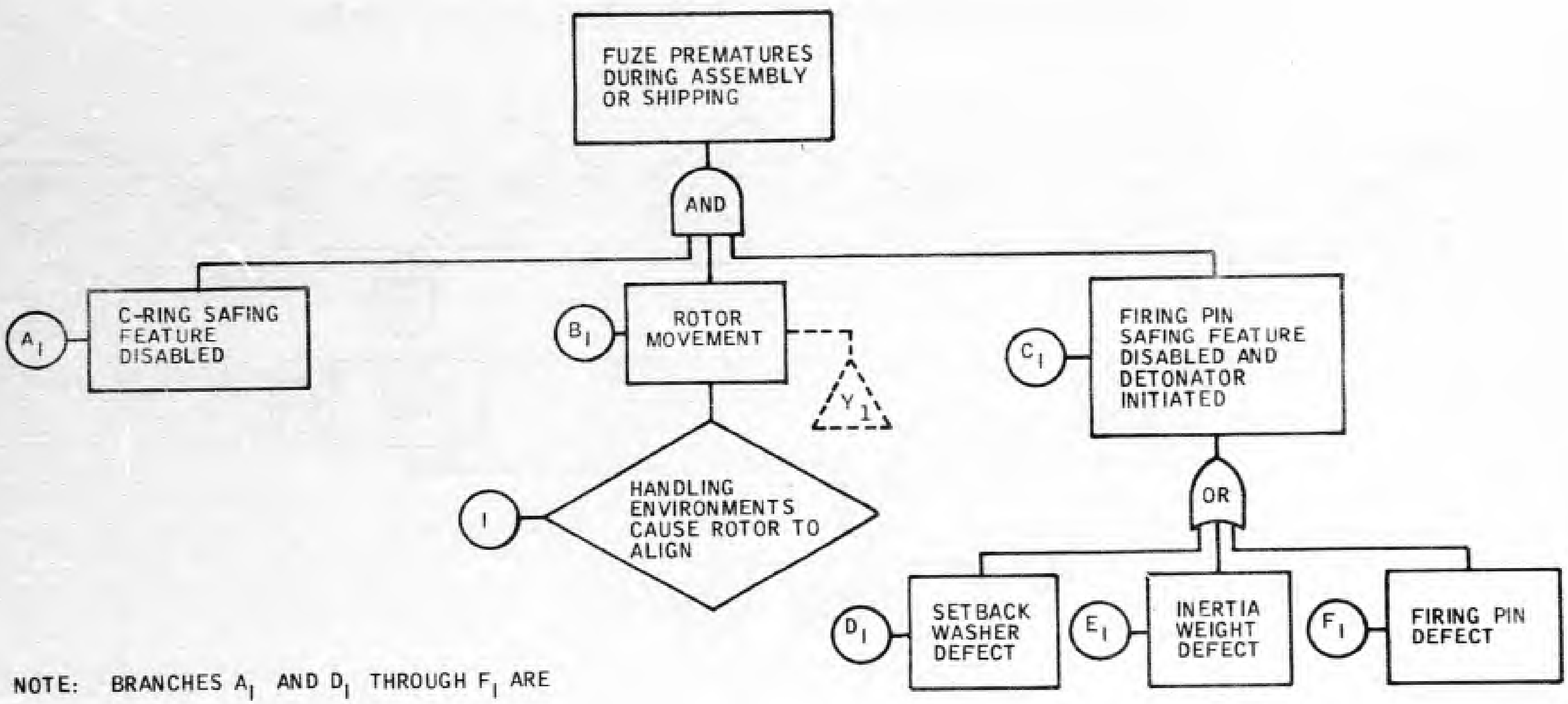

NOTE: BRANCHES A_I AND D_I THROUGH F_I ARE CONTINUED ON SUBSEQUENT PAGES.

Figure III-3. Phase I Premature Fault Tree

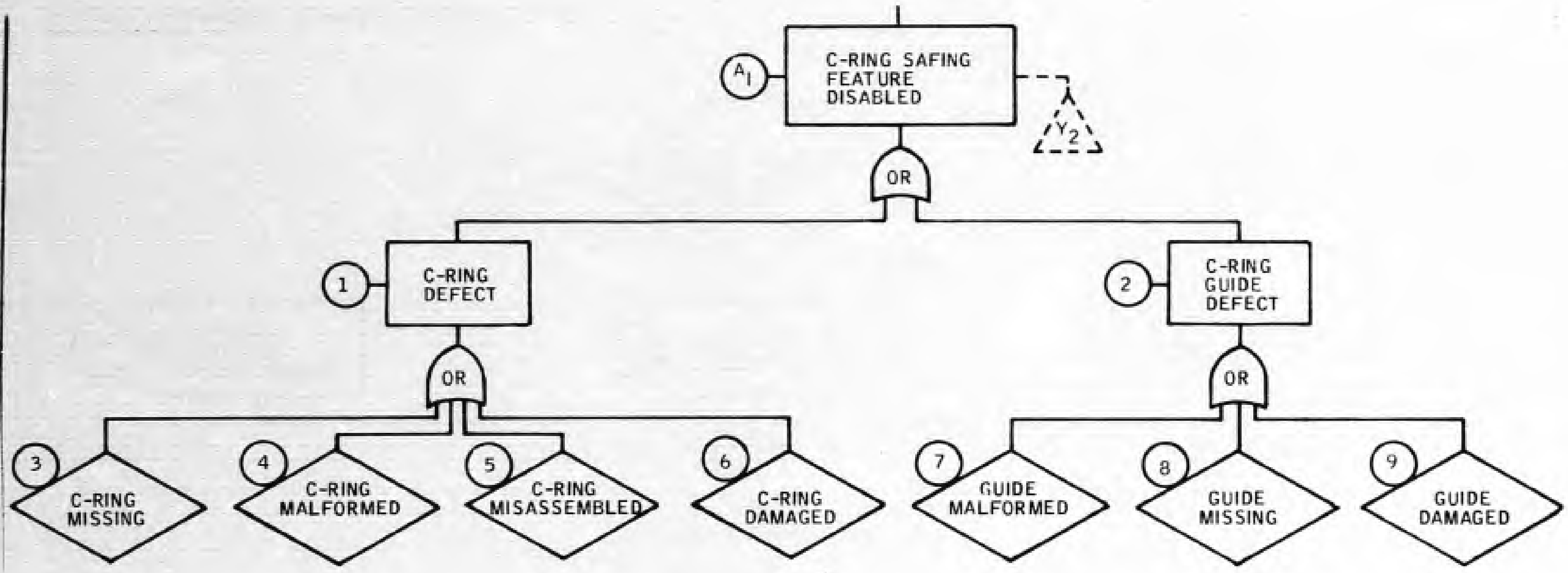

Figure III-4. C-Ring Safing Feature Disabled Fault Tree

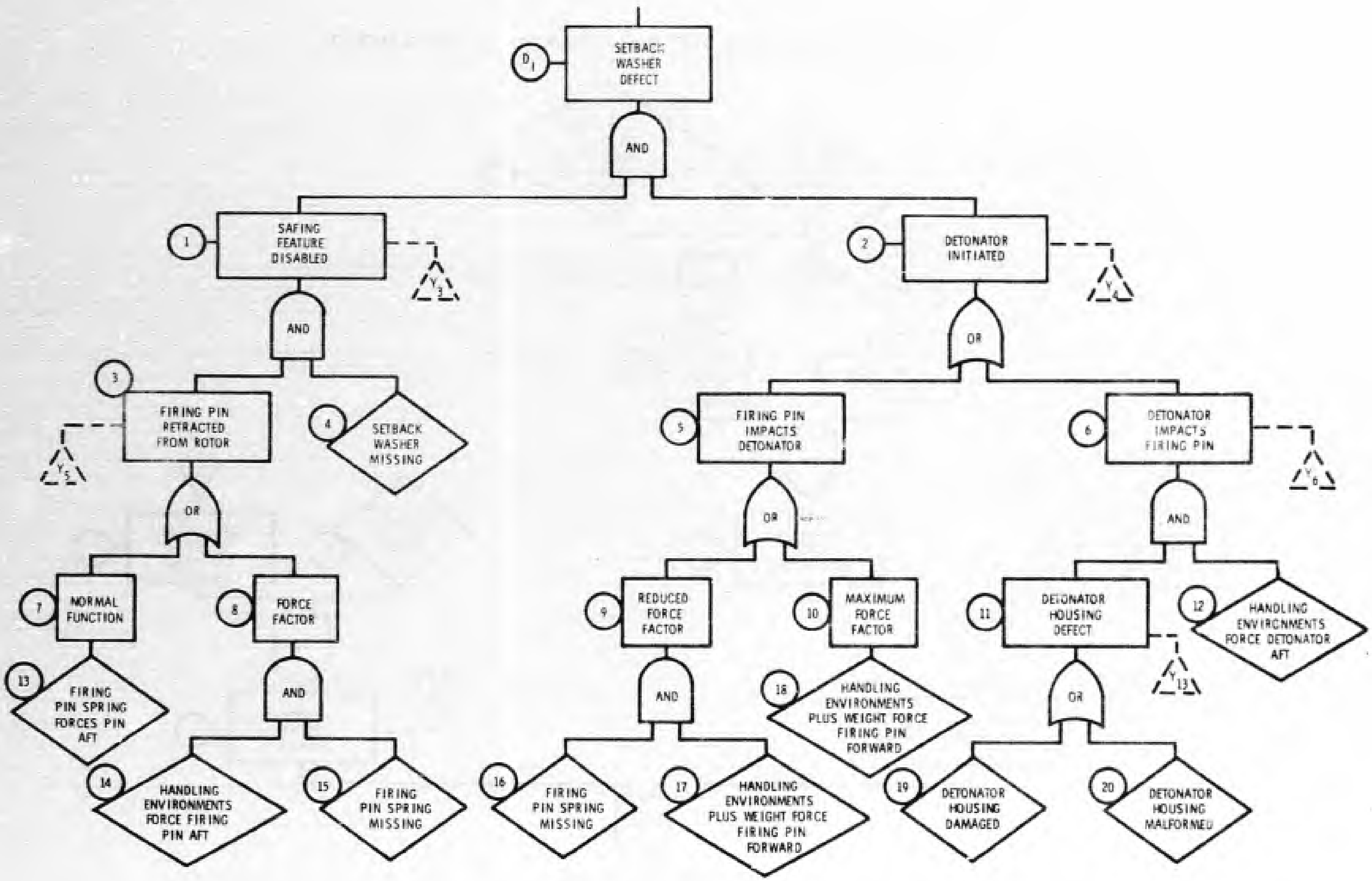

Figure III-5. Setback Washer Defect Fault Tree

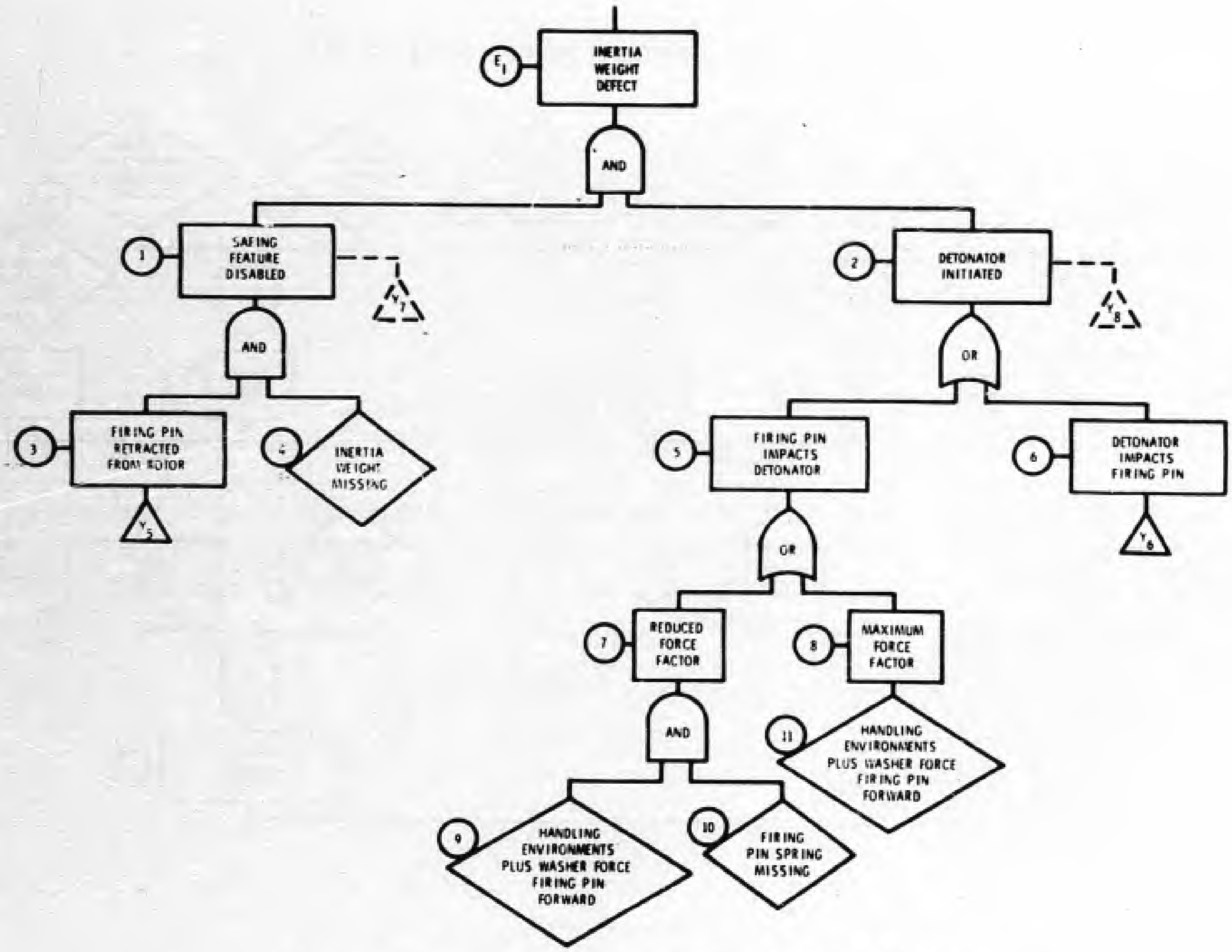

Figure III-6. Inertia Weight Defect Fault Tree

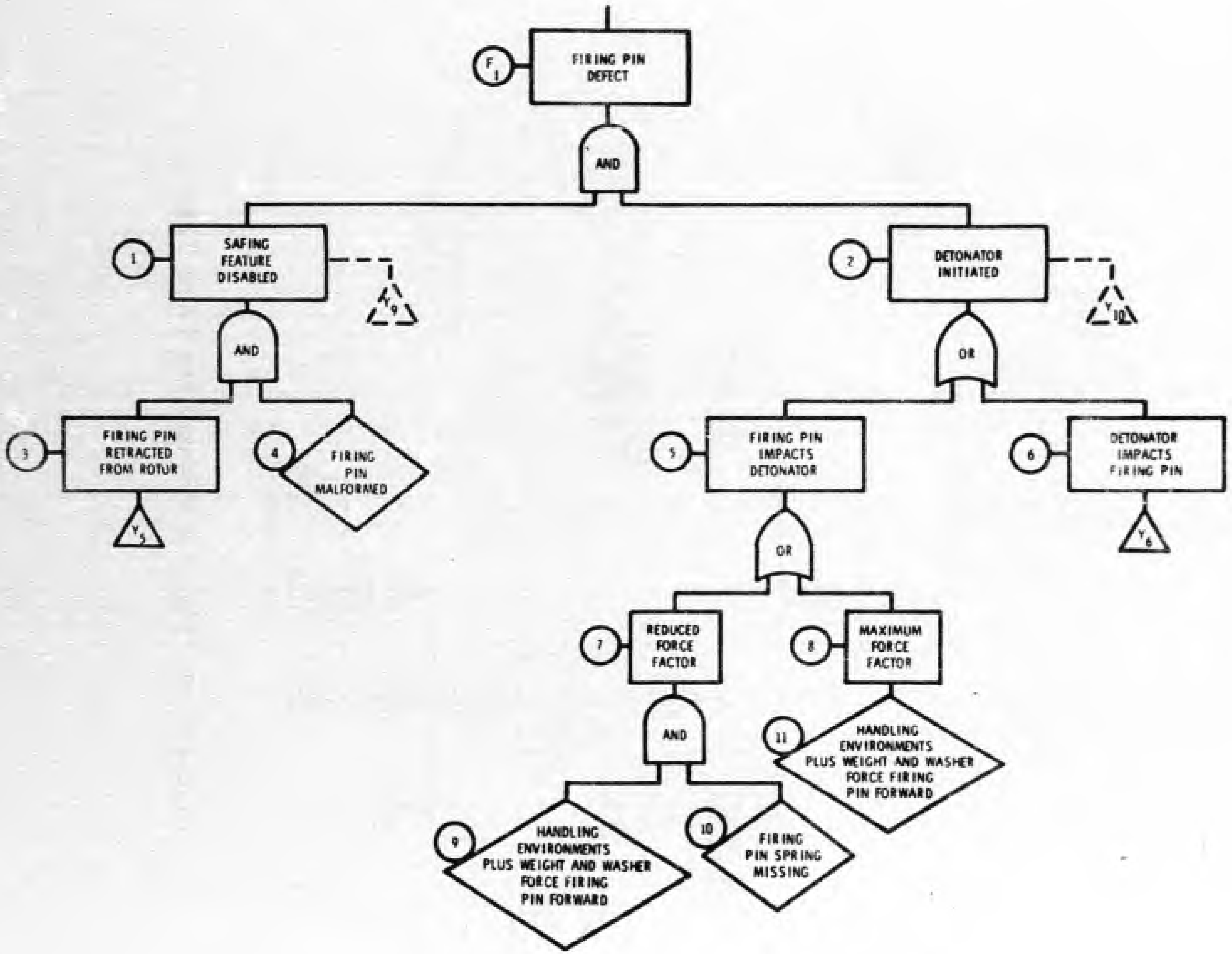

Figure III-7. Firing Pin Defect Fault Tree

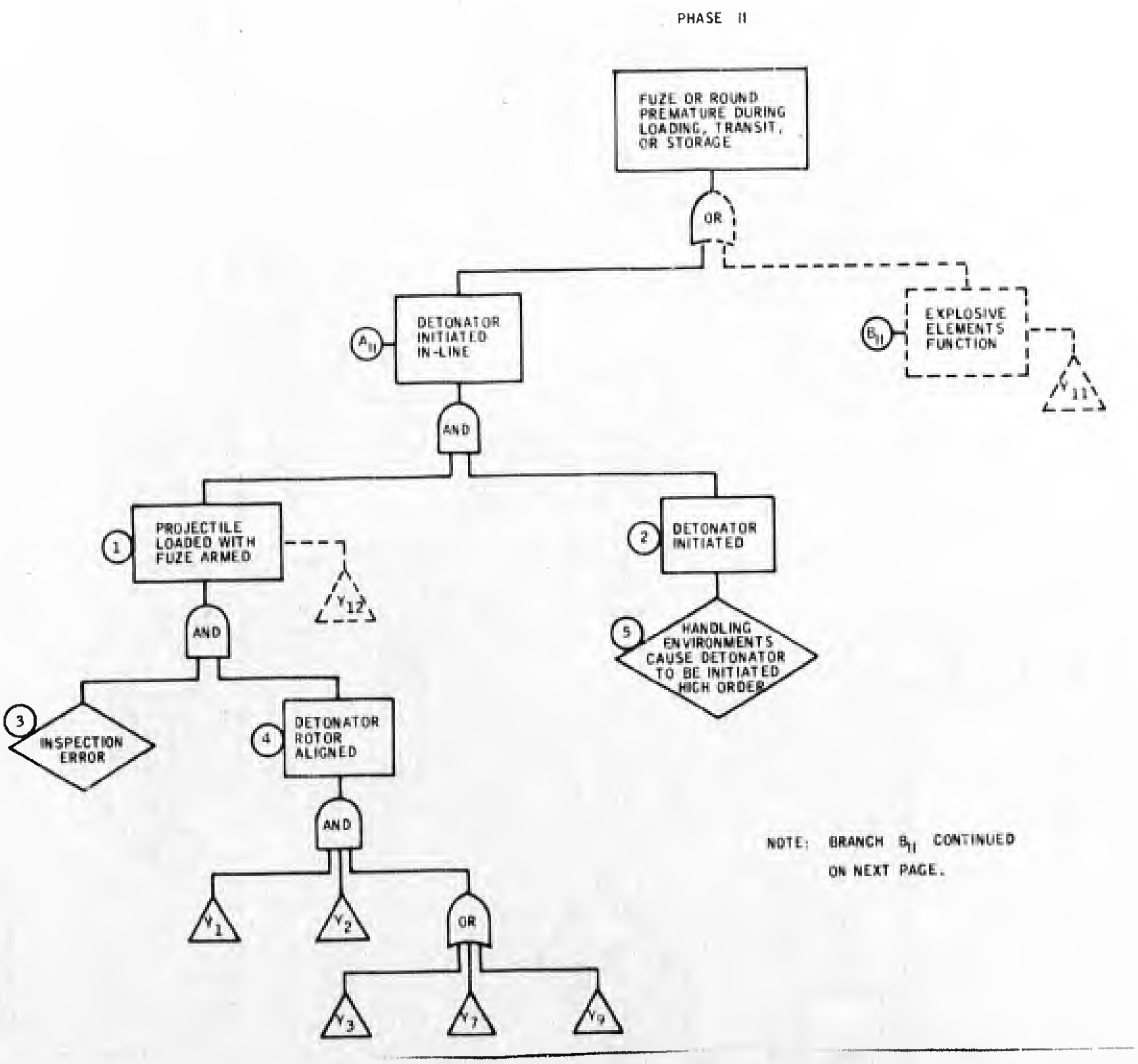

Figure III-8. Phase II Prematures Fault Tree

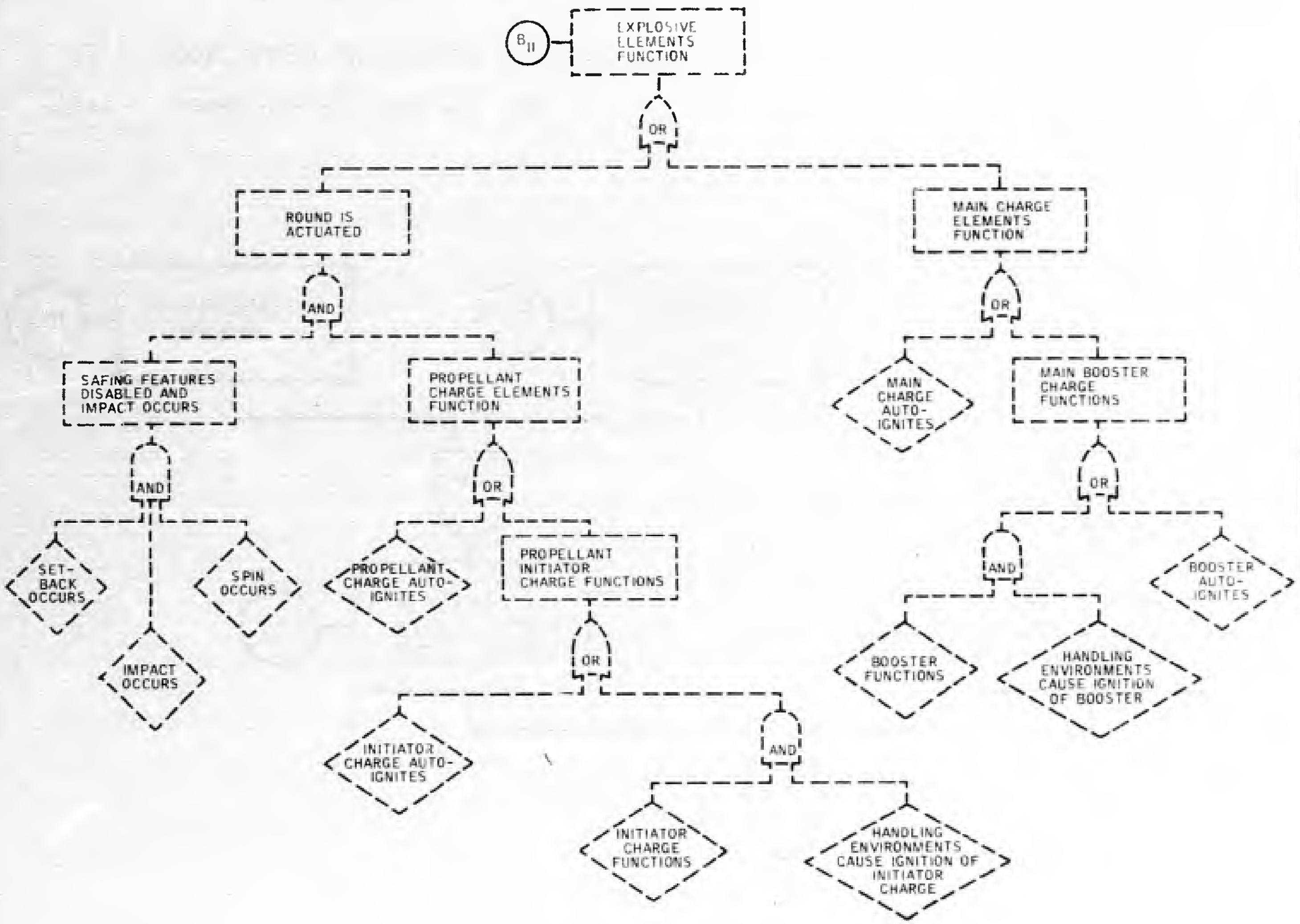

Figure III-9. Explosive Elements Function Fault Tree

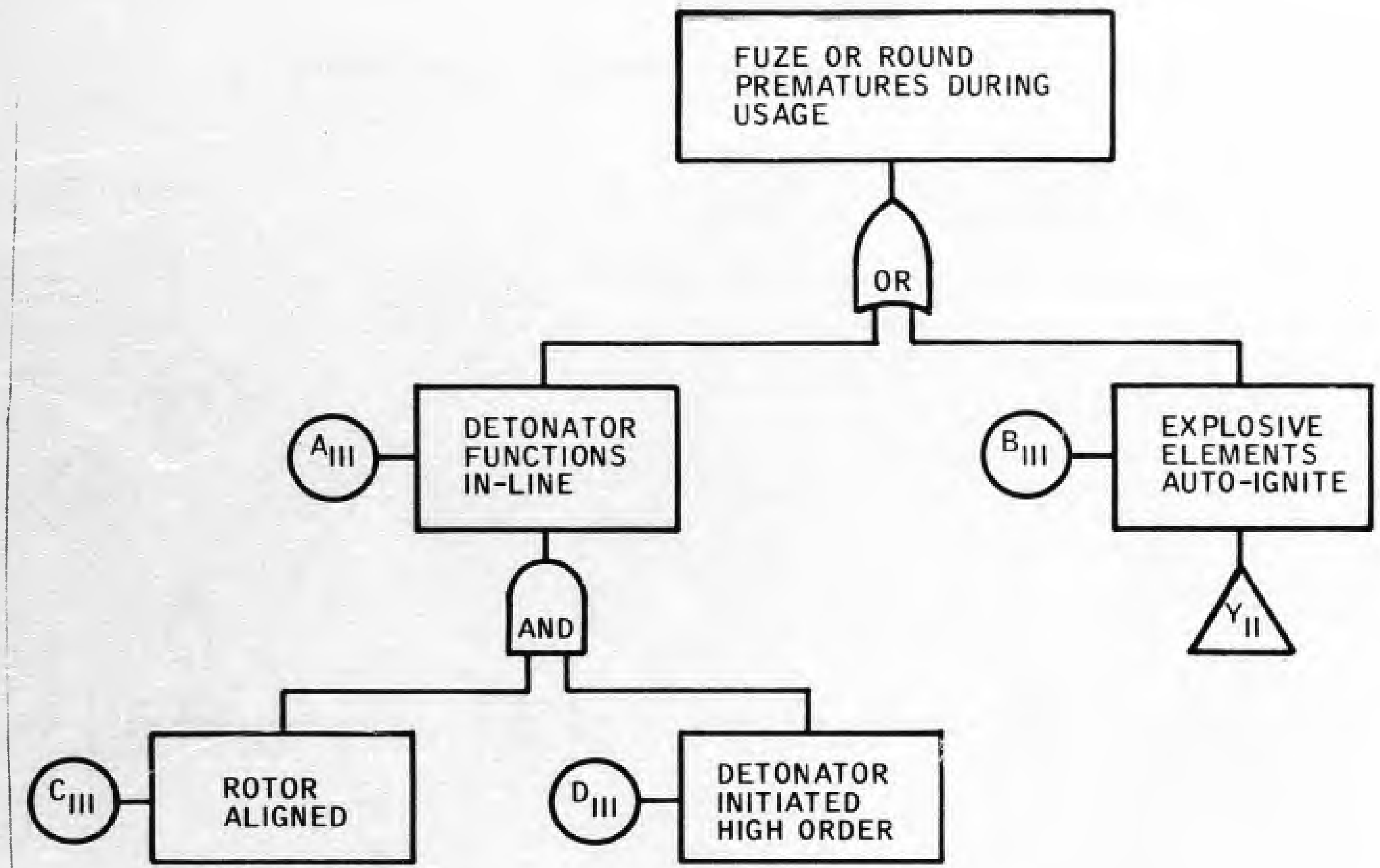

NOTE: BRANCHES C_{III} AND D_{III} ARE CONTINUED ON SUBSEQUENT PAGES.

Figure III-10. Phase III Prematures Fault Tree

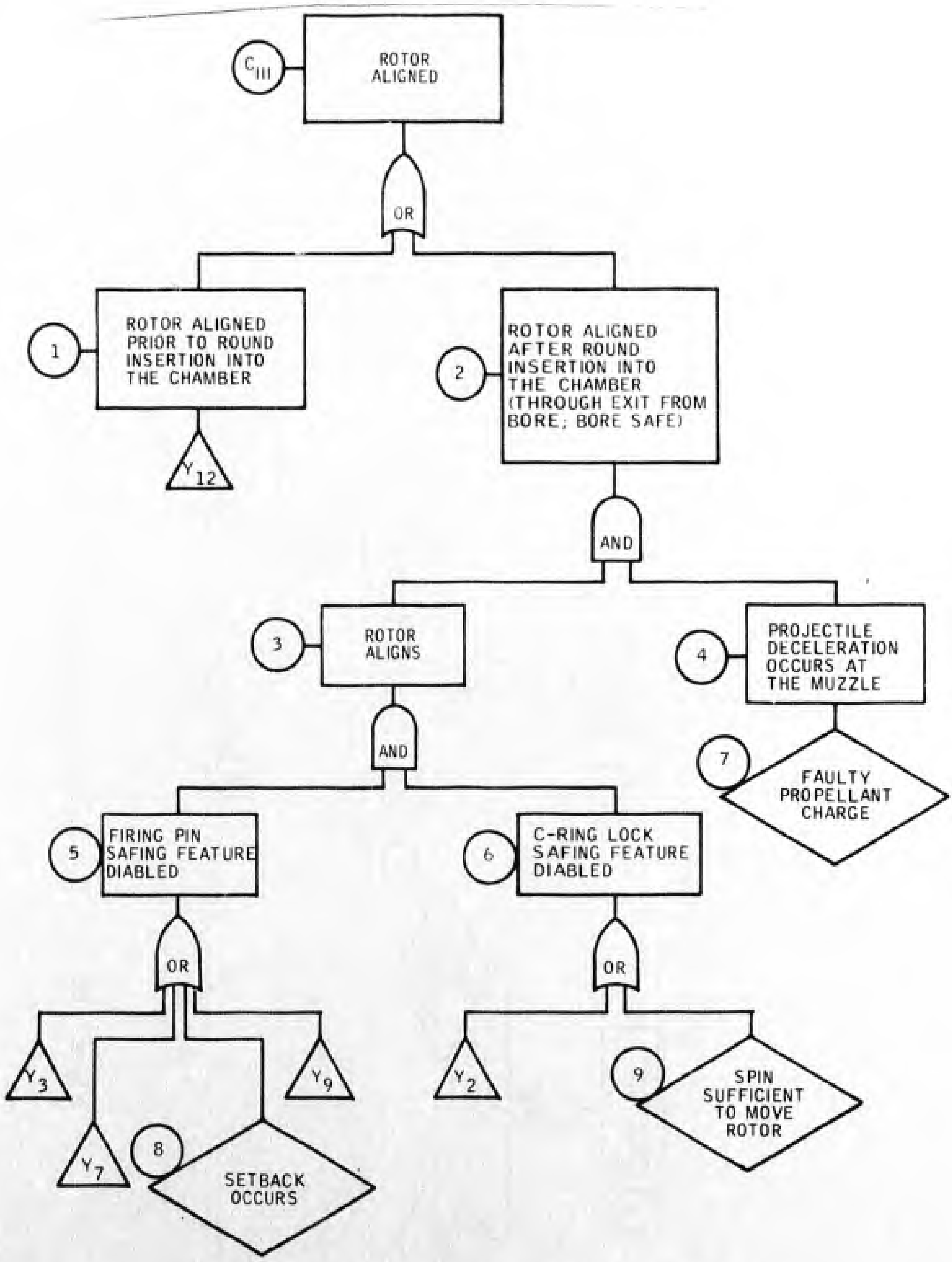

Figure III-11. Rotor Alignment Fault Tree

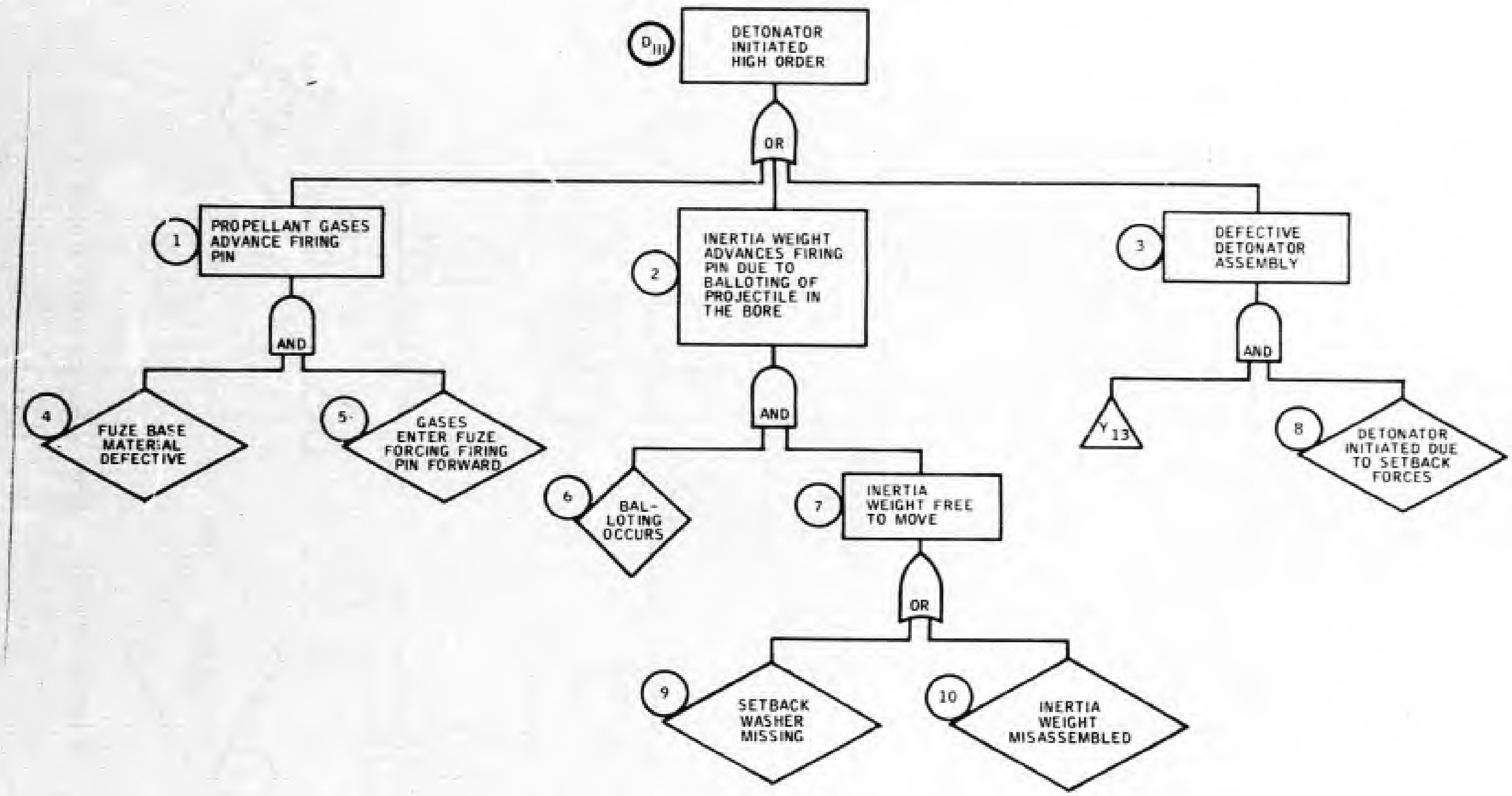

Figure III-12. Detonator Initiated High Order Fault Tree

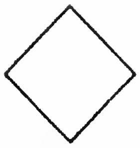

An event where analysis stopped. Further knowledge lacking or considered inconsequential. The event where basic failure rates or probabilities of occurence are employed.

A repeat symbol, with a Y and a numerical subscript, to identify which event or situation is repeated.

An indicator symbol, with a Y and a numerical subscript, to identify an event or situation which is to be repeated in another phase.

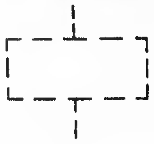

Broken line paths indicate areas that were considered but that do not contribute to safety numerics due to extremely remote probabilities of occurrence.

Identification symbol.

B. 20MM SAPHE MINIATURIZED FUZE SAFETY ANALYSIS (W6635) Contract No. F08635-70-C-0009

1. References

1. Contract No. F08635-70-C-0009, Annex No. 4, Safety Engineering Annex.

2. Honeywell Inc. Memo dated 11 March 1969, J. P. Streff, "20mm SAPHE Safety Analysis," E8002.

2. Introduction

In compliance with Reference 1, a numerical evaluation of design safety for the 20mm Semi-Armor Piercing High Explosive (SAPHE) miniaturized fuze concept was conducted. Safety fault tree diagrams were constructed and evaluated using event probabilities based on contractor test experience where possible, and based on engineering judgment when actual test data was non-existent or insufficient.

3. Summary

The probability of a safety failure during the manufacture-through-usage life cycle of the 20mm SAPHE miniaturized fuze was calculated to be 0.409×10^{-6} (one safety failure per 2.4 million units). The design goal for safety probability was 1.0×10^{-6} (one safety failure per 1.0 million units). Incorporating firing pin locking capability during the setbact-to-impact phase reduced the likelihood of premature function attributable to potential balloting or to the firing pin being unintentionally driven forward by the inertia weight during projectile flight.

4. Discussion

General -- The 20mm SAPHE miniaturized fuze design presented in Figure III-13 was used in this safety analysis. It is a modification of the Reference 2 design with reduced length. This configuration differs from that presented in Reference 2 to permit a reduction in fuze length. The more significant modifications are (1) redesign of the firing pin, (2) redesign of the inertia weight, (3) removal of the firing pin spring, and (4) incorporation of a firing pin locking capability. A functional description of normal fuze operation is presented in paragraph B.5.

Fuze Safety Numerical Evaluation -- Safety fault tree diagrams for the 20mm SAPHE miniaturized fuze design are presented in paragraph B.6. These diagrams consider the three life cycle phases depicted in Figure III-2. A numerical evaluation of fuze safety is also included in paragraph B.6. The event probabilities used in this evaluation are listed in Table III-4. Where possible, the event probabilities were derived from actual contractor test data associated with similar components. The probability of a safety failure during the life cycle of the fuze is presented in Table III-5.

TABLE III-4. EVENT PROBABILITY[a]

IDENTIFICATION CODE	FAULT TREE ENTRY (OR EVENT)	PROBABILITY[b] (PER MILLION)	DATA SOURCE
A3	CRIMP OR STAKING OPERATION INITIATES THE DETONATOR	0.1	1
A13	HANDLING ENVIRONMENTS CAUSE ROTOR TO ALIGN	P = 0.99[c]	1,2
A14	HANDLING ENVIRONMENTS FORCE DETONATOR AFT	P = 0.99[c]	1
A16	HANDLING ENVIRONMENTS PLUS INERTIA WEIGHT FORCE FIRING PIN FORWARD	P = 0.99[c]	1
A17	C-RING GUIDE DAMAGED	884.0	3
A18	C-RING GUIDE MISSING	38.0	3
A19	C-RING GUIDE MALFORMED	58.0	8
A20	DETONATOR HOUSING MALFORMED	28.0	3
A22	DETONATOR HOUSING DAMAGED	16.0	3
A23	DETONATOR STAKE OR CRIMP MISSING	16.0	1
A24	DETONATOR STAKE OR CRIMP MALFORMED	163.0	3
A25	C-RING DAMAGED	22.0	3
A26	C-RING MALFORMED	36.0	3
A27	C-RING MISASSEMBLED	7.0	3
A28	C-RING MISSING	7.0	3
A29	SETBACK WASHER MISASSEMBLED	255.0	3
A30	SETBACK WASHER MISSING	18.0	3
B4	INSPECTOR ERROR (MANUAL/VISUAL)	P = 0.01[c]	3
C9	FUZE BASE MATERIAL DEFECTIVE (POROUS)	1.0	1
C10	PROPELLANT GASES ENTER FUZE FORCING PIN FORWARD	P = 1.0[c]	1
C12	DETONATOR INITIATED DUE TO SETBACK FORCES	P = 0.99[c]	1
C15	BALLOTING OCCURS (IN THE BORE)	P = 0.1	1
C17	FAULTY PROPELLANT CHARGE (REDUCED OUTPUT)	P = 0.0001	1
C18	LOCKING BALL MISSING (ONE OF SIX)	336.0	3
C19	FUZE HOUSING BALL GROOVE MISSING	38.0	3
C24	SETBACK SUFFICIENT TO CRUSH WASHER	P = 0.9995[c]	1
C25	SPIN SUFFICIENT TO MOVE ROTOR (IN THE BORE)	P = 0.99[c]	1
C27	SPIN SUFFICIENT TO DISENGAGE C-RING LOCK	P = 0.995[c]	1

[a]PROBABILITY VALUE BASED ON CONTRACTOR EXPERIENCE FOR SIMILAR EVENTS
[b]PROBABILITY OF OCCURRENCE ESTIMATED
[c]PROBABILITY OF OCCURENCE NOT PER MILLION.

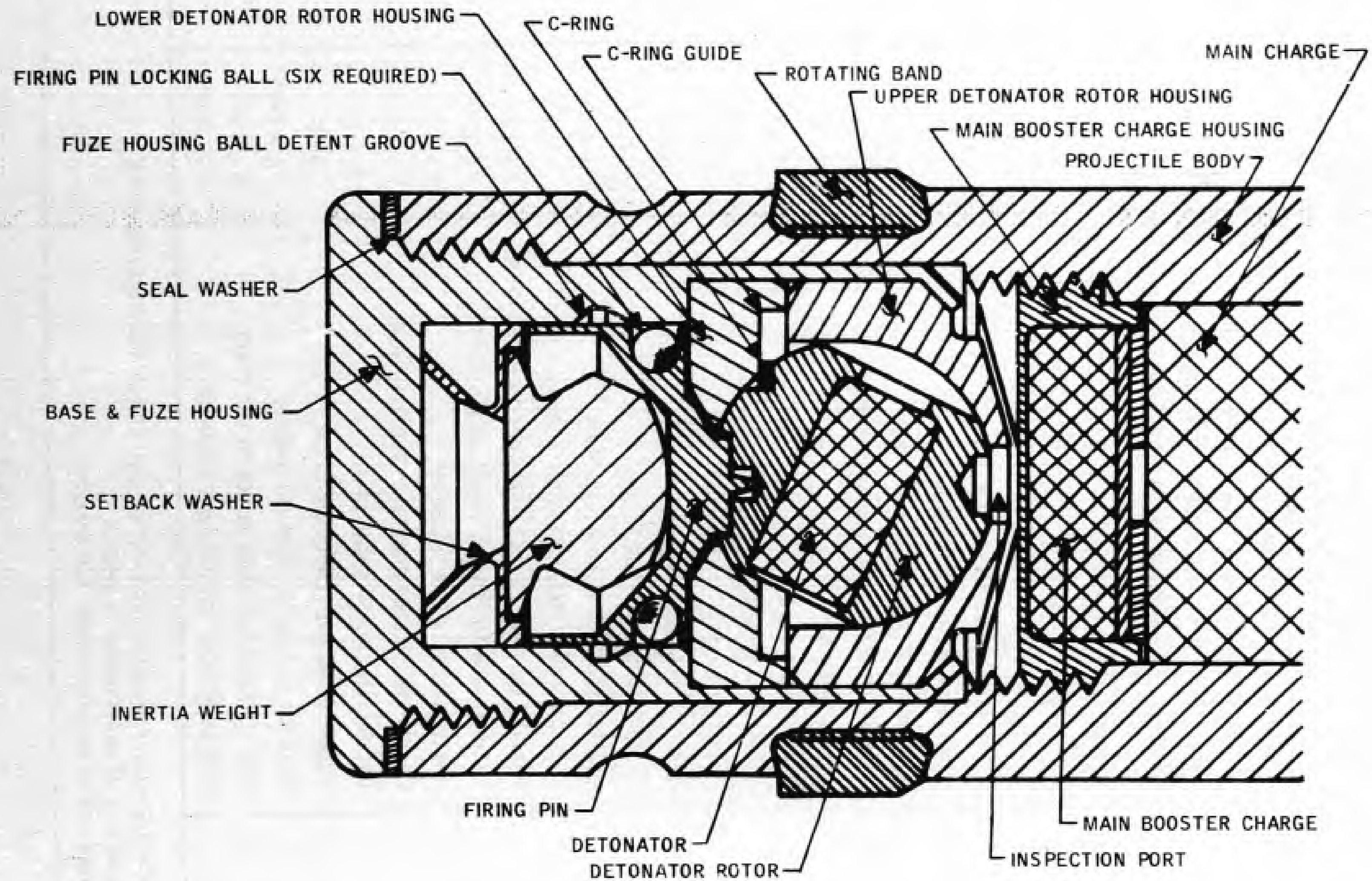

Figure III-13. 20mm SAPHE Miniaturized Fuze Design

TABLE III-5. SAFETY FAILURE PROBABILITY

Life Cycle Phase	Premature Probability (Per Million) -A-	Occurrence Rate (One Per $\bar{x}$ Million Units) -B-
I	0.381	2.6
II	0.00281	355.9
III	0.0256	39.1
Totals	0.40941	
	≈ 0.41	2.4

The above fuze safety probability is better than the design goal maximum limit of 1.0×10^{-6}, and the occurrence rate is better than the implied goal of one safety failure per million units.

5. <u>20mm SAPHE Miniaturized Fuze-Design Functional Description</u>

The following describes 20mm SAPHE miniaturized fuze function.

1. Setback forces cause the inertia weight and firing pin to crush the setback washer. This movement of the inertia weight and firing pin in the aft direction frees the first safing feature of the fuze and the firing pin is retracted from the detent in the detonator rotor.

2. Acceleration of the projectile restricts detonator rotor movement. This restriction is due to (1) the C-ring being held in the locked state by the rotor which is forced aft by the setback force, and/or (2) the frictional forces between the rotor and the lower rotor housing.

   (a) Deceleration of the projectile frees the detonator rotor from the setback forces.

   (b) Spin of the projectile causes the C-ring to open. This frees the second safing feature of the fuze, and rotor movement is no longer confined to the out-of-line orientation.

3. The detonator is free to align.

4. Spin of the projectile forces the firing pin balls into the detent groove in the fuze housing sidewall, thus locking the firing pin in the armed position.

5. Spin of the projectile causes the freed detonator rotor to seek the in-line orientation required for propagation of the explosive train.

FUZE IS ARMED

6. Impact forces cause the inertia weight to overcome the locking effect of the firing pin balls and to drive the firing pin forward into the channel of the detonator rotor which contains the stab detonator.

7. The firing pin impacts the detonator, which is rigidly mounted in the detonator rotor, and the detonator is initiated.

8. The output of the detonator crosses the air gap and initiates the booster charge.

9. The booster charge propagates across an air gap and initiates the main charge.

FUNCTION

6. 20mm SAPHE Miniaturized Fuze Design Safety Fault Tree Diagrams and Evaluation

Fault Tree Diagrams -- This section provides an analysis of the flow of events required to produce a potential hazard. These events are put in an AND/OR relationship which allows Boolean Algebra to be applied. The following logic symbols apply to Figures III-14 through III-16.

A logical AND relation. This symbol indicates that all following branches are required before achieving the previous result.

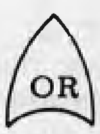

A logical OR relation. This symbol indicates that any of the following branches will permit achievement of the previous result.

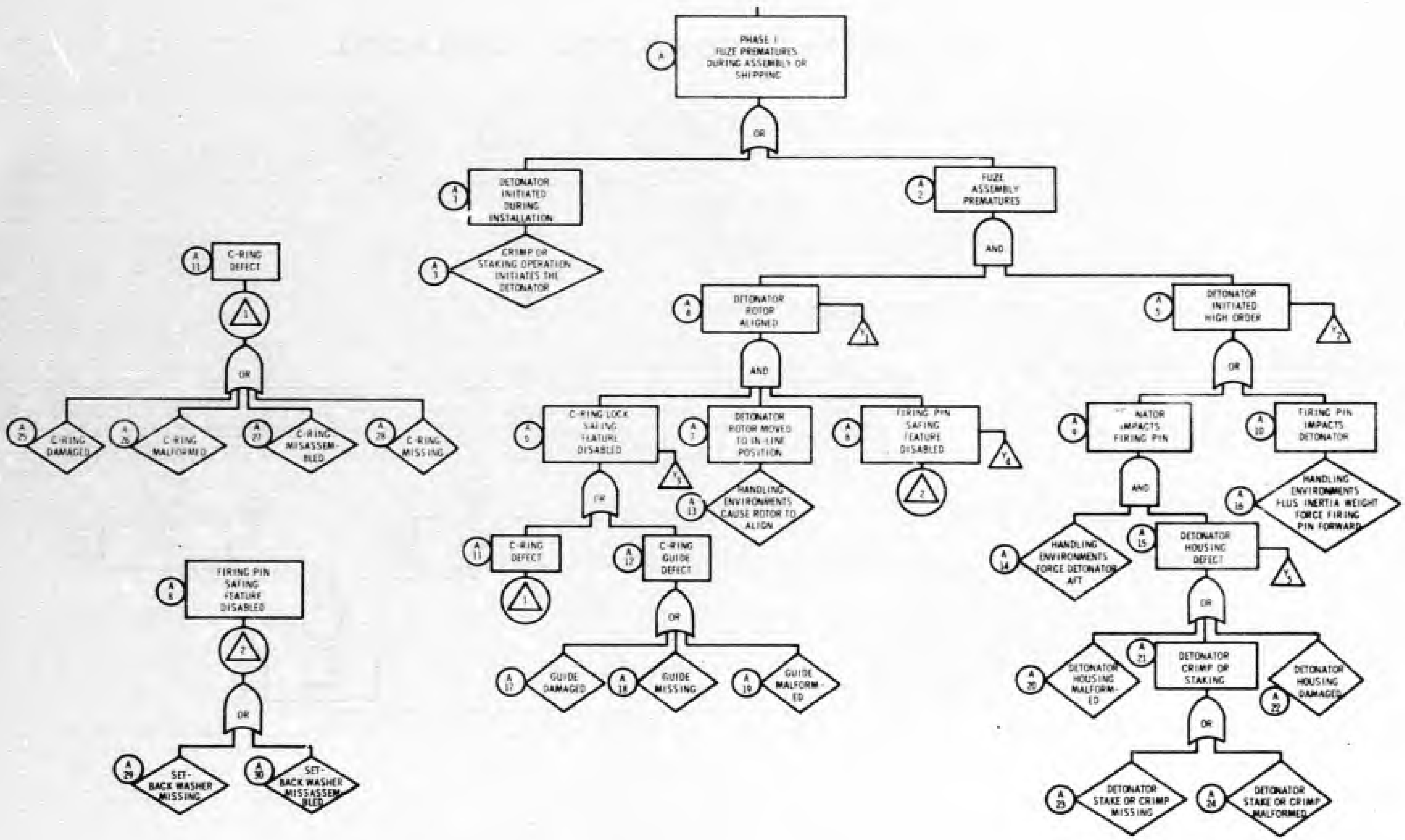

Figure III-14. Phase I Prematures Fault Tree

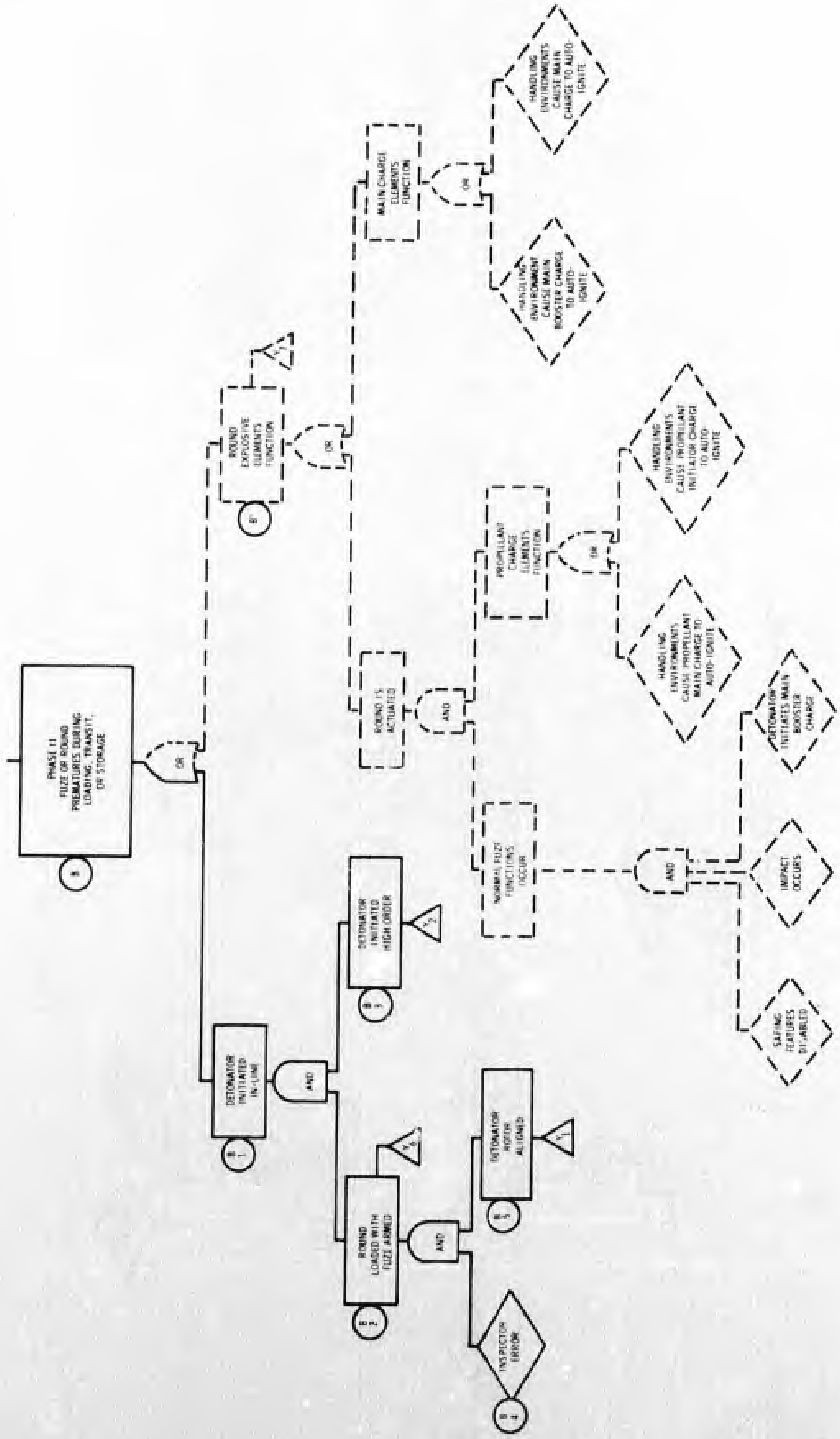

Figure III-15. Phase II Premature Fault Tree

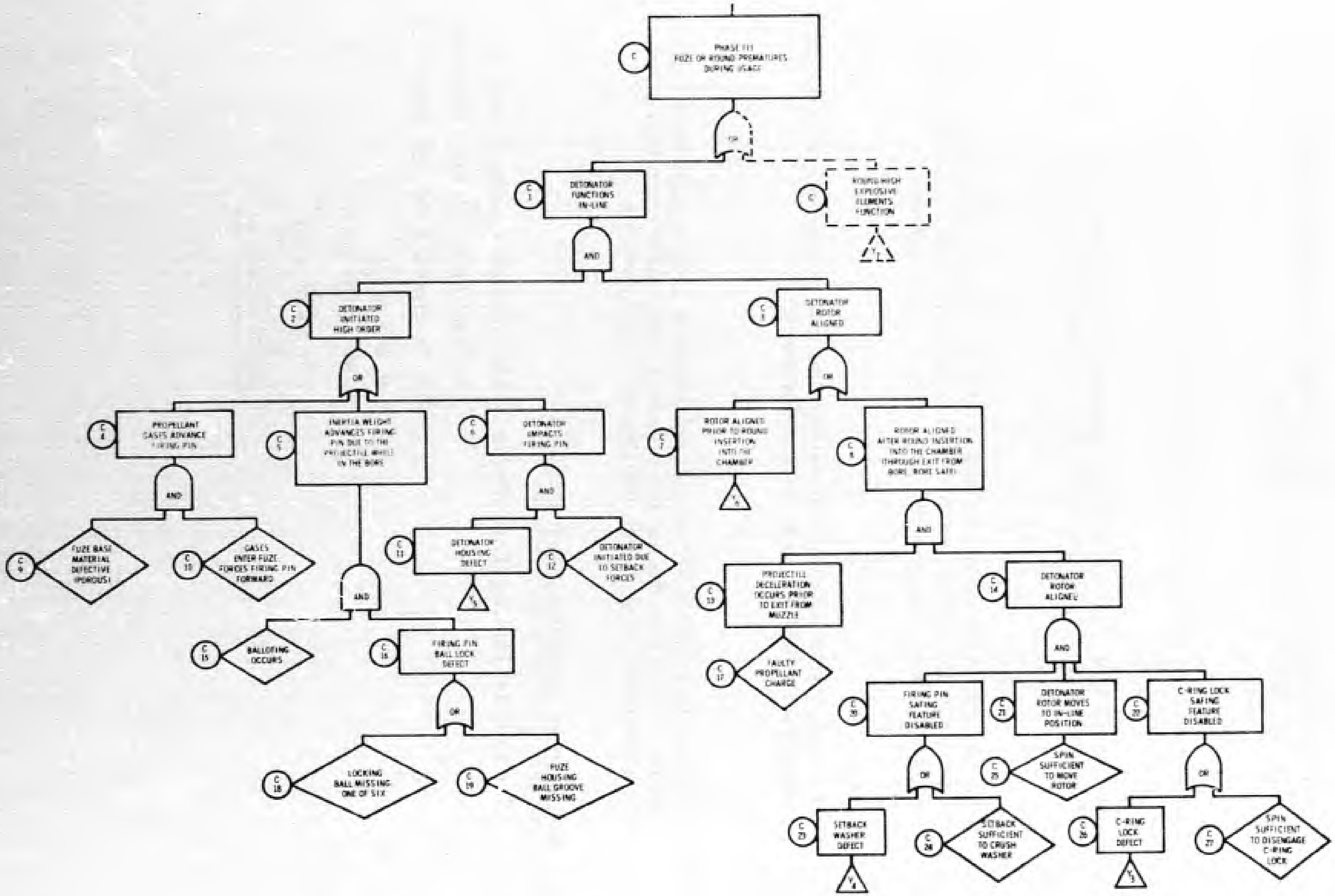

Figure III-16. Phase III Prematures Fault Tree

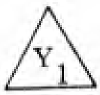

A repeat symbol containing a Y and a numerical subscript to identify which branch is repeated.

An event caused by the subsequent contributing event(s).

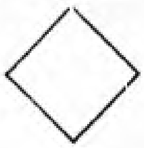

An event where the analysis stopped; this could be a basic failure mode or a lack of further knowledge.

An identification code symbol containing an alphanumeric entry. This code is used in constructing the necessary mathematical equations associated with the numerical evaluation.

A continuation symbol indicating that the remaining entries are depicted in another area of the diagram.

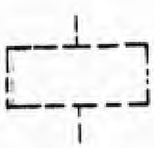

Broken line paths (or branches) indicate areas that were considered, but that do not contribute to the safety numerics due to extremely remote probabilities of occurrence.

Fuze or Round Premature Probability --

$$
\begin{aligned}
\text{Premature During Life Cycle} &= \text{Premature During Phase I} \\
&\quad + \text{Premature During Phase II} \\
&\quad + \text{Premature During Phase III} \\
&= 0.381 \times 10^{-6} \\
&\quad + 0.00281 \times 10^{-6} \\
&\quad + 0.0256 \times 10^{-6} \\
&\approx \underline{\underline{0.410 \times 10^{-6}}}
\end{aligned}
$$

APPENDIX IV

SAPHE EXPLOSIVE TRAIN DESIGN VERIFICATION TESTING

R. STRESAU LABORATORY, Inc.
RESEARCH — DEVELOPMENT — EVALUATIONS

EXPLOSIVE DEVICES, SYSTEMS AND INSTRUMENTATION

TELEPHONE: (715) 635-2777
STAR ROUTE
Spooner, Wisconsin, 54801

21 February 1972

Honeywell, Inc.
Ordnance Div.
600 2nd St. North
Hopkins, Minn 55343

Att: Mr. K. Gallant

Subject: "SAPHE Explosive Train Design Verification Testing", as outlined in the statement of work of PO 1M142207 and telephone conversations with Mr. Keith Gallant.

Gentlemen:

Test A-1 was conducted using the test arrangement as illustrated in Sk. 029-1, with the booster cup loaded at 40 Kpsi. This loading pressure was obtained from pressure-density data on hand at this laboratory which indicated that a loading pressure of 40 Kpsi should yield a density of approximately 1.73 g/cm^3. From the foregoing test a score of 6/6 was received which was as good as you could get although not significantly better than the score of 6/10 recevied and reported in the work statement. Even though the 6/6 score was not significantly better than 6/10 there was an indication that the booster loaded at 40 Kpsi was more reliable than that described in the work statement. It was then learned in a telephone conversation with Honeywell personnel that their boosters were loaded at 55 Kpsi, so test A-1 was rerun using boosters loaded at 55 Kpsi and a score of 5/6 was received. Test A-2 was then preformed and a score of 5/6 was also obtained. There is apperently no significant difference between the results of test A-1 and test A-2, although there is an indication that the boosters loaded at 40 Kpsi appear to be somewhat more sensitive than those loaded at 55 Kpsi. Test A-3 was then conducted, where a disc of aluminum 0.004 thick (P/N 28009597-001) was placed on the output end of the detonator (531680), using the test arrengement of Sk. 029-1. A score of 2/6 was received; it was therefore concluded that this approach would not improve the probability of detonation transfer between the detonator (531680) and the loaded booster cup, and that tests A-4, A-5 and A-6 should not be completed. Tests B-1 and B-2 were then preformed using the test arrangement as shown in Sk. 029-2, results of which were 9/10 and 10/10 respectively.

Since there was an indication that booster loading pressure is a factor, it was agreed that an effort to obtain quantitative data regarding the effect of this variable be obtained. Four short (10 shot total in each) Brucetons were preformed using the arrangement as shown in Sk. 029-3 with a variable (single layer) added barrier of 1100-0 aluminum in contact with the diaphram of the booster cup, with noosters loaded at 20, 30, 40 and 60 Kpsi. Densities were also calculated at these pressures by loading the PBXN-5 into brass cylinders 0.500 long with a column diameter of 0.201 (three determinations at each pressure). The results of these experiments are given in Sk. 029-4 along with the results (Mean, 50% point) of the Bruceton tests. As can be seen there appears to be an optimum loading pressure which is approximately 37 Kpsi.

Much effort was expended toward developing a method of trying to find out the density of the PBXN-5 in the five loaded boosters received from Honeywell without removing the explosive from the booster cup. The approach used was similar to that of a Brinell hardness test, where a known load is applied to a surface and the diameter of the indentation made by a hardened steel sphere (Brinell) serves to measure hardness. The method used was to apply a known load to the surface of the loaded density specimens and measure the amount of penetration of some type of penetrator.and then compare this with the amount of penetration received when the same load was applied to the surface of the loaded booster. Several different types of penetrators were tried, these included a 0.250 dia. ball, a flat ram 0.063 dia. and the "N Brale" from our hardness testor. Only the data received using the "N Brale" seemed to make much sense. There was a somewhat linear relationship between applied load and depth of penetration in the specimens at the two lower densities, but this disappeared at the higher densities. In comparing data received from the density specimens to that received from the loaded boosters it would appear that the density of the PBXN-5 in the boosters was close to what would be the optimum according to Sk. 029-4. A plot of this data can be found on Sk. 029-5. These five boosters were then fired using the test arrangement as shown in Sk. 029-1 with a 0.050 air gap, and a score of 5/5 was received.

Safety tests were preformed using the setup as illustrated in Sk. 029-6. Five shots were fired with the booster cup loaded with PETN 741 at 18 Kpsi, all five were safe according to the criteria of reference 1. Sk. 029-7 is a graphical analysis of the safety failure rate versus stimulus in DBgu for PETN 741 and PBXN-5 H-4 (loaded at 18 and 30 Kpsi respectively) based upon miniaturized gap test data taken from references two and three.

As can be seen a score of five safe in five trials with the PETN 741 pressed at 18 Kpsi would indicate a safety failure rate of less than one in $1x10^{-8}$ at a 95% confidence level. Five boosters were then loaded with lead azide (Dex) at 16 Kpsi and fired using the same test arrangement. A score of 3 safe in 5 trials was received. Sk 029-8 is a graphical analysis of NOL SSGT data for lead azide (Dex), PETN and PBXN-5. A score of 3 safe in 5 trials with the lead azide would indicate a safety failure rate of way less than one in $1x10^{-8}$, and a score of 5 safe in five trials with the PETN would also indicate a safety failure rate of less than one in $1x10^{-8}$.

From the foregoing discussion it would appear that if the loading pressure of the PBXN-5 were changed from 55 Kpsi to 37 Kpsi that the detonator (531680) should reliably transmit detonation to the booster. Concerning our determination of the density of the five boosters received from Honeywell; it is somewhat perplexing when one sees the density that we received was what should be received at the optimum loading pressure, especially in light of the 6/10 score that was received and reported in the work statement. It is recommended that some type of environmental cycling be preformed on some loaded boosters to determine if there is any apparent density change caused by expansion and contraction of the explosive material, this could be accomplished by carefully measuring the column height of the explosive before and after the cycling. It is also recommended that further testing be conducted with respect to establishing the reliability of the detonation transfer from the detonator and the booster, with the inclusion of some varicomp testing and analysis.

Sincerely,

Dale Spaulding

Dale Spaulding

REFERENCES:

1. MIL-STD-331 "Military Standard Fuze and Fuze Components, Envirnmental and Performance Tests for," Test 115, dated 10 January 1966.
2. Stresau, R. H., "Miniaturized Gap Test," for the Sandia Corporation, Albuquerque, New Mexico, Report No. 69-6-1.
3. Stresau, R. H., and D. A. Spaulding "Miniaturized Gap Test DataIII, PETN and PBX 9407, "RSLR 70-6-3 for the Sandia Corporation, Albuquerque, New Mexico.

Test Arrangement Used for Tests A-1, A-2, and A-3

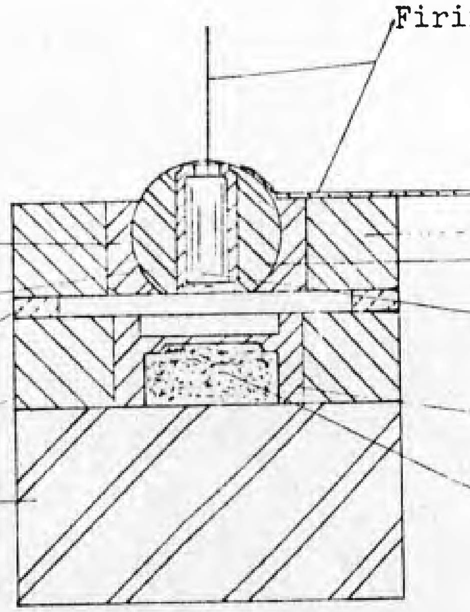

Test	Air Gap	Loading pressure Kpsi	Results(fires/trials)
A-1	0.020	40	6/6
A-1	0.020	55	5/6
A-2	0.050	55	5/6
A-3	0.020	55	2/6

Sk. 029-1

Test Arrangement For Tests B-1 and B-2

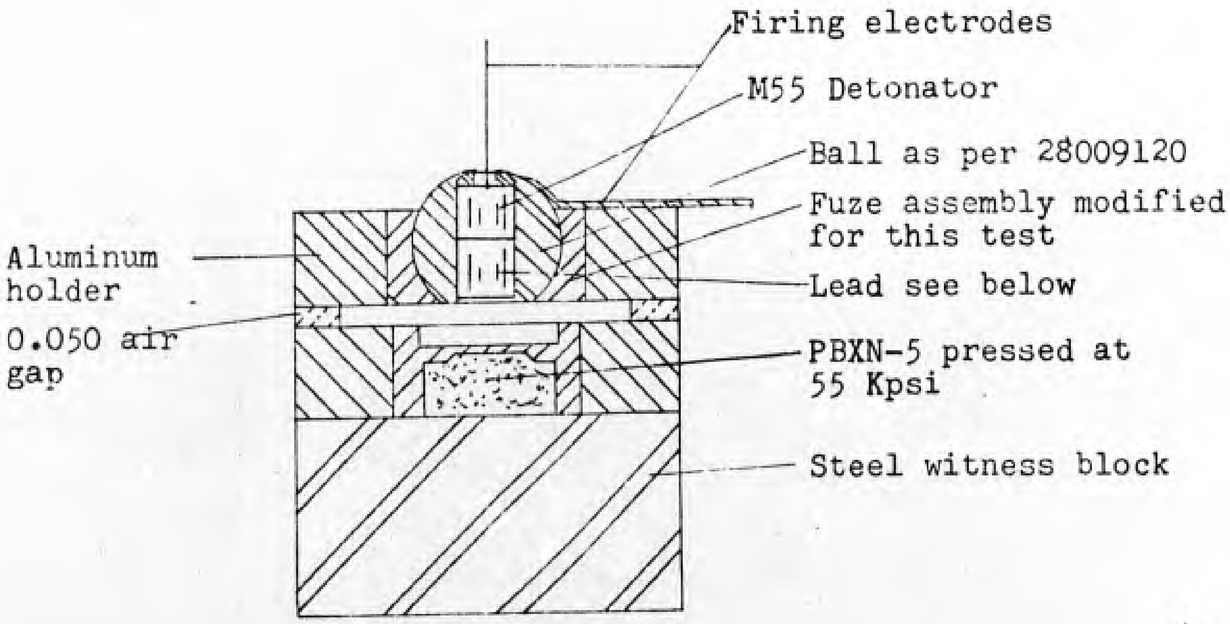

Test	Lead configuration	Test results (fires/trials)
B-1	With sleeve (reducer)	9/10
B-2	Without sleeve	10/10

Sk. 029-2

Test Arrangement Used in Bruceton Tests

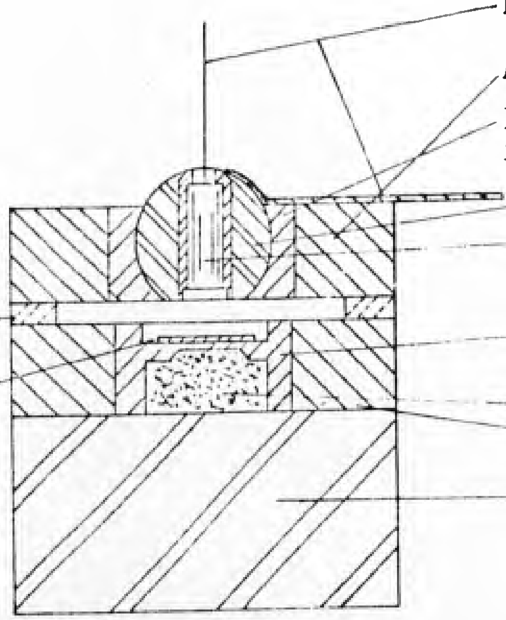

Pressure Kpsi	Density G/cm^3	Mean barrier thickness in mil (10 shot Bruceton test)
20	1.630	7.0
30	1.693	9.0
40	1.738	9.4
60	1.777	3.5

Sk. 029-3

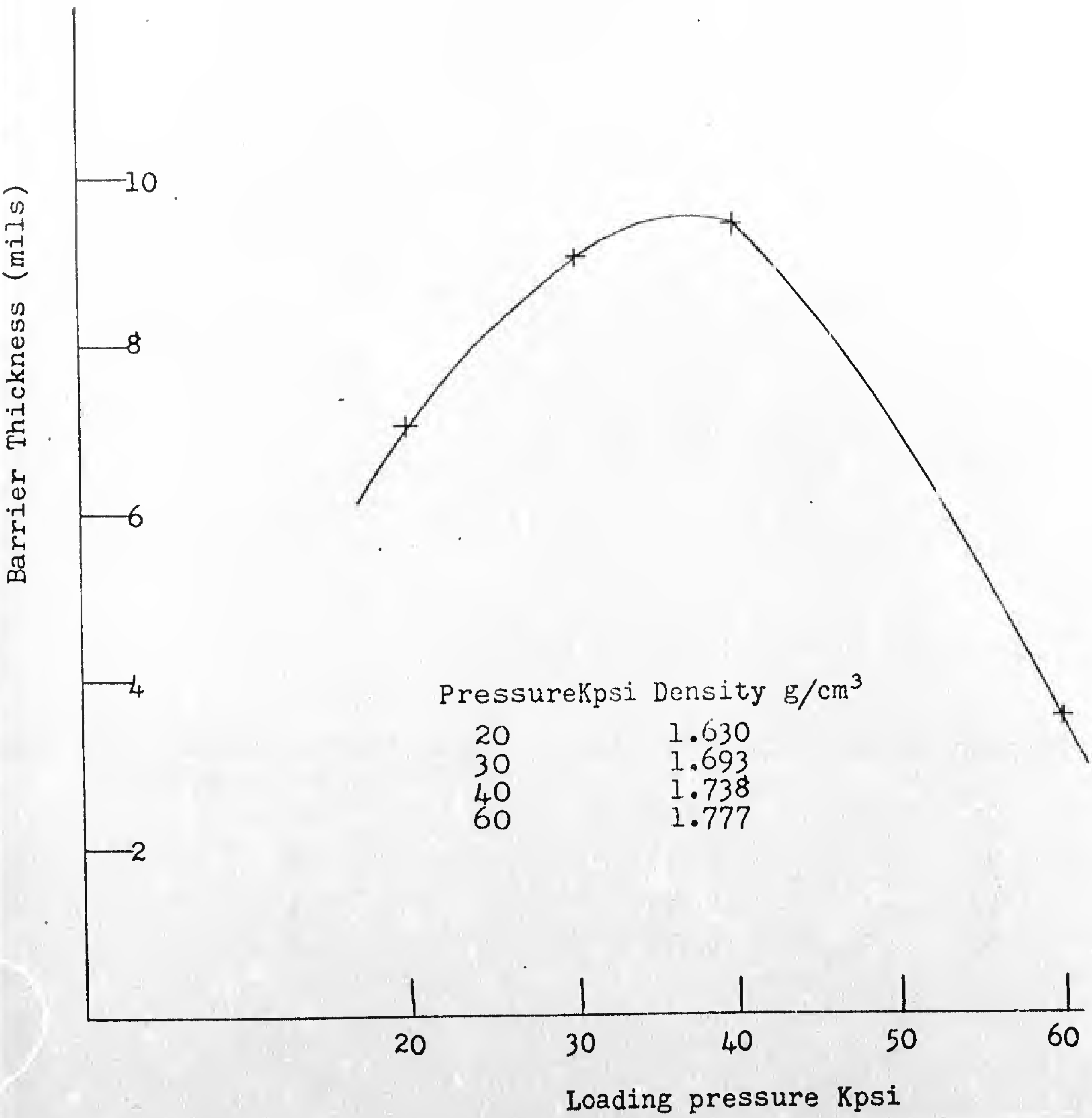
Barrier Thickness (mils)
10
8
6
4
2
PressureKpsi Density g/cm³
20 1.630
30 1.693
40 1.738
60 1.777
20
30
40
50
60
Loading pressure Kpsi

Sk. 029-4

Plot of depth of penetration of "N Brale" versus the applied pressure

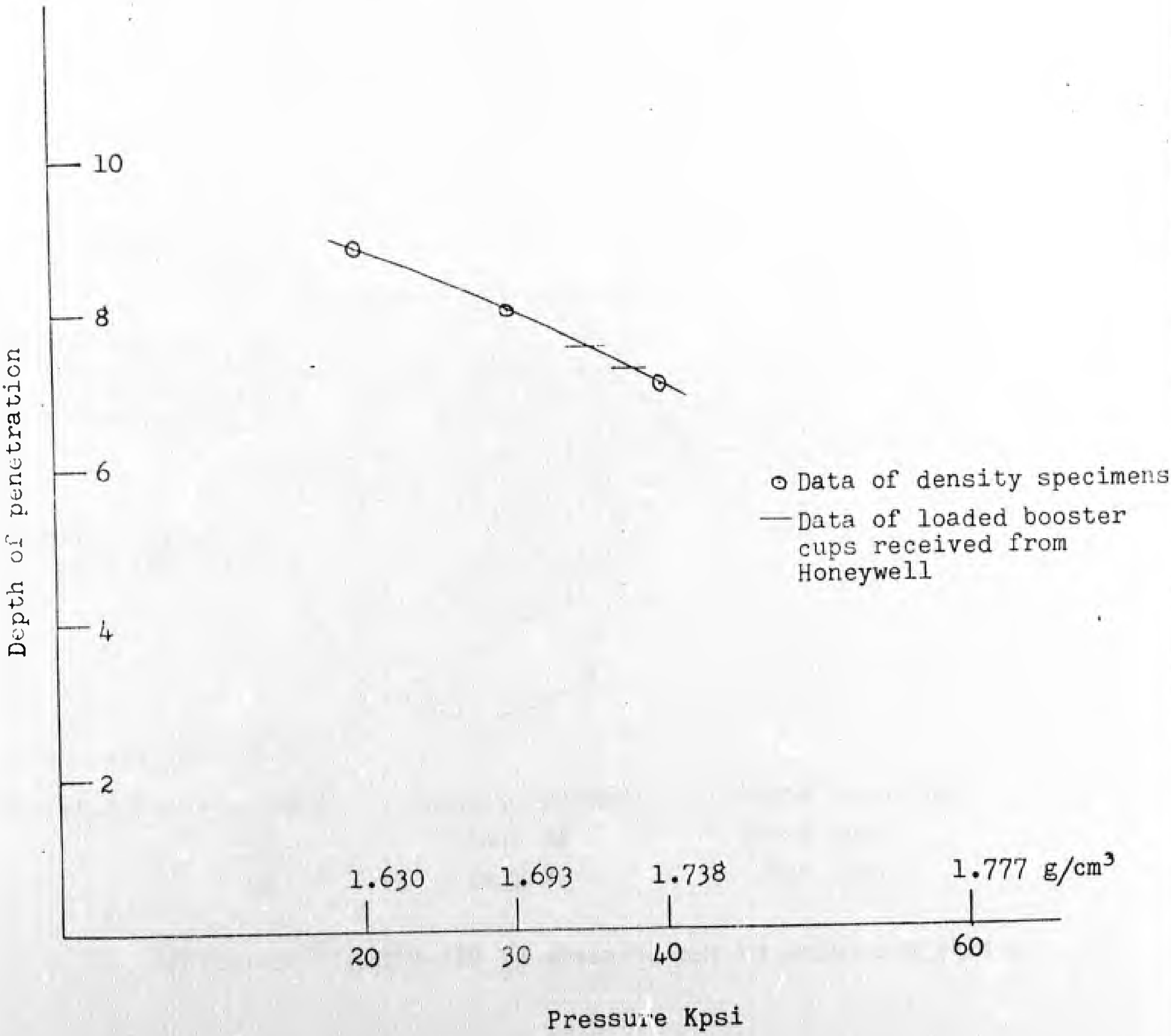

Sk. 029-5

Arrangement for Safety Tests

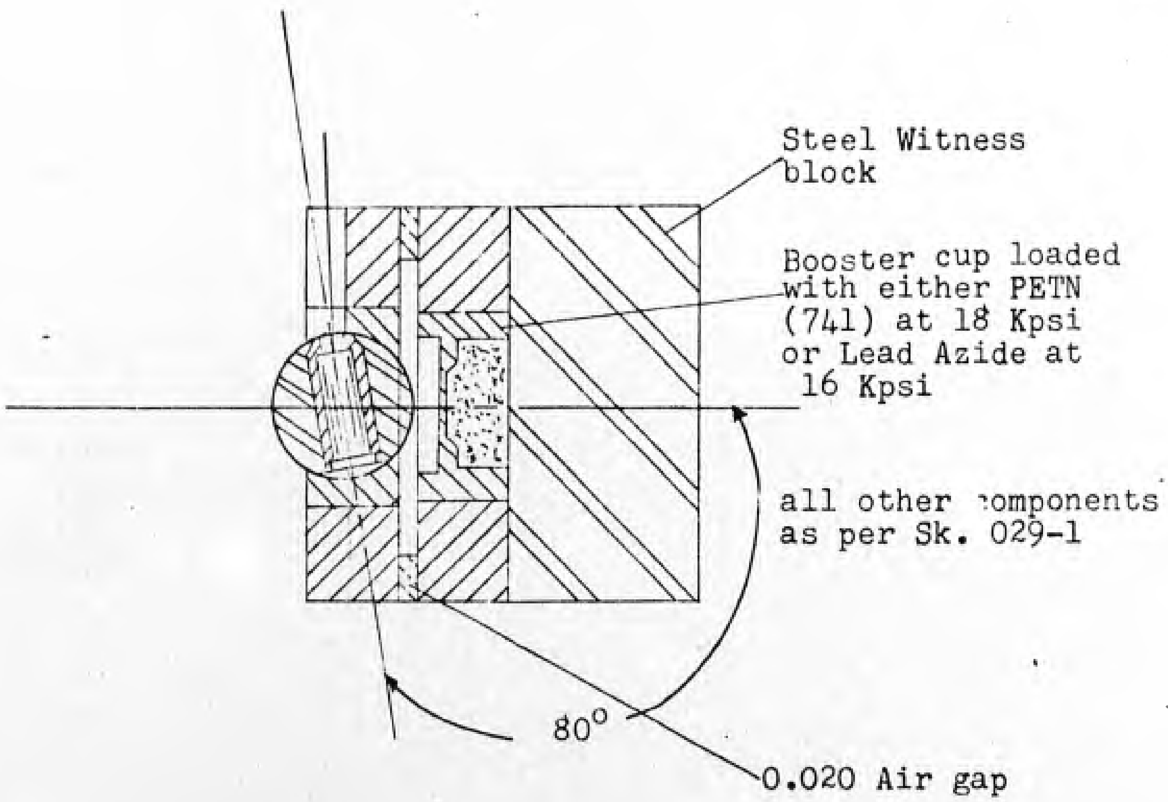

Explosive Material	Loading pressure	Results (safe[a]/trials)
Lead Azide	16 Kpsi	3/5
PETN 741	18 Kpsi	5/5

α safe according to the criteria of MIL-STD-331 test 115.

Sk. 029-6

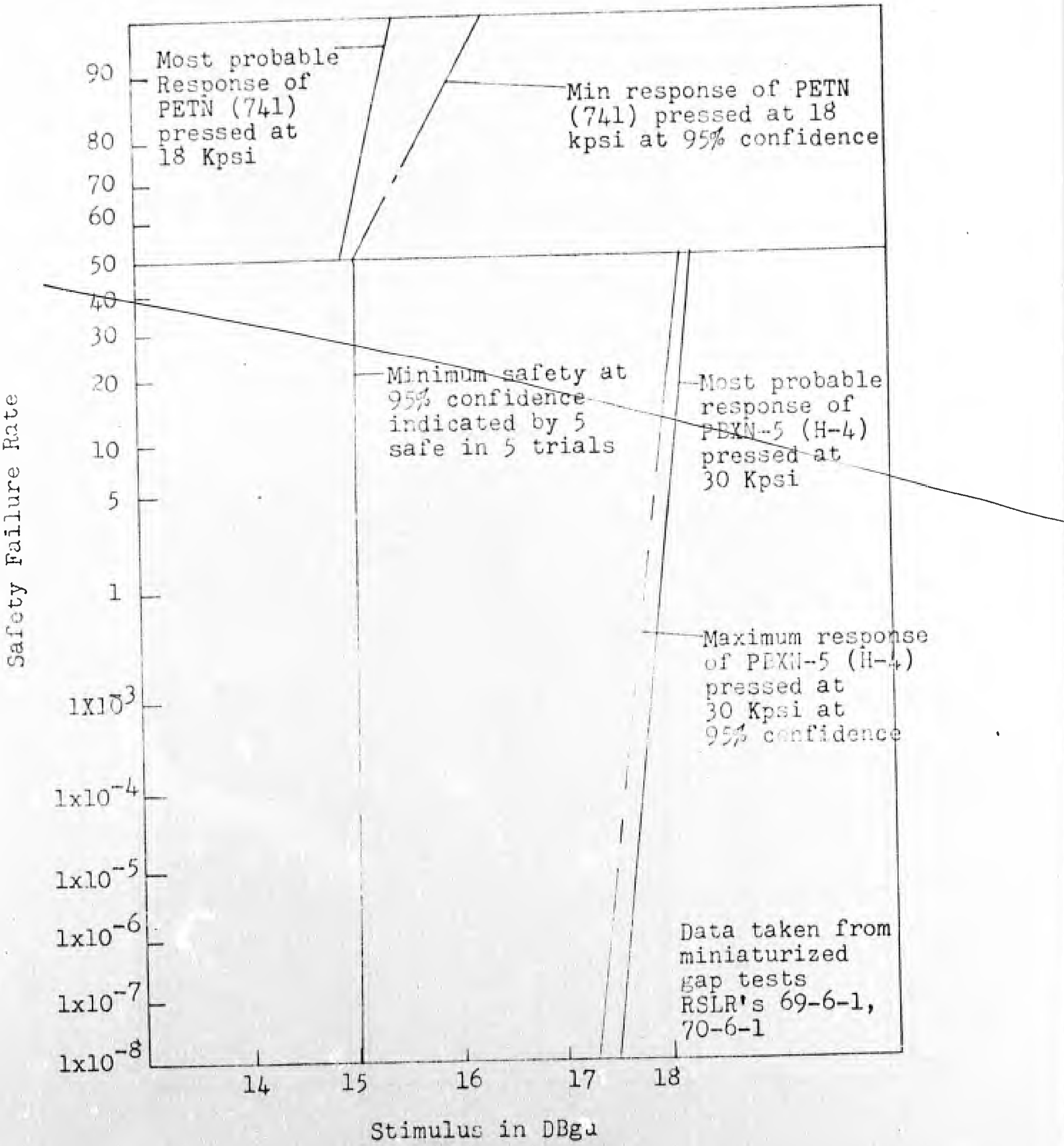
Most probable Response of PETN (741) pressed at 18 Kpsi
Min response of PETN (741) pressed at 18 kpsi at 95% confidence
Minimum safety at 95% confidence indicated by 5 safe in 5 trials
Most probable response of PBXN-5 (H-4) pressed at 30 Kpsi
Maximum response of PBXN-5 (H-4) pressed at 30 Kpsi at 95% confidence
Data taken from miniaturized gap tests RSLR's 69-6-1, 70-6-1
Safety Failure Rate
90
80
70
60
50
40
30
20
10
5
1
1X10-3
1x10-4
1x10-5
1x10-6
1x10-7
1x10-8
14
15
16
17
18
Stimulus in DBg

Sk. 029-7

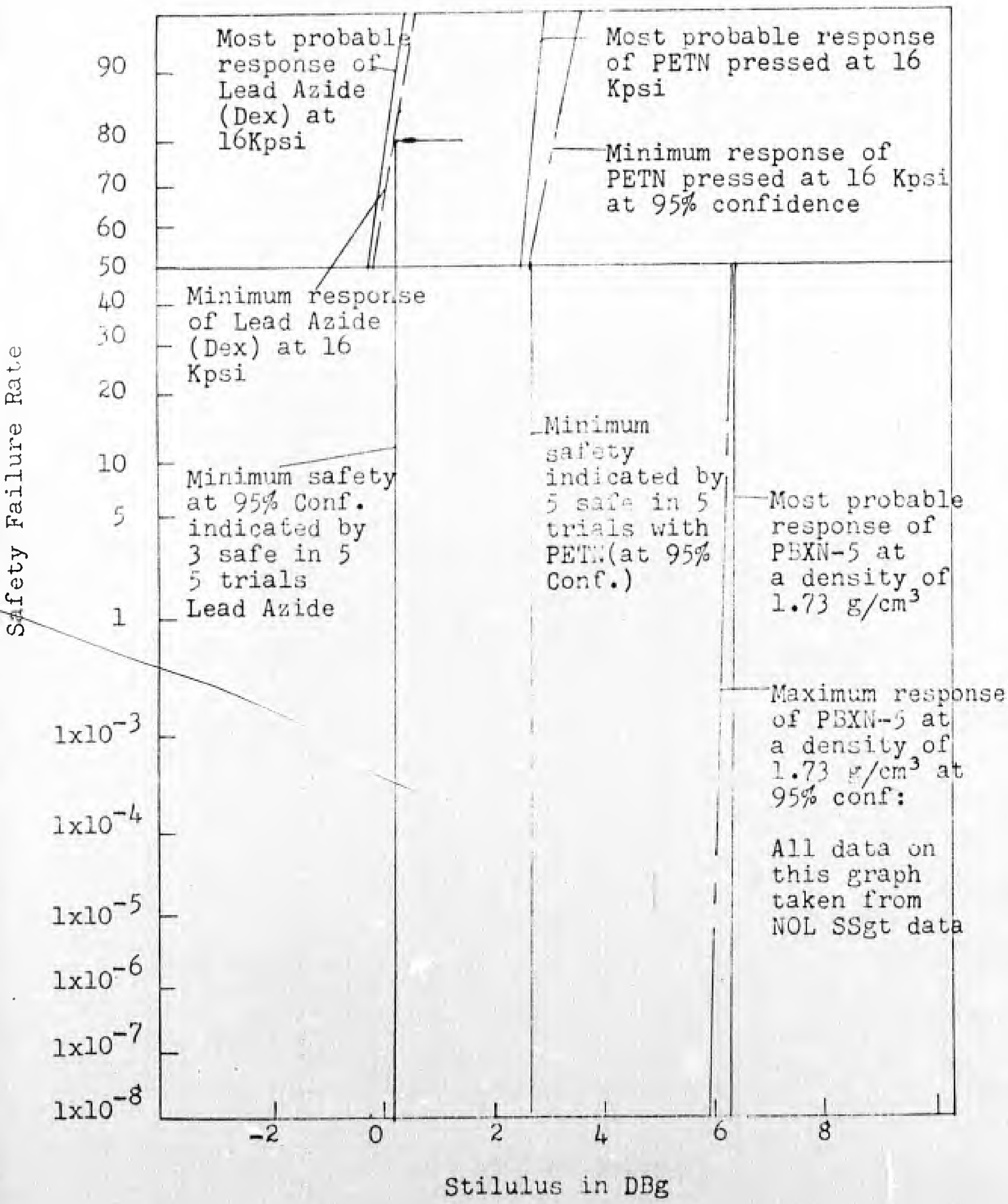

Safety Failure Rate
90
80
70
60
50
40
30
20
10
5
1
1x10-3
1x10-4
1x10-5
1x10-6
1x10-7
1x10-8
-2
0
2
4
6
8
Stilulus in DBg
Most probable response of Lead Azide (Dex) at 16Kpsi
Most probable response of PETN pressed at 16 Kpsi
Minimum response of PETN pressed at 16 Kpsi at 95% confidence
Minimum response of Lead Azide (Dex) at 16 Kpsi
Minimum safety at 95% Conf. indicated by 3 safe in 5 5 trials Lead Azide
Minimum safety indicated by 5 safe in 5 trials with PETN (at 95% Conf.)
Most probable response of PBXN-5 at a density of 1.73 g/cm3
Maximum response of PBXN-5 at a density of 1.73 g/cm3 at 95% conf:
All data on this graph taken from NOL SSgt data

Sk. 029-8

INITIAL DISTRIBUTION

Hq USAF/RDQRM	2
Hq USAF/RDPA	1
AFSC/SDWM	1
ASD/ENYS	1
AUL/AUL-LSE-70-239	1
USA Aberdeen R&D Ctr/AMXRD-BIL	1
USAF TAC Ftr Wpns Ctr/CRCD	1
DDC	2
OOAMA/MME	1
OOAMA/OONECA	1
SMUFA/J7000	1
TAC/DRA	1
TAC/LGW	1
AMSWE/REF	1
AMSMU-RE-M	1
SMULC-ATL	1
PACAF/IGY	1
AFATL/DL	1
AFATL/DLY	1
AFATL/DLR	1
AFATL/DLOSL	2
AFATL/DLDG	2
ADTC/CDCLO/DO	1

(The reverse of this page is blank.)

UNCLASSIFIED

Security Classification

DOCUMENT CONTROL DATA - R & D

(Security classification of title, body of abstract and indexing annotation must be entered when the overall report is classified)

1. ORIGINATING ACTIVITY (Corporate author) Honeywell Inc., Government and Aeronautical Products Division, 600 Second Street North, Hopkins, Minnesota 55343	2a. REPORT SECURITY CLASSIFICATION UNCLASSIFIED 2b. GROUP

3. REPORT TITLE

THE SEMI-ARMOR PIERCING HIGH EXPLOSIVE (SAPHE) ENGINEERING DEVELOPMENT PROGRAM

4. DESCRIPTIVE NOTES (Type of report and inclusive dates)

Final Report - 28 August 1969 to 15 August 1972

5. AUTHOR(S) (First name, middle initial, last name)

Ray A. Hermanson

6. REPORT DATE January 1973	7a. TOTAL NO. OF PAGES 251	7b. NO. OF REFS
8a. CONTRACT OR GRANT NO. F08635-70-C-0009 b. PROJECT NO. 4361 c. Task No. 01 d. Work Unit No.	9a. ORIGINATOR'S REPORT NUMBER(S) 9b. OTHER REPORT NO(S) (Any other numbers that may be assigned this report) AFATL-TR-73-9	

10. DISTRIBUTION STATEMENT

Distribution limited to U. S. Government agencies only; this report documents test and evaluation; distribution limitation applied January 1973. Other requests for this document must be referred to the Air Force Armament Laboratory (DLDG), Eglin Air Force Base, Florida 32542.

11. SUPPLEMENTARY NOTES Available in DDC	12. SPONSORING MILITARY ACTIVITY Air Force Armament Laboratory Air Force Systems Command Eglin Air Force Base, Florida 32542

13. ABSTRACT

Under this effort a 20mm Semi-Armor Piercing High Explosive (SAPHE) ammunition, designated the PGU-2/B, was designed, developed, fabricated, and evaluated. This design incorporated an all-impact angle base fuze evolved from the feasibility effort under Contract F08635-69-C-0134. The resulting 20mm SAPHE round is designed to meet or exceed the technical requirements of the M50 series ammunition. It is also designed to be directly interchangeable in the present M39 and M61 gun systems without change or modification to the gun or feed (with the exception of coil spring rates). The initial baseline development included contractor design, development tests, and delivery of over 3,000 cartridges for Government evaluations. Additional effort included fuze design modifications to investigate the feasibility of increasing the minimum arming distance to 6 meters, with 15 meters desired, development tests, and delivery of six cutaway display models. Although a safe-separation distance of 6 meters was not achieved within the funds and time available, it is believed that the safe-separation can be increased by using either of the two minor modifications described in the report.

DD FORM 1 NOV 65 1473 REPLACES DD FORM 1473, 1 JAN 64, WHICH IS OBSOLETE FOR ARMY USE.

UNCLASSIFIED

Security Classification

14 KEY WORDS	LINK A		LINK B		LINK C	
	ROLE	WT	ROLE	WT	ROLE	WT
Semi-Armor Piercing High Explosive						
SAPHE						
All-impact angle base fuze						
M39 Gun System						
M61 Gun System						